Polyhydroxyalkanoate production by *Bacillus thuringiensis* – An aspect of biorefining pulp and paper mill sludge

by

SARISHA SINGH

Submitted in fulfillment of the academic requirements for the degree of

Doctor of Philosophy

in the Discipline of Microbiology

School of Life Sciences

College of Agriculture, Engineering and Science

University of KwaZulu-Natal

Durban

South Africa

February 2021

As the candidate's supervisor I have approved this thesis/dissertation for submission.

Signed: [redacted] Name: Dr R Govinden Date: 12/04/2021

PREFACE

The experimental work contained in this thesis was conducted by the candidate while based in the Discipline of Microbiology, School of Life Sciences of the College of Agriculture, Engineering and Science, University of KwaZulu-Natal, Westville Campus, South Africa, under the supervision of Dr R. Govinden and the co-supervision of Prof. B. Sithole, Dr P. Lekha and Prof. K. Permaul. The research was financially supported by the National Research Foundation (NRF), Department of Science and Innovation (DSI) Biocatalysis Initiative, DSI Waste Roadmap and the Council for Scientific and Industrial Research (CSIR).

These studies represent original work by the author and the contents of this work have not otherwise been submitted in any form for any degree or diploma to another tertiary institution. Where use has been made of work by others, it is duly acknowledged in the text. The results reported are due to investigations by the candidate.

[redacted]	12 April 2021
Dr R. Govinden	Date
[redacted]	12 April 2021
Prof. B. Sithole	Date
[redacted]	12 April 2021
Dr P. Lekha	Date
[redacted]	12 April 2021
Prof. K. Permaul	Date

DECLARATION I: PLAGIARISM

I, Sarisha Singh, declare that:

(i) the research reported in this thesis, except where otherwise indicated or acknowledged, is my original research;

(ii) this thesis has not been submitted in full or in part for any degree or examination to any other university;

(iii) this thesis does not contain other persons' data, pictures, graphs or other information, unless specifically acknowledged as being sourced from other persons;

(iv) this thesis does not contain other persons' writing, unless specifically acknowledged as being sourced from other researchers. Where other written sources have been quoted, then:

a) their words have been re-written but the general information attributed to them has been referenced;

b) where their exact words have been used, their writing has been placed inside quotation marks, and referenced;

(v) where I have used material for which publications followed, I have indicated in detail my role in the work;

(vi) this thesis is primarily a collection of material, prepared by myself, published as journal articles or presented as a poster and oral presentations at conferences. In some cases, additional material has been included;

(vii) this thesis does not contain text, graphics or tables copied and pasted from the Internet, unless specifically acknowledged, and the source being detailed in the dissertation and in the References sections.

Signed: Sarisha Singh

Date: 04 February 2021

DECLARATION II: PUBLICATIONS

My role in each paper and presentation is indicated. The * indicates corresponding author.

Chapter 3:
Singh, S*., Permaul, K., Lekha, P., Sithole, B., and Govinden, R. Using pyrolysis/GC-MS to determine the effect of carbon and nitrogen nutrient source combinations on polyhydroxyalkanoate monomer production by *Bacillus thuringiensis*.
19th Annual conference of the South African Society for Microbiology, Coastlands, Umhlanga, Durban, South Africa 17-20 January 2016 (Poster presentation)
21st International Symposium on Analytical and Applied Pyrolysis, Nancy, France, 9-12 May 2016 (Oral Presentation)
I contributed to the conceptualization, conducted all of the experimental work, analyzed and interpreted all of the data, writing - original draft, reviewing, editing and presented at the respective conferences.

Chapter 5:
Singh, S*., Sithole, B., Lekha, P., Permaul, K., and Govinden, R. 2021. Pretreatment and enzymatic saccharification of sludge from a prehydrolysis kraft and kraft pulping mill. Journal of Wood Chemistry and Technology.https://doi.org/10.1080/02773813.2020.1856880
I contributed to the conceptualization, conducted all of the experimental work, analyzed and interpreted all of the data, writing - original draft, reviewing and editing.

Chapter 6:
Singh, S*., Sithole, B., Lekha, P., Permaul, K., and Govinden, R. 2021. Optimization of cultivation medium and cyclic fed-batch fermentation strategy for enhanced polyhydroxyalkanoate production by *Bacillus thuringiensis* using a glucose-rich hydrolyzate. Bioresources and Bioprocessing. 8:1-17.
I contributed to the conceptualization, conducted all of the experimental work, analyzed and interpreted all of the data, writing - original draft, reviewing and editing.

Signed: Sarisha Singh

Date: 04 February 2021

TABLE OF CONTENTS

ACKNOWLEDGMENTS

I would like to express my sincere gratitude to the following person(s):

My supervisors for their constant motivation, encouragement, guidance, support and mentoring during the course of this study;

Dr Viren Chunilall, Mr Pule Seemela and Mrs Londani Musimanyana, of the Biorefinery Industry Development Facility (BIDF), CSIR (Durban) for technical support;

Lesego Maubane from CSIR (Pretoria) for rendering services and assisting with polymer characterization;

Staff and students from UKZN (Microbiology department) for their support and guidance.

I would like to express my sincere gratitude to the following organizations for financial support;

National Research Foundation (2015-2017);

DSI Biocatalysis Inititative;

DSI Waste Roadmap, and

CSIR

LIST OF TABLES

LIST OF FIGURES

ABSTRACT

The substantial success of plastic as a material is owed to its unparalleled designs with unique properties and proved versatility in an extensive range of applications. Unfortunately, the reliance on single-use plastic commodities consequently results in the incorrect disposal and accumulation of this waste at staggering rates in our environment and landfill sites. In this regard, there is a vested interest in replacing petrochemical plastics with natural, biodegradable plastics (bioplastics). Of the many natural polymers available, microbially synthesized polyhydroxyalkanoates (PHAs) have gained popularity. Eco-friendly PHA-based bioplastics are characteristically as robust and as durable as their oil-based equivalents. Pulp and paper mill sludge (PPMS) is another solid waste stream that is predominantly disposed of via landfilling. The environmentally hazardous gases and leachate emitted from PPMS together with limited landfill space availability and the implementation of strict waste management legislation may not make landfilling practicable in the future. However, this carbohydrate-rich biomass has favorable traits that make it applicable as a feedstock for microbial biomass and PHA production. Hence, in the interest of addressing the issues mentioned above, this study aimed to beneficiate PPMS into PHAs by applying it as the sole feedstock for microbial cell proliferation and subsequent PHA production. Presently, to the best of the author's knowledge, there are no reports on PHA production as a route for valorization of PPMS from South African pulp and paper mills. Thus, the novelty of the present study is marked by the unique ways of incorporating PPMS as a low-cost substrate as well as the various fermentative strategies navigated to enhance both microbial cell biomass and PHA productivity. In the present study, it was established that *Bacillus thuringiensis* had promising PHA-producing capability. The strain synthesized a copolymer and terpolymer using untreated (raw) neutral semi-sulphite chemical pulping and cardboard recycling mill (NSSC-CR) and prehydrolysis kraft and kraft pulping mill (PHKK) PPMS in a consolidated bioprocessing fermentation. A separate hydrolysis and fermentation strategy was pursued whereby a glucose-rich hydrolyzate was obtained from enzymolysis of PPMS and subsequently utilized in a cyclic fed-batch fermentation (CFBF) strategy to obtained enhanced yields of cell biomass and PHAs. Response surface methodology (RSM) was first implemented to optimize the conditions for enzymatic saccharification of de-ashed PHKK PPMS. The optimized variables were; pH 4.89; 51°C; hydrolysis time 22.9 h; 30 U/g β-glucosidase and 60 U/g cellulase; and 6.4% of dried de-ashed PPMS fiber resulting in a hydrolyzate comprising of 48.27% glucose. Thereafter, CFBF was pursued where the glucose-rich hydrolyzate was employed as the sole carbon source for cell

proliferation and PHA production. The statistically optimized fermentation conditions to obtain high cell density biomass (OD_{600} of 2.42) were; 8.77 g L^{-1} yeast extract; 66.63% hydrolyzate (v/v); a fermentation pH of 7.18; and an incubation time of 27.22 h. The CFBF comprised of three cycles and after the third cyclic event, maximum cell biomass (20.99 g L^{-1}) and PHA concentration (14.28 g L^{-1}) were achieved. This cyclic strategy yielded an almost 3-fold increase in biomass concentration and a 4-fold increase in PHA concentration compared with batch fermentation. The properties of the synthesized PHAs were similar to commercial polyhydroxybutyrate (PHB) and polyhydroxybutyrate-co-valerate (PHBV) and also displayed slightly higher thermostability and lower crystallinity compared with commercial PHB and PHBV. This is the first report detailing the proof of concept of using PPMS from South African pulp and paper making mills for cell biomass and PHA production by *B. thuringiensis*. In addition, this study reports on the practicality and novelty of utilizing PPMS either in its raw, untreated state or as enzymatically saccharified glucose-rich hydrolyzate as cheap substrates applicable for both cell biomass and PHA production using different fermentation strategies. Finally, to the best of our knowledge, this is also the first report that has successfully applied *B. thuringiensis* in a CFBF strategy coupled with glucose-rich hydrolyzate as the sole carbon source for the production of high cell density biomass and enhanced PHA production. From this study, it is intended that innovative insights and prospective solutions to valorizing pulp and paper mill sludge are provided, whilst simultaneously generating a value-added product.

CHAPTER ONE

Introduction

1.1. Pulp and paper mill waste

The pulp and paper sector is an integral multi-faceted manufacturing industry, which represents a significant economic enterprise that generates billions of revenue towards the financial growth of many countries. The pulp and paper industry contributes significantly to South Africa's economy and society. In 2018, the forestry-to-paper value-add to South Africa's economy was R28 billion annually (PAMSA 2018). In 2019, the sector contributed R6.63 billion to the country's balance of trade. Statistically, the forestry-to-paper contribution to South Africa's total Gross Domestic Product (GDP) was an estimated R24.13 billion (0.53%), forestry contribution to manufacturing was 4.03%, and forestry contribution to agricultural GDP was 25.22% (PAMSA 2019a). In 2019 alone, South Africa produced 2.16 million tons of paper products constituting newsprint, printing/writing paper grades, corrugated materials/containerboard, wrapping paper, tissue and board (PAMSA 2019b). Consequently, the increased production of pulp and paper products to meet the daily demands will result in the inevitable generation of substantial amounts of waste. The pulp and papermaking process generates large quantities of waste such as ash, dregs, grits, lime mud and sludge (Simão et al. 2018). Pulp and paper mill sludge (PPMS) is one of the solid waste by-products generated from pulp and paper industry activities. In South Africa, PPMS production is an estimated 0.5 million tons per annum (Boshoff et al. 2016). The PPMS encompasses primary or secondary sludge and has a moisture content ranging from 50-70% depending on the pulp and paper mill (Boshoff et al. 2016). Primary sludge consists of fibrous material (e.g. cellulose fibers), inorganic fillers from the papermaking process (e.g. $CaCO_3$, kaolin and TiO_2) which constitutes the ash content and inert solids from different processes, such as the washing or screening stage, the white water circuits, etc. Secondary sludge consists of biological solids, fibers and wood-derived substances e.g. cellulose and lignin residuals. The typical fiber content accounts for 11–95% of solids in the primary sludge thus; cellulose fiber is a key characteristic component of PPMS (Chen et al. 2012; Zhang et al. 2020). In the context of this study, PPMS is an organic solid waste material containing a mixture of primary and secondary sludge.

During the pulp and papermaking process, large amounts of PPMS accumulates on the mill's premises and requires safe handling, transportation, treatment and disposal (Makgae 2011). The PPMS has been traditionally disposed of through dewatering and landfilling, land-spreading or incineration (Scott and Smith 1995; Norris and Titshall 2011). The sludge disposal process causes an undesirable emission of methane, odors from pollutants and leaching of inorganic waste thereby polluting soil, surface and/or groundwater systems (Scott and Smith 1995; Sarafadeen et al. 2014). The PPMS is a complex and changeable mixture of dozens or even hundreds of both organic and inorganic compounds with the well-known ones being heavy metals, dioxins, tannins, resin acids and organo-chlorines (Ali and Sreekrishnan 2001; Boni et al. 2004). Therefore, the PPMS waste stream is an economic burden and an environmental concern. Increasingly stringent environmental legislation can alleviate severe mismanagement, handling, soil, water and air pollution problems (Rashid et al. 2006). Waste disposal in South Africa is currently governed by means of a number of pieces of legislation including The National Environmental Management; Waste Act (NEM: WA), No 59 of 2008, which came into effect on 1 July 2009. The NEM: WA together with the minimum requirement(s) according to the Norms and Standards for Disposal of Waste to Land-fill (GN No. 636 of 23 August 2013) prohibits landfilling of waste with a moisture content > 40%, or that liberates moisture under pressure in landfill conditions, and which has not been stabilized by treatment (Department of Environmental Affairs 2013). One strategic objective of the South African government is to reduce the volume of organic waste disposed to landfill by 50% within five years (Department of Environmental Affairs 2019) thus enticing alternate uses for PPMS. Through research, innovation and development, a minimization of end-of-life waste through waste beneficiation and/or bioconversion is possible. A reduction in waste disposal costs and ongoing operational expenses such as the cost(s) associated with maintenance and fuel for waste vehicle fleets is also foreseeable. The valorization of PPMS with the aim of product development will reduce the increasing demands on fossil fuel-based materials, generate additional revenue and mitigate the environmental impact of landfilling waste.

A vested interest lies in researching the possibility of producing value-added products from PPMS. Besides being identified as a waste stream, it is also a low-cost lignocellulosic biomass substrate and a renewable resource that is currently available in surplus amounts. Moreover, PPMS presents two key advantages. Firstly, the chemo-mechanical processes during the pulp and paper making process alter the crystalline structure of the cellulose. This increases the

accessible surface area resulting in fibers more prone to enzymatic hydrolysis compared with other lignocellulosic biomass such as corncob, wheat straw, rice straw and chaff (Schroeder et al. 2015; Alkasrawi et al. 2016; Boshoff et al. 2016). Previous studies with PPMS have examined its potential in simultaneous saccharification and fermentation for cellulase or ethanol production (Kang et al. 2010; 2011; 2012; Mendes et al. 2017). Secondly, since PPMS contains 20-75% cellulose and hemicelluloses, it is rich in carbohydrates making it a desirable source of fermentable sugars (Gibril et al. 2018; Liu et al. 2018). There is great interest in the use of lignocellulosic biomass as feedstock for the production of fermentable sugars (Banerjee 2011; Min et al. 2015). Obtaining hydrolyzates from lignocellulosic substrates such as spruce sawdust (Kucera et al. 2017), various agro-waste residues (Ramadas et al. 2009; Gowda and Shivakumar 2014) and municipal waste paper (Annamalai et al. 2017) has been demonstrated. Additionally, by deriving hydrolyzates from lignocellulosic biomass where glucose and xylose are the two dominant sugars is advantageous as these sugars can be assimilated by microorganisms (Al-Battashi et al. 2019). However, successful and cost-effective conversion of cellulosic biomass to monosaccharides in high yields is still a challenge. Nevertheless, PPMS is still a good candidate for hydrolysis treatments. Hydrolyzates produced through acid or enzymatic hydrolysis stand a good chance of containing furan and/or phenol toxins derived from lignin (Du et al. 2010). The generation of these components can be detrimental to downstream enzymatic and microbial processes (Klinke et al. 2004).

1.2. Plastic pollution

Plastic pollution is another waste challenge globally. Governments worldwide have deployed policy and economic instruments, such as bans and product taxes in an effort to disincentivise the production and consumption of "single-use" plastic products and packaging. The introduction of levies and explicit prohibitions to curb plastic bag usage was successful in places like Bangladesh, Taiwan, Ireland, Italy, Denmark and Botswana (Dikgang et al. 2012). According to the United Nations Environment Agency, more than 60 countries have placed levies on single-use plastics or totally banned their use. The European Parliament finalized a law banning a range of single-use plastic items, including cutlery, straws, cotton bud and balloon sticks by 2021. Canada has also undertaken to ban single-use plastics as early as 2021. In the UK, from April 2022, a tax will apply to businesses that produce or import plastic packaging, which uses less than 30% recycled content (KPMG Tax alert 2019). Plastic carrier bags were the first to be targeted and have been banned or levied (under various conditions) by

more than 30 African governments. On 9 May 2003, The Minister of Environmental Affairs and Tourism has, under section 24 (d) of the Environment Conservation Act, 1989 (Act No. 73 of 1989) - plastic carrier bags and flat plastic bags, made regulations in the Schedule and launched a ban on plastic bags with a thickness of 30 microns along with a levy of R 0.04 per bag (Department of Environmental Affairs and Tourism 2003). The South African National Budget Speech from April 2020 states that the plastic bag levy increased to R 0.25 (Republic of South Africa National Treasury 2020). In addition, by 2021 the current levy might be extended to include all single-use plastics used for retail consumption such as beverage cups, coffee stirrers, water bottles, plastic straws, utensils and packaging such as food containers (Plastics SA 2019; 2020). The implementation of this levy aims to discourage the production and consumption of virgin plastic and ultimately reduce plastic bag consumption. Initially, consumption reduced, but once the cost of the carrier bags was included in household budgets, consumption increased again. Consumers continue to purchase plastic bags each time they shop and reuse them as bin liners (for example) resulting in an accumulation of plastic bags in landfills or dumps. The thin-walled plastic bags are especially problematic because of their lightweight and tendency to 'balloon' and be blown by the wind causing littering (Dikgang et al. 2012). In relation to the South African Industry Waste Management Plans in the packaging sectors, there is an urgent need to restrict the production and retail of single-use plastics and ultimately eradicate single-use plastics. Furthermore, exploration and research into feasible and biodegradable alternatives to plastic for single-use are desirable (Hanekom 2020). The global bioplastics production capacity is set to increase from around 2.11 million tons in 2019 to approximately 2.43 million tons in 2024. The application of bioplastics for packaging material accounts for almost 60% of the total bioplastics market in 2017. But, with rising demand for the innovation of more sophisticated biopolymers with diverse applications and the need for various biodegradable products, the market is continuously growing. Innovative biopolymers such as polylactic acid, starch blends and polyhydroxyalkanoates (PHAs) are the main drivers of this growth in the field of bio-based, biodegradable plastics. PHAs are an important polymer family that has been in development for a while and is now finally in the market at commercial scale. The production of PHA-plastics is expected to increase to $1.33 million in 2024 (European Bioplastics 2017; 2019).

Currently, commercial and academic interest lies in the production of bacterial biopolymers and functional bioplastic films. Even though traditional petrochemically synthesized polymers

possess many of the specific properties required to make useful packaging, the long-term environmental sustainability of these polymers is now being questioned (Tawakkal et al. 2014). Polyhydroxyalkanoates are a family of naturally-occurring biopolymers synthesized by bacteria that possess the enzyme PHA synthase when cultured under imbalanced nutrient conditions (Tan et al. 2014). It is desirable to use a bacterial strain capable of PHA production from a variety of substrates. Traditionally, Gram-negative bacteria are favored due to their increased PHA accumulation capability (Tan et al. 2014). However, Gram-positive *Bacillus* spp. has also demonstrated their PHA-producing potential (Valappil et al. 2007a). Biopolymers such as PHAs have been studied intensively by industry. These polyesters are 100% bio-based and are thus considered good candidates for the production of biodegradable, biocompatible plastics and elastomers that can be produced from renewable materials. The physical, mechanical and thermal characteristics of PHAs are analogous to chemically synthesized petrochemical polyesters, such as polypropylene (Albuquerque and Malafaia 2018). Thus, PHA-based materials have the potential to reduce the environmental impact associated with the disposal of petroleum-based packaging wastes (Tawakkal et al. 2014). The nature of biopolymers such as sustainable, toxicologically safe, high biocompatibility and desirable thermoplastic behavior makes them applicable in a variety of fields (Thakur et al. 2018). However, there are still economical limitations to completely substitute petrochemical plastics by PHAs. To achieve an effective PHA production scheme, the development of alternative production processes and/or the use of bacterial strains able to utilize inexpensive carbon sources has become a focus of particular interest (González-García et al. 2008; Jiang et al. 2016; Moritz and Duff 1996; Peters 2006) to substantially decrease PHA production costs. Investigations into using cellulose waste biomass directly as a nutrient source (without any pretreatment) for PHA production has proved successful (Shankar et al. 2015; Sawant et al. 2017). The convenience of using waste biomass as substrates without any prerequisite detoxification pretreatment, nutrient supplementation or fiber enhancing procedures can functionally reduce the economic hurdle of large-scale production of biopolymers. However, there is the possibility of slow bacterial growth on lignocellulosic substrates due to the lower immediate availability and accessibility of sugars compared to that of soluble sugars present in chemically defined media (Zhu et al. 2011). The application of hydrolyzates obtained from lignocellulosic substrates has shown potential as suitable feedstock and sole carbon source for bacterial PHA production (Davis et al. 2013; Al-Battashi et al. 2019).

1.3. Problem statement

South Africans use approximately 8 billion plastic carrier bags annually (Dikgang et al. 2012). The goal of banning or levying plastic bags in South Africa ultimately failed to reduce behavior and consumption due to the relatively low cost per plastic bag and the lack of affordable alternatives. Nuisance littering of plastic bags disfigures the environment and exacerbates the current solid waste crisis. Plastic pollution, mainly from single-use plastics used in consumer packaging, has significant environmental impacts. Approximately 8 million tons of plastic are currently being washed into the oceans annually causing duress to the rivers, coastal and marine environment (Department of Environmental Affairs 2018; Plastics SA 2019). Plastic waste in the oceans is also present as microbeads or microplastics and is raising concerns about the increasing microplastic load in the food chain, especially fish, and now in drinking water (Packaging SA 2018). The disposal of waste at properly licensed and regulatory compliant sanitary land-fills is a norm worldwide as it is regarded as a safe and economical option. Land-filling of hazardous waste in South Africa is driven by low landfill gate fees with typical municipal landfill gate fees of around R 200-584/ton including tax (GreenCape 2020). A few municipalities now face serious landfill airspace shortages and have increased their gate fees to around R 500- 800/ton. These low gates fees make it very difficult to implement alternative economically feasible waste treatment technologies (Godfrey and Oelofse 2017). South Africa is experiencing severe constraints in terms of the availability of landfill spaces as well as operating and decommissioning landfills in a manner that is compliant with licensing conditions. The absence of aggressive strategies to avoid generating waste and with increases in the total volumes of waste generated, greater effort is required to maintain the rapidly depleting landfill space, which is already recognized as being unsustainable (Department of Environmental Affairs 2018). The Department of Environmental Affairs and Tourism is currently reviewing the existing general waste management fees and landfill tariffs; assessing the full cost of waste management and charges; the feasibility of a disincentive landfill disposal tax to complement the existing landfill fees; and ultimately aiming to ban the landfilling of certain types of waste. For these reasons, diverting waste from landfill is a key imperative for the country's National Waste Management System. South Africa's strategy for diversion of waste from landfill is centered around building a secondary resources economy through the beneficiation of waste as part of the “circular economy” (Department of Environmental Affairs 2018). The aim, strategy, and concept of the circular economy is to reduce waste generation and

divert waste from landfill and towards supporting the growth of the South African secondary resources economy (Packaging SA 2018).

1.4. General aim of the study

Undoubtedly, PPMS has been recognized as a problematic waste stream that is an environmental threat and requires stringent management. There is an opportunity for pulp and paper mills to develop waste management strategies for PPMS, thereby beneficiating waste and simultaneously generating additional revenue streams for the industry. Therefore, the use of PPMS as a novel resource for the production of biodegradable plastics is being proposed. This study can demonstrate the novelty and practicality of biopolymer production from untreated PPMS and hydrolyzate derived from pretreated PPMS, thereby providing a solution for the remediation and valorization of PPMS. Furthermore, PHAs can be extracted from bacteria and examined for their suitability in the application of bioplastic products. This study aimed to investigate the PHA-producing potential of *Bacillus thuringiensis*, previously isolated from *Eucalyptus dunii* wood chips using commercially-sourced pure carbohydrates, untreated PPMS and carbohydrate-rich hydrolyzate derived from enzymatic saccharification of PPMS. Furthermore, different fermentation strategies were employed to produce high cell density biomass and enhance PHA productivity.

1.4.1. Specific objectives and aims

The following specific objectives were set to achieve the general aim of the study;

i) To determine the PHA-producing ability of *Bacillus thuringiensis* using simple and complex carbohydrates as carbon source.

- Using batch fermentation the isolate was cultivated in PHA-production medium where α-cellulose, glucose, glycerol, starch or sucrose was the carbon source. Extracted PHAs were profiled using Fourier transmission infrared (FTIR) spectra, pyrolysis-Gas Chromatography/Mass Spectrometry (py-GC/MS), thermogravimetric analysis (TGA) and differential scanning calorimetry (DSC).

ii) To construct a profile PPMS obtained from local prehydrolysis kraft and kraft (PHKK) and a neutral sulphite semi-chemical (NSSC) pulping mills.

- Characterization of the PPMS included; biochemical oxygen demand (BOD_5), chemical oxygen demand (COD), nitrogen content, carbohydrate composition using high-

performance liquid chromatography (HPLC), lignin and ash content. Py-GC/MS analysis of the sludge determined the presence of volatile fatty acids such as acetate, propionate, butyrate, valerate and/or hexanoate, which are typical precursors for PHA production.

iii) To determine the capacity of *B. thuringiensis* to use NSSC-CR and PHKK PPMS as feedstock and for biomass proliferation and PHA production and to characterize the extracted PHAs.

- A consolidated bioprocessing strategy was conducted using untreated PPMS. During the 72 h fermentation; bacterial proliferation, glucose consumption, BOD_5, COD were monitored. Scanning electron microscopy (SEM) was conducted to determine morphological changes in the sludge fibers. PHAs were also extracted and profiled using FTIR, py-GC/MS, TGA, and DSC.

iv) To pretreat PPMS and enzymatically saccharify PPMS for hydrolyzate production.

- A de-ashing process was conducted to obtain fibers more amenable to enzymatic treatment. Response surface methodology (RSM) was employed to determine the optimal temperature, pH, hydrolysis time, cellulase and β-glucosidase cocktail, and substrate load for the maximum recovery of sugars. HPLC analysis was employed to determine the carbohydrate content of the hydrolyzate, and py-GC/MS was used to elucidate the components of the hydrolyzate.

v) To conduct a cyclic fed-batch fermentation for increased PHA production by *B. thuringiensis* using the hydrolyzate as feedstock.

- A RSM study was conducted to determine the optimum fermentation conditions to produce high cell density biomass of *B. thuringiensis*. Using the glucose-rich hydrolyzate, cyclic-fed batch fermentation strategy was pursued to enhance PHA production by *B. thuringiensis*. After each cyclic event, PHAs were extracted and characterized using FTIR, py-GC/MS, TGA, and DSC analysis.

1.5. The organization of the thesis

This dissertation comprises seven chapters and is based on publications referred to by their titles in the text. Each chapter is self-contained, containing an abstract, an introduction for the study's motivation through literature, materials and methods, results and discussion, and conclusions.

Chapter 1 is an overview that offers background information and the rationale for the study, including the overarching aims and specific objectives of this study.

Chapter 2 consists of a literature review on background information on three topics *viz*., firstly, polyhydroxyalkanoates (PHAs), their synthesis, characterization and application. Secondly, pulp and paper mill sludge (PPMS), its composition, current disposal methods and their associated environmental challenges, and methods to beneficiate PPMS. Thirdly, the merits and drawbacks of four different fermentation strategies are discussed.

Chapter 3 focuses on determining the PHA-producing ability of *Bacillus thuringiensis* using commercially available simple and complex carbohydrates as sole carbon sources using batch fermentation. The work generated here was presented at a local and an international conference.

Chapter 4 explores the capacity of untreated PPMS to serve as the sole feedstock for PHAs using a consolidated bioprocessing fermentation strategy. The work generated here is currently being prepared into a manuscript to be submitted to Bioresource Technology.

Chapter 5 describes a scheme to pretreat and enzymatically saccharify PPMS to obtain a glucose-rich hydrolyzate. This work has been published in a peer-reviewed journal.

Chapter 6 demonstrates the application of the glucose-rich hydrolyzate in cyclic fed-batch fermentation to obtain high cell density biomass and enhanced PHA productivity. This work has been published in a peer-reviewed journal.

Chapter 7 summarises the thesis, the various findings are discussed, conclusions are drawn, and recommendations for future work are made.

1.6. References

Al-Battashi HS, Annamalai N, Sivakumar N, Al-Bahry S, Tripathi BN, Nguyen QD, Gupta VK (2019) Lignocellulosic biomass (LCB): a potential alternative biorefinery feedstock for polyhydroxyalkanoates production. Rev Environ Sci Biotechnol 18:183–205.

Albuquerque PBS, Malafaia CB (2018) Perspectives on the production, structural characteristics and potential applications of bioplastics derived from polyhydroxyalkanoates. Int J Biol Macromol 107:615–625.

Ali M, Sreekrishnan TR (2001) Aquatic toxicity from pulp and paper mill effluents: A review. Adv Environ Res 5:175–196.

Alkasrawi M, Al-Hamamre Z, Al-Shannag M, Abedin M, Singsaas E (2016) Conversion of paper mill residuals to fermentable sugars. BioResources 11:2287–2296.

Annamalai N, Al-Battashi H, Al-Bahry S, Sivakumar N (2017) Biorefinery production of poly-3-hydroxybutyrate using waste office paper hydrolysate as feedstock for microbial fermentation. J Biotechnol 265:25–30.

Banerjee S (2011) Glucose from paper mill sludge. BioResources 6:4739–4746.

Boni MR, D'Aprile L, De Casa G (2004) Environmental quality of primary paper sludge. J Hazard Mater 108:125–128.

Boshoff S, Gottumukkala LD, Rensburg E Van, Görgens J (2016) Paper sludge (PS) to bioethanol: Evaluation of virgin and recycle mill sludge for low enzyme, high-solids fermentation. Bioresour Technol 203:103–111.

Chen B-K, Lo S-H, Shih C-C, Artemov AV (2012) Improvement of thermal properties of biodegradable polymer poly(3-hydroxybutyrate) by modification with acryloyloxyethyl isocyanate. Polym Eng Sci 52:1524–1531.

Davis R, Kataria R, Cerrone F, Woods T, Kenny S, O'Donovan A, Guzik M, Shaikh H, Duane G, Gupta VK, Tuohy MG, Padamatti RB, Casey E, O'Connor KE (2013) Conversion of grass biomass into fermentable sugars and its utilization for medium chain length polyhydroxyalkanoate (mcl-PHA) production by *Pseudomonas* strains. Bioresour Technol 150:202–209.

Department of Environmental Affairs and Tourism (2019) National Environmental Management: Waste Act: Consultation: National Waste Management Strategy. Gov Gaz No. 1561:4–51.

Department of Environmental Affairs and Tourism (2018) South Africa State of Waste Report. A report on the state of the environment. Final draft:1-112.

Department of Environmental Affairs and Tourism (2013) Department of Environmental Affairs National Environmental Management: Waste Act, 2008 (Act No. 59 of 2008). Gov Not No. 36784:3–21.

Department of Environmental Affairs and Tourism (2003) Plastic carrier bags and plastic flat bags regulations. Gov Gaz No. 24839:1–3.

Dikgang J, Leiman A, Visser M (2012) Resources, conservation and recycling analysis of the plastic-bag levy in South Africa. Resour Conserv Recycl 66:59–65.

Du B, Sharma LN, Becker C, Chen S-F, Mowery RA, van Walsum GP, Chambliss CK (2010) Effect of varying feedstock-pretreatment chemistry combinations on the formation and accumulation of potentially inhibitory degradation products in biomass hydrolysates. Biotechnol Bioeng 107:430–440.

European Bioplastics (2019) Bioplastics market data. https://www.european-bioplastics.org/market/. Accessed 7 Jan 2021.

European Bioplastics (2017) Press release- Global market for bioplastics to grow by 20 percent. https://www.european-bioplastics.org/global-market-for-bioplastics-to-grow-by-20-percent/. Accessed 6 Jan 2021.

Gibril ME, Lekha P, Andrew J, Sithole B, Tesfaye T, Ramjugernath D (2018) Beneficiation of pulp and paper mill sludge: Production and characterisation of functionalised crystalline nanocellulose. Clean Technol Environ Policy 20:1835–1845.

Godfrey L, Oelofse S (2017) Historical review of waste management and recycling in South Africa. Resources 6:1–11.

González-García Y, Nungaray J, Córdova J, González-Reynoso O, Koller M, Atlic A, Braunegg G (2008) Biosynthesis and characterization of polyhydroxyalkanoates in the polysaccharide-degrading marine bacterium *Saccharophagus degradans* ATCC 43961. J Ind Microbiol Biotechnol 35:629–633.

Gowda V, Shivakumar S (2014) Agrowaste-based polyhydroxyalkanoate (PHA) production using hydrolytic potential of *Bacillus thuringiensis* IAM 12077. Brazilian Arch Biol Technol 57:55–61.

GreenCape (2020) Waste: Market Intelligence Report 2020:1-43.

Hanekom A (2020) South African initiative to end plastic pollution in the environment. S Afr J Sci 116:5–6.

Institute of Waste Management of Southern Africa (2019) Will we see the death of landfills in South Africa? http://iwmsa.co.za/media-releases. Accessed 28 Jul 2020.

Jiang G, Hill DJ, Kowalczuk M, Johnston B, Adamus G, Irorere V, Radecka I (2016) Carbon sources for polyhydroxyalkanoates and an integrated biorefinery. Int J Mol Sci 17:1–21.

Kang L, Lee YY, Yoon SH, Smith AJ, Krishnagopalan GA (2012) Ethanol production from the mixture of hemicellulose prehydrolysate and paper sludge. BioResources 7:3607–3626.

Kang L, Wang W, Pallapolu VR, Lee YY (2011) Enhanced ethanol production from de-ashed paper sludge by simultaneous saccharification and fermentation and simultaneous saccharification and co-fermentation. BioResources 6:3791–3808.

Kang L, Wang W, Lee YY (2010) Bioconversion of kraft paper mill sludges to ethanol by SSF and SSCF. Appl Biochem Biotechnol 161:53–66.

Klinke HB, Thomsen AB, Ahring BK (2004) Inhibition of ethanol-producing yeast and bacteria by degradation products produced during pre-treatment of biomass. Appl Microbiol Biotechnol 66:10–26.

KPMG Tax alert (2019) Tax on single-use plastics– Is the stick approach going to work this time? https://home.kpmg/us/en/home/insights/2019/07/tnf-south-africa-possible-tax-single-use-plastics.html. Accessed 28 Jul 2020.

Kucera D, Benesova P, Ladicky P, Pekar M, Sedlacek P, Obruca S (2017) Production of polyhydroxyalkanoates using hydrolyzates of spruce sawdust: Comparison of hydrolyzates detoxification by application of overliming, active carbon, and lignite. Bioengineering 4:1–9.

Liu S, Duncan S, Qureshi N, Rich J (2018) Fermentative production of butyric acid from paper mill sludge hydrolysates using *Clostridium tyrobutyricum* NRRL B-67062/RPT 4213. Biocatal Agric Biotechnol 14:48–51.

Makgae M (2011) Key areas in waste management: A South African perspective, integrated waste management. In: Kumar S (ed) Intech. p 472.

Mendes CVT, Rocha JMS, de Menezes FF, Carvalho MGVS (2017) Batch and fed-batch simultaneous saccharification and fermentation of primary sludge from pulp and paper mills. Environ Technol 38:1498–1506.

Min BC, Bhayani BV, Jampana VS, Ramarao BV (2015) Enhancement of the enzymatic hydrolysis of fines from recycled paper mill waste rejects. Bioresour Bioprocess 2:1–10.

Moritz JW, Duff SJB (1996) Simultaneous saccharification and extractive fermentation of cellulosic substrates. Biotechnol Bioeng 49:504–511.

Norris M, Titshall LW (2011) The potential for direct application of papermill sludge to land: A greenhouse study. Int J Environ Res 5:673–680.

Packaging SA (2018) Packaging SA: Extended producer responsibility plan. 1:1–111.

PAMSA (2018) South African Pulp and Paper Industry- Summary of 2018 production, import and export statistics. 9–11.

PAMSA (2019a) South African Paper and Pulp Industry 2019 Statistics Annual Summary. 1–10.

PAMSA (2019b) Paper Recovery and Recycling in South Africa: Facts and Statistics 2019. 1

Peters D (2006) Carbohydrates for fermentation. Biotechnol J 1:806–814.

Plastics SA (2019) Tax on single-use plastics is not the best solution. https://www.plasticsinfo.co.za/2019/07/19/tax-on-single-use-plastics-is-not-the-best-solution/#:~:text=Taxing single-use plastics is,the problem of plastic pollution.&text=The Department of Environmental Affairs,levy between 2003 and 2018. Accessed 29 Jul 2020.

Plastics SA (2020) Who will really benefit from increased levies raised on plastic bags? https://www.plasticsinfo.co.za/2020/03/03/who-will-really-benefit-from-increased-levies-raised-on-plastic-bags/. Accessed 28 Jul 2020.

Ramadas NV, Singh SK, Soccol CR, Pandey A (2009) Polyhydroxybutyrate production using agro-industrial residue as substrate by *Bacillus sphaericus* NCIM 5149. Brazilian Arch Biol Technol 52:17–23.

Rashid MT, Barry D, Goss M (2006) Paper mill biosolids application to agricultural lands: Benefits and environmental concerns with special reference to situation in Canada. Soil Environ 25:85–98.

Republic of South Africa National Treasury (2020) South Africa full budget review 2020. Natl Treas 1–285.

Sarafadeen AO, Okoya A, Enitan AF, Olusegun OA, Oluwasegun A (2014) Biosolids land application: Implications for water resources. Pensee J 76:199–230.

Sawant SS, Tran TK, Salunke BK, Kim BS (2017) Potential of *Saccharophagus degradans* for production of polyhydroxyalkanoates using cellulose. Process Biochem 57:50–56.

Schroeder BG, Zanoni PRS, Magalhães WLE, Hansel FA, Tavares LBB (2015) Evaluation of biotechnological processes to obtain ethanol from recycled paper sludge. J Mater Cycles Waste Manag 19:463–472.

Scott GM, Smith A (1995) Sludge characteristics and disposal alternatives for the pulp and paper industry. In: Proceedings of the 1995 International environmental conference. TAPPI Press, Atlanta, GA, pp 269–279.

Shankar A, D'Souza S, Narvekar M, Rao P, Tembadmani K (2015) Microbial production of polyhydroxyalkanoates (PHA) from novel sources: A Review. Int J Res Biosci 4:16–28.

Simão L, Hotza D, Raupp-Pereira F, Labrincha JA, Montedo ORK (2018) Wastes from pulp and paper mills- A review of generation and recycling alternatives. Cerâmica 64:443–453.

Tan GA, Chen C-L, Ge L, Li L, Wang L, Zhao L, Mo Y, Tan SN, Wang J-Y (2014) Enhanced gas chromatography-mass spectrometry method for bacterial polyhydroxyalkanoates analysis. J Biosci Bioeng 117:379–382.

Tawakkal ISMA, Cran MJ, Miltz J, Bigger SW (2014) A review of poly(lactic acid)-based materials for antimicrobial packaging. J Food Sci 79:1477–1490.

Thakur S, Chaudhary J, Sharma B, Verma A, Tamulevicius S, Thakur VK (2018) Sustainability of bioplastics: Opportunities and challenges. Curr Opin Green Sustain Chem 13:68–75.

Valappil SP, Boccaccini AR, Bucke C, Roy I (2007) Polyhydroxyalkanoates in Gram-positive bacteria: Insights from the genera *Bacillus* and *Streptomyces*. Antonie Van Leeuwenhoek 91:1–17.

Zhang W-H, Wu J, Weng L, Zhang H, Zhang J, Wu A (2020) Understanding the role of cellulose fiber on the dewaterability of simulated pulp and paper mill sludge. Sci Total Environ 702:134376.

Zhu M-J, Zhu Z-S, Li X-H (2011) Bioconversion of paper sludge with low cellulosic content to ethanol by separate hydrolysis and fermentation. African J Biotechnol 10:15072–15083.

CHAPTER TWO

Literature Review

2.1. Polyhydroxyalkanoates

PHAs are a family of naturally-occurring biopolyesters of various hydroxyalkanoates, synthesized by a variety of Gram-positive and Gram-negative bacteria. PHAs accumulate as granules (Fig. 2.1) at levels of 30-80% of the cell and are characteristically lipid in nature, hydrophobic, amorphous and insoluble (Tan et al. 2014). This polymeric material is synthesized

by a wide array of bacteria under imbalanced growth conditions, usually when a carbon source is provided in excess and one essential growth nutrient is subsequently limited. Furthermore, PHAs function as carbon storage and energy reserves both non-sporulating and sporulating bacteria and play a pivotal role in priming microorganisms for stress survival by promoting long-term survival of bacteria under nutrient-scarce or stressed conditions (Sheu et al. 2000; Albuquerque and Malafaia 2018). The number and size of the granules, the monomer composition, macromolecular structure and physico-chemical properties vary, depending on the producer organism. They can be observed intracellularly as light-refracting granules or as electron lucent bodies that, in overproducing mutants, cause a striking alteration of the bacterial shape (Olivera et al. 2009).

Figure 2.1: Micrograph depicting intracellular PHA accumulation (dos Santos et al. 2017).

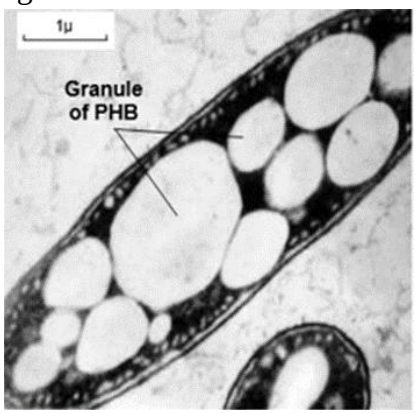

2.1.1. Chemical structure

Biologically produced PHAs are composed only of chirally pure (R)-configuration monomers (Fig. 2.2). This R-backbone makes the chemical synthesis of PHA difficult. The composition of the alkyl side chain (the R group) and the number of methylene units together determine the identity of the monomer (Kansiz et al. 2000). The alkyl side chain can manifest as saturated, aromatic, unsaturated, halogenated, epoxidized or branched monomers. The majority of PHAs are composed of R(-)-3-hydroxyalkanoic acid monomers (Muhammadi et al. 2015). Currently, there are approximately 150 known hydroxyalkanoic acids constituents of PHAs. This number continues to increase with the introduction of new types of PHAs, chemical or physical modification of current PHAs,

or through the creation of genetically modified organisms that synthesize PHAs specialized functional groups (Muhammadi et al. 2015).

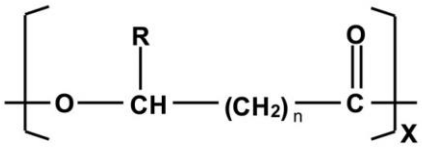

n =1	R =	hydrogen	poly (-3-hydroxypropionate)
		methyl	poly (-3-hydroxybutyrate)
		ethyl	poly (3-horoxyvalerate)
		propyl	poly (-3-hydroxyhexanoate)
		pentyl	poly (-3-hydroxyoctanoate)
		nonyl	poly (-3-hydroxydodecanoate)
n = 2	R =	hydrogen	poly (-4-hydroxybutyrate)
n = 3	R =	hydrogen	poly (-5-hydroxyvalerate)

Figure 2.2: General structure of PHA and examples of R-groups of structural derivatives (Muhammadi et al. 2015).

The molecular weight of the PHA ranges from 2×10^5 to 3×10^6 Da, depending on the number of carbon atoms constituting monomer units, the type of microorganism and the growth conditions. Based on the number of carbon atoms in the monomer units, PHAs can be divided into three groups namely; short chain length (SCL) PHAs consisting of 3–5 carbon atoms, medium chain length (MCL) PHAs, comprising 6–14 carbon atoms, and long chain length PHAs that have >14 carbon atoms. The two most common SCL PHAs are poly-3-hydroxybutyrate (PHB) and 3-hydroxyvalerate (PHV) (Wu et al. 2003).

2.1.2. PHA biosynthesis

Various factors influence PHA production and composition (Saharan et al. 2014). Common precursors to PHA synthesis include simple sugars, such as glucose and fructose and organic acids, such as acetic and propionic acid. The type of carbon substrate dictates the polymeric structure of the PHA (Koller et al. 2010). Enrichment in PHA-accumulating organisms is generally carried out by subjecting cultures to transient conditions of carbon supply. This process involves initial periods of excess followed by a lack of external carbon substrate resulting in microbial populations with an enhanced capacity to store PHA (Koller et al. 2017).

When an external carbon substrate is supplied in excess, the cell's physiological adaptation reaches maximum growth rates. During this period, substrate uptake is mainly driven towards internal polymer storage (up to 80% on a carbon-mole basis). Following substrate depletion, cells reduce their activity and considerably diminish their cellular maintenance processes, rates of enzyme synthesis and RNA transcription. The decrease in activity results in a growth limitation due to unavailability of intracellular compounds required for growth. During this phase, accumulated polymers can suffice as energy and carbon sources for cell growth and maintenance (Albuquerque et al. 2007; Albuquerque et al. 2013). The process of PHA synthesis is illustrated in Figure 2.3. Basically, PHAs are synthesized via the supply of monomer hydroxyacyl-CoA molecules and the polymerization of the monomers is catalyzed by PHA synthases. The reaction route involves conversion of alkanoic acid to PHA via the β-oxidation pathway and polymerization reaction by PHA synthase (Peña et al. 2014).

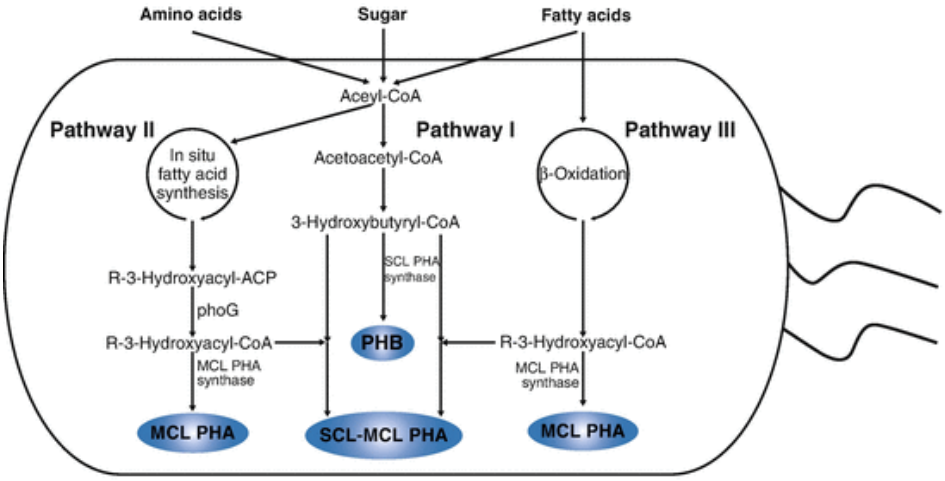

Figure 2.3: Schematic outline of the pathways and mechanisms of bacterial PHA production (Pillai and Kumarapillai 2017).

2.2. PHA Authentication and Characterization

2.2.1. Fourier-transform infrared spectroscopy

Fourier-transform infrared (FTIR) spectroscopy is a rapid and powerful tool for the quantitative analysis of the chemical nature and molecular structure of extracted PHAs. Advantages of using FTIR spectroscopy include; little amount of sample is required, minimal sample manipulation, short analysis time and the process is solvent-free. The absorption spectra represent the chemical composition of a sample with every chemical compound in the sample making its own distinct contribution to the absorbance/transmittance spectrum (Porras et al. 2018). The

intensity of peaks in a spectrum is directly related to the degrees to which each component contributes to the spectrum and the concentrations of the components of the sample. The distinctness of an individual spectrum is determined by the chemical structure of each component (Gumel et al. 2012). Figure 2.4 displays the functional groups representative of PHAs which includes; intense broad absorption band at ~3400 cm^{-1} depicting the presence of OH; prominent peaks and absorption bands around ~2800–2950 cm^{-1} representing asymmetric methyl (CH) stretches of alkanes and alkenes (CH_2-CH_3), respectively; a stretching vibration ~2920 cm^{-1} assigned to asymmetric CH_2; absorption bands at ~2850 are due to symmetrical stretches CH_3; peaks at ~1730 cm^{-1} indicative of the presence of ester carbonyl (C=O) stretching vibration; and a series of absorption bands at ~1370–600 cm^{-1} characteristic of terminal CH_3 group, asymmetric C-O-C, C-O and C-C stretching vibration, respectively (Hong et al. 1999; Gomaa 2014; Akdoğan and Çelik 2018).

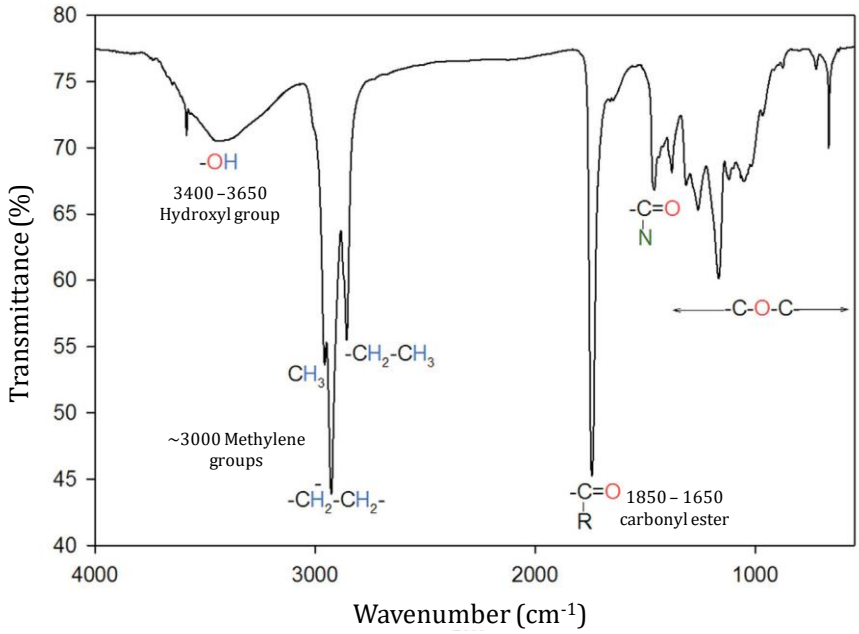

Figure 2.4: Annotated Fourier-transform infrared spectrum displaying the major functional groups present in PHAs (Gumel et al. 2014)

FTIR is a fast way to monitor PHAs in real-time mode however; the main drawback is the little information provided on the monomer composition of PHAs as the spectrum cannot be used to distinguish among hydroxybutyrate and the other hydroxyl acids. In addition, if other biomolecules such as protein or lipids that co-purify with the polymer (Isak et al. 2016), these functional groups will also be present on the spectrum thereby interfering with the detection of PHA functional groups (Torri et al. 2014).

2.2.2. Polymer composition

Gas chromatography/mass spectrometry (GC/MS) is among the most widely used analytical methods for the chemical characterization of PHA structures and to obtain an unambiguous molecular description (Pagliano et al. 2020). Pyrolysis-GC/MS (py-GC/MS) of PHAs has been applied for the analysis and characterization of methanolyzed PHAs and can be used as a direct method to determine the constituent acids present in the PHA (Ojha and Das 2018). Thermally assisted pyrolysis of PHAs (Fig. 2.5) at controlled temperatures (~400°C) in the presence of a strong organic alkali derivatising agent such as tetramethylammonium hydroxide (TMAH) achieves specific monomeric units in a polymer chain that can be identified as characteristic peaks on chromatograms (Torri et al. 2014).

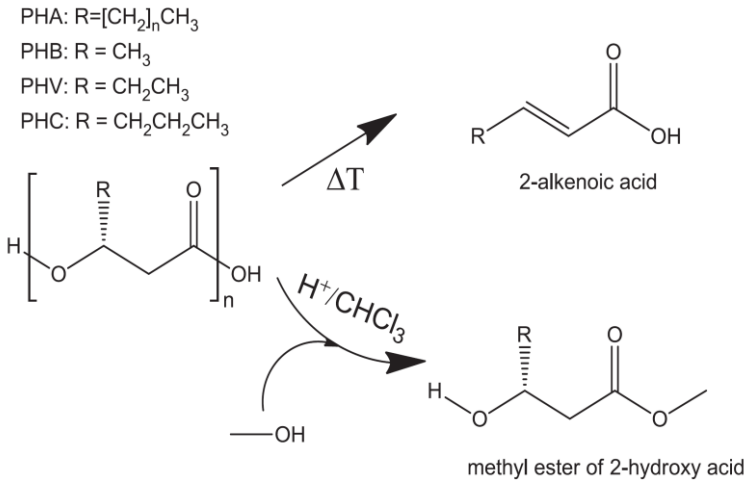

Figure 2.5: Mechanism of action of pyrolysis and methanolysis to obtain suitable monomeric constituents using GC analysis (Torri et al. 2014)

Based on the peak intensity, the main pyrolysis products (methylated alkenoic acids), homopolymer and copolymer composition can be elucidated (Anderson and Dawes 1990; Baidurah et al. 2015). The retention time observed on the mass spectrum of the chromatographic peak is compared with a mass spectral library database to determine the monomer unit corresponding to the main of the polymer. Typical retentions times observed of PHA monomers include;~2.5 min corresponds to methyl ester of 3-hydroxybutyrate; ~3 min represents the presence of HV; ~4 min reveal the presence of HB; ~8 min is ascribed to the methyl ester of HV (Ojha and Das 2018; Pagliano et al. 2020). Zribi-Maaloul et al. (2013) report on the success of employing GC/MS to determine the presence of novel PHA monomers such as; methyl esters of 3-hydroxy-hexanoic acid (HHx), 3-hydroxy-octanoic acid (HO), 3-hydroxy-decanoic acid

(HD), 3-hydroxy 5-dodecenoic acid, 3-hydroxy dodecanoic acid, and 3-hydroxy tetradecanoic acid.

2.2.3. Thermal degradation and thermal stability

The accurate determination of the thermal properties of polymers and particularly of PHAs is of fundamental importance in many processes and engineering projects aiming at the expansion of the uses of these biodegradable materials. Thermogravimetric analysis (TGA) measurements are typically employed to understand the thermal degradation processes of PHAs. The degradation behavior depends extensively on the polymer architecture, molecular weight, crystallinity, orientation, additives, and surface area (Pagliano et al. 2017). The main mechanism of degradation occurs just above melting temperature. The one-step degradation process is dominated by random chain scission reaction known as *cis*-elimination or β-elimination of ester linkages wherein carboxylic acids and ester moieties are detected (Guo et al. 2014). In the case of commercial samples, an additional degradation step is required to degrade organic additives. Here, the chain-scission degradation mechanism transitions the six-membered ring to crotonic acid and and a variety oligomers with a crotonate end group (unsaturated end groups) which can be further deconstructed into propylene, CO_2, acetaldehyde and ketene as the end products (Rivas et al. 2017). TGA analysis has been applied to quantify the degradation rates as well as understand typical processing conditions characteristics such as decomposition temperatures and related thermal stability of a variety of PHAs (Wang et al. 2011; Mendonça et al. 2014; Fadzil et al. 2018).

Differential scanning calorimetry (DSC) system is used to measure multiple transitional phases and kinetics of a sample as a result of changes in temperature and heat flow applied to the sample. The temperature at which a phase transition occurs for a particular material will appear as a peak on the thermograph (Wellen et al. 2013). The first notable observation is the glass-transition temperature (T_g) which indicates a transitional move through an endothermic process taking place. Thereafter, an exothermic process occurs where less heat is required and the sample structurally crystallizes indicating the crystallization temperature (T_c). This phase appears as an upward peak on the thermograph. Finally, an endothermic process occurs where the heat flow raises the sample temperature and the melting point (T_m) of the sample can be determined and is visualized as a downward peak on the thermograph (Salim et al. 2016; Righetti 2017). The temperatures at which these transitions occur depend heavily upon co-

monomer composition and the number of carbons in the side chain of the PHA. The T_g decreases as the length of the side chain increases from 1 to 7 carbons while T_m decreases as the side chain length increases from 4 to 7 carbons. The T_c increases with increasing length of the PHA side-chain (He et al. 2001; Dai et al. 2008). Using these transitions and measuring the area under the peaks, the enthalpies of the different processes can be calculated. Furthermore, the percent crystallinity of the sample can be calculated using information from the heat enthalpy. The percent crystallinity is directly proportional to the melting enthalpy. A reduction in heat enthalpy qualitatively reflects a less crystalline polymer. The degree of crystallinity is one of the most important properties of a polymer sample because it influences all the mechanical properties such as tensile strength, modulus, elongation, and impact strength (Shojaeiarani et al. 2019). Pure PHB is a stiff polymer due to its high crystallinity (up to 80%) and has a low melt viscosity making it applicable in injection molding of material with thin walls (Albuquerque and Malafaia 2018). Its stiffness also makes it a very brittle material that, along with its low nucleation density and formation of spherulites, can cause brittle failure. Polyhydroxybutyrate-co-hydroxyvalerate (PHBV) has a lower crystallinity (30-50%) than PHB and improved mechanical properties, including lower stiffness and brittleness and increased toughness. Therefore, increasing the length of the backbone in the polymer improves the strength and elongation resulting in an extremely elastic material. By, increasing the length of the co-monomer side chains the toughness and elongation properties of the polymer can be improved (Albuquerque and Malafaia 2018).

2.3. Applications of PHAs

The physical, mechanical and thermal characteristics of PHAs are similar to those of petrochemical polyesters, such as polypropylene, polyethylene terephthalate (PET), and polystyrene. The application of a polymer depends on the structure of the PHA polymer or copolymer. PHAs are also fully biodegradable and offer solution to management of waste and in some cases, good substitutes for conventional plastics where mechanical properties are desired (Luengo et al. 2003). The biocompatible natures of PHAs make it suitable for several applications in the biomedical field such as drug-delivery systems (Shrivastav et al. 2013) nerve and tissue repair, stents, antibiotics, tissue engineering and grafts (Ray and Kalia 2017). Commercial interest in both PHB and PHBV provided opportunities for their evaluation as medical biomaterials (Chen and Zhang 2018). Zhao et al. (2003) report on blending PHB with HHx to produce a polyhydroxybutyrate-co-hydroxyhexanoate (PHBHHx) film that displayed

better flexibility and showed improved biocompatibility compared with that of PHB alone. PHA polymers offer properties unavailable in existing synthetic absorbable polymers, such as polyglycolic acid (PGA). Marcano et al. 2017 designed a biodegradable PHA-based 3D scaffold with antibiofilm properties that is applicable for wound dressings. In the medicine sector, derivatives of 3HB such as 3-hydroxybutyrate methyl ester (HBME) have the potential to act as drug against Alzheimer's disease (Ray and Kalia 2017). PHAs are used in the packaging industry where its barrier properties prove to be valuable to preserve the flavor of packed food. Coating of paper with PHA polymers provides a way to increase the hydrophobicity of the paper. Exploration into combining nanotechnology with PHAs is leading to the development of "active packaging" which is a food packaging material with immanent antimicrobial activity that can elongate the shelf-life of food and to avoid food-borne pathogens (Koller 2014). Like oil-derived plastics, PHA-plastics can be molded, made into films, electrospun into monofilaments and blended with heteropolymers or additives to enhance their properties and broaden their range of applications (Akaraonye et al. 2010; Spierling et al. 2018).

2.4. Sustainable PHA Production

Economical limitations and high production costs prohibit the partial and/or complete substitution of petrochemical plastics by PHAs polymers. Therefore, the development of a cost-effective PHA-production scheme is desirable. Two main factors influence the industrial production costs of PHAs. Firstly, PHAs produced by pure microbial culture fermentations (both in wild form and recombinant strains) incur high operating costs. Bioreactor operations used to produce PHA consume an additional 30 to 40% in energy, which contributes to product cost (Albuquerque et al. 2007). PHA-production by pure cultures involves working under sterile conditions and often increases the costs or limits the application for these biopolymers (Bengtsson et al. 2008b). The production costs vary with the microbial species used, carbon source, PHA yield and PHA production capacity. Secondly, the raw and pure substrate materials with high market price account for about 40% of the total production cost and 12 to 33% of the total energy requirements (Chaudhry et al. 2011; Koller et al. 2017). It is possible to reduce PHA costs by sourcing less expensive feedstock, isolating new bacterial strains able to utilize inexpensive carbon sources, using mixed cultures and using cheap substrates such as waste organic carbon (Ben et al. 2011; Albuquerque et al. 2013).

2.5. Pulp and Paper Mill Sludge

2.5.1. Production and composition

Pulp and paper mill sludge (PPMS) is the resultant solid residue recovered from the wastewater stream from the pulp and paper making process and is the largest by-product of the pulp and paper industry (Suriyanarayanan et al. 2010). The physical and chemical properties of PPMS largely depend on the nature of the pulping and papermaking or recycling process, the wastewater treatment process, as well as the material feedstock used at the mill (Suriyanarayanan et al. 2010). Sludge is produced at two steps in the process of treating the effluent. Primary sludge is generated by the production of paper from virgin wood fiber, recycled fibers or deinking sludges. It is recovered at the primary clarification stage which is usually carried out by sedimentation and it is relatively easy to dewater for disposal. It normally consists of mostly fines and inorganic fillers such as calcium carbonate, china clay, and residual chemicals dissolved in the water, whereas the suspended biosolids contain mostly a mixture of cellulose, hemicelluloses and lignin, or other possible residues such as bark and additives used as filler in paper production. This composition is dependent on the recovered paper being processed (Scott and Smith 1995; Boni et al. 2004; Likon and Trebše 2012; Xu and Lancaster 2012; Soucy et al. 2014). Primary sludge can be reincorporated into the process for the board industry, but for higher grade paper products it is not suitable thus disposed of or mixed with secondary sludge (Bajpai 2016). Secondary sludge (also known as biological sludge or activated sludge) is generated when the overflow, or clarified water, is passed onto the secondary treatment plant for bacterial digestion. It consists predominantly of excess biomass produced during the biological process. Secondary sludge volumes are generally lower (~30% of total dry sludge) since most of the heavy, fibrous or inorganic solids are removed in the primary clarifier. Due to secondary sludge containing a high microbial content, the living cells trap large portions of water resulting in the sludge becoming difficult to dry therefore it will “jellify”. Compared with primary sludge, secondary sludge is far more difficult to handle or dewater (Boni et al. 2004; Xu and Lancaster 2012). The sludge can be recycled and used in another process, for example, the board industry (Soucy et al. 2014). The nature of the sludge generated from paper industries largely depends on the raw materials used in different unit processes (Suriyanarayanan et al. 2010).

2.5.2. Traditional disposal methods

2.5.2.1. Landfilling

Prior to landfilling, paper mills often blend both the primary and secondary sludges which is then dewatered to a 25-40% dry solid content (Scott and Smith 1995; Norris and Titshall 2011). Landfilling is the managed disposal of sludge waste on engineered sites after it has undergone little or no pretreatment. Nationwide, there are over 2000 waste handling facilities with only four of the nine provinces in SA having hazardous waste facilities. Currently, there is an undersupply of landfill space with the available space being rapidly depleted (Muzenda 2014). Landfills are quickly reaching their capacity and creating new sites is costly to construct and operate. The escalating costs of transportation of sludge for disposal and tipping fees together with increasingly stringent environmental regulations, diminishing land availability and public opposition has even resulted in several industries resorting to illicitly dumping their waste in order to decrease their cost of sludge disposal (Suriyanarayanan et al. 2010; Norris and Titshall 2011; Abdullah et al. 2015). Landfilled sludge is subjected to both aerobic and anaerobic decay by metabolically-active bacterial and fungal communities. The decay results in the emission of unpleasant odors and the potential production of elements which can be toxic to surrounding fauna and flora (Parrott et al. 2006; Likon and Trebše 2012). From an environmental perspective, two of the major environmental threats associated with landfills include contamination by landfill leachate and the uncontrolled release of biogas. Leachate is a strongly polluted liquid which evolves from moisture contained in the waste at the time of landfilling, rainfall percolating through the landfill, moisture added during co-disposal or moisture being biologically produced (Novella 2014). Groundwater is also at risk of becoming contaminated with leached salts, nitrates and heavy metals from the sludge (Scott and Smith 1995; Ali and Sreekrishnan 2001). Even though secondary sludges may be landfilled, the risk of leaching of soluble nutrients leads to the contamination of ground water (Bajpai 2016). The demand for land and the need to protect the limited groundwater resources in South Africa requires insight into alternative solutions to landfilling (Muzenda, 2014). Discharging organic waste to landfill sites result in the emission of methane which has ~25 times the global warming potential of CO_2. Methane gas can cause explosions or asphyxiation and is often the source of fires at landfill sites (Novella 2014). Pollutant emission from the paper mill sludge drying process found that large amounts of volatile flue gases, including paraffin gases, benzene, fatty acids, ammonia, hydrochloric acid and hydrogen cyanide were emitted during the sludge drying process (Cherian and Siddiqua 2019). Some of the other major problems associated with

landfilling include: wind dispersing debris, rodent; insect and bird infestation (sometimes disease-carrying); pollution of ground and surface water; spontaneous combustion hazards and foul odors (Muzenda 2014).

2.5.2.2. Land-spreading

Land-spreading is defined as the application of dewatered or non-dewatered sludge to agricultural land. It is a favorable technique as it reduces the dependency on landfilling by allowing for the natural reuse and recycling of sludge (Scott and Smith 1995). It is seen as a preferred and cost effective method for using paper mill sludge as it can be directly applied to land as fertilizer (Suriyanarayanan et al. 2010; Abdullah et al. 2015). Paper mill sludge has active organic material that has potential nutrient benefits for crops, therefore, land-spread sludge can improve the physical, chemical and biological properties of the soil. Organic matter from biosolids nourishes, conditions and buffers the soil and also aids in the degradation of pesticides, providing nutrients for plant growth and providing food and energy for beneficial soil microorganisms. Furthermore, it can increase water infiltration, water-holding capacity, soil granulation ability of soil or surface material to retain nutrients whilst reducing soil erosion and soil compaction. High ash sludges obtained from the deinking process can benefit sandy soils as it contains mainly kaolin clay which can aid in water retention in fast-draining soils, thereby increasing water availability for other plants (Fan et al. 2010; Sarafadeen et al. 2014). Norris and Titshall (2011) found that agricultural use of paper mill biosolids as soil organic amendment or soil conditioner was considered a favorable approach for the disposal of paper mill sludge. Furthermore, results from a nine year study by Gagnon and Ziadi (2012) indicated that application of papermill biosolids to agricultural crops had no adverse effect on agricultural soils or the environment. The biosolids increased soil organic matter and all major soil nutrients. Therefore, adding papermill biosolids to agricultural soils is advantageous as it minimizes the practice of landfilling. One of the disadvantages of land-spreading is that large surface areas of land are required onto which the sludge is spread with further difficulties arising if the land needs to be sold or leased. Other limitations for spreading paper mill sludge on agricultural land are the possible impacts on soil fertility and site quality properties. The levels of hazardous chemicals in the sludge need to be routinely checked to appropriately manage organic residues. Their chemical and physical properties need to be thoroughly and accurately characterized and it must be ensured that they are below the standard regulatory levels, otherwise they can pose potentially significant environmental and public health hazards (Suriyanarayanan et al. 2010;

Abdullah et al. 2015). The odor of the land spread sludge (especially close to residential areas) may also be problematic as it said to take about 30 days to stabilize (Scott and Smith 1995). High soluble salt levels, particularly sodium are also problematic; furthermore, there is concern over groundwater contamination and affects caused by potential leaching of nitrates and heavy metals. Land-spreading sludge material must be used very carefully as an unfavorable carbon: nitrogen ratio or high ion exchange capacity can affect the growth of plants, and there is the possibility of chromium toxicity (Vettorazzo et al. 2001; Baggs 2002). Secondary sludges which contain chlorinated organic compounds (or absorbable organo-halogens) may not be used as soil improving organic fertilizers, as most of these are acutely toxic to fauna and flora (Rosazlin et al. 2010).

2.5.2.3. Incineration

Disposal of sludge via incineration not only allows it to be a fuel source for boilers and generators at the mill as it also reduces the volume of sludge matter that needs to be land filled (Gavrilescu et al. 2012). Incineration allows for the controlled combustion of sludge, yielding steam, ash and flue gas as by-products. The recovered heat produces steam which is directed through steam turbines to generate power through an electric generator. Alternatively, steam can be used locally for process steam thereby reducing the mill's dependency on costly fossil fuels for steam production (Gavrilescu 2008). The ash by-product can be land filled or it can be used as the raw materials for light-weight aggregate and constructional brick in the building industry (Xu and Lancaster 2012; Wang et al. 2015). The stringent air pollution controls which necessitate good air quality standards are an obstacle for incineration of paper mill sludge. The major concern with burning nitrate-rich paper mill sludge in industrial boilers is the generation of greenhouse gases such as nitrate oxide and creation of acid rain (Soucy et al. 2014). The flue gas requires treatment by air pollution control before discharge. However, specifically designed fluidized-bed combustors produce fewer pollutants via the flue gas (Gavrilescu et al. 2012).

2.6. Beneficiation of pulp and paper mill sludge and effluents

The increasingly high volume of PPMS is coupled with the capital intensive and environmentally-consequential task of landfilling PPMS. In light of these concerns, attention has been directed towards valorizing PPMS with the functional aim of achieving a "green circular economy". There is a steadily growing interest in increasing the agricultural use of PPMS, processing PPMS for use in other products or the PPMS being recycled and used as a

raw material in other industries e.g., paper and board industries (Ochoa de Alda and Torrea 2006; Ochoa de Alda 2008; Huber 2015), and for energy recovery (Calace et al. 2003). Using PPMS in an applicable manner will reduce the increasing demands on limited natural resources as well as create an alternative to disposing of the sludge. Initiatives have been made to use PPMS in a suitable manner to produce value-added, eco-friendly products with an economical advantage. Some low-profile applications of PPMS are summarized in Table 2.1.

Table 2.1: Summary of the applications of pulp and paper mill sludge

Application of sludge	**Reference**
Filler in the development of medium density fiberboard panels, cement tiles, and gypsum boards	(Pervaiz and Sain 2011)
Conversion into absorbent for oil spill sanitation	(Likon and Trebše 2012)
Components in the industrial production of asphalt, tiles, plaster blends, cement or concrete	(Monosi et al. 2012)
Production of lactic acid, acetone, butanol or bioethanol	(Gurram et al. 2015; Shi et al. 2015; Guan et al. 2016)
Employed as an adsorbent matrix for the retention of cadmium and lead or phenol	(Littrell et al. 2002; Calace et al. 2003; Suryan and Ahluwalia 2012)
Agricultural systems	(Littrell et al. 2002; Suriyanarayanan et al. 2010; Torkashvand et al. 2010; 2017)
Production of wood-plastic composites	(Soucy et al. 2014)

In recent years, research has explored producing PHAs using xylan (Salamanca-Cardona et al. 2016), cellulose (Sawant et al. 2017b), and lignin (Wang et al. 2018), pulp and paper mill wastewater, effluent or low value substrates (Dionisi et al. 2004; Salmaiti et al. 2007; Bengtsson et al. 2008a; Morgan et al. 2010). However, paper mill wastes contain contaminants resulting from the pulp and papermaking processes, therefore, the characteristics of the PHAs could differ (Ben et al. 2011). The accumulation of greenhouse gases, depletion of fossil fuels and other problems related to the growing pollution of the natural environment has increased the interest in using rich sugar treasures such as PPMS as low cost, renewable raw material for PHA production. The characteristics of PPMS vary according to the technology used to pulp the wood and manufacture the paper and the different types of effluent treatment systems employed (Rashid et al. 2006). Typically, PPMS is comprised of complex mixtures of organic matter (cellulose fiber from wood or recycled paper, chemically-modified fibrous recycled paper, wood fiber, lignin, organic binders), inorganic solids (calcium carbonate, kaolinite and talc), impurities such as heavy metals, and chemical additives used in the manufacturing process and these account for the majority of the wastes (Kuokkanen et al. 2008; Norris and Titshall 2011;

Abdullah et al. 2015). The characteristic recalcitrant nature of PPMS coupled with a host of impurities gained during the pulp and paper making process necessitates the action of pretreatments prior to PPMS being employed as a successful feedstock for PHA production.

2.6.1. Pretreatment of PPMS

Excluding the impurities, PPMS is comprised of three main polymers: lignin (15-30%), hemicellulose (20-35%) and cellulose (40-50%), linked by covalent and non-covalent bonds. This organized structure hinders hydrolysis of cellulose and hemicelluloses into fermentable sugars therefore obstructing the valorization of PPMS (Zhang and Zhang 2013). Pretreatment of biomass plays a critical role in conditioning and priming material to increase its enzymatic digestibility. Different pretreatment schemes are applied to enable better hydrolysis of complex carbohydrates resulting in fermentable carbohydrates to serve as substrates for biochemical conversion to PHA (Fig. 2.6) (Baruah et al. 2018). For successful enzymatic hydrolysis, it is necessary to first perform a milling process on almost all solid feedstocks to reduce particle size making it more amenable to enzymolysis (Amin et al. 2017; Amiri and Karimi 2018; Baruah et al. 2018).

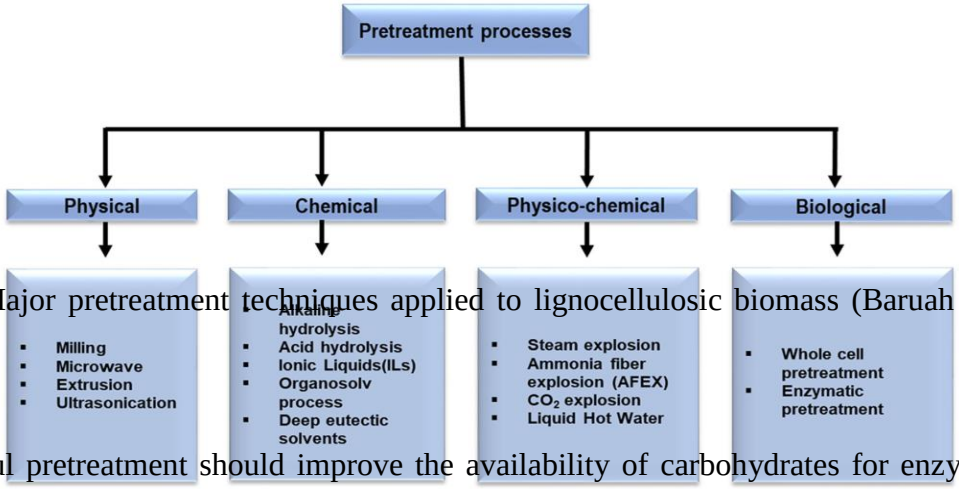

Figure 2.6: Major pretreatment techniques applied to lignocellulosic biomass (Baruah et al. 2018)

The successful pretreatment should improve the availability of carbohydrates for enzymatic saccharification, be effective in the removal of lignin, and produce no, or limited amounts of products that inhibit the action of the hydrolytic enzymes or the growth of fermentative microorganisms (Łukajtis et al. 2018). Using dilute acid in pretreatment aids in removing hemicelluloses and/or lignin, increases the surface area and porosity. This makes the cellulose chains and polysaccharides more susceptible to chemicals and enzymes resulting in improved

yields of sugars (García et al. 2015). A significant $CaCO_3$ content in the PPMS affects the enzymatic hydrolysis efficiency of paper-based solid wastes. This compound limits the solid loading capacity in the bioreactor and increases the pH of sludge suspensions, thus affecting the catalytic activity of cellulases (which have higher enzymatic activity at ~pH 5), ultimately affecting the enzymatic hydrolysis and resultant yield of the end product (Mendes et al. 2016). Ash is another powerful inhibitor and its removal has been proven to be not feasible under many industrial circumstances. This is mainly due to the filler particles binding to the fibers due to the application of different types of flotation agents in the deinking operations thus rendering it difficult to remove using conventional flotation steps (Min et al. 2015). Wang et al. (2010) and Mendes et al. (2014) report the need for a pretreatment by using an acid to remove or neutralize $CaCO_3$ and ash content and alkali treatment to adjust the pH prior to enzymatic hydrolysis.

A pretreatment is crucial prior to enzymatic saccharification of PPMS in order to alter the structure of cellulosic material and make it more amenable to hydrolysis (Kang et al. 2011; Qi et al. 2012; Singh and Bishnoi 2012). After pretreatment, acid hydrolysis and enzymatic hydrolysis are the two common methods employed for lignocellulosic biomass hydrolysis with varying efficiencies depending on treatment conditions, type of biomass, and the properties of the hydrolytic agents (Singh and Bishnoi 2012).

2.6.2. Enzymatic hydrolysis

Cellulose (β-glucan) is a polymer of glucose which can be enzymatically hydrolysed by cellulase, which is an enzyme specifically for cellulose and has the capability to break down cellulose chains. Cellulase is a mixture of endoglucanases, exoglucanases, and β-glucosidase (Fig. 2.7). Its mechanism of action entails endoglucanase exposing reducing and non-reducing ends of the linear polymer and subsequent hydrolysis by exoglucanase to form cellobiose units that are then cleaved by β-glucosidase to liberate glucose units thereby optimizing glucose production (Prasetyo et al. 2010; Leao et al. 2012; Pasma et al. 2013).

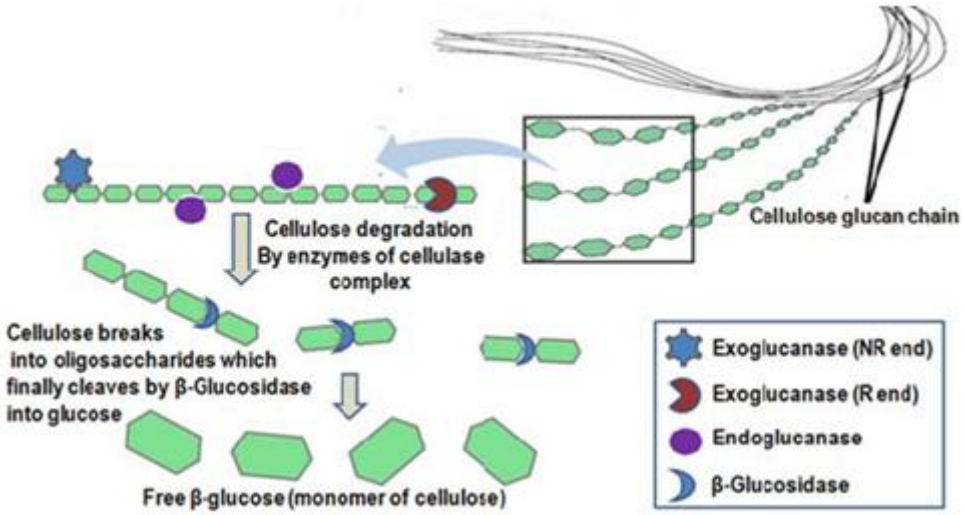

Figure 2.7: Enzymatic degradation of cellulose (Singh et al. 2016)

Cellulases do not generate inhibitors in the end product as in the case of acid hydrolysis and are promising alternatives to the use of acids (Singh and Bishnoi 2012). Optimal balanced combinations of enzymes are also needed to effectively hydrolyze the complex structure of cellulosic materials. In addition to the quality of cellulase, the digestibility of cellulose and hemicellulose is affected by pH, temperature, process time and cellulose content (Singh and Bishnoi 2012). The outcome of pretreatment and enzymatic saccharification is a glucose-rich hydrolyzate with fermentable carbohydrates to serve substrates for biochemical conversion to PHA. Hydrolyzates from lignocellulosic biomass such as: spruce sawdust (Kucera et al. 2017), wheat straw (Gasser et al. 2014), pineapples (Sukruansuwan and Napathorn 2018), oil palm fiber (Maraveas 2020), amongst others, have been successfully been applied for PHA production. Hydrolyzates from PPMS has been investigated for bioconversion to commodity products such as enzyme (Cavka et al. 2013), bioethanol (Nanda et al. 2013; Gurram et al. 2015), lactic acid (Černec et al. 2007; Shi et al. 2015), xylitol (Chen et al. 2018), and acetone (Guan et al. 2018).

2.7. Fermentation Strategies

2.7.1. Batch fermentation

Batch cultivations is still a norm for PHA production due to their simple operation, but notoriously results in intrinsically low PHA productivity (Borah et al. 2002). The system involves supplying the nitrogen and carbon source at the beginning of the fermentation and the fermentation proceeds for a pre-determined time typically, 48-72 h for PHA production. The amount of nutrients added to the fermentation medium are at a precisely calculated

concentration that considers; the physiological preconditions of the PHA-producing strain, concentrations that could be inhibitory to the strain, and concentrations that will suffice as both an imbalance to boost PHA-production yet sufficient to promote cell growth (Lai et al. 2013; Blunt et al. 2018; Koller 2018).

2.7.2. Cyclic fed-batch fermentation

Cyclic fed-batch fermentation (CFBF) was first developed by Pirt (1974) for penicillin production and since then the concept has been adapted for human serum production (Bushell et al. 2003), erythromycin production (Lynch and Bushell 1995), and metabolic acid productivity (Liu et al. 2020). CFBF is a simple "drain-and-fill" strategy used to enhance the volumetric productivity of PHA biosynthesis (Fig. 2.8). Batching of the culture occurs when two thirds of the carbon source and all of the nitrogen sources are depleted i.e., when cells are in a stationary growth phase. During batching 20% of the fermentation broth is removed (drain) and replenished with the same volume of fresh cultivation medium (fill). The medium used in the initial fermentation and during batching must be of the same composition to avoid interfering with the growth-associated PHA production (Koller 2018). Moreover, CFBF is advantageous as it avoids the down-time required to clean and sterilize bioreactors after traditional batch fermentations. To date, there are only three published reports on employing CFBF for enhanced PHA productivity by *Cupriavidus necator* (Haas et al. 2017), *Azohydromonas australica* (Gahlawat and Srivastava 2018) and *Chelatococcus* sp. strain MW10 (Ibrahim and Steinbüchel 2010), making it enticing to explore for future research.

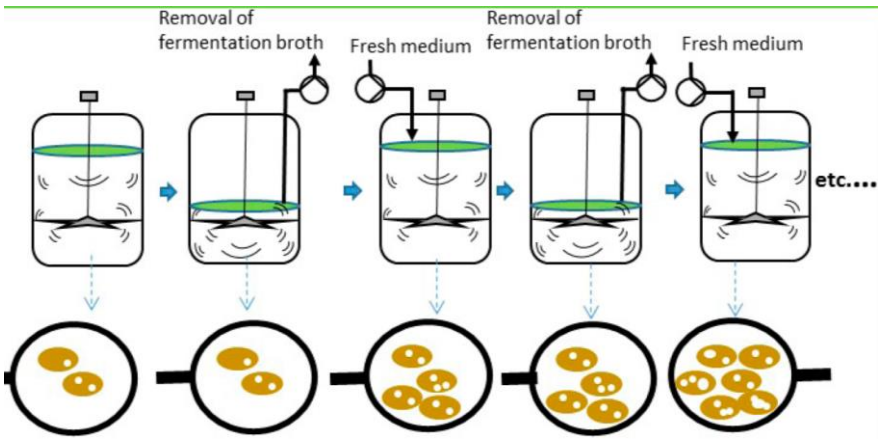

Figure 2.8: Schematic diagram of cyclic fed-batch fermentation for PHA production (Koller 2018)

2.7.3. Separate hydrolysis and fermentation

Separate hydrolysis and fermentation (SHF) is a two-step process that entails performing the enzymatic hydrolysis and subsequent fermentation of the hydrolyzate in separate bioreactors (Fig. 2.9) (Duff et al. 1994). The major advantage of performing the hydrolysis reaction separately, lies in the ability to use higher temperatures (pH 5; ~50°C for cellulase) which promotes enzyme function and stability, resulting in increased productivity of the enzyme. Thereafter, the fermentation step can be conducted using the optimal conditions for the microorganism (pH 7; ~35-40°C for bacteria) resulting in higher biomass yields (Zhu et al. 2011). Furthermore, the cell-free hydrolyzate obtained from hydrolysis can be applied to any microbial culture for fermentation processes. The unfortunate disadvantage of this system is that the accumulation of glucose during the hydrolysis step has a tendency to cause feedback inhibition of endoglucanases, exoglucanases and β-glucosidase thus affecting the yield of glucose in the hydrolyzate (Nanda et al. 2013). Nevertheless, SHF has been successfully applied for conversion of paper sludge into ethanol (Madrid and Díaz 2011; Shen and Agblevor 2011; Schroeder et al. 2015), and PHB production (García-torreiro et al. 2016).

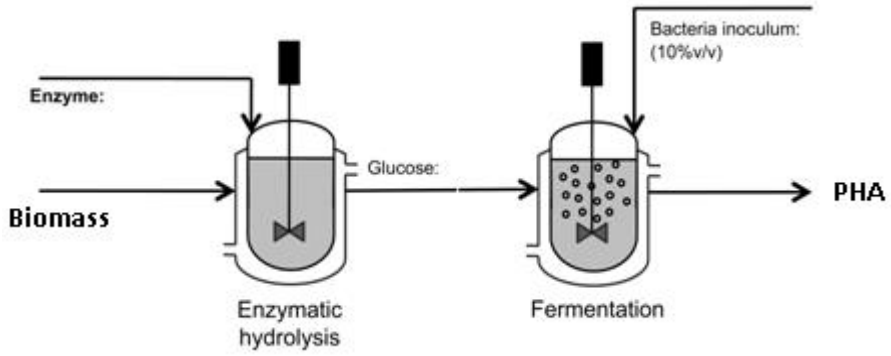

Figure 2.9: Process of separate hydrolysis and fermentation (adapted from García-Torreiro et al. 2016)

2.7.4. Consolidated bioprocessing

Consolidated bioprocessing, or CBP, is a biologically mediated process that features cellulase production, cellulose hydrolysis and fermentation in a single-unit operation (Fig. 2.10). The conversion and simultaneous fermentation of recalcitrant cellulosic biomass into desired products occurs in a one step reaction without the addition of exogenous enzymes (Olson et al. 2012). CBP might soon be the ultimate configuration as it is one process that has recognized the need for low cost hydrolysis and fermentation of cellulosic biomass (Mbaneme-Smith and Chinn 2015). In addition, CBP eliminates the need for incorporating externally synthesized

cellulase consequently lowering the operating and capital costs associated with purchasing or producing enzymes required for biomass solubilization (Lynd et al. 2016). A fully efficient CBP system must employ a CBP-enabled microbe that has inherent dual function of solubilizing a lignocellulosic biomass substrate and producing desired products at high yield and bears the potential to be employed in industrial conditions (Lynd et al. 2016). This is the main impediment of the CBP process as to date; there are no reports on a naturally occurring microbe that natively exhibit complete cellulosic substrate-utilization. Therefore, using recombinant strategy, investigation into genetically engineering a microbe or a consortium that normally exhibits partial saccharolytic enzyme is currently being pursued. The operative goal is to engineer a microbe that can rapidly grow on lignocelluloses whilst heterologously expressing sufficient quantities of several types of cellulase and/or hemicellulase enzymes that permit the conversion of pretreated lignocelluloses (Salamanca-Cardona et al. 2014; Jouzani and Taherzadeh 2015; Yan and Fong 2017; Jiang et al. 2018; Cunha et al. 2020; Wen et al. 2020). The CBP strategy is in principle applicable to production of a broad range of products derived from lignocellulosic biomass. In recent years, CBP has displayed outstanding potential for the biosynthesis of; butyric acid from rice straw (Ai et al. 2016), metabolic products from yeast (Tabañag et al. 2018), butanol (Jiang et al. 2018), hydrogen (Morales-Martínez et al. 2020), biofuel (Olguin-Maciel et al. 2020), blended copolymers (Salamanca-Cardona et al. 2016), PHAs (Salamanca-Cardona et al. 2014; Sawant et al. 2017a; Sawant et al. 2018; Wang et al. 2018; Zhou et al. 2020). But, CBP has gained the most attention for ethanol production (van Zyl et al. 2007; Anasontzis and Christakopoulos 2014; Brethauer and Studer 2014; Ali et al. 2016; Cripwell et al. 2020) systems and is being implemented for commercial production.

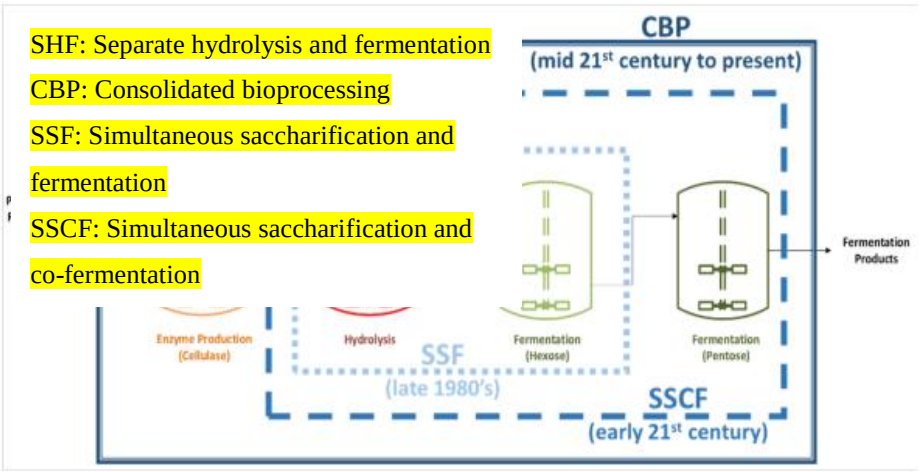

Figure 2.10: Schematic representation of consolidated bioprocessing (Tabañag et al. 2018)

2.8. References

Abdullah R, Ishak CF, Kadir WR, Bakar RA (2015) Characterization and feasibility assessment of recycled paper mill sludges for land application in relation to the environment. Int J Res Public Heal 12:9314–9329.

Ai B, Chi X, Meng J, Sheng Z, Zheng L, Zheng X, Li J (2016) Consolidated bioprocessing for butyric acid production from rice straw with undefined mixed culture. Front Microbiol 7:1–10.

Akaraonye E, Keshavarz T, Roy I (2010) Production of polyhydroxyalkanoates: The future green materials of choice. J Chem Technol Biotechnol 85:732–743.

Akdoğan M, Çelik E (2018) Purification and characterization of polyhydroxyalkanoate (PHA) from a *Bacillus megaterium* strain using various dehydration techniques. J Chem Technol Biotechnol 93:2292–2298.

Albuquerque MGE, Carvalho G, Kragelund C, Silva AF, Crespo MTB, Reis MAM, Nielsen PH (2013) Link between microbial composition and carbon substrate-uptake preferences in a PHA-storing community. Int Soc Microb Ecol J 7:1–12.

Albuquerque MGE, Eiroa M, Torres C, Nunes BR, Reis MAM (2007) Strategies for the development of a side stream process for polyhydroxyalkanoate (PHA) production from sugar cane molasses. J Biotechnol 130:411–421.

Albuquerque PBS, Malafaia CB (2018) Perspectives on the production, structural characteristics and potential applications of bioplastics derived from polyhydroxyalkanoates. Int J Biol Macromol 107:615–625.

Ali M, Sreekrishnan TR (2001) Aquatic toxicity from pulp and paper mill effluents: A review. Adv Environ Res 5:175–196.

Ali SS, Nugent B, Mullins E, Doohan FM (2016) Fungal-mediated consolidated bioprocessing: the potential of *Fusarium oxysporum* for the lignocellulosic ethanol industry. AMB Express 6:1–13.

Amin FR, Khalid H, Zhang H, Rahman S, Zhang R, Liu G, Chen C (2017) Pretreatment methods of lignocellulosic biomass for anaerobic digestion. AMB Express 7:1-12.

Amiri H, Karimi K (2018) Pretreatment and hydrolysis of lignocellulosic wastes for butanol production: Challenges and perspectives. Bioresour Technol 270:702–721.

Anasontzis GE, Christakopoulos P (2014) Challenges in ethanol production with *Fusarium oxysporum* through consolidated bioprocessing. Bioeng Bugs 5:393–395.

Anderson AJ, Dawes EA (1990) Occurrence, metabolism, metabolic role, and industrial uses of bacterial polyhydroxyalkanoates. Microbiol Rev 54:450–472.

Baggs L (2002) Nitrous oxide release from soils receiving N-rich crop residues and paper mill sludge in eastern Scotland Nitrous oxide release from soils receiving N-rich crop residues and paper mill sludge in eastern Scotland. Agric Ecosyst Environ 90:109-123.

Baidurah S, Kubo Y, Kuno M, Kodera K, Ishida Y, Yamane T, Ohtani H (2015) Rapid and direct compositional analysis of poly(3-hydroxybutyrate-co-3-hydroxyvalerate) in whole bacterial cells by thermally assisted hydrolysis and methylation-gas chromatography. Anal Sci 31:79–83.

Bajpai P (2016) Pretreatment of lignocellulosic biomass for biofuel production. In: Bajpai P (ed) Green chemistry for sustainability, 1st edn. Springer, Singapore, p 86.

Baruah J, Nath BK, Sharma R, Kumar S, Deka RC, Baruah DC, Kalita E (2018) Recent trends in the pretreatment of lignocellulosic biomass for value-added products. Front Energy Res 6:1–19.

Ben M, Mato T, Lopez A, Vila M, Kennes C, Veiga MC (2011) Bioplastic production using wood mill effluents as feedstock. 63:1196–1202.

Bengtsson S, Werker A, Christensson M, Welander T (2008a) Production of polyhydroxyalkanoates by activated sludge treating a paper mill wastewater. Bioresour Technol 99:509–516.

Bengtsson S, Werker A, Welander T (2008b) Production of polyhydroxyalkanoates by glycogen accumulating organisms treating a paper mill wastewater. Bioresour Technol 99:323–330.

Blunt W, Levin DB, Cicek N (2018) Bioreactor operating strategies for improved polyhydroxyalkanoate (PHA) productivity. Polymers (Basel) 10:1–29.

Boni MR, D'Aprile L, De Casa G (2004) Environmental quality of primary paper sludge. J Hazard Mater 108:125–128.

Borah B, Thakur PS, Nigam JN (2002) The influence of nutritional and environmental conditions on the accumulation of poly-β-hydroxybutyrate in *Bacillus mycoides* RLJ B-017. J Appl Microbiol 92:776–783.

Brethauer S, Studer MH (2014) Consolidated bioprocessing of lignocellulose by a microbial consortium. Energy Environ Sci 7:1446–1453.

Bushell ME, Rowe M, Avignone-Rossa CA, Wardell JN (2003) Cyclic fed-batch culture for production of human serum albumin in *Pichia pastoris*. Biotechnol Bioeng 82:678–683.

Calace N, Nardi E, Petronio BM, Pietroletti M, Tosti G (2003) Metal ion removal from water by sorption on paper mill sludge. Chemosphere 51:797-803.

Cavka A, Guo X, Tang SJ, Winestrand S, Jönsson LJ, Hong F (2013) Production of bacterial cellulose and enzyme from waste fiber sludge. Biotechnol Biofuels 6:1–10.

Černec F, Zule J, Likon M (2007) Chemical properties and biodegradability of waste paper mill sludges to be used for landfill covering. Waste Manag Res 25:538–546.

Chaudhry WN, Jamil N, Ali I, Ayaz MH, Hasnain S (2011) Screening for polyhydroxyalkanoate (PHA)-producing bacterial strains and comparison of PHA production from various inexpensive carbon sources. Ann Microbiol 61:623–629.

Chen G-Q, Zhang J (2018) Microbial polyhydroxyalkanoates as medical implant biomaterials. Artif Cells, Nanomedicine, Biotechnol 46:1–18.

Chen J, Dong J, Yang G, He M, Xu F, Fatehi P (2018) A process for purifying xylosugars of pre-hydrolysis liquor from kraft-based dissolving pulp production process. Biotechnol Biofuels 11:1–12.

Cherian C, Siddiqua S (2019) Pulp and paper mill fly ash: A review. Sustainability 11:1–16.

Cripwell RA, Favaro L, Viljoen-Bloom M, van Zyl WH (2020) Consolidated bioprocessing of raw starch to ethanol by *Saccharomyces cerevisiae*: Achievements and challenges. Biotechnol Adv 42:107579.

Cunha JT, Romaní A, Inokuma K, Johansson B, Hasunuma T, Kondo A, Domingues L (2020) Consolidated bioprocessing of corn cob-derived hemicellulose: Engineered industrial *Saccharomyces cerevisiae* as efficient whole cell biocatalysts. Biotechnol Biofuels 13:1–

15.
Dai Y, Lambert L, Yuan Z, Keller J (2008) Characterisation of polyhydroxyalkanoate copolymers with controllable four-monomer composition. J Biotechnol 134:137–145.
Dionisi D, Majone M, Papa V, Beccari M (2004) Biodegradable polymers from organic acids by using activated sludge enriched by aerobic periodic feeding. Biotechnol Bioeng 85:569–579.
dos Santos AJ, Valentina LVOD, Schulz AAH, Duarte MAT (2017) From obtaining to degradation of PHB: Material properties. Part I. Ing y Cienc 13:269–298.
Duff SJB, Moritz JW, Andersen KL (1994) Simultaneous hydrolysis and fermentation of pulp mill primary clarifier sludge. Can J Chem Eng 72:1013–1020.
Fadzil FIM, Mizuno S, Hiroe A, Nomura CT, Tsuge T (2018) Low carbon concentration feeding improves medium-chain-length polyhydroxyalkanoate production in *Escherichia coli* strains with defective β-oxidation. Front Bioeng Biotechnol 6:1–8.
Fan J, Ziadi N, Gagnon B, Hu Z (2010) Soil phosphorus fractions following annual paper mill biosolids and liming materials application Can J Soil Sci 90:467-479.
Gagnon B, Ziadi N (2012) Papermill biosolids and alkaline residuals affect crop yield and soil properties over nine years of continuous application. Can J Soil Sci 92:917-930.
Gahlawat G, Srivastava AK (2018) Enhancing the production of polyhydroxyalkanoate biopolymer by *Azohydromonas australica* using a simple empty and fill bioreactor cultivation strategy. Chem Biochem Eng Q 31:479–485.
García YG, Carlos, Contreras JCM, Hernández JA, Dueñas RS (2015) Procurement of fermentable sugars from cardboard waste for the cultivation of yeasts for biotechnological use. Rev Mex Ciencias For 6:88–105.
García-Torreiro M, López-Abelairas M, Lu-Chau TA, Lema JM (2016) Production of poly (3-hydroxybutyrate) by simultaneous saccharification and fermentation of cereal mash using *Halomonas boliviensis*. Biochem Eng J 114:140–146.
Gasser E, Ballmann P, Dröge S, Bohn J, König H (2014) Microbial production of biopolymers from the renewable resource wheat straw. J Appl Microbiol 117:1035–1044.
Gavrilescu D (2008) Energy from biomass in pulp and paper mills. Environ End Manag J 7:537–546
Gavrilescu D, Puitel AC, Dutuc G, Craciun G (2012) Environmental impact of pulp and paper mills. Environ Eng Manag J 11:81–86.
Gomaa EZ (2014) Production of polyhydroxyalkanoates (PHAs) by *Bacillus subtilis* and *Escherichia coli* grown on cane molasses fortified with ethanol. Brazilian Arch Biol Technol 57:145–154.
Guan W, Xu G, Duan J, Shi S (2018) Acetone-butanol-ethanol production from fermentation of hot-water-extracted hemicellulose hydrolysate of pulping woods. Ind Eng Chem Res 57:775–783.
Guan W, Shi S, Tu M, LeeYY (2016) Acetone-butanol-ethanol production from Kraft paper mill sludge by simultaneous saccharification and fermentation. Bioresour Technol 200:713-721.
Gumel AM, Annuar MSM, Heidelberg T (2014) Growth kinetics, effect of carbon substrate in

biosynthesis of mcl-PHA by *Pseudomonas putida* Bet001. Brazilian J Microbiol 45:427–438.

Gumel AM, Suffian M, Annuar M, Heidelberg T (2012) Biosynthesis and characterization of polyhydroxyalkanoates copolymers produced by *Pseudomonas putida* Bet001 isolated from palm oil mill effluent. PLoS ONE 7:1-8.

Guo J, Liu M, Liu Y, Hu C, Xia Y, Zhang H, Gong Y (2014) Rheological, thermal, and mechanical properties of P(3HB- co-4HB) and P(3HB-co-4HB)/ EVA blends. J Appl Polym Sci 41206:1–7.

Gurram RN, Al-Shannag M, Lecher NJ, Duncan SM, Singsaas EL, Alkasrawi M (2015) Bioconversion of paper mill sludge to bioethanol in the presence of accelerants or hydrogen peroxide pretreatment. Bioresour Technol 192:529–539.

Haas C, El-Najjar T, Virgolini N, Smerilli M, Neureiter M (2017) High cell-density production of poly(3-hydroxybutyrate) in a membrane bioreactor. N Biotechnol 37:117–122.

He JD, Cheung MK, Yu PH, Chen GQ (2001) Thermal analyses of poly(3-hydroxybutyrate), poly(3-hydroxybutyrate-co-3-hydroxyvalerate), and poly(3-hydroxybutyrate-co-3-hydroxyhexanoate). J Appl Polym Sci 82:90–98.

Hong K, Sun S, Tian W, Chen GQ, Huang W (1999) A rapid method for detecting bacterial polyhydroxyalkanoates in intact cells by Fourier transform infrared spectroscopy. Appl Microbiol Biotechnol 51:523–526.

Huber P (2015) Conditions for cost-efficient reuse of biological sludge for paper board manufacturing. J Clean Prod 66:65-74.

Ibrahim MHA, Steinbüchel A (2010) High-cell-density cyclic fed-batch fermentation of a poly(3-hydroxybutyrate)-accumulating thermophile, *Chelatococcus* sp. strain MW10. Appl Environ Microbiol 76:7890–7895.

Isak I, Patel M, Riddell M, West M, Bowers T, Wijeyekoon S, Lloyd J (2016) Quantification of polyhydroxyalkanoates in mixed and pure cultures biomass by Fourier transform infrared spectroscopy: Comparison of different approaches. Lett Appl Microbiol 63:139–146.

Jiang Y, Guo D, Lu J, Dürre P, Dong W, Yan W, Zhang W, Ma J, Jiang M, Xin F (2018) Consolidated bioprocessing of butanol production from xylan by a thermophilic and butanologenic *Thermoanaerobacterium* sp. M5. Biotechnol Biofuels 11:1–14.

Jouzani GS, Taherzadeh MJ (2015) Advances in consolidated bioprocessing systems for bioethanol and butanol production from biomass: A comprehensive review. Biofuel Res J 2:152–195.

Kang L, Wang W, Pallapolu VR, Lee YY (2011) Enhanced ethanol production from de-ashed paper sludge by simultaneous saccharification and fermentation and simultaneous saccharification and co-fermentation. BioResources 6:3791–3808.

Kansiz K, Billman-Jacobe H, McNaughton D (2000) Quantitative determination of the biodegradable polymer poly(β-hydroxybutyrate) in a recombinant *Escherichia coli* strain by use of mid-infrared spectroscopy and multivariative statistics. Appl Environ Microbiol 66:3415–3420.

Koller M (2018) A review on established and emerging fermentation schemes for microbial production of polyhydroxyalkanoate (PHA) biopolyesters. Fermentation 4:1-30.

Koller M, Maršálek L, de Sousa Dias MM, Braunegg G (2017) Producing microbial polyhydroxyalkanoate (PHA) biopolyesters in a sustainable manner. N Biotechnol 37:24–38.

Koller M (2014) Poly(hydroxyalkanoates) for food packaging: Application and attempts towards implementation. Appl Food Biotechnol 1:3–15.

Koller M, Salerno A, Dias M, Reiterer A, Braunegg G (2010) Modern biotechnological polymer synthesis: A review. Food Technol Biotechnol 48:255–269.

Kucera D, Benesova P, Ladicky P, Pekar M, Sedlacek P, Obruca S (2017) Production of polyhydroxyalkanoates using hydrolyzates of spruce sawdust: Comparison of hydrolyzates detoxification by application of overliming, active carbon, and lignite. Bioengineering 4:1–9.

Kuokkanen T, Nurmesniemi H, Pöykiö R, Kujala K, Kaakinen J, Kuokkanen M (2008) Chemical and leaching properties of paper mill sludge. Chem Speciat Bioavailab 20:111–122.

Lai S, Kuo P, Wu W, Jang M, Chou Y (2013) Biopolymer production in a fed-batch reactor using optimal feeding strategies. J Chem Technol Biotechnol 88: 2054–2061.

Leão A, Cherian BM, de Souza SF, Sain M, Narine S, Caldeira MS, Toldeo MAS (2012) Use of primary sludge from pulp and paper mills for nanocomposites. Mol Cryst Liq Cryst 556:254–263.

Likon M, Trebše P (2012) Recent advances in paper mill sludge management. In: Show K-Y (ed) Industrial Waste. InTech, Croatia, pp 73–90.

Littrell K, Littrell KC, Khalili NR, Campbell M, Sand G (2002) Structural characterization of activated carbon adsorbents prepared from paper mill sludge. Appl Phys 74:8–11.

Liu L, Wang F, Pei G, Cui J, Diao J, Lv M, Chen L, Zhang W (2020) Repeated fed-batch strategy and metabolomic analysis to achieve high docosahexaenoic acid productivity in *Crypthecodinium cohnii*. Microb Cell Fact 19:1–14.

Luengo JM, García B, Sandoval A, Naharroy G, Olivera ER (2003) Bioplastics from microorganims. Curr Opin Microbiol 6:251–260.

Łukajtis R, Kucharska K, Hołowacz I, Rybarczyk P, Wychodnik K, Słupek E, Nowak P, Kamínski M (2018) Comparison and optimization of saccharification conditions of alkaline pre-treated triticale straw for acid and enzymatic hydrolysis followed by ethanol fermentation. Energies 11:1–24.

Lynch HC, Bushell ME (1995) The physiology of erythromycin biosynthesis in cyclic fed batch culture. Microbiology 141:3105–3111.

Lynd LR, Guss AM, Himmel ME, Beri D, Herring C, Holwerda EK, Murphy SJ, Olson DG, Paye J, Rydzak T, Shao X, Tian L, Worthen R (2016) Advances in consolidated bioprocessing using *Clostridium thermocellum* and *Thermoanaerobacter saccharolyticum*. Ind Biotechnol 365–394.

Madrid LM, Díaz JCQ (2011) Ethanol production from paper sludge using *Kluyveromyces marxianus*. Dyna 78:185–191.

Maraveas C (2020) Production of sustainable and biodegradable polymers from agricultural waste. Polymers (Basel) 12:1–22.

Marcano A, Haidar NB, Marais S, Valleton J-M, Duncan AC (2017) Designing biodegradable

PHA-based 3D scaffolds with antibiofilm properties for wound dressings: Optimization of the microstructure/nanostructure 3:3654–3661.

Mbaneme-Smith V, Chinn MS (2015) Consolidated bioprocessing for biofuel production: Recent advances. Ind Bioprocess 3:23–44.

Mendes CVT, Cruz CHG, Reis DFN, Carvalho MGVS, Rocha JMS (2016) Integrated bioconversion of pulp and paper primary sludge to second generation bioethanol using *Saccharomyces cerevisiae* ATCC 26602. Bioresour Technol 220:161–167.

Mendes VT, Rocha JMS, Grac M (2014) Valorization of residual streams from pulp and paper mills: Pretreatment and bioconversion of primary sludge to bioethanol. Ind Eng Chem Res 53:19398-19404.

Mendonça TT, Gomez JGC, Buffoni E, Sánchez Rodriguez RJ, Schripsema J, Lopes MSG, Silva LF (2014) Exploring the potential of *Burkholderia sacchari* to produce polyhydroxyalkanoates. J Appl Microbiol 116:815–829.

Min BC, Bhayani B V, Jampana VS, Ramarao B V (2015) Enhancement of the enzymatic hydrolysis of fines from recycled paper mill waste rejects. Bioresour Bioprocess 2:1–10.

Monosi S, Sani D, Ruello ML (2012) Reuse of paper mill ash in plaster blends 1:5–10.

Morales-Martínez TK, Medina-Morales MA, Ortíz-Cruz AL, Rodríguez-De la Garza JA, Moreno-Dávila M, López-Badillo CM, Ríos-González L (2020) Consolidated bioprocessing of hydrogen production from agave biomass by *Clostridium acetobutylicum* and bovine ruminal fluid. Int J Hydrogen Energy 45:13707–13716.

Morgan F, Karlsson A, Bengtsson S, Werker A, Pratt S, Lant P, Magnusson P, Johansson P (2010) Production of bioplastics as by-products of waste treatment 1:1–9.

Muhammadi S, Afzal M, Hameed S (2015) Bacterial polyhydroxyalkanoates-eco-friendly next generation plastic: Production, biocompatibility, biodegradation, physical properties and applications. Green Chem Lett Rev 8:56–77.

Muzenda E (2014) A discussion on waste generation and management trends in South Africa. Int J Chem Environ Biol Sci 2:105–112.

Nanda S, Mohammad J, Reddy SN (2013) Pathways of lignocellulosic biomass conversion to renewable fuels 4:157-191.

Norris M, Titshall LW (2011) The potential for direct application of papermill sludge to land: A greenhouse study. Int J Environ Res 5:673–680.

Novella P (2014) Sustainable landfills– Can these be achieved? Conference 6-10 October 2014. Somerset West, Cape Town. In: Proceedings of the 20th WasteCon. pp 367–375.

Ochoa De Alda JAG (2008) Feasibility of recycling pulp and paper mill sludge in the paper and board industries. Resour Conserv Recycl 52:965–972.

Ochoa De Alda JAG, Torrea JA (2006) Applications of recycled paper mills effluents to wood substitutive products (Respro): Executive summary. Univ SEK Segovia 2:381–398.

Ojha N, Das N (2018) A statistical approach to optimize the production of polyhydroxyalkanoates from *Wickerhamomyces anomalus* VIT-NN01 using response surface methodology. Int J Biol Macromol 107:2157–2170.

Qi B, Luo J, Chen G, Chen X, Wan Y (2012) Application of ultrafiltration and nanofiltration for recycling cellulase and concentrating glucose from enzymatic hydrolyzate of steam exploded wheat straw. Bioresour Technol 104:466–472.

Olguin-Maciel E, Singh A, Chable-Villacis R, Tapia-Tussell R, Ruiz HA (2020) Consolidated bioprocessing, an innovative strategy towards sustainability for biofuels production from crop residues: An overview. Agronomy 10:1–20.

Olivera ER, Arcos M, Naharro G, Luengo JM (2009) Unusual PHA biosynthesis. In: Chen G-Q (ed) Plastics from bacteria: Natural functions and applications, 2010th edn. Springer-Verlag, Berlin Heidelberg, pp 133–168.

Olson DG, McBride JE, Joe Shaw A, Lynd LR (2012) Recent progress in consolidated bioprocessing. Curr Opin Biotechnol 23:396–405.

Pagliano G, Gugliucci W, Torrieri E, Piccolo A, Cangemi S, Di Giuseppe FA, Robertiello A, Faraco V, Pepe O, Ventorino V (2020) Polyhydroxyalkanoates (PHAs) from dairy wastewater effluent: Bacterial accumulation, structural characterization and physical properties. Chem Biol Technol Agric 7:1–14.

Pagliano G, Ventorino V, Panico A, Pepe O (2017) Integrated systems for biopolymers and bioenergy production from organic waste and by‐products: a review of microbial processes. Biotechnol Biofuels 10:1–24.

Parrott JL, Mcmaster ME, Hewitt LM (2006) A decade of research on the environmental impacts of pulp and paper mill effluents in Canada: Development and application of fish bioassays 9:297–317.

Pasma SA, Daik R, Maskat MY, Hassan O (2013) Application of Box-Behnken Design in optimization of glucose production from oil palm empty fruit bunch cellulose. Int J Polym Sci 2013:1–8.

Peña C, Castillo T, García A, Millán M, Segura D (2014) Biotechnological strategies to improve production of microbial poly-(3-hydroxybutyrate): A review of recent research work. Microb Biotechnol 7:278–293.

Pervaiz M, Sain M (2011) Protein extraction from secondary sludge of paper mill wastewater and its utilization as a wood adhesive. BioResources 6:961–970.

Pillai AB, Kumarapillai HK (2017) Bacterial polyhydroxyalkanoates: Recent trends in production and applications. In: Shukla P (ed) Recent advances in Applied Microbiology. Springer, Singapore, pp 19–53.

Pirt SJ (1974) The theory of fed batch culture with reference to the penicillin fermentation. J Appl Chem Biotechnol 24:415–424.

Porras MA, Villar MA, Cubitto MA (2018) Improved intracellular PHA determinations with novel spectrophotometric quantification methodologies based on Sudan black dye. J Microbiol Methods 148:1–11.

Prasetyo J, Kato T, Park EY (2010) Efficient cellulase-catalyzed saccharification of untreated paper sludge targeting for biorefinery. Biomass and Bioenergy 34:1906–1913.

Rashid MT, Barry D, Goss M (2006) Paper mill biosolids application to agricultural lands: Benefits and environmental concerns with special reference to situation in Canada. Soil Environ 25:85–98.

Ray S, Kalia VC (2017) Biomedical applications of polyhydroxyalkanoates. Indian J Microbiol 57:261–269.

Righetti MC (2017) Crystallization of polymers investigated by temperature-modulated DSC. Materials (Basel) 10:1-22.

Rivas LF, Casarin SA, Nepomuceno NC, Alencar MI, Agnelli JAM, de Medeiros ES, de Oliveira Wanderley AN, de Oliveira MP, de Medeiros AM, Ferreira de Santos AS (2017) Reprocessability of PHB in extrusion: ATR-FTIR, tensile tests and thermal studies. Polímeros 27:122–128.

Rosazlin A, Fauziah CI, Rasidah WW, Rosenani AB (2010) Leaching of heavy metals (Cu , Mn, Zn, Ni, Pb and As) after six months application of raw and composted recycled paper mill sludge. In: 19th World Congress of Soil Science, Soil Solutions for a Changing World. Brisbane, Australia, pp 162–165.

Salamanca-Cardona L, Scheel RA, Bergey NS, Stipanovic AJ, Matsumoto K, Taguchi S, Nomura CT (2016) Consolidated bioprocessing of poly(lactate-co-3-hydroxybutyrate) from xylan as a sole feedstock by genetically-engineered *Escherichia coli*. J Biosci Bioeng 122:406–414.

Salamanca-Cardona L, Scheel RA, Lundgren BR, Stipanovic AJ, Matsumoto K, Taguchi S, Nomura CT (2014) Deletion of the pflA gene in *Escherichia coli* LS5218 and its effects on the production of polyhydroxyalkanoates using beechwood xylan as a feedstock. Bioeng Bugs 5:284–287.

Salim YS, Saiter J-M, Natarajan VD, Kumar S, Gan SN, Chan CH (2016) Evidence of melt reaction between poly(3-hydroxybutyrate-co-3-hydroxyhexanoate) and epoxidized natural rubber as investigated by DSC, isothermal TGA and FTIR analyses. Macromol Symp Symp 365:81–86.

Salmaiti Z, Ujang MR, Salim MF, Ahmad MA (2007) Intracellular biopolymer productions using mixed microbial cultures from fermented POME. Water Sci Technol 58:179–185.

Sarafadeen AO, Okoya A, Enitan AF, Olusegun OA, Oluwasegun A (2014) Biosolids land application: Implications for water resources. Pensee J 76:199–230.

Sawant SS, Salunke BK, Kim BS (2018) Consolidated bioprocessing for production of polyhydroxyalkanotes from red algae *Gelidium amanssi*. Int J Biol Macromol 109:1012–1018.

Sawant SS, Salunke BK, Taylor LE, Kim BS (2017a) Enhanced agarose and xylan degradation for production of polyhydroxyalkanoates by co-culture of marine bacterium, *Saccharophagus degradans* and its contaminant, *Bacillus cereus*. Appl Sci 7:1-16.

Sawant SS, Tran TK, Salunke BK, Kim BS (2017b) Potential of *Saccharophagus degradans* for production of polyhydroxyalkanoates using cellulose. Process Biochem 57:50–56.

Schroeder BG, Zanoni PRS, Magalhães WLE, Hansel FA, Tavares LBB (2015) Evaluation of biotechnological processes to obtain ethanol from recycled paper sludge. J Mater Cycles Waste Manag 19:463–472.

Scott GM, Smith A (1995) Sludge characteristics and disposal alternatives for the pulp and paper industry. In: Proceedings of the 1995 International environmental conference. TAPPI Press, Atlanta, GA, pp 269–279.

Saharan BS, Grewal A, Kumar P (2014) Biotechnological production of polyhydroxyalkanoates: A review on trends and latest developments. Chinese J Biol 2014:1–18.

Shen J, Agblevor FA (2011) Ethanol production of semi-simultaneous saccharification and fermentation from mixture of cotton gin waste and recycled paper sludge. Bioprocess

Biosyst Eng 34:33–43.
Sheu D-S, Wang Y-T, Lee C-Y (2000) Rapid detection of polyhydroxyalkanoate-accumulating bacteria isolated from the environment by colony PCR. Microbiology 146:2019–2025.
Shi S, Kang L, Lee YY (2015) Production of lactic acid from the mixture of softwood pre-hydrolysate and paper mill sludge by simultaneous saccharification and fermentation. Appl Biochem Biotechnol 175:2741–2754.
Shojaeiarani J, Bajwa DS, Rehovsky C, Bajwa SG, Vahidi G (2019) Deterioration in the physico-mechanical and thermal properties of biopolymers due to reprocessing. Polymers (Basel) 11:1-17.
Shrivastav A, Kim H-Y, Kim Y-R (2013) Advances in the applications of polyhydroxyalkanoate nanoparticles for novel drug delivery system. Biomed Res Int 2013:1–13.
Singh A, Bishnoi NR (2012) Optimization of enzymatic hydrolysis of pretreated rice straw and ethanol production. Appl Microbiol Biotechnol 93:1785–1793.
Singh G, Verma AK, Kumar V (2016) Catalytic properties, functional attributes and industrial applications of β-glucosidases. 3 Biotech 6:1–14.
Soucy J, Koubaa A, Migneault S, Riedl B (2014) The potential of paper mill sludge for wood-plastic composites. Ind Crops Prod 54:248–256.
Spierling S, Knüpffer E, Behnsen H, Mudersbach M, Krieg H, Springer S, Albrecht S, Herrmann C, Endres H-J (2018) Bio-based plastics- A review of environmental, social and economic impact assessments. J Clean Prod 185:476–491.
Sukruansuwan V, Napathorn SC (2018) Biotechnology for biofuels use of agro– Industrial residue from the canned pineapple industry for polyhydroxybutyrate production by *Cupriavidus necator* strain A - 04. Biotechnol Biofuels 1–15.
Suriyanarayanan S, Mailappa AS, Jayakumar D, Nanthakumar K, Karthikeyan K, Balasubramanian S (2010) Studies on the characterization and possibilities of reutilization of solid wastes from a waste paper based paper industry. Glob J Environ Res 4:18–22.
Suryan S, Ahluwalia SS (2012) Biosorption of heavy metals by paper mill waste from aqueous solution. Int J Environ Sci 2:1331–1343.
Tabañag IDF, Chu I-M, Wei Y-H, Tsai S-L (2018) The role of yeast-surface-display techniques in creating biocatalysts for consolidated bioprocessing. Catalysts 8:1–36.
Tan GA, Chen C-L, Ge L, Li L, Wang L, Zhao L, Mo Y, Tan SN, Wang J-Y (2014) Enhanced gas chromatography-mass spectrometry method for bacterial polyhydroxyalkanoates analysis. J Biosci Bioeng 117:379–382.
Torkashvand MA (2017) The effect of paper mill sludge on chemical properties of acid soil. African J Agric Res 5:3082–3087.
Torkashvand MA, Haghighat N, Shadparvar V (2010) Effect of paper mill lime sludge as an acid soil amendment. Sci Res Essays 5:1302–1306.
Torri C, Cordiani H, Samorì C, Favaro L, Fabbri D (2014) Fast procedure for the analysis of poly(hydroxyalkanoates) in bacterial cells by off-line pyrolysis/gas-chromatography with flame ionization detector. J Chromatogr A 1359:230–236.
van Zyl WH, Lynd LR, den Haan R, McBride JE (2007) Consolidated bioprocessing for bioethanol production using *Saccharomyces cerevisiae*. Adv Biochem Eng Biotechnol

108:205–235.
Vettorazzo SC, Amaral FCS, Chitolina JC (2001) Nutrient leaching potential following application of papermill lime-sludge to an acidic clay soil. Rev Bras Cienc do Solo 25:755–763.
Wang W, Kang L, Lee YY (2010) Production of cellulase from kraft paper mill sludge by *Trichoderma reesei* Rut C-30. Appl Biochem Biotechnol 161:382–394.
Wang HH, Zhou XR, Liu Q, Chen GQ (2011) Biosynthesis of polyhydroxyalkanoate homopolymers by *Pseudomonas putida*. Appl Microbiol Biotechnol 89:1497–1507.
Wang X, Lin L, Dong J, Ling J, Wang W, Wang H, Zhang Z, Yu X (2018) Simultaneous improvements of *Pseudomonas* cell growth and polyhydroxyalkanoate production from a lignin derivative for lignin-consolidate bioprocessing. Appl Environ Microbiol 84:1–15.
Wellen RMR, Rabello MS, Fechine GJM, Canedo EL (2013) The melting behaviour of poly(3-hydroxybutyrate) by DSC. Reproducibility study. Polym Test 32:215–220.
Wen Z, Li Q, Liu J, Jin M, Yang S (2020) Consolidated bioprocessing for butanol production of cellulolytic *Clostridia*: Development and optimization. Microb Biotechnol 13:410–422.
Wu HA, Sheu D-S, Lee C-Y (2003) Rapid differentiation between short-chain-length and medium-chain-length polyhydroxyalkanoate-accumulating bacteria with spectrofluorometry. J Microbiol Methods 53:131–135.
Xu CC, Lancaster J (2012) Treatment of Secondary Sludge for Energy Recovery. 1:187-212.
Yan Q, Fong SS (2017) Challenges and advances for genetic engineering of non-model bacteria and uses in consolidated bioprocessing. Front Microbiol 8:1–16.
Zhang X-Z, Zhang Y-HP (2013) Cellulases: Characteristics, sources, production and applications. In: Yang S-T, El-Enshasy H Al, Thongchul N (eds) Bioprocessing technologies in biorefinery for sustainable production of fuels, chemicals, and polymers, 1st edn. pp 131–146.
Zhao K, Deng Y, Chen JC, Chen G (2003) Polyhydroxyalkanoate (PHA) scaffolds with good mechanical properties and biocompatibility. 24:1041–1045.
Zhou Y, Lin L, Wang H, Zhang Z, Zhou J, Jiao N (2020) Development of a CRISPR/Cas9n-based tool for metabolic engineering of *Pseudomonas putida* for ferulic acid-to-polyhydroxyalkanoate bioconversion. Commun Biol 3:1–13.
Zhu M, Zhu Z, Li X (2011) Bioconversion of paper sludge with low cellulosic content to ethanol by separate hydrolysis and fermentation. African J Biotechnol 10:15072–15083.
Zribi-Maaloul E, Trabelsi I, Elleuch L, Chouayekh H, Ben Salah R (2013) Purification and characterization of two polyhydroxyalcanoates from *Bacillus cereus*. Int J Biol Macromol 61:82–88.

CHAPTER THREE

Characterization of polyhydroxyalkanoates synthesized by *Bacillus thuringiensis* using different carbohydrates

3.1. Abstract

The plastic pollution from petrochemical-derived single-use packaging is a waste challenge globally and a severe threat to our environment. This necessitates the implementation of environmentally-friendly bioplastics. Polyhydroxyalkanoates (PHAs) are biologically-derived polymers that have limited ecological impact and are suitable alternatives for the production of biodegradable plastics. The current study aimed to induce, produce, and characterize PHAs synthesized by nutrient-stressed *Bacillus thuringiensis* using five different carbohydrates as the sole carbon sources. After the 72 h batch fermentation, analysis of the bacterial cells revealed cytoplasmic PHA granules as intracellular ovoid or spherical blue-black granules due to Sudan Black B staining using bright-field light microscopy and PHA-producing cells emitting a bright orange fluorescence under epifluorescence microscopy after Nile Blue A staining. The FTIR spectra of the extracted PHAs displayed C=O, –CH, and –OH peaks which are indicative of PHAs. Glucose was the most efficacious carbon source resulted in the highest biomass productivity (0.047 g L^{-1} h^{-1}), PHA productivity (0.031 g L^{-1} h^{-1}), and PHA yield (64.51%). Pyrolysis-gas chromatography/mass spectrometry revealed that butyrate (HB), valerate (HV), and hexanoate (HHx) were the three predominant monomers. PHB homopolymer was observed only when pure glycerol or soluble starch was used as a carbon source. A copolymer containing 97.99 mol% of HB and 2.01 mol% of HHx was elucidated using α-cellulose, whereas PHBV was obtained using glucose or sucrose. The initial and complete degradation of the extracted PHAs occurred between 86.18–269.95°C and 254–430°C, respectively. The crystallinity indices of the extracted PHAs ranged from 40–59% and the PHAs had a lower thermostability compared with commercial PHB and PHBV. The ability of *B. thuringiensis* to produce PHAs with varying compositions and characteristics using simple and complex carbohydrates as the sole carbon source, makes the strain a promising PHA producer.

Keywords: Polyhydroxyalkanoate, Sudan Black B, Nile Blue A, FTIR, Py-GC/MS

3.2. Introduction

The widespread use of plastic and plastic products undoubtedly makes plastic materials an integral part of our lifestyle. However, the recalcitrant nature of these petroleum-based synthetic plastics results in their persistence and subsequent accumulation in the environment, which

poses a risk to the natural ecosystems (Mitra et al. 2020). Thus, there has been intensive scientific investigations into the development of plastics made from polymeric material derived from biological sources, using renewable biomass as feedstock, and are biodegradable and eco-friendly (Kynadi and Suchithra 2014). There are many types of biodegradable plastics with varying degrees of biodegradability, one of which, polyhydroxyalkanoates (PHAs), has gained attention and has been studied extensively. Inherent favorable features of PHAs include non-toxicity, 100% biodegradability under aerobic and anaerobic conditions and, similar mechanical, thermoplastic, physicochemical, and biocompatible properties compared with conventional polypropylene (PP), polyethylene terephthalate (PET), and polyethylene (PE) plastics (Bhagowati et al. 2015; Kourmentza et al. 2017). PHAs are a family of biopolyesters that are synthesized by a plethora of bacteria and accumulate as intracellular granules (Masood et al. 2012; Tan et al. 2014). PHA accumulation occurs when bacteria are grown under imbalanced nutrient conditions wherein the carbon source is supplied in excess but there is a minimal supply of other essential nutrients such as nitrogen, phosphorus, oxygen, or magnesium (Anderson and Dawes 1990; Sindhu et al. 2011; Gomaa 2014; Pillai et al. 2017; Juengert et al. 2018; Mostafa et al. 2020).

PHAs are classified depending on the number of carbon atoms present in their monomers *viz*., (i) short-chain-length PHAs (scl-PHAs): C_3-C_5 monomers, (ii) medium-chain-length PHAs (mcl-PHAs): C_6-C_{14} monomers, and (iii) long-chain-length PHAs (lcl-PHAs): >C_{14} monomers (Możejko-Ciesielska and Kiewisz 2016). PHAs are further classed as homo- or hetero-polymer (copolymer) depending on composition of one or more than one type of hydroxyalkanoate as the monomeric unit, respectively. The most common and well-characterized microbial scl-PHA is polyhydroxybutyrate (PHB). However, pure PHB-based plastic material is fragile with deficiencies including: high crystallinity; stiffness; brittleness; and thermal instability, thus hindering its use in commercial and industrial applications, especially in situations where high tensile strength, extrusion, or injection processing is required (Chen et al. 2009). Mcl-PHAs such as polyhydroxyvalerate (PHV) are elastomers having both low crystallinity and low glass transition temperature (Andreeßen and Steinbüchel 2010). By carefully controlling the fermentation conditions and the feeding of carbon source results in copolymerization or blending of scl- and mcl-PHAs, which creates a modified polymer with improved and desirable properties (Shang et al. 2012). The most well-known copolymer is polyhydroxybutyrate-co-polyhydroxyvalerate (PHBV), a material with improved flexibility and melt stability, enhanced

strength, elongation and film formation, and better mechanical properties such as lower crystallinity, glass transition, and melting temperature (Zhang et al. 2009; Andreeßen and Steinbüchel 2010; Chiulan et al. 2016).

The carbon substrate and the bacterial strain are the two essential components that must be well selected in order to achieve a high production yield of PHAs. PHA production using pure, commercial substrates is expensive and limits the large-scale production and industrialization of PHAs. Nevertheless, using pure carbohydrates as a carbon source for PHA production is a worthwhile exercise as it permits the determination of bacterial strains' adaptation to and utilization of carbon substrates, production kinetics, PHA synthesis, structure, molecular weight, and properties depending on the specific carbon source used (Braunegg et al. 2004; Valappil et al. 2007a; Valappil et al. 2007b; Valappil et al. 2007c; Thomas et al. 2020). To date, a wide array of carbon sources can be exploited for PHA synthesis, and as a result, a wide range of PHAs can be synthesized (Thomas et al. 2020). The production of homo and/or copolymers were observed when multiple or single pure carbon sources were used in a fermentation (Halami 2008; Thirumala et al. 2010). Significant factors that govern PHA production and polymer properties are closely linked to the bacterial producer strain, their inherited metabolic pathways, media constituents, carbon substrates, and production mode (Mohandas et al. 2018; Thomas et al. 2020). The best PHA accumulating bacterial species should have a high growth rate, be capable of utilizing a wide variety of carbon sources, and have a high accumulation percentage (Naheed and Jamil 2014). Research has been directed towards Gram-positive strains such as *Bacillus* as they lack lipopolysaccharides and have the ability to secrete a variety of extracellular enzymes, thereby permitting proliferation on diverse substrates. The first PHA, polyhydroxybutyrate (PHB), was discovered in 1925 as a constituent of *B. megaterium* (Lemoigne 1925). Subsequently, PHA production has been reported in other *Bacillus* species (Hassan et al. 2016; Sadasivam et al. 2018), *B. cereus* (Valappil et al. 2007a; Valappil et al. 2007b; Valappil et al. 2007c; Ali and Jamil 2014), *B. megaterium* (Bhagowati et al. 2015; Akdoğan and Çelik 2018; Mohapatra et al. 2020), *B. sphaericus* (Sindhu et al. 2011), *B. subtilis* (Singh et al. 2009; Gomaa 2014; Bhagowati et al. 2015; Mohapatra et al. 2017) and *B. thuringiensis* (Odeniyi and Adeola 2017). *Bacillus* species have a unique ability to produce scl- and mcl-PHAs. Furthermore, they are among the few bacteria which can produce homopolymers and copolymers from pure substrates and biowastes of diverse origins (Singh et al. 2015; Masood et al. 2017).

The present research work aims to elucidate the PHA-producing ability of a wild-type *B. thuringiensis*. A fermentative strategy was used whereby five different carbohydrates, supplied in excess, served as the sole carbon source and limiting oganic nitrogen supplied. Intracellular PHA accumulation was visualized using Sudan Black B and Nile Blue A staining. Finally, PHAs were extracted, quantified and characterized, and compared with commercial PHB and PHBV.

3.3. Materials and Methods

3.3.1. Bacterial strain, growth, and storage conditions

Bacillus thuringiensis DF7 (accession no. KC020161), previously isolated from *Eucalyptus dunnii* wood chips obtained from a plantation in Durban, South Africa, was used as the PHA-producing isolate. The culture was grown on nutrient agar or nutrient broth at 37°C for 24 h. The bacterium was stored at 4ºC on nutrient agar for short-term maintenance and, a 40% glycerol stock culture stored at -80°C were used for long-term storage.

3.3.2. Plate screening for PHA production

The ability of *B. thuringiensis* to produce PHAs was assessed using the Nile Blue A plate screening assay. The isolate was streaked onto carbon-rich agar (CRM; 3 g beef extract, 5 g peptone, 5 g NaCl, 10 g glucose, 12 g agar (Merck), 1 L distilled H_2O) supplemented with 0.5 µg/mL Nile blue A dye (BDH chemicals) and incubated at 37°C for 3 d. Bacteria positive for PHA production exhibit a bright fluoresce under UV light irradiation (312 nm) (Naheed et al. 2012).

3.3.3. PHA production

To induce nutrient stress and subsequently PHA production, batch cultivation in shake-flask fermentation was conducted using five different carbon sources *viz*. α-cellulose (Sigma), glucose (Merck), glycerol (Sigma), starch (soluble; Merck) or sucrose (Merck) and yeast extract (Merck) as the nitrogen source. Each fermentation was conducted in a 2 L Erlenmeyer flask containing 800 mL medium comprising of minimal medium (3.7 g KH_2PO_4, 7.5 g K_2HPO_4, 1 mL of 246.5 g L^{-1} $MgSO_4.7H_2O$; 1 L distilled H_2O), carbon source (30 g L^{-1}), yeast extract (10 g L^{-1}), 1.5 mL trace elements solution (0.03 g L^{-1} $MnCl_2.4H_2O$, 0.2 g L^{-1} $CoCl_2.6H_2O$, 0.01 g L^{-1} $CuCl_2.2H_2O$, 1.4 g L^{-1} $ZnSO_4.7H_2O$, 0.3 g L^{-1} H_3BO_3, 0.02 g L^{-1} $NiCl_2.6H_2O$, 0.02 g L^{-1}

$NaMoO_4.H_2O$ dissolved in 1 L distilled H_2O) and 10% inoculum of *B. thuringiensis* culture. Following incubation at 37°C in a rotary shaker at 150 revolutions per minute (rpm) for 72 h, the bacterial biomass was harvested and assayed for PHA production.

3.3.4. Staining assays

The Sudan Black B staining assay was conducted as a rapid qualitative test for the detection of intracellular PHB granules. Heat-fixed smears were flooded with a 0.3% (w/v) ethanol solution of Sudan Black B dye for 10 min, followed by xylene for 10 s and counter-stained with 0.5% (w/v) safranin for 30 s. PHA accumulation was visualized as cells having blue-black, ovoid, or spherical intracellular granules (Abinaya et al. 2012). A bright orange fluorescence emitted by Nile Blue A-stained cells was also used to detect PHA accumulation. Heat-fixed smears were flooded with a 1% aqueous solution of Nile Blue A dye and incubated at 55°C for 10 min. Thereafter, slides were gently rinsed with water, flooded with 8% (v/v) acetic acid for 1 min, and rinsed with water (Tan et al. 2014). Slides were examined using a Nikon Eclipse 80i light microscope. For epifluorescence microscopy, a filter with an excitation wavelength of ~460 nm was used. A Nikon DS-Fi1 camera and Nikon Imaging Software D 3.00 were used to capture images at 1000× magnification.

3.3.5. PHA extraction

PHAs were recovered using solvent extraction followed by non-solvent precipitation, as per the methodology of Munir et al. (2015). The hypochlorite-chloroform dispersion method is a simple and rapid method routinely used to recover high yields of PHA from cell biomass with high purity (Kunasundari and Sudesh 2011; Aramvash et al. 2018). The bacterial biomass was harvested by centrifugation at 5752 ×*g* for 20 min to form a pellet that was washed twice with distilled water and lyophilized. The cell dry weight of the lyophilized cells was determined gravimetrically. Thereafter the lyophilized cells were transferred into a conical flask to which 100 mL of 5% sodium hypochlorite and 100 mL of chloroform were added. The mixture was agitated in a rotary shaker (New Brunswick Innova 44, Eppendorf) at 300 rpm at 37°C for 3 h. The suspension was transferred into a separating funnel and left to stand for 30 min to allow phases to separate *viz*., an upper phase containing hypochlorite solution, a middle phase containing non-PHA material (cell debris and undisrupted cells), and the bottom phase consisting of PHA solubilized in chloroform. The bottom phase was decanted into a beaker, and nine parts of methanol was added to precipitate the PHAs. Finally, the PHA-precipitate was

dried by evaporation at 30°C, resulting in white flakes or powder. The dry weight of the extracted PHAs was determined gravimetrically.

The percentage yield of PHAs was determined using the following equation:

$$\text{Yield (\%)} = \frac{\text{PHAs (g)}}{\text{CDW (g)}} \times 100$$

The volumetric bacterial biomass productivity was determined using the following equation:

$$\text{Productivity (g L}^{-1}\text{h}^{-1}) = \frac{\text{CDW (g L}^{-1})}{\text{Time (h)}}$$

The volumetric PHA productivity was determined using the following equation:

$$\text{Productivity (g L}^{-1}\text{ h}^{-1}) = \frac{\text{PHAs (g L}^{-1})}{\text{Time (h)}}$$

3.3.6. Fourier-transform infrared spectroscopy (FTIR)

The chemical structure of the extracted PHAs and commercial PHB and PHBV (Sigma Aldrich) were analyzed by FTIR (Pradhan et al. 2018). The presence of functional groups representative of PHAs were observed in infrared spectra of the powdered samples recorded in the wavenumber range from 400 to 4000 cm^{-1} using a Perkin Elmer spectrophotometer (Jasco FTIR- 6100).

3.3.7. Polymer composition

Thermally assisted hydrolysis and methylation-gas chromatography (THM-GC) using pyrolysis-gas chromatography/mass spectrometry (py-GC/MS) in the presence of the strong organic alkali, tetramethylammonium hydroxide (TMAH), was employed to qualitatively and quantitatively elucidate the polymer composition of the extracted PHAs and commercial PHB and PHBV (Sigma Aldrich) (Torri et al. 2014). The main peaks observed were identified by comparing the mass spectra with the NIST library database. The compounds were identified based on retention time and mass spectra, with only similarities ≥85% considered genuine fits. The polymer composition (mol%) of each PHA was calculated using the methodology of Martínez-Sanz et al. (2014);

$$\text{H}_{\text{a,b or c}}(\%) = \frac{\text{area H}_{\text{a,b or c}}}{\text{area H}_\text{a} + \text{area H}_\text{b} + \text{area H}_\text{c}} \times 100$$

Where a, b, and c represent the monomers polyhydroxybutyrate (HB), polyhydroxyvalerate (HV), or polyhydroxyhexanoate (HHx), respectively.

3.3.8. Thermogravimetric analysis (TGA) and differential scanning calorimetry (DSC)

TGA was used to determine the thermal stability of the extracted PHAs and commercial PHB and PHBV (Sigma). TGA was conducted using a TGA Q5000 (TA Instruments) with a temperature range from 30°C to 950°C, a heating rate of 10°C min^{-1} in a nitrogen atmosphere (N_2 flow rate = 40 mL min^{-1}). The initial degradation temperature ($T_{5\%}$) and maximum decomposition temperature (T_{max}) are the temperatures at which 5% and 95% weight loss occurred and were determined by analyzing the TGA and derivative thermogravimetric (DTG) graphs, respectively (Pradhan et al. 2018).

A differential scanning calorimeter (DSC Q2000, TA Instruments) was used to perform DSC analysis, where 10 mg of sample was loaded in an aluminum pan and heated from -10°C to 200°C at a heating rate of 10°C min^{-1}. A heating and cooling rate of 10°Cmin^{-1} was used as well as a nitrogen environment with a gas flow of 20 mL min^{-1}. The glass transition temperature (T_g) was identified as the point of inflection in the thermogram between onset and offset temperatures. The melting temperature (T_m) and melting enthalpy (ΔH_m) were determined from the peak temperature and area under the peak of an endothermic event in the second heating cycle, respectively. The crystallization temperature (T_c) and crystallization enthalpy (ΔH_c) were determined from the peak temperature and area under the peak of an exothermic event in the cooling cycle, respectively. The degree of crystallinity (X_c) was calculated by dividing ΔH_m by 146 J g^{-1} (melting enthalpy of 100% crystalline PHB) (Pradhan et al. 2018).

3.3.9. Statistical analysis

The effects of the carbon sources on CDW, PHA yields, polymer composition and thermal properties were determined using one-way ANOVA and SPSS (V 27.0). Where necessary, a Bonferroni Post-Hoc analysis was conducted and a $p < 0.05$ was considered as statistically significant.

3.4. Results and Discussion

3.4.1. Screening for PHA production

The fluorescence exhibited by *B. thuringiensis* is indicative of intracellular PHA accumulation (Fig. 3.1 A). The lack of fluorescence demonstrated by *Escherichia coli* indicates that the strain is possibly incapable of PHA-production (Fig. 3.1 B).

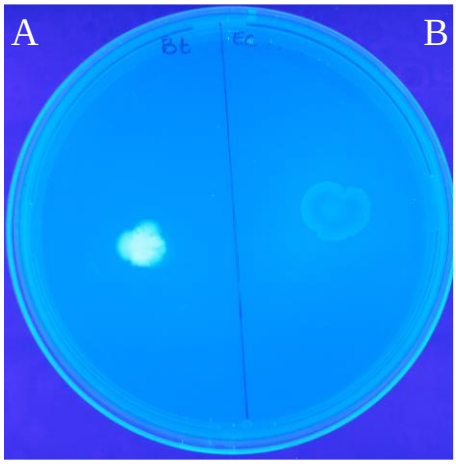

Figure 3.1: Bright fluoresce exhibited by *B. thuringiensis* (A), and non-fluorescing *E. coli* (B) when grown for 3 days at 37°C on carbon-rich agar supplemented with Nile Blue A dye and thereafter examined under UV light irradiation (312 nm).

3.4.2. Staining assays

Researchers often use staining procedures and microscopy analysis to detect and monitor PHA production in real-time i.e., while the fermentation is in progress (Bhuwal et al. 2013; Zuriani et al. 2013; Bhuwal et al. 2014). A similar approach was taken in the current study, to evaluate the suitability of five different carbon sources as substrates for PHA production by *B. thuringiensis*. Microscopic examination of Sudan Black B stained bacterial smears from the PHA production medium revealed blue-black spherical PHA inclusions within the vegetative cells (Fig. 3.2 A-E). Aljuraifani et al. (2018) used Sudan Black B staining to conclusively demonstrate the presence of PHA production by *Bacillus* sp. strain-6, with most of the granules occupying 50% of the cell's volume and surrounded by compact membranes. However, visualization of intracellular PHAs using the Sudan Black B staining procedure was difficult, and the procedure had to be repeated several times in order to make accurate observations. Often, even after washing steps, the Sudan Black B dye aggregated and remained around the bacterial cells, which could be misinterpreted as PHAs. It has been shown that Sudan Black B is non-specific to PHA, as it also stains other lipid bodies (Berlanga et al. 2006). In this study, a microscopic examination of *B. thuringiensis* smears after Nile Blue A staining was also

conducted. A bright orange fluorescence was observed at a wavelength of 460 nm (Fig. 3.2 A-E), concurring with the report on *Bacillus* sp. strain 6 (Aljuraifani et al. 2018), *B. firmus* NII 0830, *B. firmus* NII 0829 and *B. sphaericus* NII 0838 (Sindhu et al. 2011). Kumar et al. (2017) used fluorescence microscopy to establish that strong fluorescence is indicative of lipid accumulation or PHA granules inside the cells. Ali and Jamil (2014) demonstrated that Sudan Black B and Nile blue A staining tests were effective in detecting PHA-production by *B. cereus* 64-INS strain. Thus the appearance of intracellular PHA granules after both staining procedures confirm that *B. thuringiensis* was capable of using all five substrates as carbon sources for PHA production (Fig. 3.2). In the current study, Nile Blue A staining was superior to lipophilic Sudan Black B staining. It was easier to detect and visualize the presence of PHAs using epifluorescence microscopy in comparison to bright field microscopy. However, the shortfall of lipophilic dyes is their tendency to adhere to lipid structures other than PHAs, resulting in false-positive observations (Shamala et al. 2003; Muhammadi et al. 2015). In addition, staining assays are time consuming and laborious. Furthermore, it rarely provides accurate and/or conclusive results on the type of PHA produced by the bacterium (and it is often regarded as PHB only). Staining procedures are useful tools but are purely pre-screening procedures and cannot be used to identify the monomer composition(s) and quantities of the accumulated PHA (Muhammadi et al. 2015). This corroborates with findings in the present study whereby an association between fluorescence exhibited (Fig. 3.3) and the PHA yields (Table 3.1) cannot be made.

A

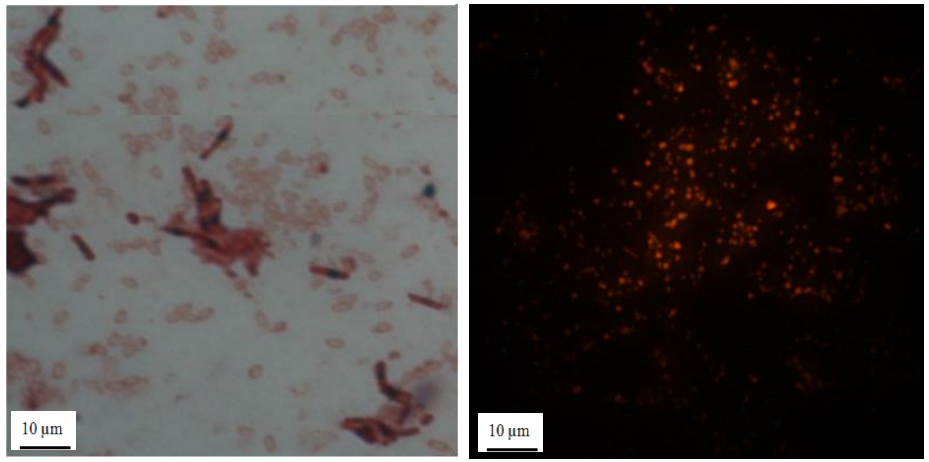

B

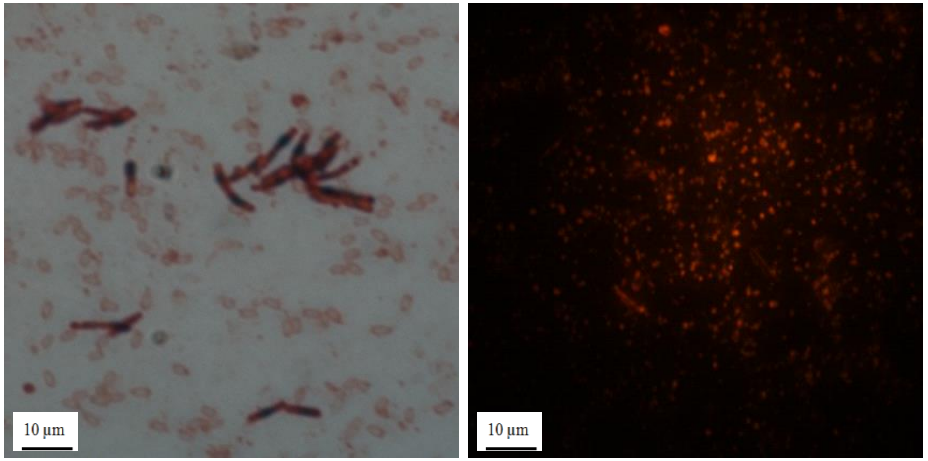

C

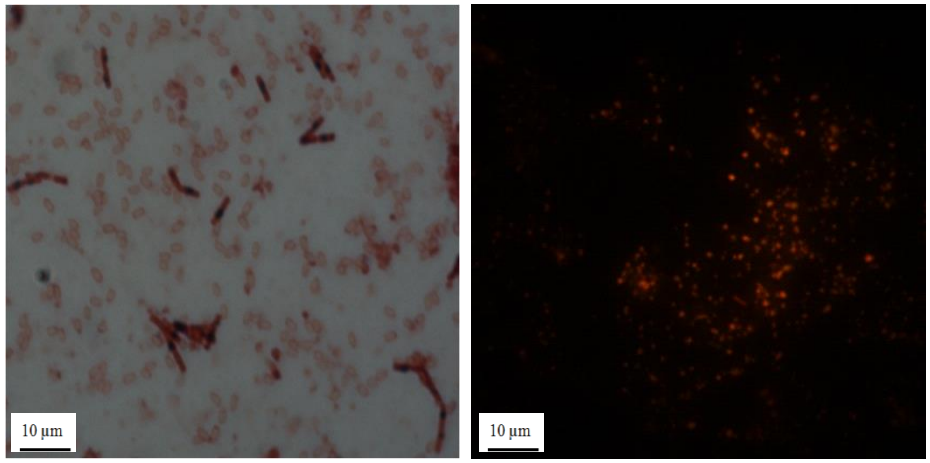

D

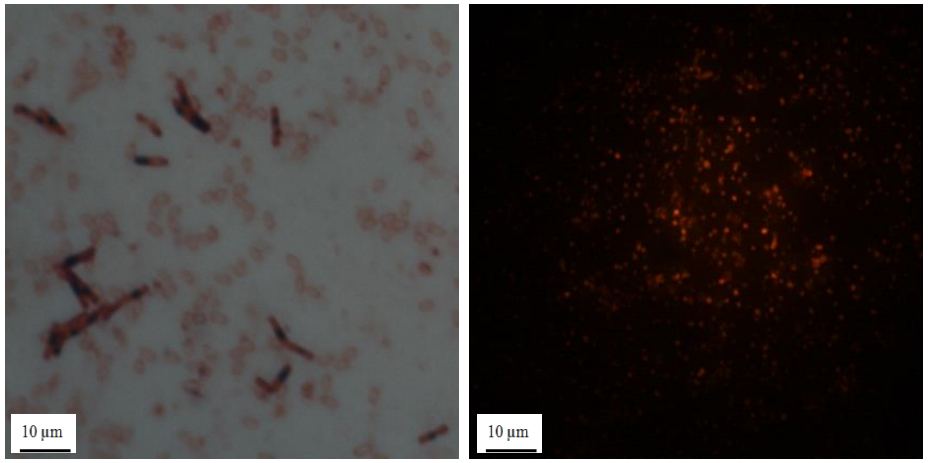

E

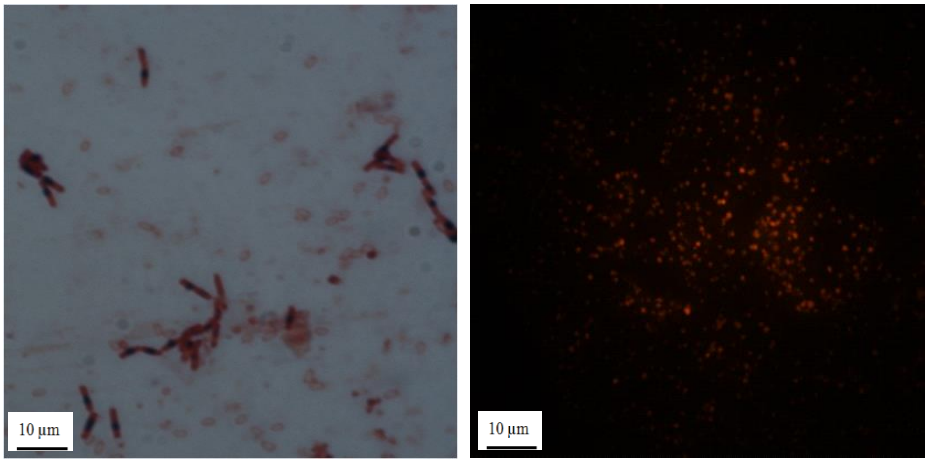

Figure 3.2: Bright-field light microscopy after Sudan Black B staining (dark intracellular granules) and epifluorescence microscopy images after Nile Blue A staining (orange fluorescence) (×1000) displaying intracellular PHA accumulation by *B. thuringiensis* when α-cellulose (A), glucose (B), glycerol (C), starch (D), and sucrose (E) were used in the 72 h batch cultivation for PHA production by *B. thuringiensis*.

3.4.3. PHA productivity

In the present study, *B. thuringiensis* exhibited nutritional versatility in terms of varied growth and PHA production when tested on the various carbon sources. The parameters from the batch cultivation of *B. thuringiensis* for PHA production for each carbon source are displayed in Table 3.1. The carbon sources had a significant effect on both the biomass (CDW) and PHA yield ($p < 0.05$). Only α-cellulose and glucose significantly affected CDW yield ($p < 0.01$), whereas α-cellulose, glucose, and sucrose significantly impacted PHA yield ($p < 0.01$). As expected, both growth and PHA yields were best using glucose as carbon source with a CDW of 3.41 g L^{-1} and PHA yield of 2.20 g L^{-1} PHA after the 72 h fermentation period. The maximum biomass productivity and PHA productivity of 0.047 g L^{-1} h^{-1} and 0.31 g L^{-1} h^{-1}, respectively, was also observed when glucose was used as the carbon source. The use of α-cellulose as a carbon source yielded 30.80% PHA (Table 3.1). The low CDW and polymer yield in comparison with the other carbon sources could be attributed to the energy the bacteria consumed to produce the extracellular enzymes required to hydrolyze the large molecule substrates for uptake as nutrients for cell proliferation (Yue et al. 2014). Previous enzyme screening studies of the *B. thuringiensis* isolate used in the present study revealed that the isolate produces cellulase (Govender 2013). The capacity of other *Bacillus* spp. to produce cellulase has been observed for *B. subtilis* AU-1 (Chan and Au 1987; Latorre et al. 2015; Nargotra et al. 2016), *Bacillus* sp. (Rastogi et al. 2009), and *B. amyloliquefaciens* (Latorre et al. 2015). *Bacillus* sp. OU40^{T} also

displayed the ability to utilize α-cellulose and hemicelluloses and produced a yield of 57.29% PHA (Nagamani and Mahmood 2013). Much lower PHA yields of 11.8% and 13-14% were observed for *Saccharophagus degradans* (Sawant et al. 2017) and *B. cereus* (Li et al. 2017), respectively. In the current study, glucose was the most efficient carbon source resulting in a maximum CDW of 3.41 g L^{-1}, 2.20 g L^{-1} PHA content and, an overall PHA yield of 64.51% (Table 3.1). Glucose is the simplest sugar and the primary carbon and preferred energy source of many PHA-producing microorganisms (Jiang et al. 2016). The yields observed in the present study are similar to *B. cereus* strain 64-INS that produced 64.35% PHA (Ali and Jamil 2014) and the 65.6% PHA yield from *B. shackletonii* K5 (CGMCC 7488) (Liu et al. 2014) when glucose was used as the carbon source. Higher yields of 67.73% PHA, 70.04% PHB, and 3.264 g L^{-1} PHA were produced by *Bacillus* sp. 112A, *Bacillus* sp. 87I (Thirumala et al. 2010) and *B. aryabhattai* PHB10 (Pillai et al. 2017), respectively when using glucose as a carbon source. Using glycerol achieved 2.98 g L^{-1} CDW, 1.55 g L^{-1} PHA and 52.01% PHA (Table 3.1). Reddy et al. (2009) report that *Bacillus* sp. 88D produced a similar yield of 1.51 g L^{-1} PHA. *B. cereus* MCCB 281 produced higher yields of 3.72 g L^{-1} CDW, 2.54 g L^{-1} PHA, and a PHA yield of 68.27% (Mohandas et al. 2018). Whereas, *Bacillus* sp. ISTVK1 produced 4.4 g L^{-1} PHA (Morya et al. 2018); a yield almost 3-fold higher than that observed in the present study. The use of soluble starch as the sole carbon source resulted in 1.54 g L^{-1} PHA and 48.13% PHA (Table 3.1). Thirumala et al. (2010) and Halami (2008) produced similar results from *Bacillus* sp. 112A (50.5% PHA) and *B. cereus* (48% PHA) respectively; when starch was used as the carbon source. Pillai et al. (2017) observed higher yields of 1.742 L^{-1} PHA and 75% PHA for *B. aryabhattai* PHB10. In contrast, Singh et al. (2013) observed a maximum PHA yield of 4.931 g L^{-1} for *B. subtilis* NG220. An overall PHA yield of 60.54% was observed when glycerol was used (Table 3.1). This yield is slightly higher than a previous report on *Bacillus* sp. 112A that produced 58.5% PHA (Thirumala et al. 2010); however, Borah et al. (2002) reported that *B. mycoides* RLJ B-017 was capable of producing 69.4% PHA.

Table 3.1: Growth and product kinetic parameters for each carbon source used in the 72 h batch cultivation for PHA production by *B. thuringiensis*

Carbon source	CDW (g L^{-1})*	PHA content (g L^{-1})	PHA yield (%)*	Biomass productivity (g L^{-1} h^{-1})	PHA productivity (g L^{-1} h^{-1})
α-Cellulose	2.11**	0.65	30.80**	0.029	0.009
Glucose	3.41**	2.20	64.51**	0.047	0.031
Glycerol	2.98	1.55	52.01	0.041	0.022
Starch	3.20	1.54	48.13	0.044	0.021
Sucrose	3.32	2.01	60.54**	0.046	0.028

**Statistically significant ($p < 0.01$) 1% level of significance *Statistically significant ($p < 0.05$) 5% level of significance

3.4.4. FTIR analysis

In this study, FTIR was used to further confirm PHA-production by identifying the presence of functional groups unique to PHA. FTIR analysis was conducted on the powdered PHAs extracted from *B. thuringiensis* and commercial PHB, PHBV. The peaks present for the ester, methylene, and terminal hydroxyl groups are typically representative of the polymeric structure of PHAs (Apparao and Krishnaswamy 2015) and are observed in the spectra for all of the extracted PHAs as well as for commercial PHB and PHBV (Fig. 3.3). The exact peak location and intensity varies, depending on the polymer chain length, concentration, and crystallinity of the PHA. The distinguishing peak of PHA is located around 1700-1738 cm^{-1} (C=O stretch) and a series of intense peaks located at 1000-1400 cm^{-1} (C-O stretch) which correspond to the ester group present in the molecular chain of highly ordered crystalline structures (Getachew and Woldesenbet 2016). The pinnacle present at 1730 cm^{-1} represents the ester carbonyl (C=O), the extending vibration of PHB. The peaks at 1300 cm^{-1} and 1600 cm^{-1} correspond to the rotations around carbon atoms of the –CH functional groups (Fig. 3.3). Adsorption bands observed around 1380, 1450, 2930, 1650, and 3400 cm^{-1} correspond to $–CH_3$, $–CH_2$, CH, C–O, and O–H groups, respectively, which was reported to be similar with pure PHB (Łabuzek and Radecka 2001). The peaks at 2850-2960 cm^{-1} are due to the C-H stretching methyl and methylene groups of alkanes, which are usually demonstrated by PHA polymers. The peaks at 500–1000 cm^{-1} correspond to (OH) separately whereas the broad peak at 3269 cm^{-1} indicates the presence of O-H stretching of alcohol (terminal OH group) (Fig. 3.3) (Sindhu et al. 2011). The presence of copolymer like PHBV is denoted by a characteristic absorption peak in the region of 2933–2972 cm^{-1}. Overall the FTIR spectra of the extracted PHAs show prominent peaks at the wavelengths which are indicative of PHAs and are comparable to the spectra of commercial PHB and PHBV as well as for PHAs recovered from other *Bacillus* sp. (Helm and Naumann 1995; Bhattacharya et al. 2016; Isak et al. 2016; Ntaikou et al. 2019).

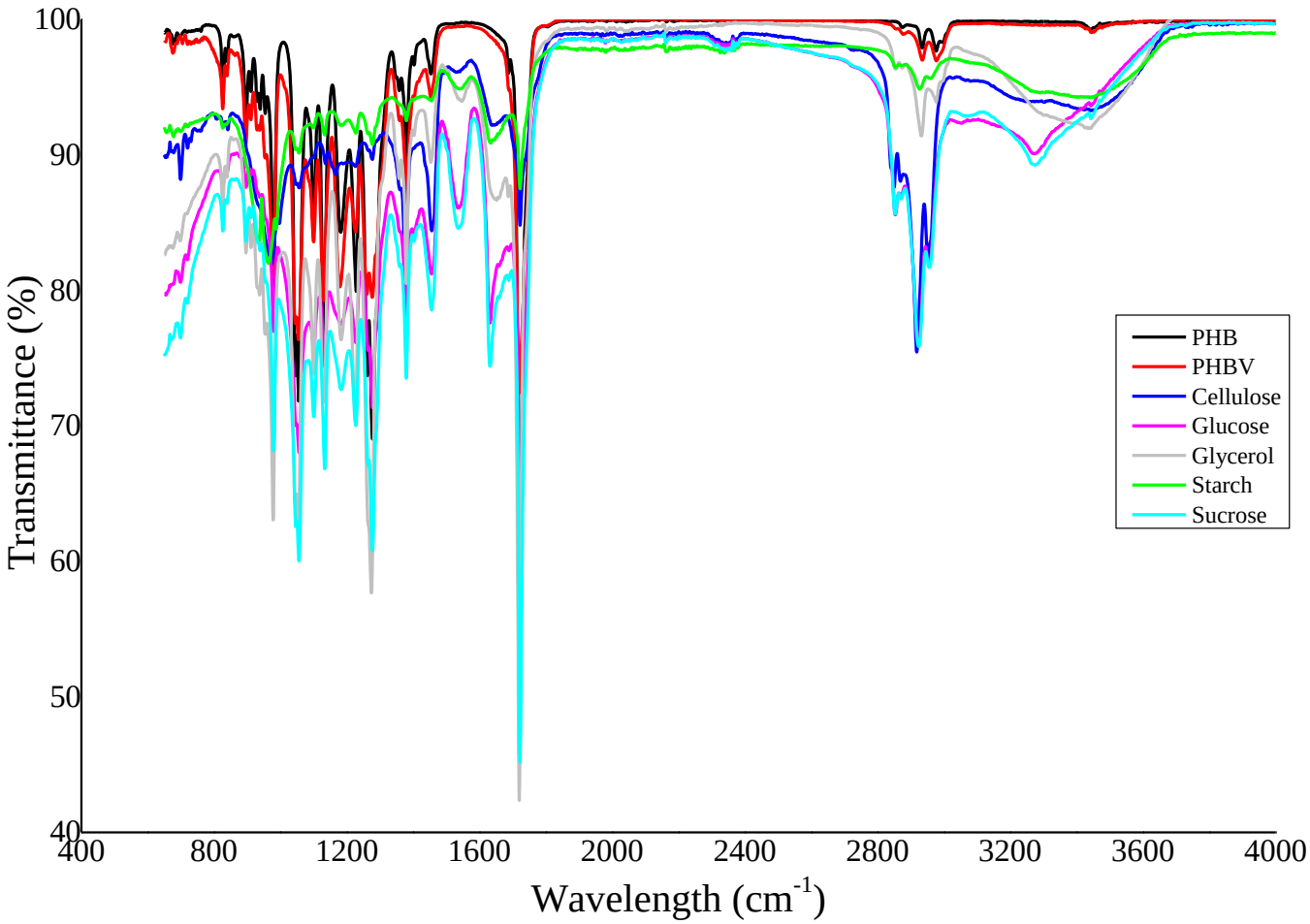

Figure 3.3: Fourier-transform infrared spectra of commercial PHB, PHBV, and the PHAs extracted from *B. thuringiensis* for each of the five carbon sources used in the 72 h batch cultivation for PHA production by *B. thuringiensis*.

3.4.5. Polymer characterization

To identify the composition of PHA pyrolysis products, GC/MS and THM-GC were employed as they permit accurate detection, characterization, and semi-quantification of PHA-monomeric moieties incorporated by the isolate (Torri et al. 2014; Baidurah et al. 2015). The monomeric composition of the polymers is summarized in Table 3.2 and the pyrograms are presented as supplementary material 1 (S 1.1-1.3). It was surprising to observe that commercial PHB also contained 10.19% HV and that it is not in fact a 100% PHB homopolymer (Table 3.2). All five carbon sources significantly affected the presence of the HB, HV or HHx ($p < 0.05$). α-Cellulose and glucose had a significant effect on the presence of HB and HV in the polymer ($p < 0.01$), whereas all five carbon sources significantly affected the presence of HHx ($p < 0.01$). Metabolism of α-cellulose resulted in a HB-HHx copolymer, comprising of 97.99 mol% of HB and 2.01 mol% of HHx (Table 3.2). This differs from previous reports whereby *Bacillus* sp.

OU40^{T} produced PHBV when α-cellulose and hemicelluloses were used as the substrate (Nagamani and Mahmood 2013). Moreover, *B. cereus* tsu1 (Li et al. 2017), and *S. degradans* (Munoz and Riley 2008) produced a PHB homopolymer when using α-cellulose. Addition of the precursors 4HB and ε-caprolactone into the production medium resulted in *Bacillus* sp. INT005 accumulating P(3HB-co-4HB-co-3HHx) and P(3HB-co-3HHx-co-6HHx), respectively (Tajima et al. 2003). Caballero et al. (1995) reported that *B. cereus* ATCC 14579 produced PHAs containing 97.7 mol% of HB and 2.3 mol% of HHx from hexanoate precursor. Those studies showed that HHx precursors were required for the respective *Bacillus* spp. to incorporate HHx into the copolymer. However, in the present study, *B. thuringiensis* produced the HB-HHx copolymer solely using α-cellulose i.e., in the absence of any precursors. The HHx component of the HB-HHx copolymer was a minor amount of only 2.01 mol% (Table 3.2). The polymer characterized by Caballero et al. (1995) also contained HHx as a minor co-monomer of the polymer; however, it reduced the melting point resulting in a PHA with the potential to be used as a melt-processable thermoplastic. In addition, biopolymers with a hexanoic acid component have the potential to function as tissue engineering material (Höfer et al. 2010). Thirumala et al. (2010) found glucose to be the most efficient substrate for the production of the scl-PHA by *Bacillus* sp. 87I. This concurs with the present study where the use of glucose resulted in the scl-polymer, PHBV (Table 3.2). In the current study, employing pure glycerol or starch as the sole carbon sources resulted in the production of PHB (Table 3.2). Studies with *B. aryabhattai* PHB10 (Pillai et al. 2017), *B. sonorensis* (Shrivastav et al. 2010), and *B. megaterium* DSM 90 (Shahid et al. 2013) also demonstrated PHB production when these substrates were used. However, *Bacillus* sp. 88D (Reddy et al. 2009), *Bacillus* sp. ISTVK1 (Morya et al. 2018) and *B. cereus* MCCB 281 (Mohandas et al. 2018) were capable of producing PHBV in the presence of glycerol. PHB production was also observed for *Bacillus* sp. 112A (Thirumala et al. 2010), *B. cereus* CFR06 (Halami 2008), *B. aryabhattai* PHB10 (Pillai et al. 2017), and *B. subtilis* NG220 (Singh et al. 2013) when starch was used as the sole carbon source thereby correlating with the observations in the present study. A PHBV copolymer was synthesized when sucrose was used as the sole carbon source (Table 3.2) whereas, *Bacillus* sp. 112A (Thirumala et al. 2010) and *B. mycoides* (Borah et al. 2002) only produced PHB. It is common for bacteria to produce PHAs with a different composition for the same substrate (Jiang et al. 2016). Overall,

the results from the current study indicate that the use of glycerol and starch resulted in only PHB. The use of glucose and sucrose resulted in the scl-copolymer, PHBV whereas, the PHA from α-cellulose was a scl-mcl copolymer. The synthesis of scl-PHAs by *B. thuringiensis* can be attributed to its *phaC* that encodes a class III PHA synthase subunit. The class III synthase is comprised of PhaC with a PhaE subunit elucidated by Paul (2018). This PhaC prefers CoA thioesters from substrates with hydroxy acyl monomer units constituting 3-5 carbon atoms, thereby producing scl-PHAs (Steinbüchel et al. 1992; Rehm 2003; Edkie and Prasad 2014). The occurrence of mcl-PHAs may be attributed to the substrate specificities of the PHA synthase and/or the monomer-supplying enzymes (Tajima et al. 2003). For industrial application, PHA copolymers are advantageous as they have improved physical and mechanical properties such as reduced crystallinity, low shrinkage, and increased flexibility, ductility, and toughness and can be bioengineered depending on the nature of the practical applications (Andreeßen and Steinbüchel 2010; Amache et al. 2013). Scl-mcl-PHAs are a highly valuable class of PHAs that have been proposed for many applications due to their desirable thermo-mechanical properties (Höfer et al. 2010).

Table 3.2: Polymer composition, degradation temperatures and thermal properties of commercial PHB and PHBV, and the PHAs extracted from *B. thuringiensis* for each carbon source used in the 72 h batch cultivation for PHA production by *B. thuringiensis*

Carbon Source	**Polymer Composition (mol%)***			**Degradation Temperature (°C)**		**Thermal Properties***					
	HB	**HV**	**HHx**	**$T_{5\%}$**	**T_{max}**	**T_g (°C)**	**T_{m1} (°C)**	**T_{m2} (°C)**	**ΔHm (J g^{-1})**	**T_c (°C)**	**X_c (%)**
α-Cellulose	97.99**	-	2.01**	200.97	430	4.70	144.89	178.43	58.45	79.08	40
Glucose	79.84**	20.16**	-	173.07	283.14	4.65	160.06	165.61	61.89	85.45	42
Glycerol	100	-	-	86.18	278.10	4.54	-	178.60	81.97	70.41	56
Starch	100	-	-	240.29	254	4.97	-	179.25	85.73	95.62	59
Sucrose	85.12	14.88	-	179.118	273.86	4.63	123.09	168.25	62.22	97.65	42
Commercial PHB	89.81	10.19	-	269.66	286.77	5.02	171.65	174.69	90.35	75.50	62
Commercial PHBV	43.35	56.65	-	264.04	288.32	4.85	138.22	146.94	60.55	113.17	41

**Statistically significant ($p < 0.01$) 1% level of significance

*Statistically significant ($p < 0.05$) 5% level of significance

3.4.6. Thermal properties

The thermal properties of commercial PHB and PHBV, as well as the PHAs extracted from *B. thuringiensis,* were evaluated using TGA and DSC. The thermal stability of polymers, especially the initial degradation temperature which polymers can withstand before complete thermal degradation, is an important factor for polymer processing (Akdoğan and Çelik 2018). The weight loss (TGA) curves and corresponding derivative weight loss (DTG plots) is displayed in Figure 3.4 and summarized in Table 3.2. All of the carbon sources were observed to significantly affect the thermal properties of the polymer(s) ($p < 0.05$). It is evident that the curves have the same shape, but the slopes differ (Fig. 3.4). Therefore, the kinetic parameters and the thermal stability temperatures would be different for each type of polymer (Carrasco et al. 2005). The thermal degradation of the PHAs occurred mainly in a two-step process whereby PHAs began to degrade at around 86.18–269.66°C ($T_{5\%}$) and completely degraded (T_{max}) between 254-430°C (Table 3.2). The major degradation of the polymer takes place at temperatures higher than the polymer melting point with a further rise in temperature (Fig. 3.4). The initial mass loss is mainly due to the evaporation of physically adsorbed solvents like methanol, chloroform, and removal of impurities from the polymer. The main thermal degradation reaction of PHAs involves a non-radical, random chain scission, and an ester cleavage of the PHB component by β-elimination. This leads to a reduction in molecular weight due to breakage and hydrolysis of the PHA into oligomers and thereafter into monomeric units (Chen et al. 2012; Chiulan et al. 2016). The varying decomposition temperatures (Table 3.2) may be attributed to the incorporation of different monomers such as HV and HHx in the case of the polymers in the current study, as the presence of different monomers also contributes to the thermal stability of the polymer (Akdoğan and Çelik 2018). The DTG results indicates that the maximum degradation temperatures for PHAs extracted when using glucose, glycerol, starch and sucrose are lower than commercial PHB and PHBV, which is indicative of a lower thermostability (Fig. 3.4; Table 3.2). The high T_{max} of 430°C for the PHB-HHx copolymer synthesized using α-cellulose as a carbon source displays better thermostability than commercial PHB and PHBV. A high decomposition temperature is a crucial factor for polymer processing in industry since the material has to be able to resist, with no structural degradation, the temperatures used for extrusion and injection molding to manufacture biodegradable films and molded pieces (Rodrigues et al. 2019). However, Shang et al. (2012) suggest polymers with thermal decomposition temperatures above 220°C, as observed in the present study, may still have a wide processing window.

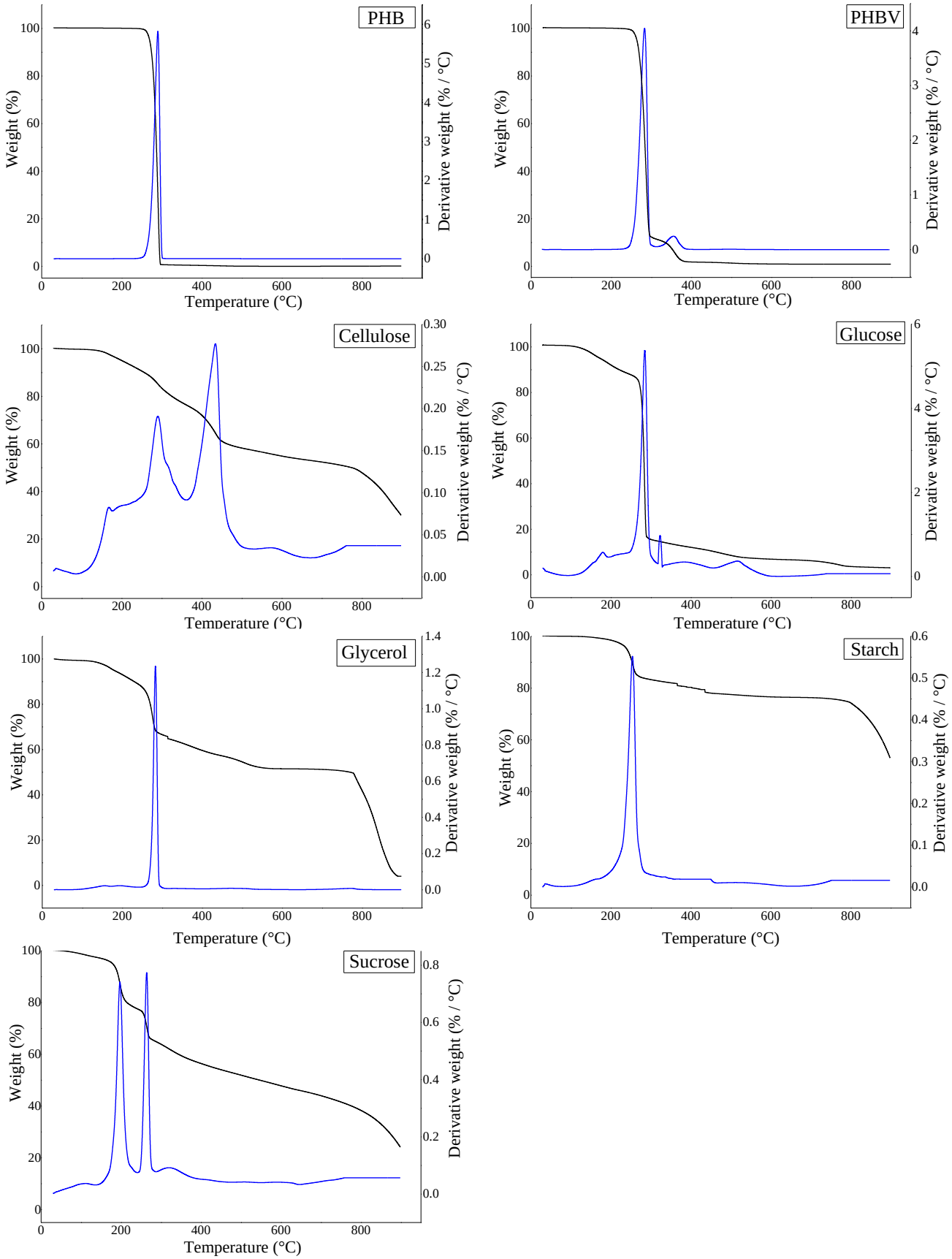

Figure 3.4: Thermograms from thermogravimetric (black) and derivative thermogravimetric (blue) analysis of commercial PHB and PHBV and the PHAs extracted for each carbon source used in the 72 h batch cultivation for PHA production by *B. thuringiensis*.

DSC was conducted to elucidate information on the thermal transitions of the polymers when heated (Chen et al. 2012). Figures 3.5 A and 3.5 B show the DSC scans for the cooling cycle and the second heating stages, respectively, and the main parameters are summarized in Table 3.2. The exothermic peaks in Figure 3.5 A correlate to the T_c, which ranges from 70.41–113.17°C (Table 3.2). The T_c observed in the present study is lower than the T_c observed for PHAs synthesized by *B. megaterium* (Pradhan et al. 2018). The narrow crystalline peak observed for PHBV (Fig. 3.5 A) is ascribed to the high HV content in the polymer (Shang et al. 2012). The endothermic peaks in Figure 3.5 B correspond to the melting temperatures (T_m) of the PHAs, which ranged between 123.09–171.65°C and 146.94–179.25°C and is within the accepted ranges for PHAs (Możejko-Ciesielska and Kiewisz 2016). However, the T_m noted in the current study is higher than the T_m of 165.6°C previously observed for PHAs synthesized by *B. thuringiensis* (Sindhu et al. 2011). The T_m is influenced by the length of the side chain and functional groups, where long side chains present with a low T_m (Saranya and Shenbagarathai 2011). The double melting behavior is not uncommon for PHB and its copolymers (Chen et al. 2012). The first melting event that occurs at a low temperature is probably due to the melting of the imperfect crystals formed during the sample preparation (Sindhu et al. 2011). However, this peak is considered to be the true melting point since it most closely represents the behavior of the original, un-annealed crystals (Ferreira et al., 2002; Chen et al., 2012). The larger area of the second melting peak suggests a large degree of re-crystallization (Chen et al. 2012). The presence of two or more melting peaks can be due to the thickness of the crystals and/or re-crystallization that occurs during the heating process in the DSC (Ferreira et al. 2002). In addition, Sindhu et al. (2011) reported that the presence of two melting temperatures can also be due to the presence of co-monomer units in the polymer chain. Commercial PHBV was observed to have a lower T_m compared with PHBV synthesized when glucose and sucrose were used as carbon sources. This can be ascribed to the proportion of HV monomer units in the biopolymer, whereby an increase in the HV monomer fraction lowers the melting point of the polymer (Akdoğan and Çelik, 2018). Polymers with a lower T_m are desirable as they are proposed to have improved workability, ductility, and flexibility (Shang et al. 2012). The T_m of the recovered PHB using glycerol or starch as the carbon source was 178.60 and 179.25°C, respectively, and is within the 174–179°C range reported by Singh et al. (2015). The T_g of the PHAs is ~5°C irrespective of their source. Pradhan et al. (2018) explain that the ordered structure of the PHA results in the initial movement of the polymer chain relatively at a lower temperature, which leads to a lower

value of T_g. Nevertheless, the T_g observed in the presented study lies within the range of 2.5–10°C reported by Singh et al. (2015). The considerable difference in melting temperature and degradation temperature noted for the PHAs in the present study is desirable as it enables convenient polymer processing (Singh et al. 2015). The degree of crystallinity (X_c) is the most important characteristic among the different mechanical performance and processability properties of PHA. It is a reflection of the molecular conformation and intermolecular packing of the atoms of the material (Rodrigues et al. 2019). Ideally, X_c should be ≤ 50%; otherwise, challenges on polymer processing emerge, resulting in corrective actions that can incur an operation price rise (Rodrigues et al. 2019). In the present study, the X_c for copolymer PHAs was ~40% whereas, the PHB homopolymer is 56-59% and is therefore highly crystalline (Table 3.2). This observation is explained by Shang et al. (2012) who state that the crystallinity of a polymer increases as the HV content in the polymer decreases. A polymer with high crystallinity is stiff and brittle in nature (Singh et al. 2015; Możejko-Ciesielska and Kiewisz 2016). A polymer with a lower crystallinity is favorable as it would be less brittle and hence increases the range of applications (Pradhan et al. 2018).

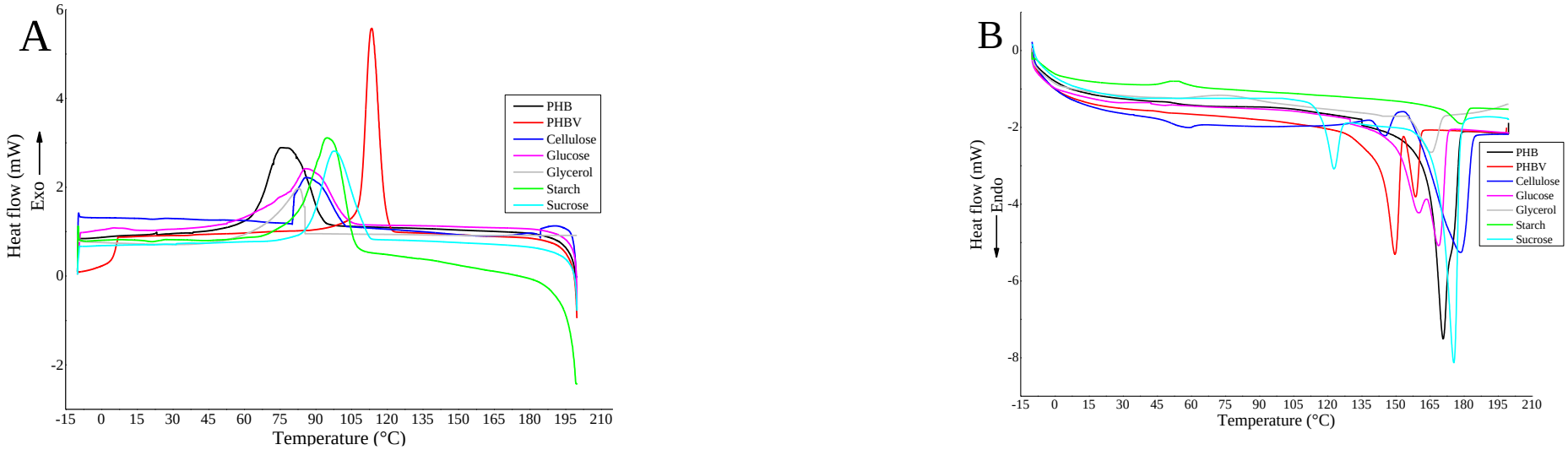

Figure 3.5: Differential scanning calorimetry thermograms of the cooling cycle (A) and the second heating cycle (B) for commercial PHB and PHBV, and the PHAs extracted for each carbon source used in the 72 h batch cultivation for PHA production by *B. thuringiensis*.

3.5. Conclusions

The present study successfully demonstrated the PHA-producing capability of *B. thuringiensis* using both simple and complex carbohydrates as sole carbon sources. While the application of staining procedures allowed for the rapid detection of PHAs and the assessment of PHA accumulation, this was not a reliable technique. The FTIR spectra of the extracted PHAs were comparable with peaks common to commercial PHB and PHBV. Of the five carbon sources tested, glucose produced the highest biomass and PHA yields. The PHAs were successfully characterized and, α-cellulose, glucose, and sucrose were superior carbon sources for the production of copolymers. However, based on DSC and TGA analysis, all carbons sources except α-cellulose resulted in PHAs that are marginally less thermostable compared with commercial PHB and PHBV. Nevertheless, this isolate is still a promising candidate as a PHA producer. The use of pure carbon sources aided in determining production kinetics and PHA yields at a lab-scale. However, the use of commercial carbohydrates for PHA production is not an economically viable approach, especially for large-scale PHA production. Thus, future studies will focus on industry waste as a carbon source for PHA production using *B. thuringiensis.*

3.6. References

Abinaya V, Balasubramanian R, Ramesh V, Natrajan N, Rajeshkannan V (2012) Exploration of polyhydroxyalkanoates production from rhizosphere soil bacteria. ENVIS Newsl 10:1–13.

Akdoğan M, Çelik E (2018) Purification and characterization of polyhydroxyalkanoate (PHA) from a *Bacillus megaterium* strain using various dehydration techniques. J Chem Technol Biotechnol 93:2292–2298.

Ali I, Jamil N (2014) Enhanced biosynthesis of poly(3-hydroxybutyrate) from potato starch by *Bacillus cereus* strain 64-INS in a laboratory-scale fermenter. Prep Biochem Biotechnol 44:822–833.

Aljuraifani AA, Berekaa MM, Ghazwani AA (2018) Perspectives of polyhydroxyalkanoate (PHAs) biopolymer production using indigenous bacteria: Screening and characterization. J Pure Appl Microbiol 12:1997–2009.

Amache R, Sukan A, Safari M, Roy I, Keshavarz T (2013) Advances in PHAs production. Chem Eng Trans 32:931–936.

Anderson AJ, Dawes EA (1990) Occurrence, metabolism, metabolic role, and industrial uses of bacterial polyhydroxyalkanoates. Microbiol Rev 54:450–472.

Andreeßen B, Steinbüchel A (2010) Biosynthesis and biodegradation of 3-hydroxypropionate-containing polyesters. Appl Environ Microbiol 76:4919–4925.

Apparao U, Krishnaswamy VG (2015) Production of polyhydroxyalkanoate (PHA) by a moderately halotolerant bacterium *Klebsiella pneumoniae* U1 isolated from rubber plantation area. Int J Environ Bioremediation Biodegrad 3:54–61.

Baidurah S, Kubo Y, Kuno M, Kodera K, Ishida Y, Yamane T, Ohtani H (2015) Rapid and direct compositional analysis of poly(3-hydroxybutyrate-co-3-hydroxyvalerate) in whole bacterial cells by thermally assisted hydrolysis and methylation-gas chromatography. Anal Sci 31:79–83.

Berlanga M, Montero MT, Hernández-Borrell J, Guerrero R (2006) Rapid spectrofluorometric screening of poly-hydroxyalkanoate-producing bacteria from microbial mats. Int Microbiol 9:95–102.

Bhagowati P, Pradhan S, Dash HR, Das S (2015) Production, optimization and characterization of polyhydroxybutyrate, a biodegradable plastic by *Bacillus* spp. Biosci Biotechnol Biochem 79:1454–1463.

Bhattacharya S, Dubey S, Singh P, Shrivastava A, Mishra S (2016) Biodegradable polymeric substances produced by a marine bacterium from a surplus stream of the biodiesel industry. Bioengineering 3:1–11.

Bhuwal AK, Singh G, Aggarwal NK, Goyal V, Yadav A (2014) Poly-β-hydroxybutyrate production and management of cardboard industry effluent by new *Bacillus* sp. NA10. Bioresour Bioprocess 1:1–11.

Bhuwal AK, Singh G, Aggarwal NK, Goyal V, Yadav A (2013) Isolation and screening of polyhydroxyalkanoates producing bacteria from pulp, paper, and cardboard industry wastes. Int J Biomater 2013:1–10.

Borah B, Thakur PS, Nigam JN (2002) The influence of nutritional and environmental conditions on the accumulation of poly-β-hydroxybutyrate in *Bacillus mycoides* RLJ B-

017. J Appl Microbiol 92:776–783.
Braunegg G, Bona R, Koller M (2004) Sustainable polymer production. Polym - Plast Technol Eng 43:1779–1793.
Caballero KP, Karel SF, Register RA (1995) Biosynthesis and characterization of hydroxybutyrate-hydroxycaproate copolymers. Int J Biol Macromol 17:86–92.
Carrasco F, Dionisi D, Martinelli A, Majone M (2005) Thermal stability of polyhydroxyalkanoates. J Appl Polym Sci 100:2111–2121.
Chan K-Y, Au KS (1987) Studies on cellulase production by a *Bacillus subtilis*. Antonie Van Leeuwenhoek 53:125–136.
Chen B-K, Lo S-H, Shih C-C, Artemov AV (2012) Improvement of thermal properties of biodegradable polymer poly(3-hydroxybutyrate) by modification with acryloyloxyethyl isocyanate. Polym Eng Sci 52:1524–1531.
Chen H, Pan S-C, Shaw G-C (2009) Identification and characterization of a novel intracellular poly(3-hydroxybutyrate) depolymerase from *Bacillus megaterium*. Appl Environ Microbiol 75:5290–5299.
Chiulan I, Panaitescu DM, Frone AN, Teodorescu M, Nicolae CA, Căşăricǎ A, Tofan V, Aurora Sălăgeanu (2016) Biocompatible polyhydroxyalkanoates/bacterial cellulose composites: Preparation, characterization, and *in vitro* evaluation. J Biomed Mater Res Part A 104A:2576–2584.
Department of Environmental Affairs and Tourism (2018) South Africa State of Waste Report. A report on the state of the environment. Final draft:1-112.
Edkie GN, Prasad DT (2014) *Bacillus* PHA synthase III C gene showed regulatory functions: An in-silico analysis. Biotechnology 13:143–151.
Ferreira BMP, Zavaglia CAC, Duek EAR (2002) Films of PLLA/PHBV: Thermal, morphological, and mechanical characterization. J Appl Polym Sci 86:2898–2906.
Getachew A, Woldesenbet F (2016) Production of biodegradable plastic by polyhydroxybutyrate (PHB) accumulating bacteria using low cost agricultural waste material. BMC Res Notes 9:1–9.
Gomaa EZ (2014) Production of polyhydroxyalkanoates (PHAs) by *Bacillus subtilis* and *Escherichia coli* grown on cane molasses fortified with ethanol. Brazilian Arch Biol Technol 57:145–154.
Govender L (2013) Seasonal variation of microflora and their effects on the quality of wood chips intended for pulping. PhD Dissertation. University of KwaZulu-Natal.
Halami PM (2008) Production of polyhydroxyalkanoate from starch by the native isolate *Bacillus cereus* CFR06. World J Microbiol Biotechnol 24:805–812.
Hassan MA, Bakhiet EK, Ali SG, Hussien HR (2016) Production and characterization of polyhydroxybutyrate (PHB) produced by *Bacillus* sp. isolated from Egypt. J Appl Pharm Sci 6:46–51.
Helm D, Naumann D (1995) Identification of some bacterial cell components by FT-IR spectroscopy. FEMS Microbiol Lett 126:75–79.
Höfer P, Choi YJ, Osborne MJ, Miguez CB, Vermette P, Groleau D (2010) Production of functionalized polyhydroxyalkanoates by genetically modified *Methylobacterium extorquens* strains. Microb Cell Fact 9:1–13.

Isak I, Patel M, Riddell M, West M, Bowers T, Wijeyekoon S, Lloyd J (2016) Quantification of polyhydroxyalkanoates in mixed and pure cultures biomass by Fourier transform infrared spectroscopy: Comparison of different approaches. Lett Appl Microbiol 63:139–146.

Jiang G, Hill DJ, Kowalczuk M, Johnston B, Adamus G, Irorere V, Radecka I (2016) Carbon sources for polyhydroxyalkanoates and an integrated biorefinery. Int J Mol Sci 17:1–21.

Juengert JR, Patterson C, Jendrossek D (2018) Poly(3-hydroxybutyrate) (PHB) polymerase PhaC1 and PHB depolymerase PhaZa1 of *Ralstonia eutropha* are phosphorylated *in vivo*. Appl Environ Microbiol 84:1–12.

Kourmentza C, Plácido J, Venetsaneas N, Burniol-Figols A, Varrone C, Gavala HN, Reis MAM (2017) Recent advances and challenges towards sustainable polyhydroxyalkanoate (PHA) production. Bioengineering 4:1–43.

Kumar M, Singhal A, Verma PK, Thakur IS (2017) Production and characterization of polyhydroxyalkanoate from lignin derivatives by *Pandoraea* sp. ISTKB. ACS Omega 2:9156–9163 .

Kynadi AS, Suchithra TV (2014) Polyhydroxyalkanoates: Biodegradable plastics for environmental conservation. In: Pramanik K, Jayanta Kumar Patra (eds) Industrial & Environmental Biotechnology. Studium Press (India) Pvt. Ltd., pp 1–15

Łabuzek S, Radecka I (2001) Biosynthesis of PHB tercopolymer by *Bacillus cereus* UW85. J Appl Microbiol 90:353–357.

Latorre JD, Hernandez-Velasco X, Kuttappan VA, Wolfenden RE, Vicente JL, Wolfenden AD, Bielke LR, Prado-Rebolledo OF, Morales E, Hargis BM, Guillermo T (2015) Selection of *Bacillus* spp. for cellulase and xylanase production as direct-fed microbials to reduce digesta viscosity and *Clostridium perfringens* proliferation using an *in vitro* digestive model in different poultry diets. Front Vet Sci 2:1–8.

Lemoigne M (1925) Etudes sur L'autolyse microbienne acidification par formation D'acide β-oxybutyrique. Ann Inst Pasteur 39:144–173.

Li H, Zhou S, Johnson T, Vercruysse K, Lizhi O, Ranganathan P, Phambu N, Ropelewski AJ, Thannhauser TW (2017) Genome structure of *Bacillus cereus* tsu1 and genes involved in cellulose degradation and poly-3-hydroxybutyrate synthesis. Int J Polym Sci 2017:1–12.

Liu Y, Huang S, Zhang Y, Xu F (2014) Isolation and characterization of a thermophilic *Bacillus shackletonii* K5 from a biotrickling filter for the production of polyhydroxybutyrate. J Environ Sci 26:1453–1462.

Martínez-Sanz M, Villano M, Oliveira C, Albuquerque MGE, Majone M, Reis M, Lopez-Rubio A, Lagaron JM (2014) Characterization of polyhydroxyalkanoates synthesized from microbial mixed cultures and of their nanobiocomposites with bacterial cellulose nanowhiskers. N Biotechnol 31:364–376.

Masood F, Abdul-Salam M, Yasin T, Hameed A (2017) Effect of glucose and olive oil as potential carbon sources on production of PHAs copolymer and tercopolymer by *Bacillus cereus* FA11. 3 Biotech 7:1–9.

Masood F, Hasan F, Ahmed S, Hameed A (2012) Biosynthesis and characterization of poly(3-hydroxybutyrate-co-3-hydroxyvalerate) from *Bacillus cereus* FA11 isolated from TNT-contaminated soil. Ann Microbiol 62:1377–1384.

Mitra R, Xu T, Xiang H, Han J (2020) Current developments on polyhydroxyalkanoates synthesis by using halophiles as a promising cell factory. Microb Cell Fact 19:1–30.

Mohandas SP, Balan L, Jayanath G, Anoop BS, Philip R, Cubelio SS, Singh ISB (2018) Biosynthesis and characterization of polyhydroxyalkanoate from marine *Bacillus cereus* MCCB 281 utilizing glycerol as carbon source. Int J Biol Macromol 119:380–392.

Mohapatra S, Pattnaik S, Maity S, Mohapatra S, Sharma S, Akhtar J, Pati S, Samantaray DP, Varma A (2020) Comparative analysis of PHAs production by *Bacillus megaterium* OUA^{T} 016 under submerged and solid-state fermentation. Saudi J Biol Sci 27:1242–1250.

Mohapatra S, Sarkar B, Samantaray DP, Daware A, Maity S, Pattnaik S, Bhattacharjee S (2017) Bioconversion of fish solid waste into PHB using *Bacillus subtilis* based submerged fermentation process. Environ Technol 38:3201–3208.

Morya R, Kumar M, Thakur IS (2018) Utilization of glycerol by *Bacillus* sp. ISTVK1 for production and characterization of polyhydroxyvalerate. Bioresour Technol Reports 2:1–6.

Mostafa YS, Alrumman SA, Otaif KA, Alamri SA, Mostafa MS, Sahlabji T (2020) Production and characterization of bioplastic by polyhydroxybutyrate accumulating *Erythrobacter aquimaris* isolated from mangrove rhizosphere. Molecules 25:1–20.

Możejko-Ciesielska J, Kiewisz R (2016) Bacterial polyhydroxyalkanoates: Still fabulous? Microbiol Res 192:271–282.

Muhammadi S, Afzal M, Hameed S (2015) Bacterial polyhydroxyalkanoates-eco-friendly next generation plastic: Production, biocompatibility, biodegradation, physical properties and applications. Green Chem Lett Rev 8:56–77.

Munir S, Iqbal S, Jamil N (2015) Polyhydroxyalkanoates (PHA) production using paper mill wastewater as carbon source in comparison with glucose. J Pure Appl Microbiol 9:1–8.

Munoz LEA, Riley MR (2008) Utilization of cellulosic waste from tequila bagasse and production of polyhydroxyalkanoate (PHA) bioplastics by *Saccharophagus degradans*. Biotechnol Bioeng 100:882–888.

Nagamani P, Mahmood SK (2013) Production of poly(3-hydroxybutyrate-co-3-hydroxyvalerate) by a novel *Bacillus* OU40^{T} from inexpensive carbon sources. Int J Pharma Bio Sci 4:182–193.

Naheed N, Jamil N (2014) Optimization of biodegradable plastic production on sugar cane molasses in *Enterobacter* sp. SEL2. Brazilian J Microbiol 426:417–426.

Naheed N, Jamil N, Hasnain S, Abbas G (2012) Biosynthesis of polyhydroxybutyrate in *Enterobacter* sp. SEL2 and Enterobacteriaceae bacterium sp. PFW1 using sugar cane molasses as media. African J Biotechnol 11:3321–3332.

Nargotra P, Vaid S, Bajaj BK (2016) Cellulase production from *Bacillus subtilis* SV1 and its application potential for saccharification of ionic liquid pretreated pine needle biomass under one pot consolidated bioprocess. Fermentation 2:1–16.

Ntaikou I, Koumelis I, Kamilari M, Iatridi Z, Tsitsilianis C, Lyberatos G (2019) Effect of nitrogen limitation on polyhydroxyalkanoates production efficiency, properties and microbial dynamics using a soil-derived mixed continuous culture. Int J Biobased Plast 1:31–47.

Odeniyi OA, Adeola OJ (2017) Production and characterization of polyhydroxyalkanoic acid

from *Bacillus thuringiensis* using different carbon substrates. Int J Biol Macromol 104:407–413.

Olivera ER, Arcos M, Naharro G, Luengo JM (2009) Unusual PHA biosynthesis. In: Chen G-Q (ed) Plastics from Bacteria: Natural Functions and Applications, 2010th edn. Springer-Verlag, Berlin Heidelberg, pp 133–168.

Paul RL (2018) Genetic engineering of *Escherichia coli* for the production of polyhydroxyalkanoates. Masters Thesis. University of KwaZulu-Natal.

Pillai AB, Kumar AJ, Thulasi K, Kumarapillai H (2017) Evaluation of short-chain-length polyhydroxyalkanoate accumulation in *Bacillus aryabhattai*. Brazilian J Microbiol 48:451–460.

Pradhan S, Dikshit PK, Moholkar VS (2018) Production, ultrasonic extraction, and characterization of poly(3-hydroxybutyrate) (PHB) using *Bacillus megaterium* and *Cupriavidus necator*. Polym Adv Technol 29:2392–2400.

Rastogi G, Muppidi GL, Gurram RN, Adhikari A, Bischoff KM, Hughes VSR, Apel WA, Bang SS, Dixon DJ, Sani RK (2009) Isolation and characterization of cellulose-degrading bacteria from the deep subsurface of the Homestake gold mine, Lead, South Dakota, USA. J Ind Microbiol Biotechnol 36:585–598.

Reddy SV, Thirumala M, Mahmood SK (2009) A novel *Bacillus* sp. accumulating poly(3-hydroxybutyrate-co-3- hydroxyvalerate) from a single carbon substrate. J Ind Microbiol Biotechnol 36:837–843.

Rehm BHA (2010) Bacterial polymers: Biosynthesis, modifications and applications. Nat Rev Microbiol 8:578–592.

Rehm BHA (2003) Polyester synthases: Natural catalysts for plastics. Biochem J 376:15–33.

Rodrigues PR, Nunes JMN, Lordelo LN, Druzian JI (2019) Assessment of polyhydroxyalkanoate synthesis in submerged cultivation of *Cupriavidus necator* and *Burkholderia cepacia* strains using soybean as substrate. Brazilian J Chem Eng 36:73–83.

Sadasivam S, Sigamani S, Venkatachalam H, Ramamurthy D (2018) A new method for the production of polyhydroxyalkanoates by *Bacillus* sp. and detect the presence of PHA synthase. Smart Sci 6:105–116.

Saranya V, Shenbagarathai R (2011) Production and characterization of PHA from recombinant *E. coli* harbouring *PHAC1* gene of indigenous *Pseudomonas* sp. LDC-5 using molasses. Brazilian J Microbiol 42:1109–1118.

Sawant SS, Tran TK, Salunke BK, Kim BS (2017) Potential of *Saccharophagus degradans* for production of polyhydroxyalkanoates using cellulose. Process Biochem 57:50–56.

Shahid S, Mosrati R, Ledauphin J, Amiel C, Fontaine P, Gaillard J-L, Corroler D (2013) Impact of carbon source and variable nitrogen conditions on bacterial biosynthesis of polyhydroxyalkanoates: Evidence of an atypical metabolism in *Bacillus megaterium* DSM 509. J Biosci Bioeng 116:302–308.

Shamala TR, Chandrashekar A, Vijayendra SVN, Kshama L (2003) Identification of polyhydroxyalkanoate (PHA)-producing *Bacillus* spp. using the polymerase chain reaction (PCR). J Appl Microbiol 94:369–374.

Shang L, Fei Q, Zhang YH, Wang XZ, Fan D-D, Chang HN (2012) Thermal properties and biodegradability studies of poly(3-hydroxybutyrate-co-3-hydroxyvalerate). J Polym

Environ 20:23–28.
Shrivastav A, Mishra SK, Shethia B, Pancha I, Jain D, Mishra S (2010) Isolation of promising bacterial strains from soil and marine environment for polyhydroxyalkanoates (PHAs) production utilizing Jatropha biodiesel byproduct. Int J Biol Macromol 47:283–287.
Sindhu R, Ammu B, Binod P, Deepthi SK, Ramachandran KB, Soccol CR, Pandey A (2011) Production and characterization of poly-3-hydroxybutyrate from crude glycerol by *Bacillus sphaericus* NII 0838 and improving its thermal properties by blending with other polymers. Brazilian Arch Biol Technol 54:783–794.
Singh G, Kumari A, Mittal A, Yadav A, Aggarwal NK (2013) Poly β-hydroxybutyrate production by *Bacillus subtilis* NG220 using sugar industry waste water. Biomed Res Int 2013:1–10.
Singh M, Kumar P, Ray S, Kalia VC (2015) Challenges and opportunities for customizing polyhydroxyalkanoates. Indian J Microbiol 55:235–249.
Singh M, Patel SK, Kalia VC (2009) *Bacillus subtilis* as potential producer for polyhydroxyalkanoates. Microb Cell Fact 8:1–11.
Steinbüchel A, Hustede E, Liebergesell M, Pieper U, Timm A, Valentin H (1992) Molecular basis for biosynthesis and accumulation of polyhydroxyalkanoic acids in bacteria. FEMS Microbiol Rev 103:217–230.
Tajima K, Igari T, Nishimura D, Nakamura M, Satoh Y, Munekata M (2003) Isolation and characterization of *Bacillus* sp. INT005 accumulating polyhydroxyalkanoate (PHA) from gas field soil. J Biosci Bioeng 95:77–81.
Tan GA, Chen C-L, Ge L, Li L, Wang L, Zhao L, Mo Y, Tan SN, Wang J-Y (2014) Enhanced gas chromatography-mass spectrometry method for bacterial polyhydroxyalkanoates analysis. J Biosci Bioeng 117:379–382.
Thirumala M, Reddy S V, Mahmood SK (2010) Production and characterization of PHB from two novel strains of *Bacillus* spp. isolated from soil and activated sludge. J Ind Microbiol Biotechnol 37:271–278.
Thomas T, Sudesh K, Bazire A, Elain A, Tan HT, Lim H, Bruzaud S (2020) PHA production and PHA synthases of the halophilic bacterium *Halomonas* sp. SF2003. Bioengineering 7:1–22.
Torri C, Cordiani H, Samorì C, Favaro L, Fabbri D (2014) Fast procedure for the analysis of poly(hydroxyalkanoates) in bacterial cells by off-line pyrolysis/gas-chromatography with flame ionization detector. J Chromatogr A 1359:230–236.
Valappil SP, Boccaccini AR, Bucke C, Roy I (2007a) Polyhydroxyalkanoates in Gram-positive bacteria: Insights from the genera *Bacillus* and *Streptomyces*. Antonie Van Leeuwenhoek 91:1–17.
Valappil SP, Misra SK, Boccaccini AR, Keshavarz T, Bucke C, Roy I (2007b) Large-scale production and efficient recovery of PHB with desirable material properties, from the newly characterised *Bacillus cereus* SPV. J Biotechnol 132:251–258.
Valappil SP, Peiris D, Langley GJ, Herniman JM, Boccaccini AR, Bucke C, Roy I (2007c) Polyhydroxyalkanoate (PHA) biosynthesis from structurally unrelated carbon sources by a newly characterized *Bacillus* spp. J Biotechnol 127:475–487.
Verster C, Bouwman H (2020) Land-based sources and pathways of marine plastics in a South

African context. S Afr J Sci 116:1–9.
Yue H, Ling C, Yang T, Chen X, Chen Y, Deng H, Wu Q, Chen J, Chen G-Q (2014) A seawater-based open and continuous process for polyhydroxyalkanoates production by recombinant *Halomonas campaniensis* LS21 grown in mixed substrates. Biotechnol Biofuels 7:1–12.
Zhang H-F, Ma L, Wang Z-H, Chen G-Q (2009) Biosynthesis and characterization of 3-hydroxyalkanoate terpolyesters with adjustable properties by *Aeromonas hydrophila*. Biotechnol Bioeng 104:582–589.
Zuriani R, Vigneswari S, Azizan MNM, Majid MIA, Amirul AA (2013) A high throughput Nile Red fluorescence method for rapid quantification of intracellular bacterial polyhydroxyalkanoates. Biotechnol Bioprocess Eng 18:472–478.

CHAPTER FOUR

Consolidated bioprocessing fermentation of pulp and paper mill sludge for polyhydroxyalkanoate production using *Bacillus thuringiensis*

4.1. Abstract

Polyhydroxyalkanoates (PHAs) are microbial biopolymers that are fully biodegradable and have similar physiochemical characteristics to conventional synthetic plastics. Carbohydrate-rich lignocellulosic biomasses such as pulp and paper mill sludge (PPMS) have the potential to serve as inexpensive feedstock in fermentation strategies for the synthesis of PHAs. In this study, neutral semi-sulphite chemical pulping and cardboard recycling mill (NSSC-CR) and prehydrolysis kraft and kraft pulping mill (PHKK) PPMS were first characterized to determine their suitability as feedstock in a consolidated bioprocessing fermentation strategy. Thereafter, both PPMS types were applied as the sole substrate for cell growth and PHA production using *Bacillus thuringiensis*. PHKK PPMS is a more favorable feedstock as it contained a higher amount of glucose (~64%), lower ash content (6.89%) and higher volatile fatty acid content (~75%) compared with NSSC-CR PPMS. After the 72 h fermentation, images from scanning electron microscopy revealed fibrils on the PPMS fibers. PHKK PPMS was also more efficacious feedstock for both cell proliferation and PHA production. A reduction in biochemical oxygen demand from 168 mg/L to 115 mg/L, chemical oxygen demand from 34 mg/L to 12 mg/L and glucose from 64% to 47% as well as biomass production of 2.74 g L^{-1} and a 25.91% PHA yield was observed. From FTIR analysis, the nature of the PHAs displayed spectra similar to commercial PHB and PHBV. Py-GC/MS analysis revealed that PHBV and a HB-HV-HHx terpolymer were synthesized using NSSC-CR and PHKK, respectively. Furthermore, the PHAs obtained using PHKK PPMS demonstrated slightly higher thermostability and lower crystallinity compared with commercial PHB and PHBV. This study explored the suitability of PPMS to be applied as a low-cost substrate in a fermentative strategy for bacterial PHA production. In addition, the potential of valorizing PPMS waste biomass whilst subsequently producing value-added PHAs with varying compositions and characteristics was also demonstrated.

Keywords: Polyhydroxyalkanoate, *Bacillus thuringiensis*, pulp and paper mill sludge, consolidated bioprocessing

4.2. Introduction

Disposal practices such as the burning and dumping of petroleum-derived plastics gives rise to distressing environmental issues regarding air and water quality as well as soil pollution (Makgae 2011). Furthermore, the finite nature and rapid depletion of fossil fuels due to growing global energy demands may consequently result in petrochemical plastics not being a viable option in the future. This has led researchers around the globe to seek solutions to petroleum derived plastics and to explore the sustainable production of eco-friendly plastic material whilst utilizing alternative renewable feedstock.

Polyhydroxyalkanoates (PHAs) are a family of naturally-occurring biopolyesters that are synthesized by a plethora of bacteria. PHAs accumulate as intracellular granules that are usually lipid in nature and also serve as carbon and energy reserves for the microbe (Tan et al. 2014). PHAs are competitive with petroleum-based plastics in terms of quality, physical and mechanical characteristics (Aldor and Keasling 2003; Zhang et al. 2009; Andreeßen and Steinbüchel 2010). However, despite their environmental advantages and their wide field of application, the use and industrial profitability of PHAs are limited by their high production costs. The production is highly expensive, mainly due to the substrate or culture medium employed, thereby preventing PHAs from being economically competitive to petrochemical plastics. To overcome this impediment, the evaluation and incorporation of low-cost, non-conventional, substrates in fermentative processes for PHA production are required.

Lignocellulosic biomass is one such renewable resource that is relatively low-cost and in plentiful supply. Lignocellulose comprises of three main polymers, 40–50% cellulose, 20–40% hemicelluloses, and 20–30% lignin, with varying compositions depending on type, species, and source of biomass (Schuster and Chinn 2013; Łukajtis et al. 2018). Cellulose is the main component of the biomass and it typically contains 50-80% complex carbohydrates consisting of C_5 and C_6 sugar units (Jouzani and Taherzadeh 2015). Lignocellulosic biomass is widely considered as an attractive substrate for PHA production (Nagamani and Mahmood 2013; Li et al. 2017; Sawant et al. 2017). Pulp and paper mill sludge (PPMS) is a lignocellulosic waste that is a by-product of the pulp and paper making process and is one of the main solid wastes from the pulp and paper industry. South Africa alone produces an estimated 0.5 million tons of PPMS per annum (Boshoff et al. 2016). PPMS can accumulate on the premises of the mill or is disposed by landfilling, landspreading and/or incineration and can result in serious handling,

soil, water and air pollution problems (Rashid et al. 2006; Abdullah et al. 2015). PPMS can also contain elevated biochemical oxygen demand (BOD) and chemical oxygen demand (COD) concentrations that have a negative impact on receiving water sources and aquatic life (Agarry and Ayobami 2011). BOD is the oxygen required to completely oxidize the pollutant and COD is the amount of organic matter that can be chemically oxidized (Agarry and Ayobami 2011). Generally, PPMS is a mixture of primary sludge and secondary sludge with typical fiber content between 11–95% and cellulose fiber being the key characteristic component in the PPMS (Gibril et al. 2018; Zhang et al. 2020). Cellulosic components of PPMS include 20-75% of cellulose and hemicellulose which is rich in carbohydrates thereby making PPMS a desirable source of sugars (Gibril et al. 2018; Liu et al. 2018). Thus, PPMS rich in cellulosic fibers is a raw material with potential to be bioconverted or valorized since it is readily available, abundant, renewable and has high carbohydrate and low lignin contents (Geng et al. 2005; Mendes et al. 2016).

However, due to the complex structure of lignocellulosic biomass, a complex multi-step depolymerizing process including pretreatment and saccharification is first required to convert the lignocellulosic biomass to simple sugars, followed by microbial fermentation. Depending on the process and biomass used, enzymatic pretreatment may also be required. Thus the process may incur time and cost constraints on the production cost of PHAs (Jouzani and Taherzadeh 2015). To this end, significant research has focused on consolidated bioprocessing (CBP). CBP technologies employ a single organism or consortia of microorganisms that produce their own cellulolytic and hemicellulolytic enzymes for lignocellulose decomposition. During the CBP process, enzyme production, enzymatic saccharification, and fermentation of the resulting sugars into valuable products proceed simultaneously (Schuster and Chinn 2013). This conversion approach combines all rate-limiting processes such as pretreatment, saccharification, and fermentation, within a single reactor thereby potentially decreasing operating cost and increases conversion efficiencies. (Jouzani and Taherzadeh 2015). CBP as a promising approach will circumvent the cost and restrictions of conventional fermentation strategies that use lignocellulosic biomass feedstock. Currently, the CBP technology is still in infancy stages of development, no commercially viable CBP microbe has been reported and ideal microorganisms and/or conditions at industrial scale are yet to be fully elucidated (Brethauer and Studer 2014). Nonetheless, CBP using lignocellulosic biomass as feedstock has been successfully applied for the production of biofuels (Olguin-Maciel et al. 2020), bioethanol

(van Zyl et al. 2007), butanol (Wen et al. 2020) and PHAs (Sawant et al. 2017; 2018; Wang et al. 2018).

Thus far, based on data from Chapter Three, *Bacillus thuringiensis* DF7 has proven to be a promising PHA-producing strain and also displayed its capability to convert commercially available α-cellulose to PHA. This study implemented a CBP strategy to evaluate the capacity of raw (untreated) neutral semi-sulphite chemical pulping and cardboard recycling mill (NSSC-CR) and prehydrolysis kraft and kraft pulping mill (PHKK) PPMS to serve as the sole feedstock for both cell proliferation and PHA production using *B. thuringiensis*. After the synthesized PHAs were extracted and quantified, they were characterized and compared with commercial PHB and PHBV.

4.3. Materials and Methods

4.3.1. Bacterial strain, growth, and storage conditions

As per section 3.3.1

4.3.2. Sample material

Neutral semi-sulphite chemical pulping and cardboard recycling mill (NSSC-CR) and prehydrolysis kraft and kraft pulping mill (PHKK) PPMS samples were collected from local pulp and paper mills in South Africa. Samples were collected in plastic bags and stored in air tight plastic containers at 4°C until further use.

4.3.3. Characterization of PPMS sample materials

4.3.3.1. High performance liquid chromatography (HPLC)

NSSC-CR and PHKK PPMS samples were prepared using standard Technical Association of the Pulp and Paper Industry (TAPPI) method T 249 cm-09. Thereafter, HPLC was used to quantitatively determine glucose, the carbohydrate that constitutes the cellulose composition of the PPMS.

4.3.3.2. Lignin content

The TAPPI method T 222 om-11 was applied to determine the percentage of acid-insoluble lignin in the NSSC-CR and PHKK PPMS samples.

The percentage lignin was calculated using the equation:

$$\text{Lignin (\%)} = \frac{\text{A} - \text{B}}{\text{W}} \times 100$$

Where, A = mass of filter paper with insoluble material (g), B = mass of pre-weighed filter paper (g) and W = mass of sample weighed out for the analysis (g)

4.3.3.3. Ash content

The percentage of ash in the samples was determined using the TAPPI protocol T 211 om-12. The percentage ash content was calculated using the equation:

$$\text{Ash (\%)} = \frac{\text{Weight of ash (g)}}{\text{Weight of original dry sample (g)}} \times 100$$

4.3.3.4. Volatile fatty acids

Thermally assisted hydrolysis and methylation-gas chromatography (THM-GC) using pyrolysis-gas chromatography/mass spectrometry (py-GC/MS) in the presence of the strong organic alkali, tetramethylammonium hydroxide (TMAH), was employed to qualitatively and quantitatively elucidate the volatile fatty acids (VFAs) present in the NSSC-CR and PHKK PPMS. A micro-furnace based Multi-Shot Pyrolyzer EGA/PY-3030D (Frontier Laboratories Ltd.) with a GCMS-QP2010 Ultra series (Shimadzu Corporation) for evolved gas analysis (EGA-MS) and single-shot analysis was used. For the analysis, a 200 µg sample of air-dried PPMS was emulsified with TMAH and added into the pyrolysis cup, and thereafter inserted into the quartz tube in the pyrolyzer furnace and pyrolyzed at 500°C for 20 msec (interface of 250°C). The pyrolyzates were introduced into a GC separation column (Ultra Alloy-5 column) with an oven temperature of 50°C with the following thermal program: initial oven temperature set at 50°C held for 2 min, followed by an increase to 200°C with a flow rate of 5°C min^{-1} and held for 4 min resulting in a total run time of 36 min. The main peaks observed were identified by comparing their mass spectra with those in NIST library database. The compounds were identified based on retention time and only mass spectra with similarities that were 85% and above were considered genuine fits.

The quantity of each VFA was determined using the following equation:

$$\text{H}_{\text{a,b,c,d,or e}}(\%) = \frac{\text{area H}_{\text{a,b,c,d,or e}}}{\text{area H}_\text{a} + \text{area H}_\text{b} + \text{area H}_\text{c} + \text{area H}_\text{d} + \text{area H}_\text{e}} \times 100$$

Where a, b, c, d and e represent the VFAs acetic acid, propanoic acid, butyric acid, valeric acid, and caproic acid, respectively.

4.3.3.5. Nitrogen, biochemical oxygen demand, and chemical oxygen demand

The total nitrogen, biochemical oxygen demand (BOD_5), and chemical oxygen demand (COD) of the samples were determined photometrically using the SpectroQuant® Nova 60 cell test (Merck). For COD analysis, digestion was conducted in a SpectroQuant® TR 420 thermoreactor (Merck) at 148°C for 2 h, following the manufacturer's instructions.

4.3.4. Consolidated bioprocessing fermentation

The consolidated bioprocessing (CBP) fermentation was conducted in a stoppered 2 L Erlenmeyer flask containing 2% (w/v) NSSC-CR or PHKK PPMS (nutrient source) and minimal salt medium (3.7 g KH_2PO_4, 7.5 g K_2HPO_4, 1 mL f 246.5 g L^{-1} $MgSO_4.7H_2O$; 1 L distilled H_2O), 1.5 mL trace elements solution (0.03 g L^{-1} $MnCl_2.4H_2O$, 0.2 g L^{-1} $CoCl_2.6H_2O$, 0.01 g L^{-1} $CuCl_2.2H_2O$, 1.4 g L^{-1} $ZnSO_4.7H_2O$, 0.3 g L^{-1} H_3BO_3, 0.02 g L^{-1} $NiCl_2.6H_2O$, 0.02 g L^{-1} $NaMoO_4.H_2O$ dissolved in 1 L distilled H_2O). The suspension was autoclaved (121°C, 15 psi, 1 h), cooled to room temperature, and 10% (v/v) inoculum of *B. thuringiensis* culture was added. Following incubation at 37°C in a rotary shaker at 200 revolutions per minute (rpm) for 72 h, different process parameters such as cell proliferation (CFU/mL), glucose content, BOD_5 and COD were analyzed after initial inoculation of *B. thuringiensis* and thereafter every 12 h for the duration of the fermentation, using the protocols described above.

4.3.5. Scanning electron microscopy

Samples taken before and after the CBP fermentation were air dried sludge and placed on a metal stub using carbon tape. Stubs were coated using a Quorum 150RES gold sputter coater. Micrographs were captured at 200× using a Carl Zeiss Field emission gun scanning electron microscope (FEG-SEM) Ultra Plus Field.

4.3.6. PHA extraction

As per section 3.3.5

4.3.7. Fourier-transform infrared spectroscopy (FTIR)

As per section 3.3.6

4.3.8. Polymer composition

As per section 3.3.7

4.3.9. Thermogravimetric analysis (TGA) and differential scanning calorimetry (DSC)

As per section 3.3.8

4.3.10. Statistical analysis

A one-way ANOVA and SPSS (V 27.0) was used to determine the effects of the PPMS on biomass, PHA yields, polymer composition, thermal properties as well as changes in glucose, BOD_5 and COD contents. Where necessary, a Bonferroni Post-Hoc analysis was conducted and a $p < 0.05$ was considered as statistically significant.

4.4. Results and Discussion

4.4.1. PPMS compositional analysis

Compositional analysis of NSSC-CR and PHKK PPMS was conducted and summarized in Table 4.1. Currently, in South Africa, there are no published guidelines on the acceptable limits for the BOD and COD of industrial solid waste to be discharged at landfill. Therefore, it is inconclusive as to whether the PPMS used in the present study is regarded as safe for disposal at landfill. However, it is known that the low BOD: COD of 0.2:1 (Table 4.1) is unfavorable for biological waste samples (Iloms et al. 2020). A ratio <0.3 indicates that toxic compounds are present and a natural, chemical or biological treatment is required to stabilize the waste prior to disposal (van der Merwe-Botha and Manus 2011; Kamali et al. 2019). The glucose content of 64.21% observed in the PHKK PPMS is higher than the glucose contents of 44% reported by Kang et al. (2011) and 24.5% by Prasetyo et al. (2010) for PPMS. The lignin and ash content of the PHKK PPMS is also lower than the 8.1% lignin and 36% ash content reported by Kang et al. (2012). Scott and Smith (1995) state that there are significant variations within the same categories of pulp and papermaking mill where varying amounts of sludge are produced, bearing distinctly different compositions. Ochoa de Alda and Torrea (2006) explain that variation in PPMS from kraft pulp and paper mills is mainly due to the efficiency of the pulping chemicals recovery system which in turn modifies the inorganic content of sludges. It was elucidated that PHKK PPMS has a lignin content of 19.28% whereas NSSC-CR PPMS has a higher lignin content of 46.1% (Table 4.1). Alkasrawi et al. (2016) and Mongkhonsiri et al. (2018) explain that sludge from kraft pulping has low lignin content due to delignification during the cooking process in Kraft mills whereby most lignin is separated from raw material into black liquor. PHKK PPMS also has a lower ash content of 6.89% compared with NSSC-

CR PPMS that has an ash content of 23.4% (Table 4.1). Ochoa de Alda (2008) proposed the concept of dividing PPMS into high-ash (> 30%, w/w) and low-ash (< 30%, w/w) categories. High-ash sludges were obtained from specialty-grade paper mills or recycled pulp mills, suggesting that the high-ash content was due to the presence of papermaking fillers. Low-ash sludges were obtained from in ground wood and some kraft pulp mills. Likon and Trebše (2012) state that low ash sludge are from primary, secondary or biological sludges generated by pulp or paper mills. This concurs with the sample from the present study which is from a kraft mill and has a low ash content of 6.89%. PPMS with low ash content has also been reported by Dabrowska et al. (2018) who report on sludge with ash content ranging from 5.19-7.11%. The low ash content in the PPMS sample can also be attributed to efforts in precipitating and collecting $CaCO_3$ and recycling it during the kraft process (Ferreira et al. 2004; He and Liu 2017; Simão et al. 2018). The low content of ash in the PHKK PPMS and the high content of ash in the NSSC-CR PPMS concurs with findings reported by Al-Kaabi et al. (2018). Py-GC/MS analysis was used to determine the presence of volatile fatty acids (VFAs) in the PPMS samples (supplementary material S2.1-S2.2). The VFAs reported here are linear short-chain fatty acids containing from two (acetic acid) to six (caproic acid) carbon atoms. PHKK PPMS was observed to have a high VFA content of 63.2% and NSSC-CR had a slightly lower content of 45.79%. VFAs are produced during anaerobic mixed culture fermentation and it is probable that the VFAs elucidated herein (Table 4.1) were produced by the native microbial population during anaerobic digestion of PPMS while in storage. Recently, much attention has been paid to the production and recovery of VFAs due to their potential to serve as renewable carbon sources, cheap precursors and a promising feedstock for PHA production (Kumar et al. 2019; Szacherska et al. 2021). The synthesis of PHAs using VFAs is considered to be an economical approach. Furthermore, PHA produced from VFAs are known to be copolymers with promising properties of PHAs analogous to the petro-derived plastics (Chakraborty et al. 2009; Ciesielski and Przybylek 2014).

Table 4.1: Compositional analysis of the neutral semi-sulphite chemical pulping and cardboard recycling mill (NSSC-CR) and prehydrolysis kraft and kraft pulping mill (PHKK) pulp and paper mill sludge samples collected from local pulp and paper mills in South Africa

					Component (%)							
					Cellulose			Volatile Fatty Acids				
PPMS	**BOD (mg/L)**	**COD (mg/L)**	**BOD:COD**	**Nitrogen (mg/L)**	**Glucose**	**Lignin**	**Ash**	**Acetic**	**Propanoic**	**Butyric**	**Valeric**	**Caproic**
NSSC-CR	40.53	190.63	0.21:1	0.5	35.48	45	22	23.54	2.59	15.35	2.12	2.19
PHKK	32.6	165.88	0.20:1	2	64.21	19.28	6.89	18.41	5.82	20.69	10.88	7.40

4.4.2. Fermentation studies

Figure 4.1 depicts the time course of CBP cultivation of *B. thuringiensis* and the kinetic parameters are presented in Table 4.2. The data from replicate CBP fermentations and the subsequent utilization of glucose were pooled to show the average growth response of *B. thuringiensis* in NSSC-CR and PHKK PPMS (Fig 4.1 A). PHKK PPMS was a better feedstock for *B. thuringiensis* and significantly impacted the yield of biomass (CDW) and PHA yield ($p < 0.05$). The culture exhibited an initial lag phase of around 8 h, after which it grew exponentially and reached stationary phase after 32 h (Fig. 4.1). A biomass and PHA yield of 2.74 g L^{-1} and 0.71 g L^{-1} was achieved using PHKK PPMS (Table 4.2). Lower biomass and PHA yields of 1.98 g L^{-1} and 0.53 g L^{-1}, respectively were achieved using NSSC-CR PPMS. From previous characterization of this *B. thuringiensis* strain, it is known that it produces hydrolytic enzymes such as cellulase, lignanase and xylanase (Govender 2013) which confer advantages for enzymolysis of lignocellulosic PPMS. Judging from the presence of fine, thin, hair-like strands emanating from a larger fiber (Fig 4.2), it is probable enzymatic degradation by *B. thuringiensis* during the fermentation facilitated the dissolution, shearing, and splitting of components from the PPMS fibers resulting in loose fibrils (Leão et al. 2012). From Figure 4.1 A it is also evident that the strain simultaneously consumed the readily available glucose resulting in a significant reduction in glucose content from 64.21% to 46.44% ($p < 0.05$). Figure 4.1 B is the average fermentation curve, showing reduction in BOD and COD during the 72 h CBP. It is also noteworthy that the strain caused a significant reduction in BOD and COD ($p < 0.05$) concentration. The average reduction in BOD and COD for NSSC-CR PPMS was

from 40.53 mg/L to 10.23 mg/L (75%) and 190.63 mg/L to 150 mg/L (21%), respectively. For PHKK PPMS, the reduction in BOD was 32.6 mg/L to 12 mg/L (63%) and 165.88 mg/L to 110.88 mg/L (33%) reduction in COD. The reduction is indicative of the biodegradability level of materials in the PPMS (Samudro and Mangkoedihardjo 2010). Oljira et al. (2018) report higher reductions in BOD and COD ranging from 73-95% using *Bacillus* sp. Kumar et al. (2012) recommend a longer fermentation period of 10 days or using a consortium of bacteria to obtain better reductions in BOD and COD of 85-94%. Nevertheless, the results herein imply that the *B. thuringiensis* can be employed as an agent in the aerobic biological treatment of PPMS thereby detoxifying and stabilizing the PPMS prior to disposal in landfill. To the best of our knowledge, this is the first report exploring a CBP strategy for cell proliferation and/or PHA formation using NSSC-CR and PHKK PPMS as a substrate. Thus, it was important to establish the growth and product kinetics of *B. thuringiensis* in PPMS in order to determine the capability of either PPMS to serve as applicable substrates for cell proliferation and/or PHA formation.

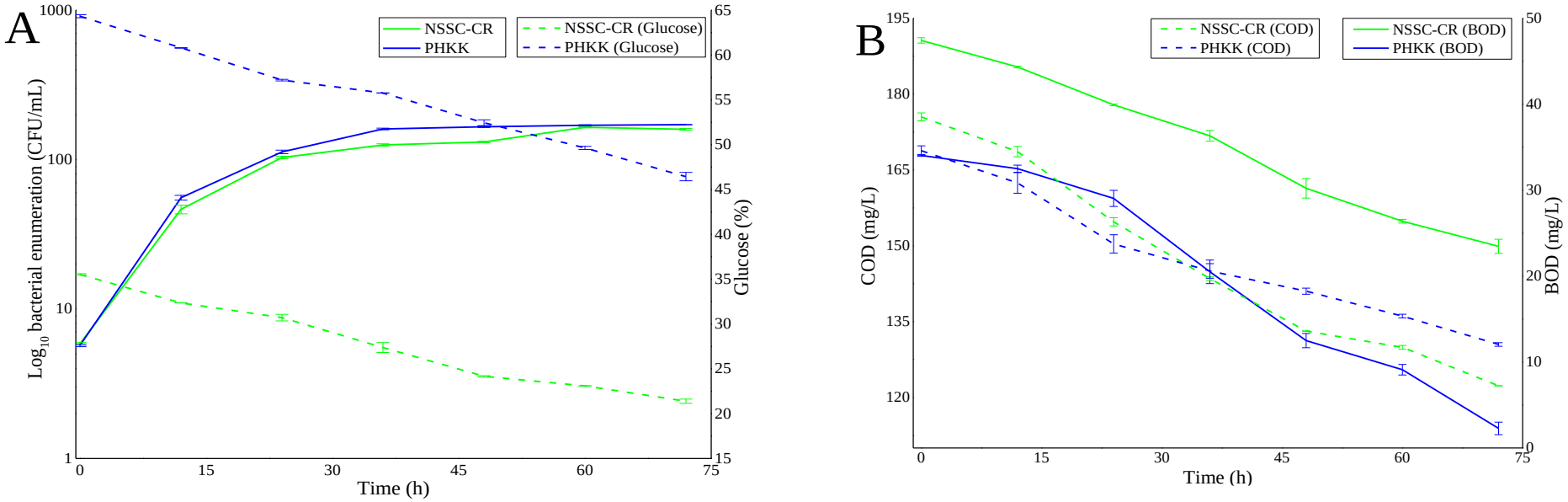

Figure 4.1: Log_{10} bacterial growth curve and glucose consumption (A) and reduction in BOD_5 and COD (B) by *B. thuringiensis* when neutral semi-sulphite chemical pulping and cardboard recycling mill (NSSC-CR) and prehydrolysis kraft and kraft pulping mill (PHKK) pulp and paper mill sludge were used as feedstock for the consolidated bioprocessing fermentation.

Table 4.2: Growth and product kinetic parameters when neutral semi-sulphite chemical pulping and cardboard recycling mill (NSSC-CR) and prehydrolysis kraft and kraft pulping mill (PHKK) pulp and paper mill sludge were used as feedstock for the consolidated bioprocessing fermentation with *B. thuringiensi*

PPMS	CDW (g L^{-1})*	PHA content (g L^{-1})	PHA yield (%)*	Biomass productivity (g L^{-1} h^{-1})	PHA productivity (g L^{-1} h^{-1})
NSSC-CR	1.98	0.53	16.67	0.028	0.005
PHKK	2.74	0.71	25.91	0.038	0.01

*Statistically significant ($p < 0.05$) 5% level of significance

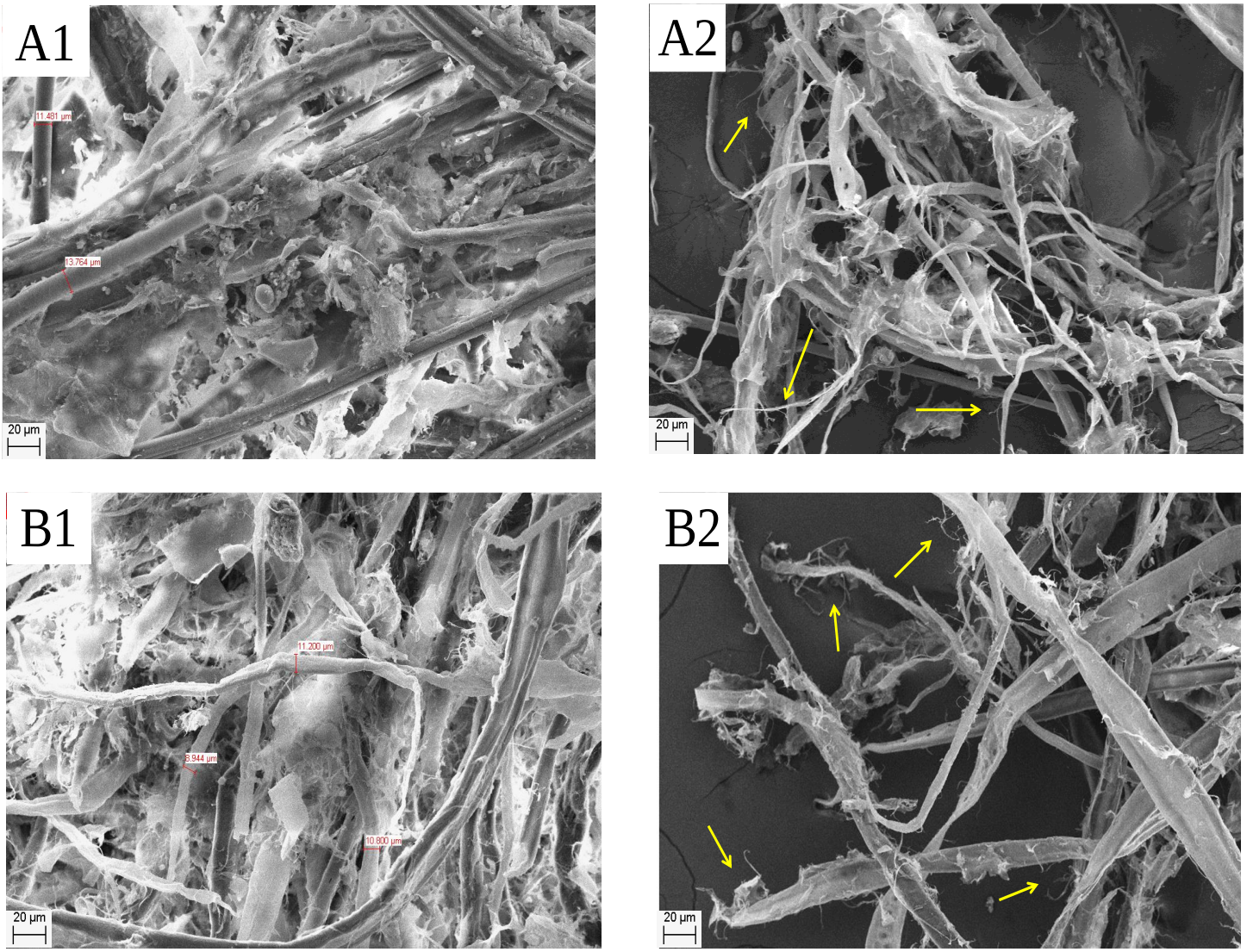

Figure 4.2: Scanning electron microscopy micrographs displaying the neutral semi-sulphite chemical pulping and cardboard recycling mill (NSSC-CR) (A) and prehydrolysis kraft and kraft pulping mill (PHKK) (B) pulp and paper mill sludge fibers before (A1 and B1) and after the 72 h (A2 and B2) consolidated bioprocessing fermentation with *B. thuringiensis*. The yellow arrows indicate fibrillation on the fiber surface.

4.4.3. PHA composition and analysis

4.4.3.1. FTIR analysis

FTIR is typically applied as a rapid method to distinguish PHAs by identifying the absorbance of the ester band. The FTIR spectra in Figure 4.3 are results of the cumulative absorbances for all of the chemical species present in a PHA sample. The intensity of a band in the spectrum is directly related to the concentration(s) of the components in the sample. The distinctness of a spectrum is determined by the chemical structure of each component in the PHA. The major PHA bands are the intense ester carbonyl (C=O) stretch between 1725 to 1740 cm^{-1}, a number of strong bands between 1000 and 1470 cm^{-1} indicative of methyl (CH_3) and methylene (CH_2) deformations and C-O-C stretches (Kansiz et al. 2007). The position and intensity of the bands depend on the PHA concentration and crystallinity (Isak et al. 2016). FTIR analysis was advantageous as it required little to no sample preparation making it useful to screen a large number or a variety of PHA samples.

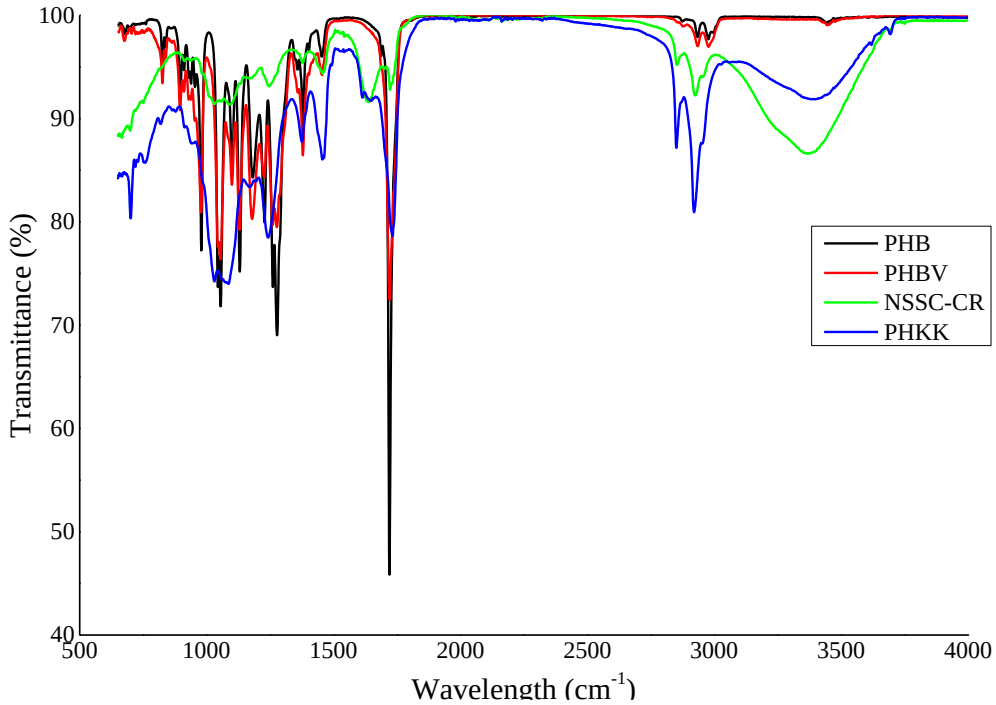

Figure 4.3: Fourier-transform infrared spectra of commercial PHB and PHBV and the PHAs extracted from *B. thuringiensis* when neutral semi-sulphite chemical pulping and cardboard recycling mill (NSSC-CR) and prehydrolysis kraft and kraft pulping mill (PHKK) pulp and paper mill sludge were used as feedstock in the consolidated bioprocessing fermentation with *B. thuringiensis*.

4.4.3.2. Polymer composition and thermal properties

From py-GC/MS analysis it was evident that a PHBV copolymer and a HB-HV-HHx terpolymer were synthesized by *B. thuringiensis* using NSSC-CR and PHKK PPMS, respectively (Table 4.3; supplementary material S2.3-S2.4). The NSSC-CR and PHKK PPMS types had a significant effect on the polymer composition ($p < 0.05$). The PHBV copolymer synthesized using NSSC-CR PPMS has a 86.35 mol% HB fraction and a 13.65 mol% HV fraction (Table 4.3). Al Battashi et al. (2020) explain the influence of VFAs on PHA composition and the incorporation of specific monomeric units in a copolymer. The HB fraction of the polymer is attributed to the abundance of acetic acid (23.54%) and butyric acid (15.35%). The HV fraction is specifically due to the presence of odd numbered VFAs such as propionic acid which contains 3 carbons, and is responsible for integrating a low fraction of HV into the polymer (Al Battashi et al. 2020). This reiterates the dynamic between VFAs and the incorporation of certain monomers into a PHAs chain previously described by Kumar et al. (2019).

An efficient CBP strategy for efficient and enhanced PHA production is still under development. Currently, there are no reports of an ideal CBP feedstock or microbial strain for PHA production. Researchers are investigating alternate low cost feedstock and microbial strains for application in CBP. To name a few, Sawant et al. (2017) report on the success of using untreated tequila bagasse as a carbon source for PHA production by *Saccharophagus degradans* ATCC 43961 and yielded 11.8-14.6% PHA. Sawant et al. (2018) demonstrated the practicality of achieving 17-27% yield of PHB by co-culturing *S. degradans* and *B.cereus* and using red algae as a non-competitive carbon source and an unconventional and promising raw material feedstock in CBP. Zhou et al. (2020) demonstrate the possibility of producing ~270 mg/L PHA using lignin-derived phenolic compounds for PHA production by *Pseudomonas putida* KT2440. Salamanca-Cardona et al. (2014; 2016) report employing genetically modified *E.coli* LS5218 in CBP using xylan as feestock and achievin a 3-fold increase in PHA production. Wang et al. (2018) also report of the successes of employing a genetically modified *P. putida* strain A514 in CBP whilst using a lignin-derivative as feedstock and obtained 40 mg/L PHA.

The TGA curve is displayed in Figure 4.3 A and the initial ($T_{5\%}$) and maximum (T_{max}) thermal degradation temperatures are summarized in Table 4.3. The NSSC-CR and PHKK PPMS types

had a significant effect on the thermal properties of the synthesized PHAs ($p < 0.05$). From Figure 3.4 A, it is evident that the curves have the same shape, but the slopes differ, resulting in changes in the kinetic parameters and the thermal stability temperatures for each type of polymer (Carrasco et al. 2005). The thermal degradation of the PHAs occurred mainly in a two-step process whereby PHAs began to degrade at around 222.58–269.66°C ($T_{5\%}$) and completely degraded (T_{max}) between 286.77-295.59°C (Table 4.3). The higher decomposition temperature (295.59°C) of the HB-HV-HHx terpolymer synthesized using PHKK PPMS is ascribed to the incorporation of HV and HHx in the polymers. The presence of these different monomers also contributes to the thermal stability of the polymer (Akdoğan and Çelik 2018). The higher T_{max} of the terpolymer indicates better thermostability than commercial PHB and PHBV. PHAs with a high decomposition temperature have a wide processing window. These polymers are also useful in industrial applications as they will able to resist high temperatures, with no structural degradation (Rodrigues et al. 2019). The DSC cooling and second heating cycle curves of commercial PHB and PHBV, as well as the PHAs, extracted from *B. thuringiensis* using NSSCR-CR and PHKK PPMS are shown in Figure 4.3. There was a wide variation in the T_c ranging from 75.5°C to 113.52°C (Table 4.3; Fig. 4.3 A). The increasing T_c relates to gain of mobilization of the polymer chains therefore, higher temperatures will be required for polymer processing (Beber et al. 2018). In Figure 4.3 B, two distinct T_m endothermic peaks are observed for each sample. The first T_m ranged from 78.14 -171.65°C, whereas the second T_m ranged from 146.94 -174.69°C (Table 4.3). Multiple melting peaks are a common feature of semi-crystalline polymers (Wellen et al. 2015). The lower T_m observed for the multi-component HB-HV-HHX terpolymer is ascribed to the alkanoate components or long side chains (Saranya and Shenbagarathai 2011; Sandhya et al. 2013). A PHA with low T_m is desirable as it implies that the polymer can be processed at a low temperature for the production of soft material such as films. The degree of crystallinity (X_c) is another important characteristics of a PHA and X_c should ideally be ≤ 50%. In the present study, the PHA synthesized using PHKK PPMS is more favorable due to its low crystallinity (X_c = 35%) (Table 4.3). Highly crystalline PHAs, such as the PHA synthesized using NSSC-CR PPMS is less desirable as these PHAs require corrective actions thereby incurring challenges during polymer processing and increased operation costs (Rodrigues et al. 2019).

Table 4.3: Polymer composition, degradation temperatures and thermal properties of commercial PHB and PHBV, and the PHAs extracted from *B. thuringiensis* when neutral semi-sulphite chemical pulping and cardboard recycling mill (NSSC-CR) and prehydrolysis kraft and kraft pulping mill (PHKK) pulp and paper mill sludge were used as feedstock in the consolidated bioprocessing fermentation with *B. thuringiensis*

Polymer Source	**Polymer Composition (mol%)***			**Degradation Temperature (°C)**		**Thermal Properties***					
	HB	**HV**	**HHx**	**$T_{5\%}$**	**T_{max}**	**T_g (°C)**	**T_{m1} (°C)**	**T_{m2} (°C)**	**ΔHm (J g^{-1})**	**T_c (°C)**	**X_c (%)**
NSSC-CR	86.35	13.65		226.72	286.98	4.98	168.23	170.23	85.59	81.83	59
PHKK	60.59	27.97	11.44	222.58	295.59	4.88	78.14	148.02	51.11	100.51	35
Commercial PHB	89.81	10.19	-	269.66	286.77	5.02	171.65	174.69	90.35	75.50	62
Commercial PHBV	43.35	56.65	-	264.04	288.32	4.85	138.22	146.94	60.55	113.17	41

*Statistically significant ($p < 0.05$) 5% level of significance

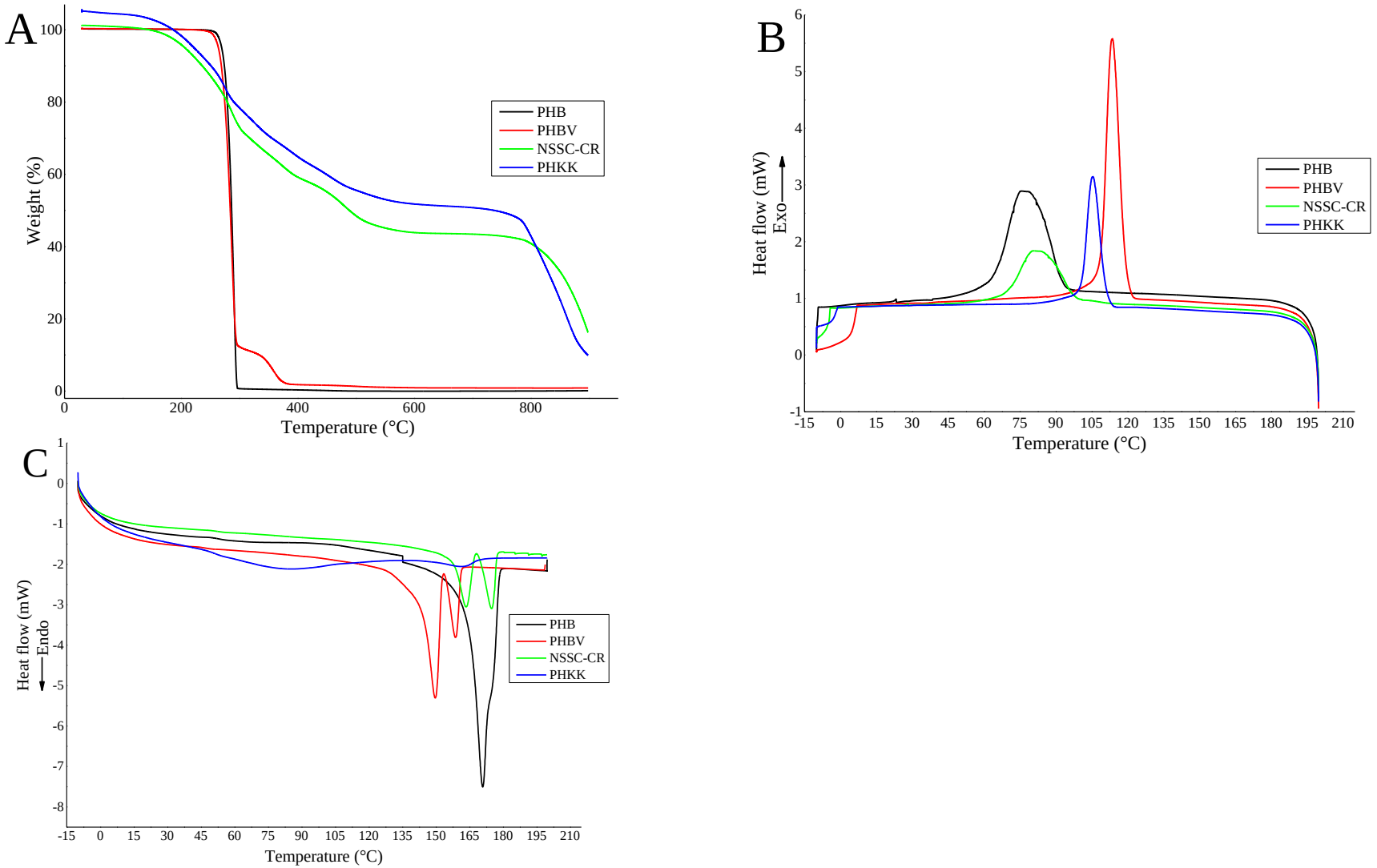

Figure 4.4: Thermograms from thermogravimetric analysis (A), differential scanning calorimetry of the cooling cycle (B) and the second heating cycle (C) used to characterize commercial PHB and PHBV, and the PHAs extracted from *B. thuringiensis* when neutral semi-sulphite chemical pulping and cardboard recycling mill (NSSC-CR) and prehydrolysis kraft and kraft pulping mill (PHKK) pulp and paper mill sludge were used as feedstock in the consolidated bioprocessing fermentation with *B. thuringiensis*.

4.5. Conclusions

Taken together, the results presented herein demonstrates the unique and promising potential of coupling the CBP strategy with untreated NSSC-CR and PHKK PPMS for *B. thuringiensis* cell growth and PHA production. From compositional analysis, characteristics such as high glucose, nitrogen, and VFAs levels but low lignin and ash contents made PHKK PPMS a better suited feedstock compared with NSSC-CR PPMS. Nevertheless, cell biomass and PHA production were achieved utilizing both NSSC-CR and PHKK PPMS, albeit in relatively low yields of 1.98 g L^{-1} and 2.74 g $L^{-1}$and 16.67% and 25.91%, respectively. It is noteworthy that the HB-HV-HHx terpolymer obtained using PHKK PPMS displayed slightly higher thermostability and lower crystallinity in comparison with commercial PHB and PHBV, compared with the copolymer retrieved using NSSC-CR PPMS as feedstock. CBP was successfully adapted for the purposes of the present study and was a beneficial exercise. An additional advantage is that this was a one-process technique and only one fermentation vessel was used. Since PHKK PPMS has more favorable characteristics, it will be a better candidate in forthcoming strategies. Future studies can involve pretreating the PPMS biomass followed by implementing a separate hydrolysis and fermentation study to enhance the yield of cell biomass and/or PHAs produced by *B. thuringiensis*.

4.6. References

Abdullah R, Ishak CF, Kadir WR, Bakar RA (2015) Characterization and feasibility assessment of recycled paper mill sludges for land application in relation to the environment. Int J Res Public Heal 12:9314–9329.

Agarry S, Ayobami O (2011) Evaluation of microbial systems for biotreatment of textile waste effluents in Nigeria: Biodecolourization and biodegradation of textile dye. J Appl Sci Environ Manag 15:79-86.

Akdoğan M, Çelik E (2018) Purification and characterization of polyhydroxyalkanoate (PHA) from a *Bacillus megaterium* strain using various dehydration techniques. J Chem Technol Biotechnol 93:2292–2298.

Al-Kaabi Z, Pradhan R, Thevathasan N, Arku P, Gordon A, Dutta A (2018) Beneficiation of renewable industrial wastes from paper and pulp processing. AIMS Energy 6:880–907.

Al Battashi H, Al-Kindi S, Gupta VK, Sivakumar N (2020) Polyhydroxyalkanoate (PHA) production using volatile fatty acids derived from the anaerobic digestion of waste paper. J Polym Environ 29:250–259.

Aldor IS, Keasling JD (2003) Process design for microbial plastic factories: Metabolic engineering of polyhydroxyalkanoates. Curr Opin Biotechnol 14:475–483.

Alkasrawi M, Al-Hamamre Z, Al-Shannag M, Abedin M, Singsaas E (2016) Conversion of paper mill residuals to fermentable sugars. BioResources 11:2287–2296.

Andreeßen B, Steinbüchel A (2010) Biosynthesis and biodegradation of 3-hydroxypropionate-containing polyesters. Appl Environ Microbiol 76:4919–4925.

Beber VC, de Barros S, Banea MD, Brede M, de Carvalho LH, Hoffmann R, Costa ARM, Bezerra EB, Silva IDS, Haag K, Koschek K, Wellen RMR (2018) Effect of Babassu natural filler on PBAT/PHB biodegradable blends: An investigation of thermal, mechanical, and morphological behavior. Materials (Basel) 11:1–16.

Boshoff S, Gottumukkala LD, Rensburg E Van, Görgens J (2016) Paper sludge (PS) to bioethanol: Evaluation of virgin and recycle mill sludge for low enzyme, high-solids fermentation. Bioresour Technol 203:103–111.

Brethauer S, Studer MH (2014) Consolidated bioprocessing of lignocellulose by a microbial consortium. Energy Environ Sci 7:1446–1453.

Carrasco F, Dionisi D, Martinelli A, Majone M (2005) Thermal stability of polyhydroxyalkanoates. J Appl Polym Sci 100:2111–2121.

Chakraborty P, Gibbons W, Muthukumarappan K (2009) Conversion of volatile fatty acids into polyhydroxyalkanoate by *Ralstonia eutropha*. J Appl Microbiol 106:1996–2005.

Ciesielski S, Przybylek G (2014) Volatile fatty acids influence on the structure of microbial communities producing PHAs. Brazilian J Microbiol 45:395–402.

Dabrowska M, Kuittinen S, Pappinen A, Swietochowski A (2018) Physical and chemical properties of pulp waste for energy purposes. In: Proceedings of the International Scientific Conference-Engineering for Rural Development. Jelgava 23-25 May 2018, Finland:1716-1720.

Ferreira LMGA, Amaral L, Machado (2004) Removal of chloride in the kraft chemical recovery cycle of pulp mills using the ion-exchange process. Ind Eng Chem Res 43:7121-7128.

Geng X, Zhang SY, Deng J (2005) Characteristics of paper mill sludge and its utilization for the manufacture of medium density fiberboard. Wood Fiber Sci 39:345–351.

Gibril ME, Lekha P, Andrew J, Sithole B, Tesfaye T, Ramjugernath D (2018) Beneficiation of pulp and paper mill sludge: Production and characterisation of functionalised crystalline nanocellulose. Clean Technol Environ Policy 20:1835–1845.

Govender L (2013) Seasonal variation of microflora and their effects on the quality of wood chips intended for pulping. PhD Dissertation. University of KwaZulu-Natal.

He T, Liu (2017) Recovery of calcium carbonate waste as paper filler in the causticising process of bamboo kraft pulping. J Bioresour Bioprod 2:82-88.

Iloms E, Ololade OO, Ogola HJO, Selvarajan R (2020) Investigating industrial effluent impact on municipal wastewater treatment plant in Vaal, South Africa. Int. J. Environ. Res. Public Health 17:1-18.

Isak I, Patel M, Riddell M, West M, Bowers T, Wijeyekoon S, Lloyd J (2016) Quantification of polyhydroxyalkanoates in mixed and pure cultures biomass by Fourier transform infrared spectroscopy: Comparison of different approaches. Lett Appl Microbiol 63:139–146.

Jouzani GS, Taherzadeh MJ (2015) Advances in consolidated bioprocessing systems for bioethanol and butanol production from biomass: A comprehensive review. Biofuel Res J 2:152–195.

Kamali M, Alavi-borazjani SA, Khodaparast Z (2019) Additive and additive-free treatment technologies for pulp and paper mill effluents: Advances, challenges and opportunities. Water Resour Ind 21:100109.

Kang L, Lee YY, Yoon SH, Smith AJ, Krishnagopalan GA (2012) Ethanol production from the mixture of hemicellulose prehydrolysate and paper sludge. BioResources 7:3607–3626.

Kang L, Wang W, Pallapolu VR, Lee YY (2011) Enhanced ethanol production from de-ashed paper sludge by simultaneous saccharification and fermentation and simultaneous saccharification and co-fermentation. BioResources 6:3791–3808.

Kansiz M, Domínguez-Vidal A, McNaughton D, Lendl B (2007) Fourier-transform infrared (FTIR) spectroscopy for monitoring and determining the degree of crystallisation of polyhydroxyalkanoates (PHAs). Anal Bioanal Chem 388:1207–1213.

Kumar G, Ponnusamy VK, Bhosale RR, Shobana S, Yoon JJ, Bhatia SK, Rajesh Banu J, Kim SH (2019) A review on the conversion of volatile fatty acids to polyhydroxyalkanoates using dark fermentative effluents from hydrogen production. Bioresour Technol 287:121427.

Kumar V, Dhall P, Kumar R, Singh YP, Kumar A (2012) Bioremediation of agro-based pulp mill effluent by microbial consortium comprising autochthonous bacteria. Sci World J 2012:1–7.

Leão AL, Cherian BM, de Souza SF, Sain M, Narine S, Caldeira MS, Toledo MAS (2012) Use of primary sludge from pulp and paper mills for nanocomposites. Mol Cryst Liq Cryst 556:254–263.

Li H, Zhou S, Johnson T, Vercruysse K, Lizhi O, Ranganathan P, Phambu N, Ropelewski AJ, Thannhauser TW (2017) Genome structure of *Bacillus cereus* tsu1 and genes involved in cellulose degradation and poly-3-hydroxybutyrate synthesis. Int J Polym Sci 2017:1–12.

Likon M, Trebše P (2012) Recent advances in paper mill sludge management. In: Show K-Y (ed) Industrial Waste. InTech, Croatia, pp 73–90.

Liu S, Duncan S, Qureshi N, Rich J (2018) Fermentative production of butyric acid from paper mill sludge hydrolysates using *Clostridium tyrobutyricum* NRRL B-67062/RPT 4213. Biocatal Agric Biotechnol 14:48–51.

Łukajtis R, Kucharska K, Hołowacz I, Rybarczyk P, Wychodnik K, Słupek E, Nowak P, Kamínski M (2018) Comparison and optimization of saccharification conditions of alkaline pre-treated triticale straw for acid and enzymatic hydrolysis followed by ethanol fermentation. Energies 11:1–24.

Makgae M (2011) Key areas in waste management: A South African perspective, integrated waste management. In: Kumar S (ed) Intech. p 472.

Martínez-Sanz M, Villano M, Oliveira C, Albuquerque MGE, Majone M, Reis M, Lopez-Rubio A, Lagaron JM (2014) Characterization of polyhydroxyalkanoates synthesized from microbial mixed cultures and of their nanobiocomposites with bacterial cellulose nanowhiskers. N Biotechnol 31:364–376.

Mendes CVT, Cruz CHG, Reis DFN, Carvalho MGVS, Rocha JMS (2016) Integrated bioconversion of pulp and paper primary sludge to second generation bioethanol using *Saccharomyces cerevisiae* ATCC 26602. Bioresour Technol 220:161–167.

Mongkhonsiri G, Gani R, Malakul P, Assabumrungrat S (2018) Integration of the biorefinery concept for the development of sustainable processes for pulp and paper industry. Comput Chem Eng 119:70–84.

Munir S, Iqbal S, Jamil N (2015) Polyhydroxyalkanoates (PHA) production using paper mill wastewater as carbon source in comparison with glucose. J Pure Appl Microbiol 9:1–8.

Nagamani P, Mahmood SK (2013) Production of poly(3-hydroxybutyrate-co-3-hydroxyvalerate) by a novel *Bacillus* OU40^{T} from inexpensive carbon sources. Int J Pharma Bio Sci 4:182–193.

Ochoa De Alda JAG (2008) Feasibility of recycling pulp and paper mill sludge in the paper and board industries. Resour Conserv Recycl 52:965–972.

Ochoa De Alda JAG, Torrea JA (2006) Applications of recycled paper mills effluents to wood substitutive products (Respro): Executive summary. Univ SEK Segovia 2:381–398.

Olguin-Maciel E, Singh A, Chable-Villacis R, Tapia-Tussell R, Ruiz HA (2020) Consolidated bioprocessing, an innovative strategy towards sustainability for biofuels production from crop residues: An overview. Agronomy 10:1–20.

Oljira T, Muleta D, Jida M (2018) Potential applications of some indigenous bacteria isolated from polluted areas in the treatment of brewery effluents. Biotechnol Res Int 2018:1–13.

Pradhan S, Dikshit PK, Moholkar VS (2018) Production, ultrasonic extraction, and characterization of poly(3-hydroxybutyrate) (PHB) using *Bacillus megaterium* and *Cupriavidus necator*. Polym Adv Technol 29:2392–2400.

Prasetyo J, Kato T, Park EY (2010) Efficient cellulase-catalyzed saccharification of untreated paper sludge targeting for biorefinery. Biomass and Bioenergy 34:1906–1913.

Rashid MT, Barry D, Goss M (2006) Paper mill biosolids application to agricultural lands: Benefits and environmental concerns with special reference to situation in Canada. Soil Environ 25:85–98.

Rodrigues PR, Nunes JMN, Lordelo LN, Druzian JI (2019) Assessment of polyhydroxyalkanoate synthesis in submerged cultivation of *Cupriavidus necator* and *Burkholderia cepacia* strains using soybean as substrate. Brazilian J Chem Eng 36:73–83.

Salamanca-Cardona L, Scheel RA, Bergey NS, Stipanovic AJ, Matsumoto K, Taguchi S, Nomura CT (2016) Consolidated bioprocessing of poly(lactate-co-3-hydroxybutyrate) from xylan as a sole feedstock by genetically-engineered *Escherichia coli*. J Biosci Bioeng 122:406–414.

Salamanca-Cardona L, Scheel RA, Lundgren BR, Stipanovic AJ, Matsumoto K, Taguchi S, Nomura CT (2014) Deletion of the pflA gene in *Escherichia coli* LS5218 and its effects on the production of polyhydroxyalkanoates using beechwood xylan as a feedstock. Bioeng Bugs 5:284–287.

Samudro G, Mangkoedihardjo S (2010) Review on BOD, COD and BOD/COD ratio: A triangle zone for toxic, biodegradable and stable levels. Int J Acad Res 2:235–239.

Sandhya M, Aravind J, Kanmani P (2013) Production of polyhydroxyalkanoates from *Ralstonia eutropha* using paddy straw as cheap substrate. Int J Environ Sci Technol 10:47–54.

Saranya V, Shenbagarathai R (2011) Production and characterization of PHA from recombinant *E. coli* harbouring *PHAC1* gene of indigenous *Pseudomonas* sp. LDC-5 using molasses. Brazilian J Microbiol 42:1109–1118.

Sawant SS, Salunke BK, Kim BS (2018) Consolidated bioprocessing for production of polyhydroxyalkanotes from red algae *Gelidium amanssi*. Int J Biol Macromol 109:1012–1018.

Sawant SS, Tran TK, Salunke BK, Kim BS (2017) Potential of *Saccharophagus degradans* for production of polyhydroxyalkanoates using cellulose. Process Biochem 57:50–56.

Schuster B, Chinn M (2013) Consolidated bioprocessing of lignocellulosic feedstocks for ethanol fuel production. BioEnergy Res 6:416–435.

Simão L, Hotza D, Raupp-Pereira F, Labrincha JA, Montedo ORK (2018) Wastes from pulp and paper mills- A review of generation and recycling alternatives. Cerâmica 64:443–453.

Szacherska K, Oleskowicz-Popiel P, Ciesielski S, Mozejko-Ciesielska J (2021) Volatile fatty acids as carbon sources for polyhydroxyalkanoates production. Polymers (Basel) 13:1–21.

Tan GA, Chen C-L, Ge L, Li L, Wang L, Zhao L, Mo Y, Tan SN, Wang J-Y (2014) Enhanced gas chromatography-mass spectrometry method for bacterial polyhydroxyalkanoates analysis. J Biosci Bioeng 117:379–382.

Torri C, Cordiani H, Samorì C, Favaro L, Fabbri D (2014) Fast procedure for the analysis of poly(hydroxyalkanoates) in bacterial cells by off-line pyrolysis/gas-chromatography with flame ionization detector. J Chromatogr A 1359:230–236.

van der Merwe-Botha M, Manus L (2011) Wastewater risk abatement plan: A W_2RAP guideline to plan and manage towards safe and complying municipal wastewater collection and treatment in South Africa. Water Res Comm. Report No. TT 489/11:121.

van Zyl WH, Lynd LR, den Haan R, McBride JE (2007) Consolidated bioprocessing for bioethanol production using *Saccharomyces cerevisiae*. Adv Biochem Eng Biotechnol 108:205–235.

Wang X, Lin L, Dong J, Ling J, Wang W, Wang H, Zhang Z, Yu X (2018) Simultaneous improvements of *Pseudomonas* cell growth and polyhydroxyalkanoate production from a

lignin derivative for lignin-consolidate bioprocessing. Appl Environ Microbiol 84:1–15.
Wellen RMR, Rabello MS, Júnior ICA, Fechine GJM, Canedo EL (2015) Melting and crystallization of poly(3-hydroxybutyrate): Effect of heating/cooling rates on phase transformation. Polímeros 25:296–304.
Wen Z, Li Q, Liu J, Jin M, Yang S (2020) Consolidated bioprocessing for butanol production of cellulolytic *Clostridia*: Development and optimization. Microb Biotechnol 13:410–422.
Zhang H-F, Ma L, Wang Z-H, Chen G-Q (2009) Biosynthesis and characterization of 3-hydroxyalkanoate terpolyesters with adjustable properties by *Aeromonas hydrophila*. Biotechnol Bioeng 104:582–589.
Zhang W-H, Wu J, Weng L, Zhang H, Zhang J, Wu A (2020) Understanding the role of cellulose fiber on the dewaterability of simulated pulp and paper mill sludge. Sci Total Environ 702:134376.
Zhou Y, Lin L, Wang H, Zhang Z, Zhou J, Jiao N (2020) Development of a CRISPR/Cas9n-based tool for metabolic engineering of *Pseudomonas putida* for ferulic acid-to-polyhydroxyalkanoate bioconversion. Commun Biol 3:1–13.

CHAPTER FIVE

Pretreatment and enzymatic saccharification of sludge from a prehydrolysis kraft and kraft pulping mill

5.1. Abstract

The South African pulp and paper industry generates an estimated 0.5 million tons of pulp and paper mill sludge (PPMS) annually. As PPMS is generated, it requires safe, efficient, and economical collection and disposal. However, PPMS is typically land-filled and subsequently emits nuisance odors, methane, and leaches toxins. Thus, PPMS is an environmental hazard and a potential pollutant of air, soil, and water systems. PPMS is primarily composed of cellulose and coupled with the prospect of biorefinery practices, a value-added product such as glucose-rich hydrolyzate can be derived from this lignocellulosic waste stream. The current study applied a Box-Behnken Design to establish the appropriate conditions to obtain the highest possible yield of glucose from PPMS. The PPMS contained 6.89% ash and 64.21% cellulose. De-ashing using acidic pretreatment reduced the ash content by 51%, thereby increasing the amenability of the cellulose fibers to enzymatic hydrolysis. The optimized conditions for the model from the Box-Behnken Design were; pH 4.89, 51°C, hydrolysis time 22.9 h, 30 U/g β-glucosidase, and 60 U/g cellulase, and a substrate load of 6.4%. The model was validated using these conditions, and recovery of 0.48 g glucose per 1 g of fiber was attained. The hydrolyzate contained trace amounts of xylose and mannose. Pyrolysis gas chromatography-mass spectrometry elucidated that the hydrolyzate also contained low concentrations of toxins such as hemicellulose-derived acetic acid (0.25%), sugar-derived furans (1.06%), and lignin-derived phenols (0.58%). This study proposes a scheme that resulted in a 75% yield of glucose and validated the use of PPMS as a viable candidate for enzymatic saccharification. The glucose-rich hydrolyzate retrieved has potential capability as an inexpensive source of fermentable sugars in downstream applications.

Keywords: prehydrolysis kraft and kraft pulping mill sludge, pretreatment, Box-Behnken model, enzymatic hydrolysis, glucose recovery

5.2. Introduction

Pulp and paper mill sludge (PPMS) is the main solid waste from the pulp and paper industry. On average, about 50 kg of sludge is generated per ton of paper product (Zambare and Christopher 2020). South Africa produces an estimated 0.5 million tons of PPMS per annum (Boshoff et al. 2016). The PPMS is typically disposed by land-filling, land-spreading and/or incineration (Rashid et al. 2006). The disposal of waste at properly licensed and regulatory-compliant sanitary landfills is a norm worldwide as it is regarded as a safe and economical option. Waste disposal in South Africa is currently governed by several legislations including The National Environmental Management: Waste Act (NEM: WA), No. 59 of 2008. The NEM: WA together with the minimum requirement(s) according to the Norms and Standards for Disposal of Waste to Landfill (GN No. 636 of 23 August 2013) prohibits land-filling of waste with a moisture content > 40%, or that liberates moisture under pressure in landfill conditions, and which has not been stabilized by treatment (Department of Environmental Affairs 2013). In addition, landfill space in South Africa is rapidly depleting. The on-going land-filling of general and hazardous waste in South Africa makes it very difficult to implement alternative economical waste disposal technologies (Godfrey and Oelofse 2017).

Generally, PPMS is composed of 70% primary sludge and 30% secondary sludge. Primary sludge consists of fibrous material (e.g. cellulose fibers), inorganic fillers from the papermaking process (e.g. $CaCO_3$, kaolin and TiO_2), which constitutes the ash content (Kuokkanen et al. 2008), and inert solids from processes such as the washing or screening stage, the white water circuits, etc. secondary sludge consists of biological solids, fibers and wood derived substances e.g., cellulose and lignin residuals. The typical fiber content accounts for 11-95% of solids in the primary sludge (Gibril et al. 2018; Zhang et al. 2020). The cellulosic material in the PPMS is composed of 20-75% of cellulose and hemicelluloses and is thus rich in carbohydrates, making it a desirable source of sugars (Gibril et al. 2018; Liu et al. 2018). Pretreatment of PPMS prior to enzymatic saccharification is crucial in order to effectively reduce the lignin and ash content thereby making the cellulosic material more amenable to enzymatic hydrolysis (Wang et al. 2010; Kang et al. 2011). Compared to other cellulosic options such as corncob, wheat straw, rice straw and chaff, PPMS is more amenable to hydrolysis treatments, since it has already been exposed to a great deal of mechanical and chemical processing during pulping (Boshoff et al. 2016). PPMS rich in cellulosic fibers is a raw material with potential to be bio-converted or valorized since it is readily available, abundant, renewable and has high carbohydrate and low lignin contents. However the successful and effective

conversion of PPMS biomass to monosaccharides in high yields is still a challenge. Optimization of reaction parameters is one of the most important stages in the development of efficient and economic production of high value products from renewable sources (Pasma et al. 2013). Response surface methodology (RSM) using a Box-Behnken Design (BBD) is an effective optimization tool that fulfils this requirement and is widely used in various fields (Khat-udomkiri et al. 2018).

Research has focused on beneficiation of waste residue to produce value-added, eco-friendly products with an economical advantage. PPMS has been investigated for bioconversion to commodity products such as butyric acid (Liu et al. 2018), bio-ethanol, lactic acid, xylitol and unicellular protein (Gurram et al. 2015; Shi et al. 2015). Waste biomass is an attractive source of fermentable sugars for application as an inexpensive feedstock (Duff et al. 1994; Madrid and Díaz 2011; Marques et al. 2016). Hydrolyzates obtained from enzymolysis of; recycled paper sludge were used in simultaneous saccharification and fermentation and separate hydrolysis and fermentation for production of lactic acid by bacteria (Schroeder et al. 2015), whereas primary clarifier sludge from kraft and low yield sulfite pulping operations (Duff et al. 1994) or recycled paper sludge (Marques et al. 2008; Madrid and Díaz 2011) was used in bio-ethanol production.

This study firstly aimed to develop an effective process for the removal of ash from the PHKK PPMS with minimal loss of fiber and glucose. The study also assessed the application and efficiency of enzymatic hydrolysis using cellulolytic enzymes on de-ashed PPMS fiber. A RSM with a 3-level and 5 factor BBD was used to evaluate the influence and interaction of process parameters, namely, pH of the fermentation broth, reaction time and temperature, enzyme cocktail dosage and substrate load on the glucose yield. The optimal conditions for enzymatic hydrolysis to recover the maximum yield of reducing sugars from the PPMS were determined. Finally, the hydrolyzate was analyzed to quantitatively determine the, sugar yield, the individual sugars and the presence of potentially toxic compounds in the hydrolyzate.

5.3. Materials and Methods

5.3.1. Sample material

Prehydrolysis kraft and kraft pulping mill (PHKK) sludge samples were collected from a pulp and paper mill in South Africa. The mill typically uses *Eucalyptus* (hardwood) wood fiber.

Samples were collected in transparent plastic bags and stored in air tight plastic containers at 4°C.

5.3.2. High performance liquid chromatography (HPLC)

As per section 4.3.3.1

5.3.3. Lignin content

5.3.3.1. Acid-insoluble lignin

As per section 4.3.3.2

5.3.3.2. Acid-soluble lignin

The TAPPI UM 250 method was applied to determine the percentage of acid-soluble lignin in the sample. The absorbance of the acid-soluble lignin is measured at 205 nm (Varian Cary 50 UV/Vis spectrophotometer; Agilent Technologies) where the risk of interference from the furan aldehydes is considerably less. A 1 mL sample from the HPLC prepared sample was transferred to a fused silica absorption cell having a 10 mm light path and 3% sulfuric acid solution was used as a blank.

5.3.4. Ash content

As per section 4.3.3.3

5.3.5. Moisture content

Moisture content was determined using the Kett model FD-610 Infrared Moisture Determination Balance (California, USA). A 0.5 g aliquot of sample was placed onto the sample dish, which was heated and dried using infrared light until there was no weight change per unit of time. The moisture content of the solid component was determined as a percentage of weight loss compared with the initial mass of the sample.

5.3.6. De-ashing process

Firstly, to remove acid-insoluble ash, a 10% w/v suspension was made using untreated (raw) PPMS and distilled water with homogenization for 18 h at room temperature, followed by filtration and oven drying (50°C) (termed “sludge A”). Secondly, to remove acid-soluble ash, a 10% w/v suspension was made using “sludge A” and 1 N H_2SO_4 with homogenization for 18 h at room temperature followed by filtration (termed “sludge B”). Thirdly, to wash off excess

acid, “sludge B” was suspended in distilled water (10% w/v), homogenized (15 min), filtered, resuspended and homogenized in distilled water and filtered again (termed “sludge C”). Finally, 1 N NaOH was used to neutralize the pH of the “sludge D” for further use. The filtration steps involved passing the respective sludge suspensions through 8 different sieves with pore sizes of 1.7 mm, 1 mm, 710 µm, 150 µm, 53 µm, 45 µm, 38 µm and 11 µm, respectively. The use of sieves with various pore sizes allowed PPMS fibers to be retained on sieves with pore sizes 1.7 mm, 1 mm, 710 µm whereas impurities such as sand or clay that can pass through the bigger pore sized sieves, are retained on smaller pore sized sieves. PPMS fibers retained on sieves with pore sizes 1.7 mm, 1 mm, 710 µm were pooled and used in downstream processes. The sieves were air dried and the amounts of fibers recovered and lost were determined gravimetrically. Percentage carbohydrates, lignin and ash content of the retentate and filtrate were determined using the respective protocols outlined previously. This sequential process resulted in de-ashed PPM sludge fibers which were oven dried, mechanically milled and autoclaved (20 min; 121°C; 0.12 – 0.14 MPa) and stored in air-tight containers for further use.

5.3.7. Statistical analysis

The effects of the de-ashing process on the components characterized were determined using one-way ANOVA and SPSS (V 26.0). Where necessary a Bonferroni Post-Hoc analysis was conducted where a $p < 0.05$ was considered as statistically significant.

5.3.8. Statistical optimization of enzymatic saccharification parameters

5.3.8.1. Box-Behnken Design

For this study, a BBD was applied to study the effect of; pH; reaction temperature; hydrolysis time; enzyme cocktail (U/g dry de-ashed PPMS fiber) and substrate load (independent variables) on the recovery of reducing sugar (g L^{-1}) (response); any interaction(s) between different combination(s) of variables; and to optimize the conditions of the five parameters for the maximum recovery of reducing sugars (g L^{-1}). The five factors studied in the design were designated as X_1, X_2, X_3, X_4 and X_5, respectively and prescribed at 3 different levels i.e. low (-1), middle (0) and upper (+1) ranges (Table 5.1).

Table 5.1: Independent variables with their respective coded values and levels used in the 3-level 5-factor Box-Behnken Design to optimize the conditions for the maximum recovery of

reducing sugars from de-ashed prehydrolysis kraft and kraft pulping mill (PHKK) pulp and paper mill sludge fiber

Coded value	Independent variable	Level		
		Low	Middle	Upper
		-1	0	+1
X_1	pH	4	5	6
X_2	Temperature (°C)	40	50	60
X_3	Time (h)	18	24	30
		1	2	3
X_4	Enzyme cocktail	β-glucosidase: 7.5 U/g Cellulase: 15 U/g	β-glucosidase: 15 U/g Cellulase: 30 U/g	β-glucosidase: 30 U/g Cellulase: 60 U/g
X_5	Substrate load (%)	2	5	8

The design generated a total of 46 experimental runs (Table 5.3), which were conducted according to the enzyme saccharification procedure mentioned above. Recovered reducing sugar yield (g L^{-1}) was determined for each trial and using multiple regression analysis of independent variables, a second order polynomial was fitted to the response data obtained from the design. The design and results of the experimental runs were analyzed and interpreted using Statistica software V 13.4.0.14 (TIBCO Software Inc.).

The second-order polynomial equation was generated as follows;

$$Y = \beta_0 + \beta_i x_i + \beta_{ij} x_i x_j + \beta_{ii} x_i^2$$

Where, Y is the predicted response, β_0 is the model constant, β_i is the linear coefficient, β_{ii} is the quadratic coefficient, βij is the interaction coefficient and x_i is the independent variable. The statistically not significant parameters ($p > 0.05$) and their interactions were omitted from the equation.

5.3.8.2. Enzymatic saccharification

The oven dried de-ashed PPMS fibers were mechanically milled to increase the surface area for enzymatic saccharification. Enzymatic hydrolysis was achieved with Primafast Gold HSL cellulase (83 U/mL; Ecozyme, South Africa) and β-glucosidase (2 U/mg; Sigma-Aldrich), which were prepared as per manufacturers' specifications and stored at 4°C until further use. The experiments were conducted in 50 mL stoppered conical flasks. The pH, enzyme and substrate loading were as per the RSM model (Table 5.3) and the total reaction volume was made up to 5 mL with 100 mM citrate-phosphate buffer. Samples were incubated in an orbital shaker (New Brunswick Innova 44, Eppendorf) at 200 revolutions per minute (RPM) under the relevant temperature and reaction time conditions (Table 5.3). After incubation, the supernatant

(hydrolyzate) was aspirated and the concentration of glucose (g L^{-1}) released through enzymatic hydrolysis was assayed using the colorimetric 3, 5-dinitrosalicyclic acid (DNS) method (Miller 1959) and HPLC analysis.

5.3.8.3. Data analysis

Data from the BBD were subjected to a second-order multiple regression analysis using the least squares regression methodology to obtain the parameter estimates of the mathematical model. The ANOVA test was applied to determine the statistical significance of the BBD where $p < 0.05$ was considered as statistically significant. Adequacy of the model was checked by model analysis and R^2 analysis. An R^2 close to 1 implies a better fit design to experimental data which is also supported with the R^2 adjusted. The adjusted R^2 value also explains the suitability of the design. The *F*-value indicates the significance of the fitted equation at 5% level of significance. The higher *F*-value is observed, the more significant factor. If the probability associated with the *F*-ratio is small, then the model is considered a better statistical fit. To visualize the relationship between response and experimental levels of statistically significant factor(s) and to determine the optimum conditions, the fitted equations are expressed as 3D surface plots. The surface plots depict the interaction between two factors whilst holding the other independent parameters at a constant middle range value (Tesfaye et al. 2018).

5.3.8.4. Model validation

In order to validate the optimum values for variables given by the second-order polynomial equation, critical values and response surface plots experimental trials were conducted to validate the predicted value by determining the observed value of the responses. The optimal conditions for recovering reducing sugar were used for further downstream applications.

5.3.9. Hydrolyzate compositional analysis

HPLC was used to qualitatively and quantitatively evaluate the carbohydrates constituting the hydrolyzate thereby deducing the g of glucose per g of dry weight de-ashed PPMS fiber. In addition, pyrolysis/ gas chromatography-mass spectrometry (py-GC/MS) was employed to elucidate the presence and quantity of fermentation inhibitory compounds produced during enzymatic saccharification of the PPMS. A micro-furnace based Multi-Shot Pyrolyzer EGA/PY-3030D (Frontier Laboratories Ltd.) with a GCMS-QP2010 Ultra series (Shimadzu Corporation) for evolved gas analysis (EGA-MS) and single-shot analysis was used. For the

analysis, 5 µL samples of the hydrolyzate was added into the pyrolysis cups and thereafter transferred into the quartz tube in the pyrolyzer furnace and pyrolyzed at 500°C for 20 msec (interface of 250°C). The pyrolyzates were introduced into a GC separation column (Ultra Alloy-5 column) with an oven temperature of 50°C with the following thermal program: initial oven temperature set at 50°C held for 2 min, followed by an increase to 200°C with a flow rate of 5°C min^{-1} and held for 4 min resulting in a total run time of 36 min. The main peaks observed were identified by comparing their mass spectra with those in NIST library database. The compounds were identified based on retention time and mass spectra with only similarities that were 85% and above were considered genuine fits.

5.4. Results and Discussion

5.4.1. Characterization of the PHKK PPMS

A compositional analysis was carried out to quantitatively determine the weight % (wt %) of hemicellulose, cellulose, acid-insoluble lignin, acid-soluble lignin, ash and moisture content of the PPMS. This analysis revealed that the PPMS comprised of 9.62% hemicellulose (comprising of 0.64% arabinose, 1.12% galactose, 4.39% xylose and 3.47% mannose), 64.21% cellulose, 16.33% acid-insoluble lignin and 2.95% acid-soluble lignin, and ash content of 6.89% (Table 5.2). The composition of PPMS in the present study differs slightly from other reports by Kang et al. (2010) and Kang et al. (2011) where the authors found that their kraft mill sludge contained a lower content of glucan (44.5%) and lignin (8.1%) and a notably higher ash content of 36%. Variation in PPMS composition from kraft pulp and paper mills is mainly due to the efficiency of the pulping chemicals recovery system which in turn impacts the inorganic content of sludges (Ochoa de Alda and Torrea 2006). Sludge from kraft pulping has low lignin content due to delignification during the cooking process wherein most of the lignin is separated from raw material into black liquor. Low-ash sludges (< 30%, w/w) are typically obtained from ground wood and kraft pulp mills (Ochoa de Alda and Torrea 2006; Ochoa de Alda 2008; Alkasrawi et al. 2016; Mongkhonsiri et al. 2018). This concurs with the sample from the present study which is from a kraft mill and has a low ash content of 6.89%. The low ash content in the PPMS sample can also be attributed to the $CaCO_3$ recycling efforts during the kraft process by precipitation and collection (He and Liu 2017; Simão et al. 2018). The moisture content of the sludge was 79.82%, thereby deeming it unsuitable for land-filling according to South African legislation. It is not unusual for PPMS to have high moisture content as Ochoa De Alda (2008) and Simão et al. (2018) reported PPMS with moisture contents ranging from 43-78% and 52.7-

77.1%, respectively. Simão et al. (2018) also found that kraft PPMS with a low ash content (13-15%) had a higher moisture content (74-78%), which correlates with the findings in the current study.

5.4.2. De-ashing of sludge

The effect of each step in the de-ashing process on compositional changes of the PPMS is given in Table 5.2. Each of the components characterized were significantly affected by the de-ashing process ($p < 0.05$). The combination of water washing and sulfuric acid washing of raw sludge only significantly affected the percentage recovered and lost fibers ($p < 0.05$). The combination of water washing, acid washing followed by another two water washes significantly affected the arabinose, mannose, recovered and lost fibers ($p < 0.05$). There are multiple reports on increases in total carbohydrates after the de-ashing (Kang et al. 2010; Wang et al. 2010; Kang et al. 2011); however, in the current study an increase of only 1.08% for xylose and 0.76% for mannose were noted by the end of the de-ashing process. It is known that during the homogenization process fine particles dissociate from sludge and remain in suspension resulting in fibers passing through the screen with the filtrate (Kang et al. 2011). Thus, it is plausible that the acid treatment in the present study caused partial fiber degradation and fiber loss during the filtration process. However, the degradation and loss of fibers cannot necessarily be attributed to the duration of homogenizing sludge with acid. Aslanzadeh et al. (2017) explained that a 0.8 M HCl and 10 g sludge mixture required 24 h to effectively dissolve all of the $CaCO_3$. The de-ashing process in the present study significantly affected the galactose, glucose and ash content as well as the recovered fibers ($p < 0.05$) (Table 5.2). No carbohydrates were detected in the filtrate; therefore the sugars did not leach out of the fibers during the de-ashing process. Furthermore, insignificant ($p > 0.05$) and minute quantities (< 0.03%) of acid-soluble lignin were detected in the filtrate during the de-ashing.

The present study adopted the method of Wang et al. (2010) who elaborated on the success of using acid and base treatments to de-ash sludge whilst sequentially removing compounds that are inhibitory to cellulase. The de-ashing process did significantly reduce the ash content ($p < 0.05$) in the PPMS from 6.89% to 3.37% resulting in a 51% reduction of ash in the sludge. It has been proven that the removal of ash components that normally inhibit enzymatic hydrolysis result in an improved enzymatic activity (Kang et al. 2011; Chen et al. 2014). However, these authors also noted that during the de-ashing process, the removal of ash was accompanied by a

loss of carbohydrates, which was also noted in the present study. Paper sludge with high cellulose and low ash content as found in the present study is preferable due to potential for high yields, while avoiding the negative effect of ash on the enzymatic hydrolysis, through adsorption and/or inactivation of cellulase (Kang et al. 2010; Kang et al. 2011; Chen et al. 2014). However, it is imperative to consider the economics of a process and the application of the end product. As effective as it was, there are disadvantages to using acid treatment in the de-ashing process such as; the need to intensively wash PPMS to remove the acid before the fermentation is performed; the need to neutralize the acid by alkali which generates a stream of reagents and/or vacuum distillation to recover and reuse the acid. Boshoff et al. (2016) state that additional de-ashing steps incur additional processing costs, therefore, for their study the PPMS was de-ashed by washing over a screen until an ash content of 10.08% was achieved, which they found was sufficient for effective cellulase activity. In the present study, ash removal was attempted; however, considering the effects of acid on the fibers and the questionable economic and environmental impacts of generating wastewater during the washing steps, it might not be possible to pursue the entire de-ashing process in future. The use of excessive water washing steps generates wastewater and would increase the energy consumption for the entire process thereby affecting the final production cost and can prove uneconomical. Therefore, the de-ashing process used on PPMS in downstream processes can involve; preparing a 10% (w/v) PPMS suspension in distilled water and homogenization for 18 h; passing the slurry through sieves; oven drying and mechanically milling and, autoclaved for further use. Even though the water washing step in the de-ashing process increased glucose content by only 0.2%, it had the highest recovery of fibers of 78.58%. Furthermore, it has been demonstrated that PPMS with > 10% ash content was successfully enzymatically hydrolyzed (Kang et al. 2010; Kang et al. 2011; Boshoff et al. 2016). Therefore, it is plausible that the de-ashed PPMS fibers in the current study with an ash content of 5.54% might be susceptible to enzymolysis.

Table 5.2: Effect of the de-ashing process on the composition of prehydrolysis kraft and kraft pulping mill (PHKK) pulp and paper mill sludge and the percentage of fiber recovered and lost during the de-ashing process

	Component (wt %)									
	Hemicellulose				Cellulose	Lignin			Fiber (%)	
Treatment	**Arabinose*** [c]	**Galactose*** [d]	**Xylose***	**Mannose*** [c]	**Glucose*** [d]	**Acid-insoluble***	**Acid-soluble***	**Ash*** [d]	**Recovered** * [a, b, c, d]	**Lost** * [a, b, c]
Untreated (Raw PPMS)	0.64	1.12	4.39	3.47	64.21	16.33	2.95	6.89	100.00	0.00
Water wash [a]	0.41	0.87	4.41	3.56	64.79	15.97	2.92	5.54	78.58	10.55
Acid wash [b]	0.00	0.82	4.68	3.70	62.09	15.18	3.01	4.99	74.99	7.65
Water wash 2[c]	3.36	1.16	3.02	1.24	60.11	15.13	1.53	4.88	71.66	6.38
Base wash [d]	0.00	0.63	5.47	4.23	56.84	15.12	2.74	3.37	71.33	4.90

* Component of the sample that was significantly affected by the de-ashing process ($p < 0.05$)
[a] Sludge suspension after homogenization with water ("sludge A")
[b] Water washed sludge homogenized with H_2SO_4 ("sludge B")
[c] Acid washed sludge washed with distilled water ("sludge C")
[d] Water washed 2 sludge after neutralization with NaOH ("sludge D")

5.4.3. Statistical optimization of enzymatic saccharification parameters

The experimental conditions, batch runs as well as the corresponding experimental, predicted and residual responses for recovered reducing sugar are represented in Table 5.3 and as a plot in Figure 5.1. An increase in yield from 7.50 g L^{-1} to 15.89 g L^{-1} occurred when the enzyme concentration was changed (runs 29 and 31). The effect of substrate load is observed in runs 5 and 19 where a yield of 14.56 g L^{-1} for 5% substrate load decreased to 12.11 g L^{-1} for 8% substrate load. The reducing sugar yield increased from 5.36 g L^{-1} to 12.47 g L^{-1} with an increased hydrolysis time from 18 to 30 h (runs 32 and 33). The effect of pH and temperature is observed in runs 1 and 4 where a yield of 9.96 and 7.75 g L^{-1} was obtained, respectively, when the low and high ranges were used. An average yield of 18.26 g L^{-1} was observed in runs 21-23 and 44-46 where pH 5 and 50°C (middle range) was used. The predicted and the experimental responses of recovered reducing sugar are comparable with minimal difference noted between the data (Fig. 5.1). Most of the points are concentrated along the line, indicating a satisfactory correlation between experimental data and predictive data thus proving a high prognostic ability of the BBD.

Table 5.3: Box-Behnken Design model for enzymatic saccharification of de-ashed prehydrolysis kraft and kraft pulping mill (PHKK) pulp and paper mill sludge fibers and the observed, predicted, and residual responses (g L^{-1}) for each experimental run

	Variables					Recovered reducing sugar (g L^{-1})		
Run	**pH**	**Temperature (°C)**	**Time (h)**	**Enzyme cocktail**	**Substrate load (%)**	**Observed**	**Predicted**	**Residual**
11	5	40	24	2	8	10.25	13.43	-3.18
34	5	50	18	2	8	19.90	17.76	2.14
21	5	50	24	2	5	17.11	18.09	-0.99
14	6	50	18	2	5	15.02	12.60	2.42
32	5	50	18	2	2	5.26	12.70	-7.44
6	5	50	30	1	5	8.09	9.33	-1.24
42	5	40	24	3	5	14.37	14.82	-0.45
29	6	50	24	1	5	7.50	8.26	-0.76
3	4	60	24	2	5	11.66	12.70	-1.04
22	5	50	24	2	5	19.79	18.09	1.70
23	5	50	24	2	5	17.81	18.09	-0.28
26	5	40	30	2	5	16.24	11.89	4.35
4	6	60	24	2	5	7.75	11.15	-3.40
30	4	50	24	3	5	19.21	16.66	2.55
45	5	50	24	2	5	19.37	18.94	0.43
9	5	40	24	2	2	11.29	8.38	2.92
38	4	50	24	2	8	18.10	16.12	1.98
24	5	40	18	2	5	10.65	13.16	-2.50
13	4	50	18	2	5	15.89	14.14	1.75
8	5	50	30	3	5	16.97	16.18	0.79
31	6	50	24	3	5	15.89	15.11	0.78
39	6	50	24	2	8	15.10	14.57	0.52
16	6	50	30	2	5	10.20	11.33	-1.13
25	5	60	18	2	5	15.10	15.18	-0.08
46	5	50	24	2	5	18.85	18.94	-0.10
43	5	60	24	3	5	13.99	16.85	-2.86
15	4	50	30	2	5	10.27	12.88	-2.61
19	5	50	24	1	8	12.11	11.72	0.39
33	5	50	30	2	2	12.47	11.43	1.04
41	5	60	24	1	5	14.45	10.00	4.45
17	5	50	24	1	2	4.49	6.66	-2.17
10	5	60	24	2	2	13.16	10.40	2.76
40	5	40	24	1	5	6.90	7.97	-1.07
20	5	50	24	3	8	17.67	18.57	-0.90
28	4	50	24	1	5	6.24	9.81	-3.56
35	5	50	30	2	8	15.33	16.49	-1.16
27	5	60	30	2	5	13.88	13.92	-0.04
2	6	40	24	2	5	9.78	9.12	0.65
18	5	50	24	3	2	13.87	13.51	0.35
44	5	50	24	2	5	18.18	18.94	-0.76

5	5	50	18	1	5	14.56	10.59	3.97
7	5	50	18	3	5	17.18	17.44	-0.27
1	4	40	24	2	5	9.96	10.67	-0.71
37	6	50	24	2	2	10.42	9.52	0.90
12	5	60	24	2	8	15.67	15.46	0.21
36	4	50	24	2	2	12.71	11.06	1.64

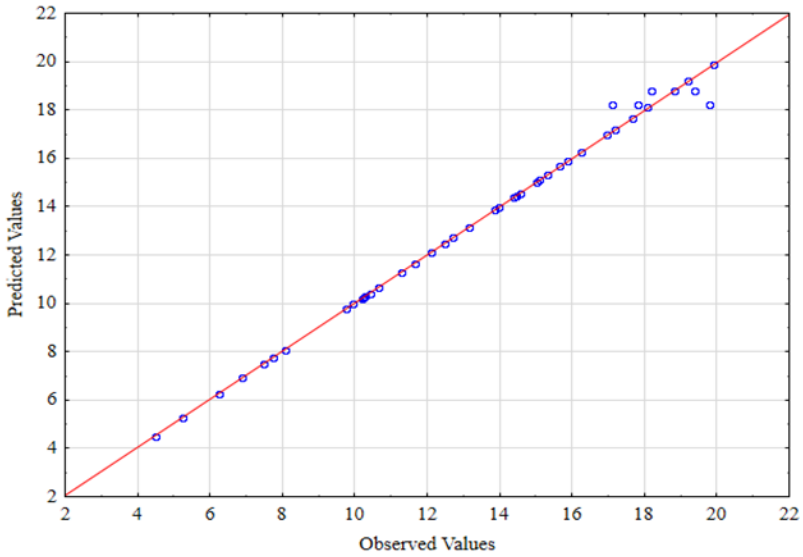

Figure 5.1: Observed versus predicted responses for the Box-Behnken Design

After a multiple regression analysis of the observed responses for recovered reducing sugar (g L^{-1}) the second-order polynomial equation is:

Response (Y): *Recovered reducing sugar (g L^{-1}) = 4.5408 – 5.5733C+ 5.8222D – 3.4058BC – 3.9656BD + 3.1377CD – 5.8856CE – 2.9056A^2B^2 + 3.2702CA^2 + 2.4874EB^2 + 2.3305CD^2 + 8.8812A^2 + 8.0594B^2 + 4.4901C^2 + 6.1011D^2 + 3.8624E^2*

Where, A^2, B^2, C, C^2, D, D^2, E^2, A^2B^2, CA^2, BC, BD, EB^2, CD, CD^2 and CE were the statistically significant model terms indicating that the results are unlikely to be due to chance.

Analysis of the regression equation draws the conclusion that the recovery of reducing sugar in the selected factor ranges is influenced by all of the independent variables either in linear or quadratic terms. In linear terms, only time (C) and enzyme cocktail (D) showed the highest influence on the recovery of reducing sugar. This suggests that the recovered reducing sugar should be relatively insensitive to linear variations of pH, temperature, and substrate load. With respect to quadratic terms, all five variables had positive significance on recovered reducing sugar (Table 5.4). Interactive effect of variables, pH and temperature (quadratic terms; A^2B^2), time and pH (CA^2), temperature and time (BC), temperature and enzyme cocktail (BD),

substrate load and temperature (EB^2), time and enzyme cocktail (CD) and time and substrate load (CE) also had positive significance on recovered reducing sugar (Table 5.4) indicating a strong interaction between these variables and that sugar recovery depends on the interactions between these factors. Negative values of coefficients of the regression equation confirm that increases in the value of any of the factors leads a decrease in the yield of reducing sugar. The model *F*-value of 35.9137 and ($p < 0.01$) implies the model is significant, and there is only a 0.01% chance that a model *F*-value this large could occur due to noise. The ANOVA indicated that this regression model was significant ($p < 0.01$) with a "Lack of Fit" *F*-value of 49.0418 therefore the Lack of Fit is not significant relative to the pure error. A non-significant lack of fit ($p = 0.1126$) is good especially for process optimization and considers that the model is fit. The value of $p > F < 0.001$, implies that the model terms are significant and that there is a < 1% chance that the observed values were due to chance alone. The R^2 value is the coefficient of determination and for a good fit of a model, R^2 should be ≥ 80% (Cao et al. 2008). A satisfactory R^2 value of 0.9939 was obtained. Therefore, 99.39% of the variability in the response could be explained by the model and that 1% of the variations occurs while performing the experiments, thus indicating a realistic fit of the model to the experimental data (Table 5.4). The adjusted determination coefficient R^2 value of 0.93241 indicated adequate signal and this high value also supports that the model was significant. The coefficient of variation (CV) is the ratio of the standard error of the estimate to the mean value of the observed response, expressed as a percentage and a model with a CV <15% is considered reasonably reproducible as it suggests higher reliability of the experiment and demonstrates a greater reliability of the trials (Cao et al. 2008; Tesfaye et al. 2018). For the current study, the CV was 9.60% indicating a high degree of precision in the experiment.

Table 5.4: ANOVA for response surface quadratic model from the Box-Behnken Design to recover the maximum concentration of reducing sugar from de-ashed prehydrolysis kraft and kraft pulping mill (PHKK) pulp and paper mill sludge fibers

Source	Sum of squares (SS)	Degrees of freedom (df)	Mean square (MS)	*F*-value	Probability > *F*
Model	762.9686	40	19.0742	35.9137	0.00001**
A- pH	0.0338	1	0.0338	0.0295	0.8720
B- Temperature	0.1908	1	0.1908	0.1665	0.7041
C- Time	13.3119	1	13.3119	11.6155	0.0271*
D- Enzyme cocktail	14.5277	1	14.5277	12.6764	0.0236*
E- Substrate load	6.7546	1	6.7546	5.8938	0.0722
AB	3.4721	1	3.4721	3.0297	0.15673
AB^2	0.1813	1	0.1813	0.1582	0.71110
BA^2	7.2300	1	7.2300	6.3087	0.0659
A^2B^2	22.5136	1	22.5136	19.6446	0.0114*

AC	0.1615	1	0.1615	0.1409	0.7265
AC^2	2.3611	1	2.3611	2.0602	0.2245
CA^2	21.3890	1	21.3890	18.6633	0.0124*
A^2C^2	4.8236	1	4.8236	4.2089	0.1095
AD	5.2185	1	5.2185	4.5535	0.0998
AD^2	1.3031	1	1.3031	1.1370	0.3463
DA^2	5.1602	1	5.1602	4.5027	0.1011
A^2D^2	6.8926	1	6.8926	6.0142	0.0703
AE	0.1255	1	0.1255	0.1095	0.7573
EA^2	0.2279	1	0.2279	0.1988	0.6787
BC	11.5995	1	11.5995	10.1214	0.0335*
BC^2	3.3751	1	3.3751	2.9450	0.1613
CB^2	0.3700	1	0.3700	0.3229	0.6003
B^2C^2	1.1032	1	1.1032	0.9626	0.3821
BD	15.7259	1	15.7259	13.7219	0.0208*
BD^2	0.0020	1	0.0020	0.0017	0.9689
DB^2	7.8589	1	7.8589	6.8574	0.0589
B^2D^2	1.3817	1	1.3817	1.2056	0.3338
BE	3.1589	1	3.1589	2.7563	0.1722
EB^2	12.3738	1	12.3738	10.7970	0.0303*
CD	9.8449	1	9.8449	8.5903	0.0428*
CD^2	10.8621	1	10.8621	9.4779	0.0369*
DC^2	1.4751	1	1.4751	1.2871	0.3199
CE	34.6406	1	34.6406	30.2262	0.0053**
EC^2	4.6223	1	4.6223	4.0332	0.1150
DE	3.6401	1	3.6401	3.1762	0.1493
A^2	46.7416	1	46.7416	40.7852	0.0031**
B^2	24.1689	1	24.1689	21.0890	0.0101**
C^2	21.5048	1	21.5048	18.7643	0.0123*
D^2	19.2117	1	19.2117	16.7635	0.0149*
E^2	55.0809	1	55.0809	48.0617	0.0023**
Residual	233.6842	31	7.5382		
Lack of fit	233.5255	30	7.7842	49.0418	0.1126
Pure error	4.5842	4	1.1460		
R^2	0.99399				
R^2 adjusted	0.93241				

** Statistically significant ($p < 0.01$) 1% level of significance *Statistically significant ($p < 0.05$) 5% level of significance

The relationship and interactive effects between the dependent variable and the independent variables is graphically represented in three-dimensional (3D) response surface plots generated by the model (Fig. 5.2). Firstly, the nature of the response plot shape in Figure 5.2 was examined. The presence of an elliptical or circular shape of contours in 3D plots is indicative of significant interactions between the variables (Tesfaye et al. 2018). The interactive effect of variables, A^2B^2, CA^2, BC, BD, EB^2, CD, CD^2 and CE were significant ($p < 0.05$). Figure 5.2 represents the overall contribution of each independent variable to yield of sugar. Figure 5.2 A describes the quadratic effect of both pH and temperature on the yield of reducing sugar. Figures 5.2 A, and D displays the quadratic effect of temperature and Figure 5.2 B displays the linear effect of temperature. From these plots it is evident that a pH of 4.8 to 5 and a reaction temperature of 48-52°C will yield of ~18-20 g L^{-1} reducing sugar. The yield dropped at lower or higher pH and/or increased or decreased incubation time. Figure 5.2 B displays the linear

effects of temperature and time on yield of reducing sugar where yields of > 18 g L^{-1} is obtainable if the enzymatic saccharification occurs for 22-26 h, ~50°C. Kulsuwan and Kongkiattikajorn (2012) obtained 52.4%-67.7% reducing sugar from recycled paper mill sludge using the optimum conditions for two different cellulases which were: 24 h incubation at pH 5.0; and 40-70°C where a higher yield of reducing sugar was obtained at 50°C. According to Min et al. (2015) commercially available cellulases are optimally applied at 50°C and further explain the strong effect of temperature on hydrolysis. They also observed that at 40°C hydrolysis, yield decreased by 15–20% compared with 50°C. Figure 5.2 C displays the linear effect of enzyme cocktail and time on yield. It is observed that enzyme cocktail 2 or 3 will result in a yield of ~28 g L^{-1} at a reaction time of 22-26 h. Min et al. (2015) demonstrate that increasing enzyme dosage was very effective for the enzymolysis of unbleached kraft pulp samples and their study obtained yields as high as 60% using high enzyme loadings. Figure 5.2 D represents the effect of temperature (linear) and substrate load (quadratic) on the yield. It is evident that a substrate load of 6-7% at a reaction temperature of 48-52°C will result in a reducing sugar yield > 18 g L^{-1}. For solid substrates with high water retention capacity, such as kraft PPMS, enzymatic hydrolysis at solid loadings >10% is difficult to operate in shaking flasks as the suspension becomes highly viscous with little free water available in the flask. Therefore, enzymatic hydrolysis at high substrate loading can be significantly inhibited by a high solids concentration resulting in a low hydrolysis efficiency and low concentration of reducing sugars (Zhu et al. 2011; Guan et al. 2018). From Figure 5.2 it is deduced that the optimal conditions for maximum recovery of reducing sugars are: fermentation pH of 4.8-5; reaction temperature of 48-52°C; hydrolysis time of 22-26 h; enzyme cocktail 2 or 3 and a substrate load of 6-7%. Values outside this range resulted in low efficiency recovery of reducing sugar. This confirms that the range of the chosen variables, in the experimental design, were conducive to obtaining high yields of reducing sugar.

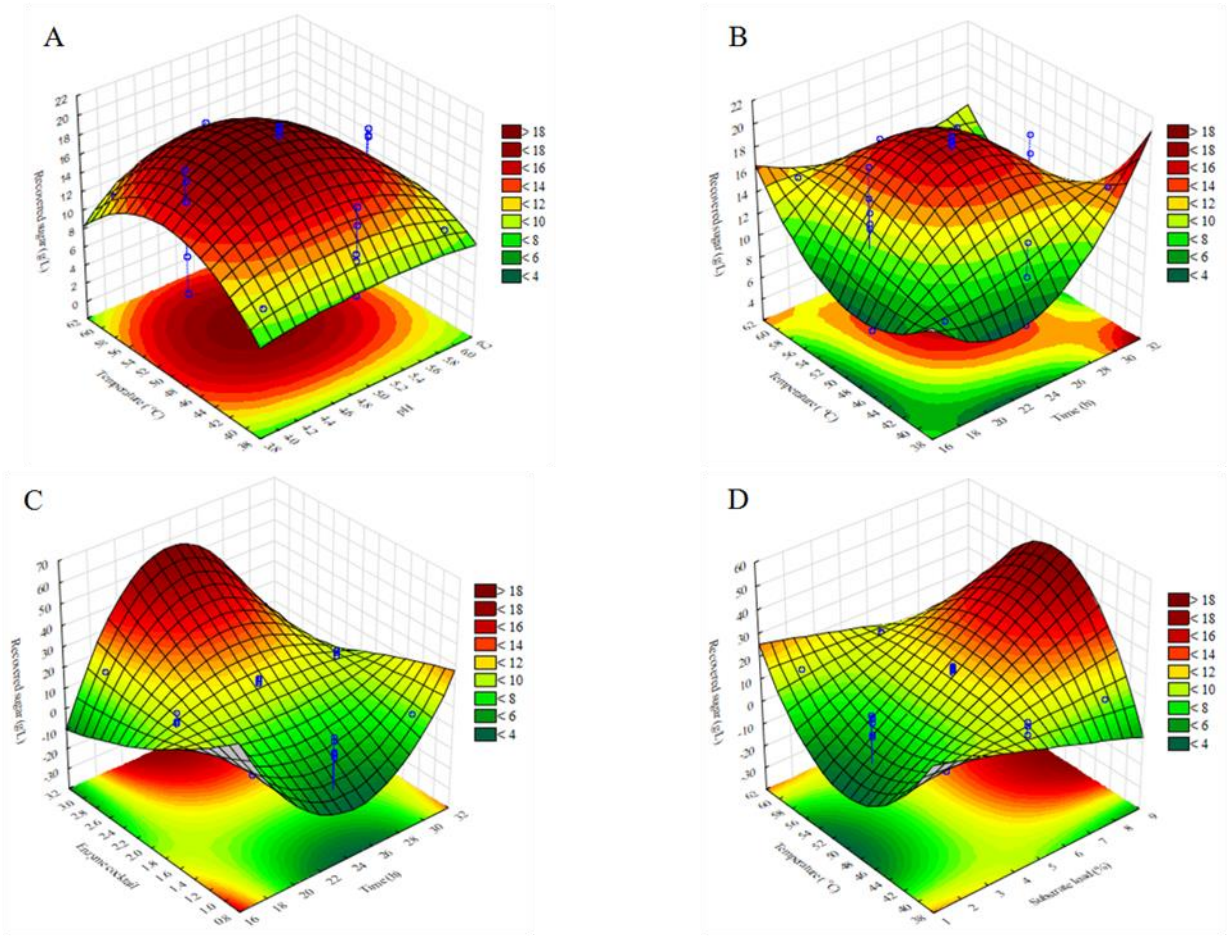

Figure 5.2: Three-dimensional (3D) response surface generated by the Box-Behnken Design model for the independent variables that significantly affect the yield of recovered reducing sugar: temperature and pH (A); temperature and time (B); enzyme cocktail and time (C), and temperature and substrate load (D) for the enzymatic saccharification of de-ashed prehydrolysis kraft and kraft pulping mill (PHKK) pulp and paper mill sludge fibers.

5.4.4. Model validation

The model was validated by conducting experiments under the predicted conditions. For this, a post-hoc analysis revealed critical values which are the exact optimum conditions to obtain a predicted yield (Hanrahan et al. 2007). The validation of the model was performed using reaction conditions: pH 4.89; 51°C; hydrolysis time 22.9 h; enzyme cocktail 3; and a substrate load of 6.4%. The predicted value was a yield of 19.89 g L^{-1} of reducing sugar. From duplicate experimental trials on two separate occasions the observed yield was slightly higher at 20.56 g L^{-1}. The marginal difference between experimental and predicted values revealed a good

correlation amongst the observed and predicted results, thus verifying the validity of the response model and the accuracy of optimal conditions for the variables.

5.4.5. Hydrolyzate characterization

The DNS assay used in the present study is an accurate analytical method to evaluate reducing sugars in solutions or supernatants obtained from enzymatic saccharification of cellulosics, if glucose is the sole product (Rivers et al. 1984). The DNS assay was efficacious in determining reducing sugars of a diverse array of hydrolyzates obtained from: cellulolytic hydrolysis of primary clarifier sludge from kraft operations (Duff et al. 1994); primary clarifier sludge (Moritz and Duff 1996); hydrolysis recycled paper sludge samples (Madrid and Díaz 2011) and enzymatic hydrolysis of paper sludge (Peng and Chen 2011). Pairing the DNS assay with HPLC to determine monosaccharide content in hydrolyzate from PPMS is a common practice (Prasetyo et al. 2010; Zhu et al. 2011; Dwiarti et al. 2012; Kemppainen et al. 2012; Mendes et al. 2016; Buzała et al. 2017; Mendes et al. 2017). After establishing the concentration of reducing sugar, HPLC was employed to profile and measure specific sugars. The individual monosaccharides in the hydrolyzate were: 2.62% xylose; 0.89% mannose; and 48.27% of glucose (Table 5.5). Therefore, 48.27% from a possible 64.79% of glucose was recovered, resulting in a yield of 75%. In terms of quantitative sugar yield (g g^{-1}), 0.482 g glucose was obtained per 1 g dry weight of de-ashed PPMS fiber. The hydrolyzate is composed of a mixture of carbohydrates, containing mainly glucose, xylose and trace amounts of arabinose, galactose and mannose. The composition of the hydrolyzate is important because microbes have varying affinity for carbohydrate intake, with greater capacity to absorb glucose than xylose (García et al. 2015). Due to the cellulose content of the PPMS, it is not surprising that the carbohydrate in this hydrolyzate is predominately glucose but it also contained some hemicellulose-derived xylose (2.62%) and mannose (0.89%).

Table 5.5: Percentage carbohydrates in the hydrolyzate (recovered) and remaining fibers after saccharification (unrecovered) of de-ashed prehydrolysis kraft and kraft pulping mill (PHKK) pulp and paper mill sludge (PPMS) fibers

		Hemicellulose			**Cellulose**
	Arabinose	**Galactose**	**Xylose**	**Mannose**	**Glucose**
De-ashed fiber	0.41	0.87	4.41	3.56	64.79
Recovered	0	0	2.62	0.89	48.27
Unrecovered	0	0	1.79	2.81	16.01

Achieving a yield of approximately 75% has been previously documented (Banerjee 2011; Min et al. 2015; Alkasrawi et al. 2016). The optimal conditions provided by the RSM model were used for bulk production of hydrolyzate. The inability to recover 100% of the reducing sugars could be an impact of hornification. It is a phenomenon whereby hydrolytic enzymes have restricted access to cellulosic fibers or the fines as a result of the drying process. The drying of PPMS fibers and fines results in a loss of amorphous cellulose and a reduced internal porosity thereby reducing the fibers hydration capacity and increasing its crystallinity. The effect seems to be responsible for the reduction in the yields by nearly 30% (Min et al. 2015).

5.4.6. Detection of toxins in the hydrolyzate

Py-GC/MS was conducted to determine the chemical components of the hydrolyzate. Analysis of the hydrolyzate revealed a total of 44 different components categorized into 14 major chemical functional groups as listed in Table 5.6, representing 100% composition of the hydrolyzate. The intensity of peaks of the constituents are displayed in Figure 5.3. The major compound types identified were hydrocarbon (28.81%), sugar (24.99%) and sugar alcohol (24.12%). The minor component types were amide (12.1%) and ketone (2.85%) whereas the other components constituted less than 2% of the total yield (Table 5.6). Despite its advantages, the use of acid during pretreatment results in the hydrolysis of lignocellulosic components such as cellulose, hemicellulose and lignin and the formation of a plethora of inhibitory by-products (Jönsson and Martín 2016) with varying modes of action (Palmqvist and Hahn-Hägerdal 2000; Pienkos and Zhang 2009). Commonly produced toxic compounds present in lignocellulosic hydrolyzates include: acetic acid; furanics; phenolics; inorganic salts; aromatics; bioalcohols; and aliphatic acids. Its presence in hydrolyzate contributes to acidification, inhibition of subsequent microbial fermentation and/or downstream biochemical processes (Klinke et al. 2004). The hydrolyzate obtained in the present study contains (below 1%) of acetic acid, 2-vinylfuran, 2-butenal and 2-propanone (Table 5.6 and Fig. 5.3), which are confirmed pyrolysis products of lignin from pulp mill effluents (Moldoveanu 1998). Compounds such as acetic acid, furanics and phenolics constitute 0.25%, 0.58% and 1.06% of the hydrolyzate, respectively (Table 5.6). The acetic acid in the hydrolyzate is a result of acetyl groups from hemicellulose being released during acid pretreatment (Lourenço et al. 2018). Zha et al. (2012) also identified the inhibitory compounds formic acid (0.57 g/L) and acetic acid (8.0 g/L) in hydrolyzates of sugar cane bagasse and oak saw dust. 2-Furaldehyde (furfural) and 2-furancarboxaldehyde, 5-methyl-hydroxy (HMF) are degradation products of pentoses (xylose) and hexoses (Barbosa et

al. 2014; Costa et al. 2016), respectively, and are known to be toxic to biocatalysts at low concentrations. Zha et al. (2014) identified the inhibitory compounds in hydrolyzates from lignocellulosic biomass such as sugar cane bagasse, corn stover, wheat straw, barley straw, willow wood chips and oak sawdust. The authors report that HMF showed toxicity at 1.0 g/L towards fermenting yeast but, when HMF was combined with another inhibitory compound such as syringaldehyde, the inhibitory effect was lowered to 0.5 g/L. Therefore, it is possible that the toxicity threshold can be lowered when multiple inhibitors are present. 2-Methoxy-phenol (guaiacol) is known to be derived from kraft lignin (Moldoveanu 1998). The effect of phenolics as inhibitors to microbial growth and product yield are variable as the mechanism of toxicity has not been elucidated. One possibility is that phenolics interfere with the cell membrane by influencing its function and changing its protein-to-lipid ratio (Jönsson and Martín 2016). With the presence of catechol in the hydrolyzate (Table 5.6), it can be assumed that the hydrolyzate also contains para- and orthobenzoquinones (Jönsson and Martín 2016). In the current study, the presence of each possible inhibitor in hydrolyzate is less than 1% and this concentration can be attributed to the use of a less recalcitrant type of biomass such as PPMS coupled with mild, acidic pretreatment conditions.

Detoxification steps can be implemented to curtail the toxic nature of lignocellulosic hydrolyzate; however, there are repercussions such as increased process costs due to additional steps or constraints on solids loading in the fermentation step. However, using micro-organisms as biological methods of detoxification of inhibitory compounds is also possible and advantageous. Yeasts, fungi, and bacteria and/or their enzymes can naturally detoxify lignocellulosic hydrolyzates by degrading the furfural, HMF and/or phenolic compounds and change their composition or structure to less toxic ones (Parawira and Tekere 2011).

Table 5.6: Composition of the prehydrolysis kraft and kraft pulping mill (PHKK) pulp and paper mill sludge (PPMS) hydrolyzate elucidated by py-GC/MS

Retention time (min)	Name of compound	Quantity (%)
	Alcohol	
3.919	(S)-2,5-Dimethyl-3-vinylhex-4-en-2-ol	0.13
4.691	2-Pentanol, 3-chloro-4-methyl	0.14
5.271	2-Propanol, 1-ethoxy-	0.25
8.931	7-Octen-2-ol	0.06
25.163	3-Ethyl-4-methyl-3-heptanol	1.35
	Aldehyde	

2.946	2-Butenal	0.1
	Amide	
30.123	4-Methylmannonic amide	12.1
	Carboxylic acid	
2.186	Acetic acid, methoxy-, methyl ester	0.25
18.46	Cyclopropanecarboxylic acid, 3-formyl-2,2-dimethyl-, ethyl ester	0.14
	Benzene	
15.749	Benzene, 1,4-dimethoxy-	0.1
	Fatty acid	
3.487	2-Propenoic acid, 2-methyl-, 2-aminoethyl ester, hydrochloride	0.22
10.86	Pentanoic acid, 4-oxo-, methyl ester	0.03
15.564	Hepten-2-yl angelate, 6-methyl-5-	0.1
	Furan	
3.423	Furan, 2,5-dimethyl-	0.15
3.674	2-Vinylfuran	0.1
6.228	Furfural	0.39
8.09	2-Furanmethanol	0.04
9.944	2-Furancarboxaldehyde, 5-methyl-hydroxy	0.38
	Hydrocarbon	
2.124	Cyclopentane, ethyl-	0.36
2.23	1,3-Cyclopentadiene	0.14
3.777	Oxazolidine, 3-methyl-	0.24
29.659	(18S,19S)-18,19-Dihydroxy-1,4,7,10,13,16-hexaoxocycloencosane	28.07
	Imidazole	
8.383	1-(3H-Imidazol-4-yl)-ethanone	1.43
	Ketone	
3.309	2,3-Pentanedione	0.28
6.067	1-Hydroxy-2-butanone	0.19
6.58	2-Cyclopenten-1-one	0.35
8.191	2-Cyclopenten-1-one, 2-methyl-	0.27
10.599	2-Cyclopenten-1-one, 3-methyl-	0.05
13.038	1,2-Cyclopentanedione, 3-methyl-	1.28
13.453	2-Cyclopenten-1-one, 3-ethyl-2-hydroxy-	0.43
	Phenol	
13.832	Phenol, 2-methoxy-	0.25
20.82	Catechol	0.33
	Sugar	
4.953	2-Methyl-l-methylmannopyranoside	1.96
27.284	.Beta.-D-Mannopyranose, 2,4,6-tri-O-methyl-, diacetate	4.36
32.306	Methyl 4-O-methyl-d-arabinopyranoside	18.67
	Sugar alcohol	
18.258	D-Glucitol, 1,4:3,6-dianhydro-2,5-di-O-methyl-	10.24
19.17	Dianhydromannitol	0.96
21.129	1,3:2,5-Dimethylene-4-methyl-d-rhamnitol	0.4

22.553	4-Methyl-1,3:2,5-dimethylene-l-rhamnitol	0.07
25.661	D-(+)-Arabitol, pentamethyl ether	0.84
26.697	D-Galactitol, 3,6-anhydro-1,2,4,5-tetra-O-methyl-	5.46
28.551	Adonitol, pentamethyl ether	6.15
	Terpenoid	
4.097	Oxirane, 2,3-diethyl-	0.46
4.278	Oxirane, 3-ethyl-2,2-dimethyl-	0.73

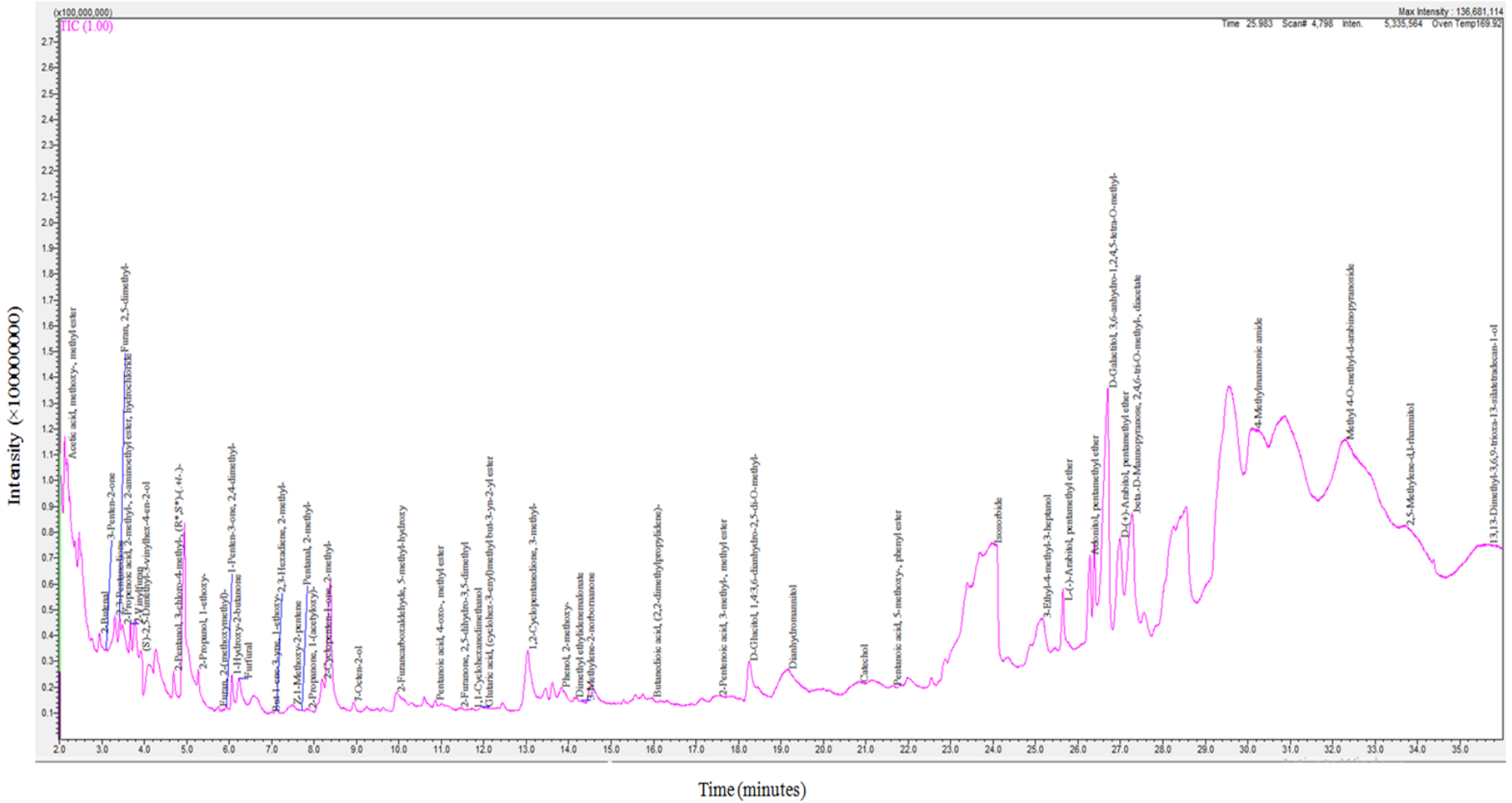

Figure 5.3: Pyrogram profiling compounds present in the prehydrolysis kraft and kraft pulping mill (PHKK) pulp and paper mill sludge (PPMS) hydrolyzate.

5.5. Conclusions

Pulp and paper mills generate large volumes of sludge waste which is normally landfilled, landspread or incinerated. Due to the economic and environmental impacts of these traditional disposal methods, they might not be viable options in the future. Therefore, using PPMS for bioconversion in low cost processes is a possibility as it contains a significant amount of carbohydrate-containing cellulose, which is readily available for saccharification and release of fermentable sugars. In this study, the PHKK PPMS was characterized using a variety of analytical techniques. The main components of the sludge are the fiber and ash and the quantity of these influence downstream applications. The PPMS can be described as 9.62% hemicellulose, 64.21% cellulose, 19.28% lignin and 6.89% ash. The de-ashing process was successful for the removal of ash and significantly reduced the ash content by 51%; however, the economic and environmental impacts of the entire de-ashing process is concerning. For further use, the PPMS can be water washed, filtered and oven dried in order to retain the majority of glucose and fibers. RSM and the BBD was time and labor saving and this was a useful statistic tool for optimizing recovery of reducing sugar. Simultaneous elucidation of statistically significant independent variables as well as their mutual interactions and combinatory interactions were also determined. The RSM test was an effective method to determine the optimal conditions for maximum yield of reducing sugar. The experimental value was consistent with the value of the predicted experiments, thereby validating the model. After optimization, HPLC analysis revealed that a 75% yield of glucose was obtained and py-GC/MS revealed presence of potentially inhibitory compounds in the hydrolyzate. Currently there is a limited amount of literature on the optimization of reducing sugars recovered from PPMS. In this experiment, PPMS was a suitable candidate for enzymatic saccharification, thus diversifying the use of PPMS. The resultant glucose-rich hydrolyzate has potential application in separate hydrolysis and fermentation studies that wish to incorporate inexpensive carbon source in the feedstock.

5.6. References

Alkasrawi M, Al-Hamamre Z, Al-Shannag M, Abedin M., Singsaas E (2016) Conversion of paper mill residuals to fermentable sugars. BioResources 11:2287–2296.

Aslanzadeh S, Kemal RA, Pribowo AY (2017) Strategies for characterizing compositions of industrial pulp and paper sludge. In: International Conference on Chemistry and Material Science (IC2MS) 2017. IOP Publishing, Malang, East Java, Indonesia, pp 299: 1–8.

Banerjee S (2011) Glucose from paper mill sludge. BioResources 6:4739–4746.

Barbosa BM, Colodette JL, Júnior DL, Gomes FJB, Martino DC (2014) Preliminary studies on furfural production from lignocellulosics. J Wood Chem Technol 34:178–190.

Boshoff S, Gottumukkala LD, Rensburg E Van, Görgens J (2016) Paper sludge (PS) to bioethanol: Evaluation of virgin and recycle mill sludge for low enzyme, high-solids fermentation. Bioresour Technol 203:103–111.

Buzała KP, Kalinowska H, Przybysz P, Małachowska E (2017) Conversion of various types of lignocellulosic biomass to fermentable sugars using kraft pulping and enzymatic hydrolysis. Wood Sci Technol 51:873–885.

Cao Y, Meng D-J, Lu J, Long J (2008) Statistical optimization of xylanase production by *Aspergillus niger* AN-13 under submerged fermentation using response surface methodology. African J Biotechnol 7:631–638.

Chen H, Venditti R, Gonzalez R, Phillips R, Jameel H, Park S (2014) Economic evaluation of the conversion of industrial paper sludge to ethanol. Energy Econ 44:281–290.

Costa VLD, Gomes TP, Simões RMS (2016) Effect of acid sulphite pretreatment on enzymatic hydrolysis of Eucalypt, Broom, and Pine. J Wood Chem Technol 36:63–75.

Department of Environmental Affairs (2013) Department of Environmental Affairs National Environmental Management: Waste Act, 2008 (Act No. 59 of 2008). Gov Not No. 36784:3–21.

Duff SJB, Moritz JW, Andersen KL (1994) Simultaneous hydrolysis and fermentation of pulp mill primary clarifier sludge. Can J Chem Eng 72:1013–1020.

Dwiarti L, Boonchird C, Harashima S, Park EY (2012) Simultaneous saccharification and fermentation of paper sludge without pretreatment using cellulase from *Acremonium cellulolyticus* and thermotolerant *Saccharomyces cerevisiae*. Biomass and Bioenergy 42:114–122.

García YG, Carlos, Contreras JCM, Hernández JA, Dueñas RS (2015) Procurement of fermentable sugars from cardboard waste for the cultivation of yeasts for biotechnological use. Rev Mex Ciencias For 6:88–105.

Gibril ME, Lekha P, Andrew J, Sithole B, Tesfaye T, Ramjugernath D (2018) Beneficiation of pulp and paper mill sludge: Production and characterisation of functionalised crystalline nanocellulose. Clean Technol Environ Policy 20:1835–1845.

Godfrey L, Oelofse S (2017) Historical review of waste management and recycling in South Africa. Resources 6:1–11.

Guan W, Xu G, Duan J, Shi S (2018) Acetone-butanol-ethanol production from fermentation of hot-water-extracted hemicellulose hydrolysate of pulping woods. Ind Eng Chem Res 57:775–783.

Gurram RN, Al-Shannag M, Lecher NJ, Duncan SM, Singsaas EL, Alkasrawi M (2015)

Bioconversion of paper mill sludge to bioethanol in the presence of accelerants or hydrogen peroxide pretreatment. Bioresour Technol 192:529–539.

Hanrahan G, Garza C, Garcia E, Miller K (2007) Experimental design and response surface modeling: A method development application for the determination of reduced inorganic species in environmental samples. J Environ Informatics 9:71–79.

He T, Liu M (2017) Recovery of calcium carbonate waste as paper filler in the causticizing process of bamboo kraft pulping. J Bioresour Bioprod 2:82–88.

Jönsson LJ, Martín C (2016) Pretreatment of lignocellulose: Formation of inhibitory by-products and strategies for minimizing their effects. Bioresour Technol 199:103–112.

Kang L, Wang W, Lee YY (2010) Bioconversion of kraft paper mill sludges to ethanol by SSF and SSCF. Appl Biochem Biotechnol 161:53–66.

Kang L, Wang W, Pallapolu VR, Lee YY (2011) Enhanced ethanol production from de-ashed paper sludge by simultaneous saccharification and fermentation and simultaneous saccharification and co-fermentation. BioResources 6:3791–3808.

Kemppainen K, Ranta L, Sipilä E, Anders Ö, Vehmaanperä J, Puranen T, Langfelder K, Hannula J, Kallioinen A, Siika-aho M, Sipilä K, von Weymarn N (2012) Ethanol and biogas production from waste fibre and fibre sludge- The FibreEtOH concept. Biomass and Bioenergy 46:60–69.

Khat-udomkiri N, Sivamaruthi BS, Sirilun S, Lailerd N, Peerajan S, Chaiyasut C (2018) Optimization of alkaline pretreatment and enzymatic hydrolysis for the extraction of xylooligosaccharide from rice husk. AMB Express 8:1–10.

Klinke HB, Thomsen AB, Ahring BK (2004) Inhibition of ethanol-producing yeast and bacteria by degradation products produced during pre-treatment of biomass. Appl Microbiol Biotechnol 66:10–26.

Kulsuwan N, Kongkiattikajorn J (2012) Study on optimal conditions for reducing sugars production from recycled paper sludge by diluted acid and enzymes. KKU Res J 17:622–629.

Kuokkanen T, Nurmesniemi H, Pöykiö R, Kujala K, Kaakinen J, Kuokkanen M (2008) Chemical and leaching properties of paper mill sludge. Chem Speciat Bioavailab 20:111–122.

Liu S, Duncan S, Qureshi N, Rich J (2018) Fermentative production of butyric acid from paper mill sludge hydrolysates using *Clostridium tyrobutyricum* NRRL B-67062/RPT 4213. Biocatal Agric Biotechnol 14:48–51.

Lourenço A, Gominho J, Pereira H (2018) Chemical characterization of lignocellulosic materials by analytical pyrolysis. In: Kusch P (ed) Analytical Pyrolysis. InTech, Croatia, pp 1–23.

Madrid LM, Díaz JCQ (2011) Ethanol production from paper sludge using *Kluyveromyces marxianus*. Dyna 78:185–191.

Marques S, Gírio FM, Santos JAL, Roseiro JC (2016) Pulsed fed-batch strategy towards intensified process for lactic acid production using recycled paper sludge. Biomass Convers Biorefinery 7:127–137.

Mendes CVT, Cruz CHG, Reis DFN, Carvalho MGVS, Rocha JMS (2016) Integrated bioconversion of pulp and paper primary sludge to second generation bioethanol using

Saccharomyces cerevisiae ATCC 26602. Bioresour Technol 220:161–167 .

Mendes CVT, Rocha JMS, de Menezes FF, Carvalho MGVS (2017) Batch and fed-batch simultaneous saccharification and fermentation of primary sludge from pulp and paper mills. Environ Technol 38:1498–1506.

Miller GL (1959) Use of dinitrosalicylic acid reagent for determination of reducing sugar. Anal Chem 31:426–428.

Min BC, Bhayani B V, Jampana VS, Ramarao B V (2015) Enhancement of the enzymatic hydrolysis of fines from recycled paper mill waste rejects. Bioresour Bioprocess 2:1–10.

Moldoveanu S. (1998) Analytical pyrolysis of lignins. In: Moldoveanu S. (ed) Analytical Pyrolysis of Natural Organic Polymers. Techniques and Instrumentation in Analytical Chemistry. Elsevier Science Publishing Co Inc, pp 327–351.

Mongkhonsiri G, Gani R, Malakul P, Assabumrungrat S (2018) Integration of the biorefinery concept for the development of sustainable processes for pulp and paper industry. Comput Chem Eng 119:70–84.

Moritz JW, Duff SJB (1996) Simultaneous saccharification and extractive fermentation of cellulosic substrates. Biotechnol Bioeng 49:504–511.

Ochoa De Alda JAG (2008) Feasibility of recycling pulp and paper mill sludge in the paper and board industries. Resour Conserv Recycl 52:965–972.

Ochoa De Alda JAG, Torrea JA (2006) Applications of recycled paper mills effluents to wood substitutive products (Respro): Executive summary. Univ SEK Segovia 2:381–398.

Palmqvist E, Hahn-Hägerdal B (2000) Fermentation of lignocellulosic hydrolysates I: Inhibition and detoxification. Bioresour Technol 74:17–24.

Parawira W, Tekere M (2011) Biotechnological strategies to overcome inhibitors in lignocellulose hydrolysates for ethanol production: Review. Crit Rev Biotechnol 31:20–31.

Pasma SA, Daik R, Maskat MY, Hassan O (2013) Application of Box-Behnken Design in optimization of glucose production from oil palm empty fruit bunch cellulose. Int J Polym Sci 2013:1–8.

Peng L, Chen Y (2011) Conversion of paper sludge to ethanol by separate hydrolysis and fermentation (SHF) using *Saccharomyces cerevisiae*. Biomass and Bioenergy 35:1600–1606.

Pienkos PT, Zhang M (2009) Role of pretreatment and conditioning processes on toxicity of lignocellulosic biomass hydrolysates. Cellulose 16:743–762.

Prasetyo J, Kato T, Park EY (2010) Efficient cellulase-catalyzed saccharification of untreated paper sludge targeting for biorefinery. Biomass and Bioenergy 34:1906–1913.

Rashid MT, Barry D, Goss M (2006) Paper mill biosolids application to agricultural lands: Benefits and environmental concerns with special reference to situation in Canada. Soil Environ 25:85–98.

Rivers DB, Gracheck SJ, Woodford LC, Emert GH (1984) Limitations of the DNS assay for reducing sugars from saccharified lignocellulosics. Biotechnol Bioeng 26:800–802.

Schroeder BG, Zanoni PRS, Magalhães WLE, Hansel FA, Tavares LBB (2015) Evaluation of biotechnological processes to obtain ethanol from recycled paper sludge. J Mater Cycles Waste Manag 19:463–472.

Simão L, Hotza D, Raupp-Pereira F, Labrincha JA, Montedo ORK (2018) Wastes from pulp and paper mills- A review of generation and recycling alternatives. Cerâmica 64:443–453.

Tesfaye T, Sithole B, Ramjugernath D, Ndlela L (2018) Optimisation of surfactant decontamination and pre-treatment of waste chicken feathers by using response surface methodology. Waste Manag 72:371–388.

Wang W, Kang L, Lee YY (2010) Production of cellulase from kraft paper mill sludge by *Trichoderma reesei* Rut C-30. Appl Biochem Biotechnol 161:382–394.

Zambare V, Christopher L (2020) Integrated biorefinery approach to utilization of pulp and paper mill sludge for value-added products. J Clean Prod 274:122791.

Zha Y, Muilwijk B, Coulier L, Punt PJ (2012) Inhibitory compounds in lignocellulosic biomass hydrolysates during hydrolysate fermentation processes. J Bioproces Biotechniq 2:1-11.

Zha Y, Westerhuis JA, Muilwijk B, Overkamp KM, Nijmeijer BM, Coulier L, Smilde KA, Punt PJ (2014) Identifying inhibitory compounds in lignocellulosic biomass hydrolysates using an exometabolomics approach. BMC Biotechnol 14:1-16.

Zhang W-H, Wu J, Weng L, Zhang H, Zhang J, Wu A (2020) Understanding the role of cellulose fiber on the dewaterability of simulated pulp and paper mill sludge. Sci Total Environ 702:134376.

Zhu Z-S, Li X-H, Zheng Q-M, Zhang Z, Yu Y, Wang J-F, Liang S-Z, Zhu M-J (2011) Bioconversion of a mixture of paper sludge and extraction liquor from water prehydrolysis of *Eucalyptus* chips to ethanol using separate hydrolysis and fermentation. BioResources 6:5012–5026.

CHAPTER SIX

Optimization of cultivation medium and cyclic fed-batch fermentation strategy for enhanced polyhydroxyalkanoate production by *Bacillus thuringiensis* using a glucose-rich hydrolyzate

---

6.1. Abstract

The accumulation of petrochemical plastic waste is detrimental to the environment. Polyhydroxyalkanoates (PHAs) are bacterial-derived polymers utilized for the production of bioplastics. PHA-plastics exhibit mechanical and thermal properties similar to conventional plastics. However, high production cost and obtaining high PHA yield and productivity impedes the widespread use of bioplastics. This study demonstrates the concept of cyclic fed-batch fermentation (CFBF) for enhanced PHA productivity by *Bacillus thuringiensis* using a glucose-rich hydrolyzate as the sole carbon source. The statistically optimized fermentation conditions used to obtain high cell density biomass (OD_{600} of 2.4175) were: 8.77 g L^{-1} yeast extract; 66.63% hydrolyzate (v/v); a fermentation pH of 7.18; and an incubation time of 27.22 h. The CFBF comprised three cycles of 29 h, 52 h, and 65 h, respectively. After the third cyclic event, cell biomass of 20.99 g L^{-1}, PHA concentration of 14.28 g L^{-1}, PHA yield of 68.03%, and PHA productivity of 0.219 g L^{-1} h^{-1} was achieved. This cyclic strategy yielded an almost 3-fold increase in biomass concentration and a 4-fold increase in PHA concentration compared with batch fermentation. FTIR spectra of the extracted PHAs display prominent peaks at the wavelengths unique to PHAs. A copolymer was elucidated after the first cyclic event, whereas, after CFBF cycles 2-4, a terpolymer was detected. The PHAs obtained after CFBF cycle 3 have a slightly higher thermal stability compared with commercial PHB. The cyclic events decreased the melting temperature and degree of crystallinity of the PHAs. The approach used in this study demonstrates the possibility of coupling fermentation strategies with hydrolyzate derived from lignocellulosic waste as an alternative feedstock to obtain high cell density biomass and enhanced PHA productivity.

Keywords: Polyhydroxyalkanoate, glucose-rich hydrolyzate, response surface methodology, cyclic fed-batch fermentation, PHA productivity, pulp and paper mill sludge

6.2. Introduction

An estimated 240 million tons of plastics are produced globally every year. Most of these plastic materials are petroleum-based and are resistant to degradation resulting in accumulation and pollution of forestry and marine environments (Gholamveisi et al. 2018). With crude oil reserves dwindling, the dependence on exhaustible fossil fuel resources is unsustainable. This can be mitigated by the exploitation of biopolymers, i.e., natural polymers generated by living organisms, consisting of monomeric units that are covalently bonded to form larger molecules. Examples include polyhydroxyalkanoates (PHAs) such as polyhydroxybutyrate (PHB) and polyhydroxybutyrate-valerate copolymer (PHBV) that occur as intracellular granules produced by bacteria and are accumulated by the cell to act as carbon and energy storage reserves (Sheu et al. 2000; Sin et al. 2014). PHAs are considered to be carbon-neutral and environment-friendly. Research into PHAs has intensified since the discovery that PHA-bioplastics are non-toxic, biodegradable and that their mechanical, physical, and thermal characteristics are similar to fossil-fuel-based plastics, such as polypropylene and polyethylene (Muhammadi et al. 2015). Thus, PHAs have the potential to replace fossil fuel-derived plastics. However, the PHA production cost is a significant problem as carbon source alone accounts for 45% of the total production cost, hindering the market growth of PHA-based plastics (Annamalai et al. 2017). For PHAs to be cost-competitive with petroleum-derived plastics, sustainable, renewable, and cheaper alternative carbon source substrates need to be explored. Furthermore, employing microbial strains capable of high cell density growth and PHA production in waste-derived cultivation media will also be beneficial.

Waste biomass is an attractive alternative source of fermentable sugars for application as inexpensive feedstock for the production of platform chemicals (Moritz and Duff 1996; Peters 2006; Prasetyo et al. 2010; Martin-Sampedro et al. 2011). Glucose-rich hydrolyzate obtained from corrugated cardboard was used as a nutrient source for yeast proliferation (García et al. 2015). Hydrolyzates obtained from enzymolysis of recycled paper sludge was used for the production of lactic acid by bacteria (Marques et al. 2008), primary clarifier sludge from kraft and low yield sulfite pulping operations (Duff et al. 1994) and recycled paper sludge (Madrid and Díaz 2011; Schroeder et al. 2015) was used in bio-ethanol production. Moreover, hydrolyzates from wheat bran (Annamalai and Sivakumar 2016), waste office paper (Annamalai et al. 2017), and wheat straw (Ferreira and Schlottbom 2016) were successful as alternative substrates for PHB production. *Bacillus* species have an innate ability to produce a

variety of hydrolytic enzymes enabling them to metabolize complex residues and utilize a diverse array of carbon wastes (Rohini et al. 2006). Thus, there is a growing interest in exploring *Bacillus* strains and their potential to use agro-wastes residues and hydrolyzates for PHA production. *Bacillus* strains such as *B. thuringiensis* B417-5 and *B. thuringiensis* strain IAM 12077 displayed PHB-producing capability when using hydrolyzates from agro-waste residues (Gowda and Shivakumar 2014; Thammasittirong et al. 2017).

To enhance product yields, high cell density cultivations and high productivity during fermentation should be achieved, particularly for intracellular compounds. The development of high cell density cultivations strategies fundamentally uses different types of bioreactors and cultivation strategies (Ibrahim and Steinbüchel 2010). One such strategy is cyclic fed-batch fermentation (CFBF) that was first described by Pirt (1974) for penicillin production and has since been applied for enhanced production of antibiotics (Lynch and Bushell 1995), recombinant proteins (Argyropoulos and Lynch 1997), and PHAs (Ibrahim and Steinbüchel 2010; Haas et al. 2017; Gahlawat and Srivastava 2018). The CFBF process entails the partial withdrawal of fermentation medium and subsequent re-filling with an equal volume of fresh fermentation medium. The chemical composition of the fermentation medium must be consistent throughout the "empty-and-fill" process. The CFBF strategy prevents increases in concentrations of toxic by-products and enhances cell growth to achieve high concentrations of final biomass and increased PHA yields (Ibrahim and Steinbüchel 2010; Gahlawat and Srivastava 2018).

This study reports the practicality of employing *Bacillus thuringiensis* in a CFBF cultivation using glucose-rich hydrolyzate derived from enzymatic saccharification of pulp and paper mill sludge as the sole carbon source. Firstly, a statistical optimization study was conducted to elucidate the optimal fermentation medium to produce high cell density biomass. The initial use of batch fermentation was to assist in determining kinetic parameters. Thereafter, the CFBF cultivation strategy was used to enhance cell density and PHA production by *B. thuringiensis*. A comparison between batch fermentation and CFBF was performed to evaluate PHA yield and productivity. Lastly, PHAs were extracted after each cycle and characterized to determine their composition and thermal stability and compared with commercial PHB and PHBV.

6.3. Materials and Methods

6.3.1. Bacterial strain, growth, and storage conditions

As per section 3.3.1

6.3.2. Hydrolyzate production

A glucose-rich hydrolyzate was extracted from dry de-ashed pulp and paper mill sludge (PPMS) as per the method outlined in Chapter Five. Briefly, PPMS obtained from a prehydrolysis kraft and kraft (PHKK) pulping mill was de-ashed using acidic pretreatment. A five-factor Box-Behnken Design was used to optimize the conditions for the maximum recovery of glucose (g L^{-1}) from dry de-ashed PPMS fiber. After model validation, the observed yield of glucose was 20.56 g L^{-1}.

6.3.3. Cultivation medium for high cell density production

Biomass production was conducted using shake-flask cultivation in 25 mL stoppered conical flasks. The cultivation medium included: 1.5 g L^{-1} $(NH_4)_2SO_4$, 0.2 g L^{-1} $MgSO_4.7H_2O$, 2.5 g L^{-1} NaCl, 1.5 g L^{-1} KH_2PO_4, and 1.5 mL trace element solution. The concentration of yeast extract and glucose-rich hydrolyzate and the medium pH were varied as per the model design (Table 6.2). All flasks were incubated at 37°C in an orbital shaker (New Brunswick Innova 44, Eppendorf) at 200 revolutions per minute (rpm) for the relevant times (Table 6.2). After incubation, a 1 mL aliquot was aspirated, and cell density was recorded as the optical density at 600 nm (OD_{600}) using a spectrophotometer (Varian Cary 60 UV/Vis spectrophotometer; Agilent Technologies) against a blank of the 1 mL respective uninoculated cultivation medium.

6.3.4. Statistical optimization of fermentation medium

For this study, a Box-Behnken Design (BBD) was applied to elucidate the optimal cultivation medium to obtain high cell density biomass. The design determined the concentration of yeast extract, the concentration of glucose-rich hydrolyzate, incubation time, and pH (independent variables) to obtain maximum cell density and any interaction(s) between different combination(s) of variables. The four factors studied in the design were designated as X_1, X_2, X_3, and X_4, respectively, and prescribed at three different levels (Table 6.1). The design generated a total of 27 experimental runs.

Table 6.1: Independent variables with their respective coded values and levels used in the 3-level 4-factor Box-Behnken Design to elucidate the optimal cultivation medium to obtain high cell density biomass production by *B. thuringiensis*

Coded value	Independent variable	Level		
		Low	Middle	Upper
		-1	0	+1
X_1	Yeast extract (g L^{-1})	6	8	10
X_2	Hydrolyzate (% v/v)	50	75	100
X_3	Time (h)	18	24	30
X_4	pH	7.0	7.2	7.4

The results from the experimental runs were analyzed and interpreted using Design-Expert software V 12 (StatEase). Based on the cell density response and interaction of the variables, a multiple regression analysis of independent variables was used, and a second-order polynomial was fitted to the response data obtained from the design.

The second-order polynomial equation generated was as follows:

$$Y = \beta_0 + \beta_i X_i + \beta_{ij} X_i X_j + \beta_{ii} X_i^2$$

Where Y is the predicted response, β_0 is the model constant, β_i is the linear coefficient, β_{ii} is the quadratic coefficient, βij is the interaction coefficient, and X_i is the independent variable. The statistically not significant parameters ($p > 0.05$) and their interactions were omitted from the equation.

6.3.4.1. Data analysis

The ANOVA test was applied to determine the statistical significance ($p < 0.05$) of the BBD. Adequacy of models was checked by analysis of R^2 and the R^2 adjusted. The capability and statistical significance of the model equation and the model terms were evaluated by the *F*-test (Cao et al. 2008). The *F*-value is also checked to find out the significance of all the fitted equations at a 5% level of significance (Hanrahan et al. 2007; Smitha and Pradeep 2017; Czyrski and Sznura 2019). To visualize the relationship between response and experimental levels of a statistically significant factor(s) and to determine the optimum conditions, the fitted equations were expressed as 3-dimensional (3D) surface plots. Surface plots were determined by holding the other independent parameters at a constant middle range value.

6.3.4.2. Model validation

To validate the predicted value, experimental trials were conducted to determine the observed value using the optimum values for variables given by the second-order polynomial equation, critical values, and response surface plots. After model validation, the statistically optimized

medium was used for seed and inoculum development, as well as the cultivation medium for the batch and CFBF.

6.3.5. Batch fermentation and CFBF

Based on the results obtained from statistical optimization of the cultivation medium, the medium was prepared and used in downstream processes. For the batch and CFBF, the pre-inoculum was developed in 10% (v/v) suspensions in stoppered conical flasks and incubated at 37ºC in an orbital shaker (New Brunswick Innova 44, Eppendorf) at 200 rpm; for the optimal incubation time to produce high cell density biomass as determined from the BBD. The batch and CFBF cultivations of *B. thuringiensis* were conducted in a 2 L stoppered conical flask containing 500 mL optimized cultivation medium. For the fermentation, flasks were incubated at 37ºC in an orbital shaker (New Brunswick Innova 44, Eppendorf) and maintained at 200 rpm. CFBF was initiated as described for batch fermentation; however, when glucose concentration had depleted to a limiting concentration (~8 g L^{-1}), the batch cultivation was converted to nutrient feed cycle mode wherein 20% (v/v) of the fermentation medium was removed from the flask and replenished with an equal volume of fresh medium (having the same composition as the starting medium). Four cycles of repeated-batch cultivation were executed in this manner. At the end of the batch cultivation and after each cycle of the CFBF, the residual carbohydrate content (g L^{-1}), cell biomass (cell dry weight; CDW; g L^{-1}), and PHA produced (g L^{-1}) were determined. The PHAs extracted at the end of each cycle were confirmed by polymer characterization analyses. The batch and CFBF were conducted in duplicate on two separate occasions.

6.3.6. PHA extraction

As per section 3.3.5

6.3.7. High performance liquid chromatography (HPLC)

As per section 4.3.3.1

6.3.8. Fourier-transform infrared spectroscopy (FTIR)

As per section 3.3.6

6.3.9. Polymer analysis

As per section 3.3.7

6.3.10. Thermogravimetric analysis (TGA) and differential scanning calorimetry (DSC)

As per section 3.3.8

6.3.11. Statistical analysis

The effects of batch fermentation and each cycle of the CFBF on the yield of CDW and PHA as well as on polymer composition and thermal properties were determined using one-way ANOVA and SPSS (V 27.0). Where necessary, a Bonferroni Post-Hoc analysis was conducted, and a $p < 0.05$ was considered as statistically significant.

6.4. Results and Discussion

6.4.1. Statistical optimization of biomass fermentation medium

A BBD with four factors, with replicated center points, was used for statistical optimization of the fermentation medium for the production of high cell density biomass. The parameters tested were; yeast extract (A), hydrolyzate concentration (B), incubation time (C), and pH (D) of the fermentation medium (Table 6.2). This model was used to determine the effects of individual or combined interactions of the four independent variables on the yield of biomass. The experimental conditions, batch runs, as well as the corresponding actual, predicted, and residual responses for biomass yield are represented in Table 6.2 and Figure 6.1. An increase in cell density from OD_{600} of 1.8094 to 1.8923 occurred when the concentration of yeast extract decreased from 10 to 6 g L^{-1} (runs 10 and 11). Increasing the concentration of hydrolyzate from 50% to 100% adversely affected cell proliferation (runs 14 and 15) whereby cell density decreased from OD_{600} of 1.7275 to 1.2236. The effect of pH is observed in runs 23 and 25; a pH of 7 (closer to neutral) favored high cell density production with an OD_{600} of 2.1408 noted compared with pH 7.4, where an OD_{600} of 1.8025 was observed. A longer fermentation time also favored high cell density production (runs 5 and 6), where an increase in cultivation time from 18 h to 30 h increased cell density from OD_{600} 1.6736 to 1.9265 (Table 6.2). The highest OD_{600} of 2.3309 was noted for run 22 using the conditions: 10 g L^{-1} yeast extract; 75% hydrolyzate; incubation for 30 h; and a fermentation medium at pH 7.2. The predicted and the actual experimental responses of biomass are comparable, with minimal difference noted between the data (Figure 6.1). The minimal deviation from the straight line indicates less variation from the predicted value and is a satisfactory correlation between experimental data and predictive data, thus proving a high prognostic ability of the BBD (Tesfaye et al. 2018a).

Table 6.2: The actual, predicted, and residual responses for each experimental run from the 3-level 4-factor Box-Behnken Design used to elucidate the optimal cultivation medium to obtain high cell density biomass production by *B. thuringiensis*

	Variables				Cell Density (OD_{600})		
Run	**Yeast extract (g L^{-1})**	**Hydrolyzate (% v/v)**	**Time (h)**	**pH**	**Actual**	**Predicted**	**Residual**
1	6	50	24	7.2	2.0359	2.0517	-0.0158
2	10	50	24	7.2	2.1195	2.0293	0.0902
3	6	100	24	7.2	1.3056	1.4088	-0.1032
4	10	100	24	7.2	1.7119	1.7091	0.0028
5	8	75	18	7.0	1.6736	1.5987	0.0749
6	8	75	30	7.0	1.9265	1.9670	-0.0405
7	8	75	18	7.4	1.6336	1.6061	0.0275
8	8	75	30	7.4	1.8854	1.9733	-0.0879
9	8	75	24	7.2	2.2129	2.1609	0.0519
10	6	75	24	7.0	1.8923	1.8377	0.0546
11	10	75	24	7.0	1.8094	1.8706	-0.0613
12	6	75	24	7.4	1.8057	1.7384	0.0672
13	10	75	24	7.4	1.9349	1.9835	-0.0486
14	8	50	18	7.2	1.7275	1.7876	-0.0601
15	8	100	18	7.2	1.2236	1.1973	0.0262
16	8	50	30	7.2	2.0264	2.0466	-0.0203
17	8	100	30	7.2	1.7399	1.6739	0.0660
18	8	75	24	7.2	2.1112	2.1349	-0.0238
19	6	75	18	7.2	1.7387	1.7779	-0.0392
20	10	75	18	7.2	1.8382	1.8676	-0.0294
21	6	75	30	7.2	2.1328	2.09634	0.0364
22	10	75	30	7.2	2.3309	2.2847	0.0463
23	8	50	24	7.0	2.1408	2.1552	-0.0144
24	8	100	24	7.0	1.2805	1.2938	-0.0133
25	8	50	24	7.4	1.8025	1.7821	0.0203
26	8	100	24	7.4	1.7019	1.6804	0.0214
27	8	75	24	7.2	2.2071	2.2352	-0.0281

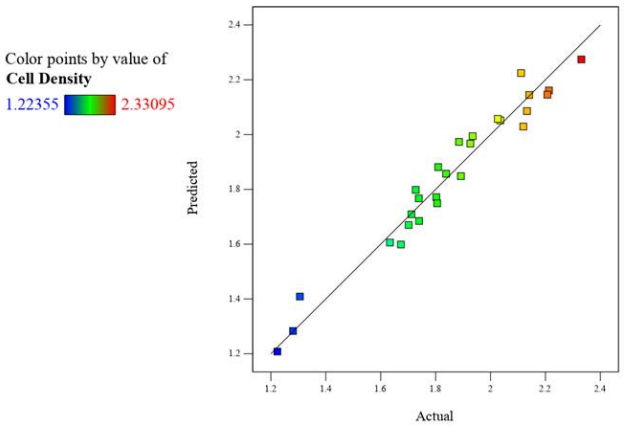

Figure 6.1: Graphical representation of the minimal difference between the actual (straight line) and predicted responses (squares) for the 3-level 4-factor Box-Behnken Design to obtain high cell density biomass production by *B. thuringiensis*.

The responses of predicted and experimental values were computed by means of ANOVA to determine the ability of the polynomial expression to predict the responses statistically. The ANOVA for the quadratic model of the response for cell density yield is presented in Table 6.3. The processed data from the experimental design enabled the calculation of the coefficients of the regression equation. The second-order polynomial equation is as follows;

Response (Y): $Biomass\ (OD_{600}) = +2.18 + 0.0695A + 0.2408B + 0.0034C + 0.1839D + 0.0807AB + 0.0530AC + 0.0247AD + 0.1899BC + 0.0544BD - 0.0003CD - 0.0656A^2 - 0.2956B^2 - 0.2117C^2 - 0.1630D^2$

Where A, B, D, BC, B^2, C^2, and D^2 were the statistically significant model terms indicating confidence in the results for the parameters yeast extract concentration (A), hydrolyzate concentration (B), incubation time (C), and pH (D).

The mathematical model equation for the production of biomass is within the limits of the conditions tested. Analysis of the regression equation infers that maximum cell density production of 2.3309 at OD_{600} is within the selected factor ranges and is influenced by all of the independent variables either in linear or quadratic terms. When considered in linear terms, the concentration of hydrolyzate (B) and incubation time (D) showed the greatest influence on biomass production. This suggests that biomass production should be relatively insensitive to linear variation of the other parameters. When considered with respect to quadratic terms, the concentration of hydrolyzate, reaction time, and pH had positive significance on biomass production (Table 6.3). The only significant interactive effect of variables was between

hydrolyzate concentration and time (BC) ($p < 0.05$), indicating that this strong interaction has a positive significance on yielding high cell density biomass (Table 5.3). The negative values of coefficients of the regression equation confirm that an increase in the value of any of the factors will decrease the biomass yield. The model *F*-value of 16.13 and $p < 0.01$ implies that the model is significant, and there is a 0.01% chance that an *F*-value this large can be due to noise. The ANOVA indicated that this regression model was significant ($p < 0.01$). The value of $p > F < 0.001$ implies that the model terms are significant and that there is less than a 1% chance that the observed values were due to chance. R^2 or coefficient of determination is the proportion of variation in the response attributed to the model rather than to random error, and for a good fit of a model, R^2 should be at least 80% (Cao et al. 2008). The suitability of the model was confirmed by a satisfactory R^2 value of 0.9576, which means that 95.76% of the variability in the response could be explained by the model and that 5% of the variations occur while performing the experiments, thus indicating a realistic fit of the model to the experimental data (Table 6.3). The R^2 coefficient measures the number of reductions in the variability of the response obtained using the independent factors within the model and confirms a satisfactory adjustment of the proposed model to the experimental data. The adjusted determination coefficient R^2 value was 0.8982 indicating adequate signal, and this high value also supports that the model was significant. The coefficient of variation (CV) is the ratio of the standard error of the estimate to the mean value of the observed response, expressed as a percentage, and a model with a CV below 15% can be considered reasonably reproducible as it suggests higher reliability of the experiment and demonstrates greater reliability of the trials (Cao et al. 2008; Tesfaye et al. 2018b; Limkar et al. 2019). In the current study, the CV of 5.01% indicates a high degree of precision in the experiment. Adequate precision measures the signal to noise ratio, and a ratio greater than four is desirable. For the present BBD, a ratio of 14.501 indicates an adequate signal suggesting that this model can be used to navigate the design space.

Table 6.3: ANOVA for response surface quadratic model for the 3-level 4-factor Box-Behnken Design used to elucidate the optimal cultivation medium to obtain high cell density biomass production by *B. thuringiensis*.

Source	Sum of Squares	Degrees of Freedom	Mean Square	*F*-value	*p*-value
Model	1.94	14	0.1384	16.13	< 0.0001**
A-Yeast extract	0.0580	1	0.0580	6.75	0.0266*
B-Hydrolyzate	0.6956	1	0.6956	81.04	< 0.0001**
C-pH	0.0001	1	0.0001	0.0162	0.9012
D-Time	0.4058	1	0.4058	47.27	< 0.0001**
AB	0.0260	1	0.0260	3.03	0.1122
AC	0.0113	1	0.0113	1.31	0.2789

AD	0.0024	1	0.0024	0.2837	0.6059
BC	0.1443	1	0.1443	16.81	0.0021*
BD	0.0118	1	0.0118	1.38	0.2677
CD	3.306×10^{-7}	1	3.306×10^{-7}	0.0000	0.9952
A^2	0.0230	1	0.0230	2.68	0.1329
B^2	0.4661	1	0.4661	54.30	< 0.0001**
C^2	0.2391	1	0.2391	27.85	0.0004**
D^2	0.1417	1	0.1417	16.50	0.0023*
Residual	0.0858	10	0.0086		
R^2	0.9576				
Adjusted R^2	0.8982				

**Statistically significant ($p < 0.01$) 1% level of significance
*Statistically significant ($p < 0.05$) 5% level of significance

The interactive effects between the response variable and the test variables are graphically illustrated as 3D-response surface plots generated by the model, as represented in Figure 6.2. The elliptical or circular shape of contours in 3D plots helps to predict the major interaction between the variables (Tesfaye et al. 2018b). An elliptical contour plot is indicative of significant interactions between the variables. From these plots, it is evident that a pH of 7.1-7.2 and a cultivation time of ~27 h will result in high cell density (OD_{600} of 2.2). The cell density decreases at higher pH or decreased cultivation time (Fig. 6.2 A). It is evident that yeast extract of ~8 g L^{-1} enhanced biomass production (Fig. 6.2 B). Nitrogen is an absolute requirement for cell growth and is assimilated for the synthesis of amino acids glutamine and glutamate (Cheng et al. 2015). Yeast extract comprises the water-soluble components of the yeast cell and is the main nitrogen source for bacterial growth. It is rich in growth-stimulating compounds such as peptides, carbohydrates, salts, vitamins, and free amino acids. Therefore it is a useful ingredient in media for the cultivation of microorganisms as it supports protein synthesis and cell growth, and reduces the consumption rate of the carbon source, and minimizes the accumulation of by-products (Cheng et al. 2015; Nguyen and Tran 2018). Ferreira and Schlottbom (2016) found that as little as 1 g L^{-1} of yeast extract was sufficient to obtain high yields of *B. sacchari* whereas Andersen and Jayaraman (2003) obtained the maximum cell density of *B. thuringiensis* subsp. g*alleriae* when 19.7196 g L^{-1} was used in the cultivation medium. A hydrolyzate concentration of ~65% allowed for a cell density of OD_{600} of 2.2, with concentrations above or below this range being less effective for yielding high cell density biomass (Fig. 6.2 B). During the hydrolysis of cellulosic biomass, sugars are not the only by-product. Toxic cell inhibitors such as volatile organic acids, furfurals, and acid-soluble lignin are also released during enzymolysis (Larsson et al. 1999). The inhibitory effect of phenolic and other aromatic compounds on microbial growth and product yield is variable. One possible mechanism is that phenolic compounds such as furfural and 5-hydroxymethylfurfural (5-HMF) interfere with the cell

membrane by influencing its functions and changing its protein-to-lipid ratio (Peters 2006; Zhang et al. 2018). Two common detoxification procedures to eliminate microbial inhibitors include separation by adsorption of inhibitors using activated carbon and over-liming. Such detoxification methods significantly reduce the concentration of inhibitors, thereby having a positive influence on the growth of biomass. However, detoxification processes are time-consuming and expensive (Kucera et al. 2017). Yu and Stahl (2008) observed that diluting hydrolyzate to about 50% (v/v) was better for cell growth and that the dilution effect significantly reduced the toxicity of the hydrolyzate. In the present study, it is possible that when using 100% (v/v) hydrolyzate, the presence of toxic compounds negatively affected cell proliferation resulting in lower cell density. In order to achieve a concentration of 50 or 75% of hydrolyzate, the hydrolyzate was diluted with a basal salt medium. Therefore, it is plausible that the simple dilution of hydrolyzate reduced the concentration of cell inhibiting toxic compounds, thus making the medium more favorable for cell growth. Furthermore, previous enzyme screening assays revealed that *B. thuringiensis* used in the present study synthesizes ligninase (Govender 2013). Ligninases can degrade furfural, HMF, or change their composition or structure to less toxic forms, thereby detoxifying lignocellulosic hydrolyzates (Yang et al. 2018). Values outside this range showed low efficiency for biomass production, confirming that the range of the chosen variables in the experimental design was conducive to obtain high yields of cell biomass.

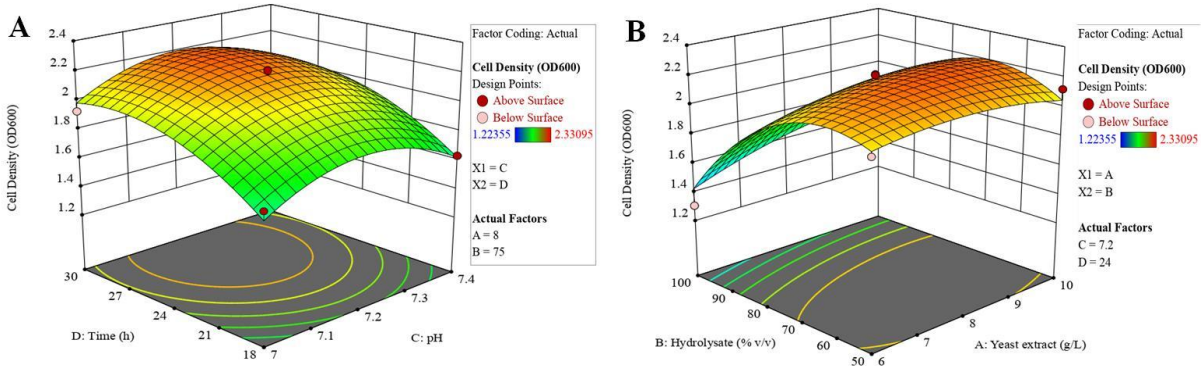

Figure 6.2: Three-dimensional (3D) response surface generated by the Box-Behnken Design model for the independent variables that affect the yield of obtain high cell density biomass production by *B. thuringiensis*; time and pH (A) and concentration of hydrolyzate and yeast extract (B).

6.4.2. Model validation

The model in the present study was validated by conducting experiments under the predicted conditions. Post-analysis of the design was used to determine the point prediction, and a mean cell density at OD_{600} of 2.28011 was predicted using the factors; 8.77 g L^{-1} yeast extract; 66.63% hydrolyzate (v/v); a fermentation pH of 7.18; and an incubation time of 27.22 h. After duplicate experimental trials on two separate occasions, a maximum OD_{600} of 2.4175 was attained. The difference between experimental and predicted values revealed a good correlation amongst the observed and predicted results, thus verifying the validity of the response model and the reality and accuracy of optimal conditions for the variables.

6.4.3. Batch fermentation and CFBF

Figure 6.3 A depicts the time course of batch cultivation of *B. thuringiensis* for PHA production, and the kinetic parameters are presented in Table 6.4. CFBF cycles 2, 3, and 4 were observed to significantly affect the yield of biomass (CDW) and PHA yield ($p < 0.05$). During batch cultivation, the culture exhibited an initial lag phase of around 4 h, after which it grew exponentially, resulting in a biomass yield of 7.75 g L^{-1} (CDW) and 3.22 g L^{-1} of PHA in 30 h, resulting in a PHA productivity of 0.107 g L^{-1} h^{-1}. The culture reached the stationary phase after 38 h. It was important to establish the batch growth and product kinetics since this established the basic kinetic parameters that were used for the CFBF for enhanced PHA formation. Wang and Liu (2014) found that wood extract hydrolyzate contributed to enhanced PHB production by *Burkholderia cepacia* in batch fermentation and obtained 16.8 g L^{-1} of PHB after 9 days. A 72 h batch fermentation of *Cupriavidus necator* using waste office paper hydrolyzate resulted in cell biomass, PHB production, and PHB content of 7.74 g L^{-1}, 4.45 g L^{-1}, and 57.52%, respectively (Annamalai et al. 2017). The CFBF cultivation of *B. thuringiensis* is depicted in Figure 6.3 B, and the kinetic parameters are presented in Table 6.4. The conversion of the batch fermentation to CFBF started at 29 h when the glucose concentration was 8.09 g L^{-1}, resulting in the first cycle of removal and subsequent re-filling of an equal volume of fresh medium. The slight decrease in cell concentration observed during the cycles is due to the addition of fresh medium that diluted the remaining fermentation medium; however, it gradually increased with continuous cell proliferation. The second cycle occurred at 52 h, and the third cycle at 65 h. It was observed that the culture continuously maintained its metabolic activities and continued to produce PHA even after three cycles. Based on the observation of continuously high cell density and PHA yields and glucose consumption, a

fourth cycle was initiated at 72 h. This however, was not successful, and the yields decreased in comparison with cycles CFBF 1-3. The decreased yields observed after CFBF 4 is explained by Ibrahim and Steinbüchel (2010) who state that that CFBF is typically performed to obtain high cell density. Once the highest possible cell density is reached, the culture enters decline phase during which excessive degradation of PHA occurs. Therefore, three cycles were sufficient to successfully achieve high cell density and PHA yields using the CFBF strategy. At the end of the third CFBF cycle (after 65 h), cell biomass of 20.99 g L^{-1} was noted with a PHA concentration of 14.28 g L^{-1} resulting in a yield of 68.03%. This cyclic strategy yielded an overall PHA productivity of 0.219 g L^{-1} h^{-1}. The CFBF resulted in an almost 3-fold increase in biomass concentration and 4-fold increase in PHA concentration, respectively, as compared with batch cultivation (Table 6.4). During batch cultivations, nutrients such as carbon and nitrogen substrates become limited during the course of fermentation, particularly during the exponential growth phase, thus affecting the growth of the culture. Furthermore, initiating batch fermentation with very high concentrations of substrates in the cultivation medium stands a risk of substrate inhibition phenomenon. Therefore, CFBF could be a better option as it ensures a controlled feeding of the substrate and adequate nutrient availability during the entire cultivation, thereby curbing the potential problem of substrate inhibition. CFBF also eliminates time-consuming activities such as cleaning, filling, and sterilizing a bioreactor to initiate batch cultivation (Gahlawat and Srivastava 2018). To the best of our knowledge, to date, there are no reports on CFBF cultivation for biomass and PHA production by *B. thuringiensis.* Gahlawat and Srivastava (2018) used CFBF to increase PHB concentration and productivity by *Azohydromonas australica*. They observed that at the end of the 60 h fermentation, the biomass and PHB yield was 24.90 g L^{-1} and 18.79 g L^{-1}, respectively, with a PHA productivity of 0.29 g L^{-1} h^{-1}. Ibrahim and Steinbüchel (2010) also investigated the use of CFBF to achieve high biomass growth and PHB productivity by the thermophilic bacterium, *Chelatococcus* sp. MW10 in a 42-liter bioreactor. After three cycles and 265 h fermentation, a cell density of 115 g L^{-1}, PHB concentration of 13.6 g L^{-1} h^{-1}, and PHB yield of 11.8% was noted. The CFBF strategy employed by Haas et al. (2017) found that *Cupriavidus necator* achieved a high PHB concentration of 3.1 g L^{-1} and reached a cell density of 148 g L^{-1}, which yielded 76% PHB.

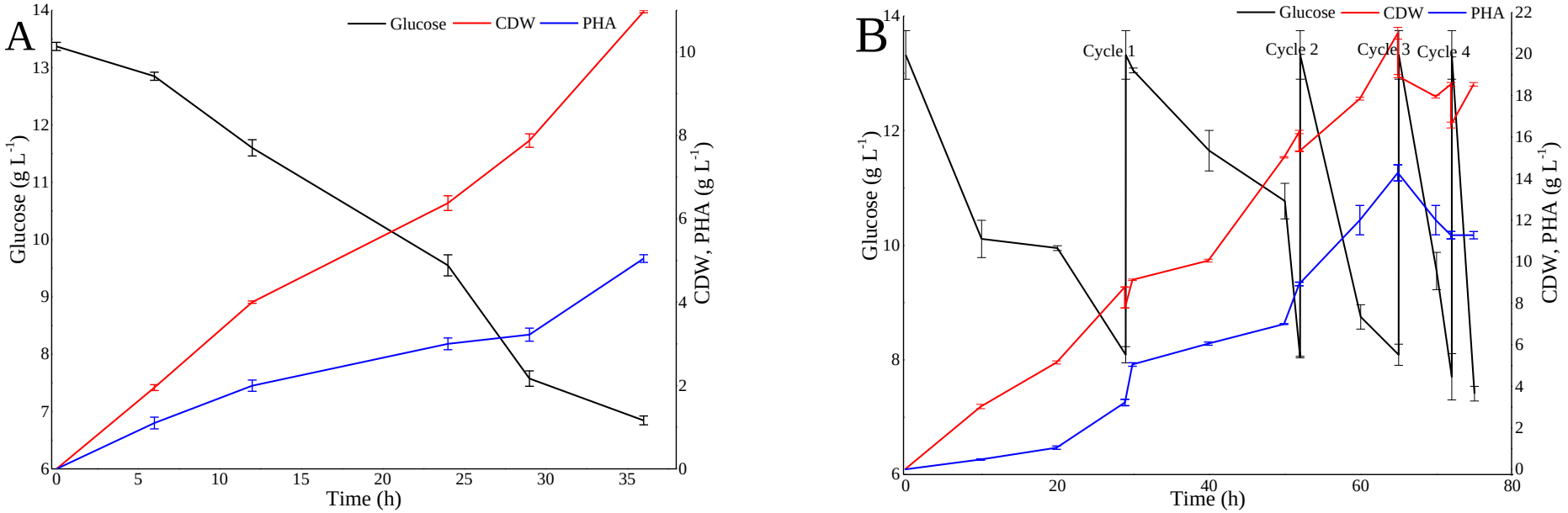

Figure 6.3: Kinetics of cell proliferation, carbon consumption and PHA production by *B. thuringiensis* in batch fermentation (A) and cyclic fed-batch fermentation (B) using the statistically optimized cultivation medium.

Table 6.4: Growth and product kinetic parameters of *B. thuringiensis* during the batch fermentation and cyclic fed-batch fermentation using the statistically optimized cultivation medium

Fermentation	Time (h)	Residual glucose (g L^{-1})	CDW (g L^{-1})	PHA (g L^{-1})	PHA yield (%)	Biomass productivity (g L^{-1} h^{-1})	PHA productivity (g L^{-1} h^{-1})
Batch	36	6.98	7.75	3.22	41.54	0.258	0.107
CFBF Cycle 1	29	8.09	8.75	3.22	36.8	0.302	0.111
CFBF Cycle 2	52	8.05	16.29*	8.95	54.94*	0.313	0.172
CFBF Cycle 3	65	7.94	20.99*	14.28	68.03*	0.323	0.219
CFBF Cycle 4	72	7.96	18.52*	11.28	60.90*	0.257	0.157

*Statistically significant ($p < 0.05$) 5% level of significance

6.4.4. FTIR characterization of PHAs

FTIR was used to confirm PHA-production by identifying the presence of functional groups present in PHA (Fig. 6.4). The peaks present at the ester, methylene, and terminal hydroxyl group are typically representative of the polymeric structure of PHAs (Apparao and Krishnaswamy 2015). The exact peak location and intensity are known to vary with the polymer chain length, concentration, and crystallinity of the PHA. The distinguishing peak of PHA is located around 1700-1738 cm^{-1} (C=O stretch) and a series of intense peaks located at 1000-1400 cm^{-1} (C-O stretch), which correspond to the ester group present in the molecular chain of highly ordered crystalline structures (Getachew and Woldesenbet 2016). The prominent pinnacle present at ~1708 cm^{-1} corresponds to ester carbonyl (C=O) extending the vibration of PHB (Fig. 6.4). Observation of adsorption bands around 1380, 1450, 2930, 1650, and 3400 cm^{-1} corresponds to $–CH_3$, $–CH_2$, CH, C–O, and O–H groups, respectively, which is typically present in pure PHB (Łabuzek and Radecka 2001). The strong peaks at 2923-2975 cm^{-1} are due to the C-H stretching methyl and methylene groups of alkanes, which are usually demonstrated by PHA polymers. The broad peak at 3396 cm^{-1} indicates the presence of O-H stretching of alcohol (terminal OH group) (Fig. 6.4) (Sindhu et al. 2016). The presence of a copolymer like PHBV is denoted by a characteristic absorption peak in the region of 2933–2972 cm^{-1}. Overall, the FTIR spectra of the extracted PHAs are comparable with commercial PHB and PHBV as they display prominent peaks at the wavelengths unique to PHA.

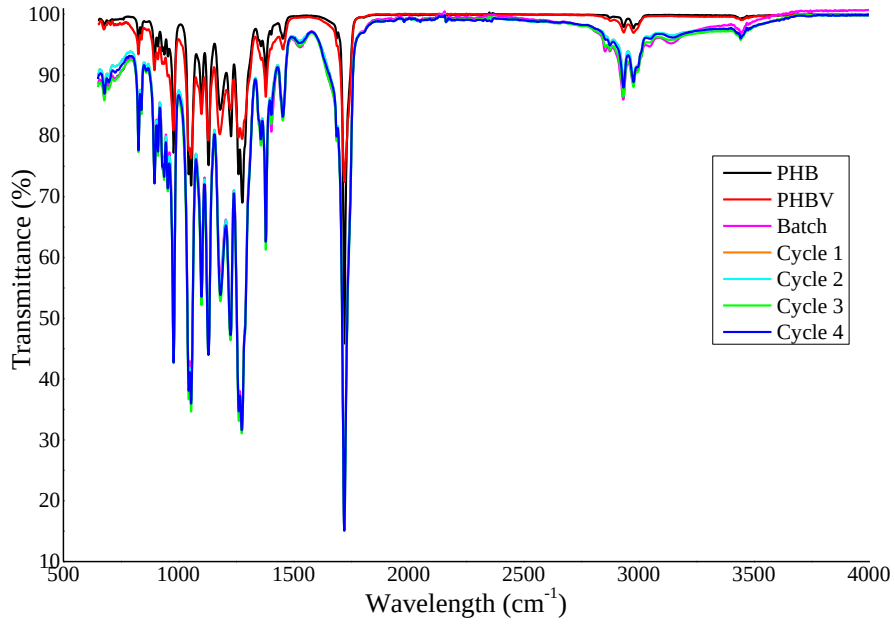

Figure 6.4: Fourier-transform infrared spectra of commercial PHB and PHBV compared with the PHAs extracted from *B. thuringiensis* after batch fermentation and after each cycle of the cyclic fed-batch fermentation.

6.4.5. Polymer composition

To identify the composition of the produced PHAs, py-GC/MS and THM-GC were employed as these techniques permit accurate detection, characterization, and semi-quantification of PHA-monomeric moieties incorporated by the isolate (Torri et al. 2014; Baidurah et al. 2015). The variations in the polymer composition of PHAs extracted after batch and CFBF are significant ($p < 0.01$). Statistical analysis revealed that cycles CFBF 2, 3, and 4 significantly affected the mol% of HB and HV in the polymer ($p < 0.05$), whereas only CFBF cycles 3 and 4 significantly affected the mol% of HHx in the polymers ($p < 0.05$). It was surprising to observe that the commercial PHB used in the present study is not a PHB homopolymer as it contained 10.19% HV (Table 6.5). In the present study, it was observed that after the first cyclic event, a copolymer containing 62.61% HB and 37.39% HV was elucidated, whereas after CFBF cycles 2-4, the HB-HV-HHx terpolymer was noted (Table 6.5 and S 3.1-3.5). This differs from previous reports, which state that PHB was the predominant biopolymer synthesized when agro-waste-derived hydrolyzates from bagasse (Yu and Stahl 2008), wheat bran (Annamalai and Sivakumar 2016), rice straw (Sindhu et al. 2016), wood (Wang and Liu 2014), wheat straw (Ferreira and Schlottbom 2016), and waste office paper (Annamalai et al. 2017) were the sole carbon source in the fermentation.

6.4.6. Thermal properties

6.4.6.1. TGA analysis

The thermal degradation profiles for commercial PHB and PHBV and the PHAs extracted from *B. thuringiensis* after each cyclic event are shown in Figure 6.5. The initial ($T_{5\%}$) and maximum (T_{max}) degradation temperatures for each sample are presented in Table 6.5 and Figure 6.5. All of the samples displayed a similar thermal decomposition pattern, and the thermal degradation for all the samples occurs in a one-stage decomposition trend under a nitrogen atmosphere (Fig. 6.5 A). The TGA curve shows that the weight loss (%) of all the samples occurs in two stages. In comparison with commercial PHB and PHBV, there is a noticeable difference in the initial and maximum thermal degradation. The initial degradation occurred in the range of 255.54-269.66°C with a weight loss of ~1-8% of the total mass noted (Table 6.5; Fig. 6.5 A). This weight loss results from the evaporation of physically adsorbed impurities or solvents like methanol, chloroform, etc., used during the extraction and separation processes (Pradhan et al. 2018). The maximum thermal degradation of the samples occurred around 286.77°C to 292.21°C, beyond the melting point of PHB (Table 6.5; Fig. 6.5 B). The main mechanism of

thermal decomposition of PHB corresponds to β-elimination of PHB chains that facilitate the formation of crotonic acid, dimeric, trimeric, and tetrameric volatiles (Vahabi et al. 2019). A shift in maximum degradation temperature of the PHAs is observed whereby T_{max} increased after each cyclic event compared with commercial PHB and PHBV (Table 6.5, Fig. 6.5 B). Thus, it can be concluded that these PHAs have a slightly higher thermal stability compared with commercial PHB. The higher thermal stability of the extracted polymer could also be attributed to a more crystalline morphology (Pradhan et al. 2018). It is important to acknowledge high decomposition temperatures as it is a crucial factor for polymer processing in the industry since the material has to be tolerant and resist structural degradation, considering the high temperatures used for extrusion and injection molding to manufacture biodegradable films and molded pieces (Pradhan et al. 2018). Hassan et al. (2016) reported that the maximum thermal degradation for PHA obtained from *Bacillus* sp.34 occurred between 237-320°C, a range that was also observed in the present study. A similar observation was made for polymers obtained from *Alcaligenes* sp., where the maximum thermal degradation was between 220°C and 315°C (Melo et al. 2012). Pillai et al. (2017) found the thermal degradation of the PHB synthesized by *B. aryabhattai* to have an initial polymer degradation temperature at 247°C and maximum degradation at 287°C, which is similar to the degradation temperatures of the terpolymer PHA retrieved after the second cyclic event (Table 6.5). However, their standard PHB showed the initial and maximum degradations at 212°C and 266°C, respectively, which is substantially lower compared with the commercial PHB used in the present study (Table 6.5). The cyclic events resulted in PHAs having a noticeable shift in maximum thermal degradation temperature ranging from 250.77-262.56°C, which is higher than the commercial PHB and PHBV, respectively. However, Sandhya et al. (2013) concluded that their sample contained many different hydroxyalkanoate monomers since they observed lower degradation temperatures compared to that of the standard PHB.

6.4.6.2. DSC analysis

Differential scanning calorimetry analysis was conducted to elucidate the thermal transitions that a polymer undergoes as the sample is heated. The thermal transitions are manifested in terms of glass transition temperature (T_g), melting point (T_m), melting enthalpy (ΔH_m), crystallization temperature (T_c), crystallization enthalpy (ΔH_c), and degree of crystallinity (X_c) are summarized in Table 6.5. The DSC cooling and second heating cycle curves of commercial PHB and PHBV, as well as the PHAs, extracted from *B. thuringiensis* after each cyclic event,

are shown in Figure 6.6. The variations observed for T_g, T_m T_c, and X_c of PHAs extracted after batch fermentation and each cyclic event of CFBF are significant ($p < 0.01$). The T_g varied from 4.60-5.02°C (Table 6.5). The structure of the polymer results in the initial movement of the polymer chain at a relatively lower temperature resulting in a decreased value of glass transition temperature (Pradhan et al. 2018). There was a wide variation in the T_c ranging from 75.5°C to 118.54°C (Table 6.5; Fig. 6.6 A). Crystallization occurs due to the gain of mobilization of the polymer chains, which allows the polymer chains to organize and form crystals. The increasing T_c relates to the crystalline region in the polymer where the molecular chains are closely packed, and the secondary links are stronger in contrast to amorphous regions of a polymer. Therefore, high temperatures are required for the deformation of the polymer chain (Beber et al. 2018). PHAs with low T_c are problematic for melt-processing polymer procedures (Volova et al. 2013). The T_c for PHB synthesized from *B. megaterium* was ~113°C, which is comparable to commercial PHBV analyzed in the present study (Chaijamrus and Udpuay 2008). The narrower crystallization peaks for PHBV and PHA from CFBF cycles 2, 3, and 4 observed in Figure 6.6 A are owed to the higher content of HV in the respective polymers and are also indicative of crystals with a more homogeneous size distribution. The larger crystallization peaks as observed for commercial PHB, PHA from batch fermentation and CFBF cycle 1 (Fig. 6.6 A) are less desirable as they represent the formation of crystals with lower perfection and larger size distribution (do Amaral Montanheiroa et al. 2016). In Figure 6.6 B, two distinct T_m endothermic peaks are observed for each sample, which is presented as a minor peak, followed by a dominant major peak at a higher temperature. For commercial PHB, the second peak appears as a shoulder peak of the main peak. The first T_m ranged from 129.53-171.65°C, whereas the second T_m ranged from 140.82 -174.69°C (Table 6.5). The first melting peak originates from the melting of crystals formed during PHA sample preparation, and the second peak is due to the fusion of crystals formed during the heating phase of the DSC (Buzarovska and Grozdanov 2009). Other major contributors to the double melting behavior that results in multiple melting peaks include two different crystalline domains; the melting-re-crystallization-remelting mechanism; melting of different types of crystals with different sizes; different modifications; and thermal stabilities; or the melting of crystals with different lamellar thickness. Small and less perfect crystals melt at a lower temperature, and the larger and more perfect ones melt at a higher temperature (Wellen et al. 2015; do Amaral Montanheiroa et al. 2016; Vahabi et al. 2019). Multiple melting peaks are a common feature of semi-crystalline polymers (Wellen et al. 2015). Multi-component PHAs, as

observed herein, have other alkanoate components or long side chains and tend to have a lower T_m (Saranya and Shenbagarathai 2011; Sandhya et al. 2013). Sharma et al. (2017) report that copolymer PHBV produced by *Pseudomonas putida* had a T_m of 137-170°C, which is higher than the T_m of PHBV observed in the present study. The low T_m of the PHA characterized at CFBF cycle 4 is not unusual. Surendran et al. (2020) explain that incorporation of a minor quantity (5 mol%) of HHx can reduce the melting point to below 155°C. The decreasing T_m in the present study is consistent with previous reports that had shown a decrease in melting temperature when the non-HB monomer fraction of the copolymer increased (Kehail et al. 2015). A low T_m is indicative of a polymer containing a high HV fraction (Surendran et al. 2020). A low T_m is also desirable as it implies that the polymer can be processed at a low temperature, making the polymer suitable for soft products such as films with improved ductility and flexibility (Liu et al. 2019). The presence of a pronounced gap between T_m and T_{max} (Table 6.5) is an important favorable characteristic of a polymer. It is indicative of polymers with a wide melt-processing window, thereby increasing the range of products (films, fibers, hollow forms etc.) that can potentially be produced from the polymer, as well as increasing the range of processing methods the polymer can withstand (solution spinning, extrusion, injection molding etc.) (Volova et al. 2013). The degree of crystallinity (X_c) is one of the most important characteristics among the different mechanical performance and processability properties of the polymer and is summarized in Table 6.5. To minimize polymer processing challenges, X_c should ideally be $\leq$ 50%; otherwise, corrective actions are required resulting in challenges during polymer processing that can increase the operation price (Rodrigues et al. 2019). The X_c for the cyclic events decreased from 52% at CFBF 1 to 34% after CFBF 4 (Table 6.5). Thus, the synthesized PHAs are less crystalline compared with commercial PHB and PHBV. Chaijamrus and Udpuay (2008) reported X_c = 60% for PHA extracted from *B. megaterium*, resulting in a highly crystalline polymer. That X_c is substantially higher compared with the X_c observed for PHAs in the present study. The X_c of the PHAs extracted from *B. thuringiensis* are lower than that of the commercial PHB and PHBV (Table 6.5). The decreasing X_c observed for PHAs from CFBF cycles 2, 3, and 4 is attributed to the presence of HHx specifically, as the incorporation of HHx in the polymer chain reduces the crystallinity of the PHA (Surendran et al. 2020). The,X_c for PHBV obtained after batch fermentation and CFBF cycle 1 is 59% and 57%, respectively, which is a relatively high

crystalline PHBV copolymer. In addition, the X_c for the PHBV copolymers observed in the present study is similar to the X_c of commercial PHB (62%) than the X_c of commercial PHBV (41%) (Table 6.5). Shang et al. (2012) explain that a high HV content in the polymer, as observed in commercial PHBV, decreases the crystallinity of a polymer. Surendran et al. (2020) further explain the isodimorphism behavior phenomenon that occurs exclusively in PHBV copolymers. When the HV fraction of the copolymer is < 37%, the HV lattice can co-crystallize into the same lattice as HB. The properties of the resultant polymer are similar to PHB, such as high crystallinity. A polymer with high crystallinity is stiff and brittle in nature (Singh et al., 2015; Możejko-Ciesielska and Kiewisz, 2016). Therefore, a PHA with low crystallinity, such as the terpolymer obtained after CFBF cycles 2, 3, and 4, is advantageous as it is less brittle, thus increasing the range of applications of the polymer (Chaijamrus and Udpuay 2008). Furthermore, incorporating HV and HHx monomers into PHAs as well as having a combination of a low T_g and a low X_c, as observed for PHAs in the present study, are favorable (Table 6.5). These characteristics change the mechanical performance of the polymer as it imparts elastomeric behavior rendering flexible polymers suitable for medical applications (Rai et al. 2011). In the present study, TGA and DSC analysis aided in highlighting the critical role that incorporation of non-HB units into the polymer chain plays for the enhancement of physical properties of PHA polymers.

Table 6.5: Polymer composition, thermal degradation and thermal properties of the PHAs extracted from *B. thuringiensis* after batch fermentation and after each cycle of the cyclic fed-batch fermentation compared with commercial PHB, and PHBV

	Polymer Composition (mol %)**			**Degradation Temperature (°C)**		**Thermal Properties****						
	HB	**HV**	**HHx**	**$T_{5\%}$**	**T_{max}**	**T_g (°C)**	**T_{m1} (°C)**	**T_{m2} (°C)**	**ΔHm (J g^{-1})**	**T_c (°C)**	**ΔHc (J g^{-1})**	**X_c (%)**
Batch fermentation	82.13	17.87	-	217.15	286.81	4.98	155.4	166.64	85.59	78.07	62.61	59
CFBF Cycle 1	77.45	22.55	-	222.52	286.87	4.95	149.89	160.77	83.93	83.69	65.89	57
CFBF Cycle 2	54.56	42.80	2.64	248.60	289.96	4.71	147.17	158.35	59.76	115.18	54.96	40
CFBF Cycle 3	52.48	43.78	3.74	253	290.66	4.65	143.77	154.53	55.77	118.54	53.50	38
CFBF Cycle 4	48.43	46.39	5.18	275.54	292.21	4.60	129.53	140.82	49.77	122.14	46.53	34
Commercial PHB	89.81	10.19	-	269.66	286.77	5.02	171.65	174.69	90.35	75.5	63.92	62
Commercial PHBV	43.35	56.65	-	264.04	288.32	4.85	138.22	146.94	60.55	113.17	58.06	41

** Statistically significant ($p < 0.01$) 1% level of significance

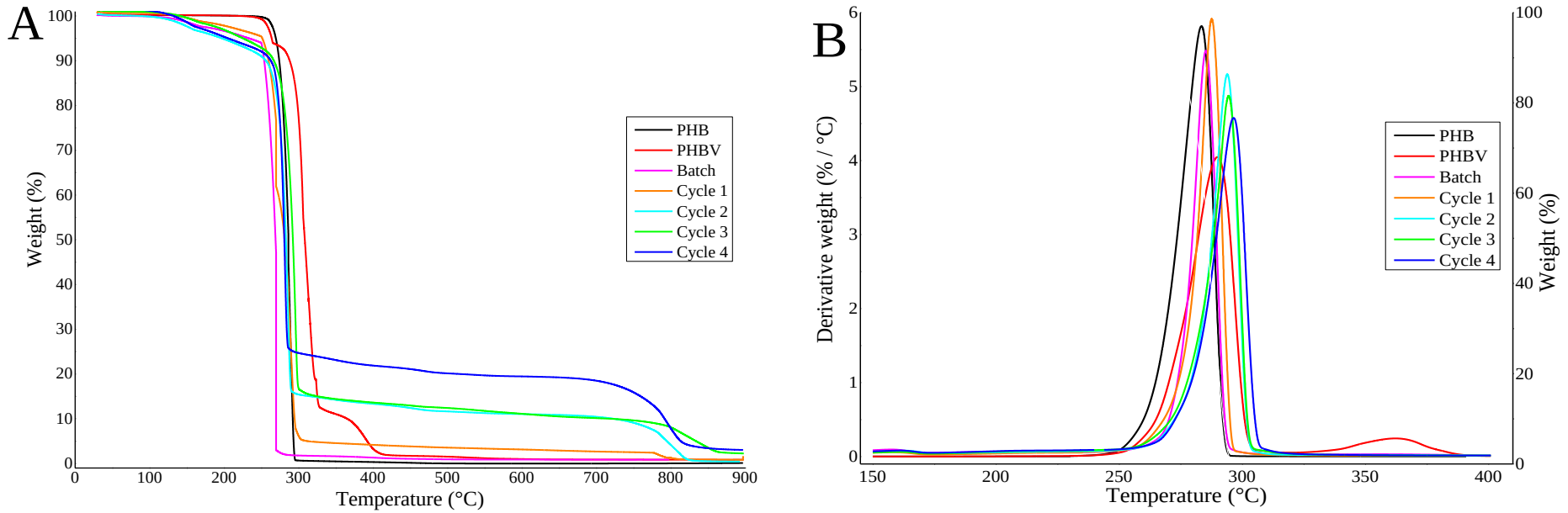

Figure 6.5: Thermograms from thermogravimetric (A) and derivative thermogravimetric (B) analysis of commercial PHB and PHBV, and the PHAs extracted from *B. thuringiensis* after batch fermentation and after each cycle of the cyclic fed-batch fermentation using the statistically optimized cultivation medium.

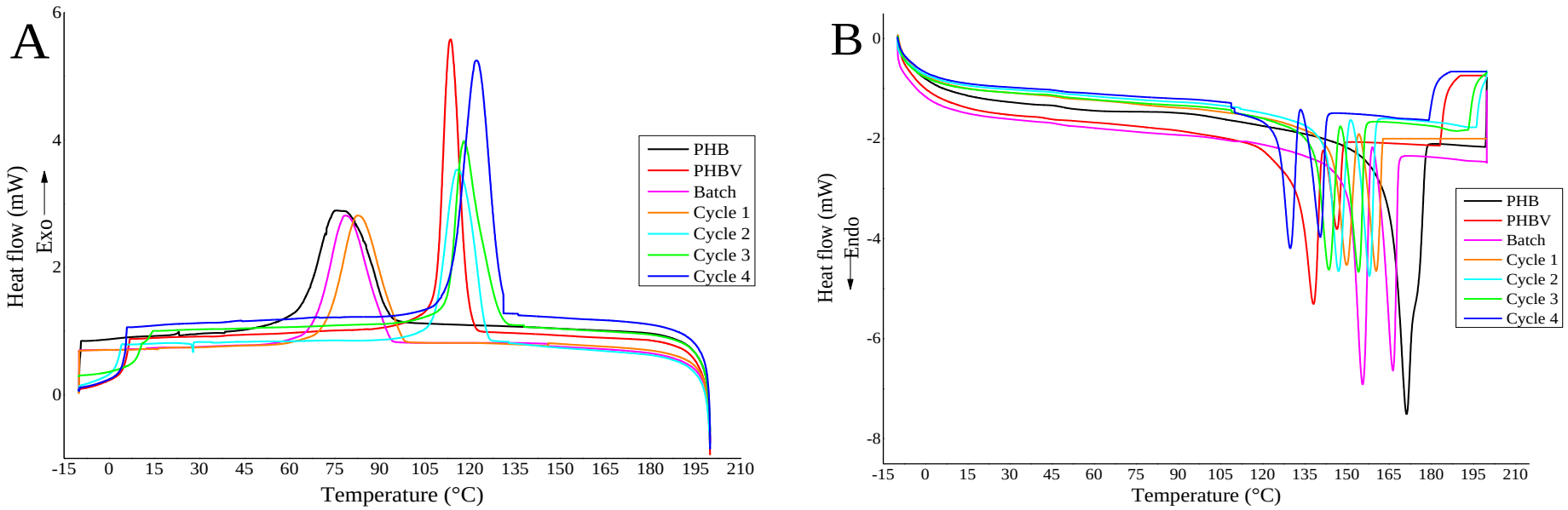

Figure 6.6: Differential scanning calorimetry thermograms displaying the cooling cycle (A), and the second heating cycle (B) used to characterize commercial PHB and PHBV, and the PHAs extracted from *B. thuringiensis* after batch fermentation and after each cycle of the cyclic fed-batch fermentation using the statistically optimized cultivation medium.

6.5. Conclusions

This study assessed the ability and efficiency of *B. thuringiensis* to assimilate glucose-rich hydrolyzate produced from enzymatic saccharification of PPMS. The isolate was able to use this hydrolyzate as a sole carbon source for cell proliferation and PHA production. The statistical optimization using BBD aided in determining an optimal cultivation medium to produce high cell density biomass and also determined the success of the CFBF strategy. The CFBF strategy proved successful for simultaneously achieving high cell density and enhancing PHA production by *B. thuringiensis*. Three cycles of culture broth removal and subsequent re-filling with fresh medium at 29 h, 52 h and 65 h resulted in a maximum PHA yield of 14.28 g L^{-1} with the overall productivity of 0.219 g L^{-1} h^{-1}. The present work demonstrated a 3-fold increase in PHA yield and a 4-fold increase in productivity compared with batch cultivation. The isolate was a good producer of co- and ter-polymers. However, the polymer composition, and thermal properties varied after each cyclic event. On the basis of proof of concept, this study exhibits encouraging results. A range of very cheap raw materials are available for industrial PHA production, and coupled with the practicality of this strategy, it has potential to be scaled-up to pilot level for techno-economic feasibility analysis.

6.6. References

Andersen RKI, Jayaraman K (2003) Influence of carbon and nitrogen sources on the growth and sporulation of *Bacillus thuringiensis* var *galleriae* for biopesticide production. Chem Biochem Eng Q 17:225–231.

Annamalai N, Al-Battashi H, Al-Bahry S, Sivakumar N (2017) Biorefinery production of poly-3-hydroxybutyrate using waste office paper hydrolysate as feedstock for microbial fermentation. J Biotechnol 265:25–30.

Annamalai N, Sivakumar N (2016) Production of polyhydroxybutyrate from wheat bran hydrolysate using *Ralstonia eutropha* through microbial fermentation. J Biotechnol 237:13–17.

Apparao U, Krishnaswamy VG (2015) Production of polyhydroxyalkanoate (PHA) by a moderately halotolerant bacterium *Klebsiella pneumoniae* U1 isolated from rubber plantation area. Int J Environ Bioremediation Biodegrad 3:54–61.

Aramvash A, Moazzeni Zavareh F, Gholami Banadkuki N (2018) Comparison of different solvents for extraction of polyhydroxybutyrate from *Cupriavidus necator*. Eng Life Sci 18:20–28.

Argyropoulos D, Lynch HC (1997) Recombinant β-glucanase production and plasmid stability of *Bacillus subtilis* in cyclic fed batch culture. Biotechnol Tech 11:187–190.

Baidurah S, Kubo Y, Kuno M, Kodera K, Ishida Y, Yamane T, Ohtani H (2015) Rapid and direct compositional analysis of poly(3-hydroxybutyrate-co-3-hydroxyvalerate) in whole bacterial cells by thermally assisted hydrolysis and methylation-gas chromatography. Anal Sci 31:79–83.

Beber VC, de Barros S, Banea MD, Brede M, de Carvalho LH, Hoffmann R, Costa ARM, Bezerra EB, Silva IDS, Haag K, Koschek K, Wellen RMR (2018) Effect of Babassu natural filler on PBAT/PHB biodegradable blends: An investigation of thermal, mechanical, and morphological behavior. Materials (Basel) 11:1–16.

Buzarovska A, Grozdanov A (2009) Crystallization kinetics of poly(hydroxybutyrate-co-hydroxyvalerate) and poly(dicyclohexylitaconate) PHBV/PDCHI blends: Thermal properties and hydrolytic degradation. J Mater Sci 44:1844–1850.

Cao Y, Meng D-J, Lu J, Long J (2008) Statistical optimization of xylanase production by *Aspergillus niger* AN-13 under submerged fermentation using response surface methodology. African J Biotechnol 7:631–638.

Chaijamrus S, Udpuay N (2008) Production and characterization of polyhydroxybutyrate from molasses and corn steep liquor produced by *Bacillus megaterium* ATCC 6748. Agric Eng Int CIGR Ejournal 1–12.

Cheng L, Wang J, Fu Q, Miao L, Yang X, Li S, Li F, Shen Z (2015) Optimization of carbon and nitrogen sources and substrate feeding strategy to increase the cell density of *Streptococcus suis*. Biotechnol Biotechnol Equip 29:779–785.

Czyrski A, Sznura J (2019) The application of Box-Behnken-Design in the optimization of HPLC separation of fluoroquinolones. Sci Rep 9:1–10.

do Amaral Montanheiroa TL, Passadora FR, de Oliveiraa MP, Durán N, Lemes AP (2016) Preparation and characterization of maleic anhydride grafted poly(hydroxybutirate-co-hydroxyvalerate)-PHBV-g-MA. Mater Res 19:229–235.

Duff SJB, Moritz JW, Andersen KL (1994) Simultaneous hydrolysis and fermentation of pulp mill primary clarifier sludge. Can J Chem Eng 72:1013–1020.

Ferreira BS, Schlottbom C (2016) Production of polyhydroxybutyrate from lignocellulosic hydrolysates– Optimization of *Bacillus sacchari* fermentation and scale up from 2 L to 200 L. Eppendorf 1–6.

Gahlawat G, Srivastava AK (2018) Enhancing the production of polyhydroxyalkanoate biopolymer by *Azohydromonas australica* using a simple empty and fill bioreactor cultivation strategy. Chem Biochem Eng Q 31:479–485.

García YG, Carlos, Contreras JCM, Hernández JA, Dueñas RS (2015) Procurement of fermentable sugars from cardboard waste for the cultivation of yeasts for biotechnological use. Rev Mex Ciencias For 6:88–105.

Getachew A, Woldesenbet F (2016) Production of biodegradable plastic by polyhydroxybutyrate (PHB) accumulating bacteria using low cost agricultural waste material. BMC Res Notes 9:1–9.

Gholamveisi N, Azar SM, Moravej R (2018) *Bacillus thuringiensis* strain NG, a novel isolated strain for production of various polyhydroxyalkanoates. Biol J Microorg 6:13–20.

Govender L (2013) Seasonal variation of microflora and their effects on the quality of wood chips intended for pulping. PhD Dissertation. University of KwaZulu-Natal.

Gowda V, Shivakumar S (2014) Agrowaste-based polyhydroxyalkanoate (PHA) production using hydrolytic potential of *Bacillus thuringiensis* IAM 12077. Brazilian Arch Biol Technol 57:55–61.

Haas C, El-najjar T, Virgolini N, Smerilli M, Neureiter M (2017) High cell-density production of poly(3-hydroxybutyrate) in a membrane bioreactor. N Biotechnol 37:117–122.

Hanrahan G, Garza C, Garcia E, Miller K (2007) Experimental design and response surface modeling: A method development application for the determination of reduced inorganic species in environmental samples. J Environ Informatics 9:71–79.

Hassan MA, Bakhiet EK, Ali SG, Hussien HR (2016) Production and characterization of polyhydroxybutyrate (PHB) produced by *Bacillus* sp. isolated from Egypt. J Appl Pharm Sci 6:46–51.

Ibrahim MHA, Steinbüchel A (2010) High-cell-density cyclic fed-batch fermentation of a poly(3-hydroxybutyrate)-accumulating thermophile, *Chelatococcus sp*. strain MW10. Appl Environ Microbiol 76:7890–7895.

Kehail AA, Foshey M, Chalivendra V, Brigham CJ (2015) Thermal and mechanical characterization of solvent-cast poly(3-hydroxybutyrate-co-3-hydroxyhexanoate). J Polym Res 22:1–8.

Kucera D, Benesova P, Ladicky P, Pekar M, Sedlacek P, Obruca S (2017) Production of polyhydroxyalkanoates using hydrolyzates of spruce sawdust: Comparison of hydrolyzates detoxification by application of overliming, active carbon, and lignite. Bioengineering 4:1–9.

Kunasundari B, Sudesh K (2011) Isolation and recovery of microbial polyhydroxyalkanoates. Express Polym Lett 5:620–634.

Łabuzek S, Radecka I (2001) Biosynthesis of PHB tercopolymer by *Bacillus cereus* UW85. J Appl Microbiol 90:353–357.

Larsson S, Palmqvist E, Hahn-Hägerdal B, Tengborg C, Stenberg K, Zacchi G, Nilvebrant N-O (1999) The generation of fermentation inhibitors during dilute acid hydrolysis of softwood. Enzyme Microb Technol 24:151–159.

Limkar MB, Pawar SV, Rathod VK (2019) Statistical optimization of xylanase and alkaline protease co-production by *Bacillus* spp using Box-Behnken Design under submerged fermentation using wheat bran as a substrate. Biocatal Agric Biotechnol 17:455–464.

Liu J, Zhao Y, Diao M, Wang W, Hua W, Wu S, Chen P, Ruan R, Cheng Y (2019) Poly(3-hydroxybutyrate-co-3-hydroxyvalerate) production by *Rhodospirillum rubrum* using a two-step culture strategy. J Chem 2019:1–8.

Lynch HC, Bushell ME (1995) The physiology of erythromycin biosynthesis in cyclic fed batch culture. Microbiology 141:3105–3111.

Madrid LM, Díaz JCQ (2011) Ethanol production from paper sludge using *Kluyveromyces marxianus*. Dyna 78:185–191.

Marques S, Alves L, Roseiro JC, Gírio FM (2008) Conversion of recycled paper sludge to ethanol by SHF and SSF using *Pichia stipitis*. Biomass and Bioenergy 32:400–406.

Martin-Sampedro R, Eugenio ME, Revilla E, Martín JA, Villar JC (2011) Integration of kraft pulping on a forest biorefinery by the addition of a steam explosion pretreatment. BioResources 6:513–528.

Martínez-Sanz M, Villano M, Oliveira C, Albuquerque MGE, Majone M, Reis M, Lopez-Rubio A, Lagaron JM (2014) Characterization of polyhydroxyalkanoates synthesized from microbial mixed cultures and of their nanobiocomposites with bacterial cellulose nanowhiskers. N Biotechnol 31:364–376.

Melo JDD, Carvalho LFM, Medeiros AM, Souto CRO, Paskocimas CA (2012) A biodegradable composite material based on polyhydroxybutyrate (PHB) and carnauba fibers. Compos Part B Eng 43:2827–2835.

Moritz JW, Duff SJB (1996) Simultaneous saccharification and extractive fermentation of cellulosic substrates. Biotechnol Bioeng 49:504–511.

Możejko-Ciesielska J, Kiewisz R (2016) Bacterial polyhydroxyalkanoates: Still fabulous? Microbiol Res 192:271–282.

Muhammadi S, Afzal M, Hameed S (2015) Bacterial polyhydroxyalkanoates-eco-friendly next generation plastic: Production, biocompatibility, biodegradation, physical properties and applications. Green Chem Lett Rev 8:56–77.

Munir S, Iqbal S, Jamil N (2015) Polyhydroxyalkanoates (PHA) production using paper mill wastewater as carbon source in comparison with glucose. J Pure Appl Microbiol 9:1–8.

Nguyen H-YT, Tran G-B (2018) Optimization of fermentation conditions and media for production of glucose isomerase from *Bacillus megaterium* using response surface methodology. Scientifica (Cairo) 2018:1–11.

Peters D (2006) Carbohydrates for fermentation. Biotechnol J 1:806–814.

Pillai AB, Kumar AJ, Thulasi K, Kumarapillai H (2017) Evaluation of short-chain-length polyhydroxyalkanoate accumulation in *Bacillus aryabhattai*. Brazilian J Microbiol 48:451–460.

Pirt SJ (1974) The theory of fed batch culture with reference to the penicillin fermentation. J Appl Chem Biotechnol 24:415–424.

Pradhan S, Dikshit PK, Moholkar VS (2018) Production, ultrasonic extraction, and characterization of poly(3-hydroxybutyrate) (PHB) using *Bacillus megaterium* and *Cupriavidus necator*. Polym Adv Technol 29:2392–2400.

Prasetyo J, Kato T, Park EY (2010) Efficient cellulase-catalyzed saccharification of untreated paper sludge targeting for biorefinery. Biomass and Bioenergy 34:1906–1913.

Rai R, Keshavarz T, Roether JA, Boccaccini AR, Roy I (2011) Medium chain length polyhydroxyalkanoates, promising new biomedical materials for the future. Mater Sci Eng R Reports 72:29–47.

Rodrigues PR, Nunes JMN, Lordelo LN, Druzian JI (2019) Assessment of polyhydroxyalkanoate synthesis in submerged cultivation of *Cupriavidus necator* and *Burkholderia cepacia* strains using soybean as substrate. Brazilian J Chem Eng 36:73–83.

Rohini D, Phadnis S, Rawal SK (2006) Synthesis and characterization of poly-β-hydroxybutyrate from *Bacillus thuringiensis* R1. Indian J Biotechnol 5:276–283.

Sandhya M, Aravind J, Kanmani P (2013) Production of polyhydroxyalkanoates from *Ralstonia eutropha* using paddy straw as cheap substrate. Int J Environ Sci Technol 10:47–54.

Saranya V, Shenbagarathai R (2011) Production and characterization of PHA from recombinant *E. coli* harbouring *PHAC1* gene of indigenous *Pseudomonas* sp. LDC-5 using molasses. Brazilian J Microbiol 42:1109–1118.

Schroeder BG, Zanoni PRS, Magalhães WLE, Hansel FA, Tavares LBB (2015) Evaluation of biotechnological processes to obtain ethanol from recycled paper sludge. J Mater Cycles Waste Manag 19:463–472.

Shang L, Fei Q, Zhang YH, Wang XZ, Fan D-D, Chang HN (2012) Thermal properties and biodegradability studies of poly(3-hydroxybutyrate-co-3-hydroxyvalerate). J Polym Environ 20:23–28.

Sharma PK, Munir RI, de Kievit T, Levin DB (2017) Synthesis of polyhydroxyalkanoates (PHAs) from vegetable oils and free fatty acids by wild-type and mutant strains of *Pseudomonas chlororaphis*. Can J Microbiol 63:1009–1024.

Sheu D-S, Wang Y-T, Lee C-Y (2000) Rapid detection of polyhydroxyalkanoate-accumulating bacteria isolated from the environment by colony PCR. Microbiology 146:2019–2025.

Sin MC, Tan IKP, Annuar MSM, Gan SN (2014) Viscoelastic, spectroscopic, and microscopic characterization of novel bio-based plasticized poly(vinyl chloride) compound. Int J Polym Sci 2014:1–11.

Sindhu R, Kuttiraja M, Prabisha TP, Binod P, Sukumaran RK, Pandey A (2016) Development of a combined pretreatment and hydrolysis strategy of rice straw for the production of bioethanol and biopolymer. Bioresour Technol 215:110–116.

Singh M, Kumar P, Ray S, Kalia VC (2015) Challenges and opportunities for customizing polyhydroxyalkanoates. Indian J Microbiol 55:235–249.

Singh S, Sithole B, Lekha P, Permaul K, Govinden R (2021) Pretreatment and enzymatic saccharification of sludge from a prehydrolysis kraft and kraft pulping mill. J Wood Chem Technol. https://doi.org/10.1080/02773813.2020.1856880

Smitha KV, Pradeep BV (2017) Application of Box-Behnken design for the optimization of culture conditions for novel fibrinolytic enzyme production by *Bacillus altitudinis* S-CSR 0020. J Pure Appl Microbiol 11:1447–1456.

Surendran A, Lakshmanan M, Chee JY, Sulaiman AM, Van Thuoc D, Sudesh K (2020) Can polyhydroxyalkanoates be produced efficiently from waste plant and animal oils? Front Bioeng Biotechnol 8:1–15.

Tesfaye T, Sithole B, Ramjugernath D, Ndlela L (2018a) Optimisation of surfactant decontamination and pre-treatment of waste chicken feathers by using response surface methodology. Waste Manag 72:371–388.

Tesfaye T, Sithole B, Ramjugernath D, Ndlela L (2018b) Valorisation of waste chicken feathers: Optimisation of decontamination and pre-treatment with bleaching agents using response surface methodology. Waste Manag 72:371–388.

Thammasittirong A, Saechow S, Thammasittirong SN-R (2017) Efficient polyhydroxybutyrate production from *Bacillus thuringiensis* using sugarcane juice substrate. Turkish J Biol 41:992–1002.

Torri C, Cordiani H, Samorì C, Favaro L, Fabbri D (2014) Fast procedure for the analysis of poly(hydroxyalkanoates) in bacterial cells by off-line pyrolysis/gas-chromatography with flame ionization detector. J Chromatogr A 1359:230–236 .

Vahabi H, Michely L, Moradkhani G, Akbari V, Cochez M, Vagner C, Renard E, Saeb MR, Langlois V (2019) Thermal stability and flammability behavior of poly(3-hydroxybutyrate) (PHB) based composites. Materials (Basel) 12:1–14.

Volova TG, Zhila NO, Shishatskaya EI, Mironov P V., Vasil'ev AD, Sukovatyi AG, Sinskey AJ (2013) The physicochemical properties of polyhydroxyalkanoates with different chemical structures. Polym Sci - Ser A 55:427–437.

Wang Y, Liu S (2014) Production of (R)-3-hydroxybutyric acid by *Burkholderia cepacia* from wood extract hydrolysates. AMB Express 4:1–10.

Wellen RMR, Rabello MS, Júnior ICA, Fechine GJM, Canedo EL (2015) Melting and crystallization of poly(3-hydroxybutyrate): Effect of heating/cooling rates on phase transformation. Polímeros 25:296–304.

Yang S, Franden MA, Yang Q, Chou YC, Zhang M, Pienkos PT (2018) Identification of inhibitors in lignocellulosic slurries and determination of their effect on hydrocarbon-producing microorganisms. Front Bioeng Biotechnol 6:1–14.

Yu J, Stahl H (2008) Microbial utilization and biopolyester synthesis of bagasse hydrolysates. Bioresour Technol 99:8042–8048.

Zhang W, Alvarez-Gaitan JP, Dastyar W, Saint CP, Zhao M, Short MD (2018) Value-added products derived from waste activated sludge: A biorefinery perspective. Water 10:1–20.

CHAPTER SEVEN

Summary, Recommendations and Future possibilities

7.1. Summary

Plastics are an incredible and versatile innovation that is available in a multitude of types and forms which are beneficial in everyday life. However, many of the plastics we use daily are produced from chemicals derived from fossil fuels, a finite and rapidly depleting resource. In addition, the majority of plastics are not readily biodegradable thus persist in the natural environment for extended periods of time, increasing the environmental pollution burden (Andrady and Neal 2009). Therefore, in an effort to alleviate this plastic pollution crisis, investigation into microbial biopolymers that can be applied in the production of bio-based plastics, has become a key interest of researchers. The favorable physical, chemical and thermal properties of bio-based polyhydroxyalkanoates (PHAs) make them suitable for the production of bioplastics which are "green", eco-friendly and biodegradable (Andreeßen and Steinbüchel 2010; Tan et al. 2014).

The requirements of an efficient PHA-accumulating strain include; high growth rate, ability to utilize a wide variety of carbon sources and a high PHA productivity (Naheed and Jamil 2014). However, there are two key challenges that hinder the economic competitiveness and industrial application of PHAs. The first issue is attributed to the high production cost. Choosing a substrate that serves a dual function of supporting both microbial cell proliferation and PHA production is beneficial in reducing production cost. Many studies have reported on successful PHA production, initially from pure carbon substrates then advancing onto the exploitation of cheaper renewable biomass such as lignocellulosic waste biomass. Pulp and paper mill sludge (PPMS) is one such lignocellulosic biomass that is cheap and abundantly available. In South Africa, this waste stream is presently being landfilled, contributing to green house gas emission and environmental pollution. Recently, implementation of strict environmental legislation has resulted in management of this waste stream becoming a major concern for the pulp and paper industry. Thus, using PPMS as feedstock for PHA production provides a lucrative management strategy for this waste stream. Its inherent desirable characteristic of a high carbohydrate content makes it worthwhile to explore PPMS as a potential feedstock candidate. The second problem revolves around employing a fermentative strategy that generates high cell density

cultivation whilst simultaneously enhancing PHA to obtain high yields of the biopolymer. To the best of the author's understanding, the work presented here is a first for the country. There are no studies that report on PHA production as a route for valorization of PPMS from South African pulp and paper mills. Thus, the novelty of the present study is marked by the multiple ways of using PPMS as a substrate in fermentative strategies to enhance both microbial cell biomass and PHA productivity.

This study revealed the capacity of *B. thuringiensis* to produce PHAs from a variety of carbohydrates which is a common characteristic amongst *Bacillus* species (Valappil et al. 2007; Valappil et al. 2008). Using the Sudan Black B and Nile Blue A staining procedures coupled with microscopy analysis, PHA granules were visualized as blue-black spherical or fluorescent intracellular inclusions, respectively (Aljuraifani et al. 2018). The presence of PHA granules also confirmed that all five carbon sources tested were efficacious substrates for PHA production. Even though the microscopic examination enabled the rapid detection of PHA granules, it was a tedious, laborious and time-consuming exercise. Furthermore, it was not possible to deduce correlations between the fluorescence intensities and PHA productivity. *B. thuringiensis* exhibited nutritional versatility in terms of varied growth and PHA production for the various carbon sources used. However, for the purposes of obtaining high biomass and PHA productivity, glucose is the best carbon source. It is noteworthy that a higher biomass and PHA productivity of 0.258 g L^{-1} h^{-1} and 0.107 g L^{-1} h^{-1}, respectively, was achieved using the glucose-rich hydrolyzate in comparison to commercial glucose. Both the biomass and PHA productivity observed when using commercial α-cellulose or PPMS as the sole carbon source was similar ~0.03 g L^{-1} h^{-1} and ~0.01 g L^{-1} h^{-1}, respectively. Jiang et al. (2016) attributed the higher biomass and PHA productivity achieved on glucose-based substrates to the higher affinity that bacteria have for monosaccharides and disaccharides, substrates that are easily fermented directly to produce PHAs. The carbohydrates in polysaccharide material, like α-cellulose or PPMS, are in a polymerized form that must first be hydrolyzed by the microbe and thereafter fermented to produce PHAs. This becomes a rate limiting step of PHA production due to the time taken to metabolize the substrate followed by the up-take of nutrients required for subsequent cell activities.

Characterizing and profiling *B. thuringiensis*, NSSC-CR and PHKK PPMS were vital procedures, as this insight enabled the development of an appropriate fermentation strategy

capable of yielding both cell biomass and PHA using untreated (raw) PPMS. Previous characterization of the *B. thuringiensis* strain used in this study reported the presence of cellulase, xylanase and ligninase (Govender 2013), three enzymes that are imperative for the hydrolysis of lignocellulosic biomass during a consolidated bioprocessing (CBP) strategy. PHKK PPMS served as the better substrate than NSSC-CR PPMS for biomass and PHA production producing yields of 2.74 g L^{-1} and 0.71 g L^{-1}, respectively. This finding is of significant importance as most studies do not investigate the use of PPMS for PHA production and rather explore its applicability for bioethanol production (Kang et al. 2010; Phillips et al. 2013; Ko et al. 2015; Nandan et al. 2015; Zambare and Christopher 2020). Inherent characteristics of NSSC-CR PPMS include low glucose content (35.48%), relatively high lignin (45%) and ash content (22%). The high ash content (> 30%) is possibly due to papermaking fillers used during the pulp and paper making process (Ochoa de Alda 2008). It is well established that high ash content affects the enzymatic hydrolysis efficiency of the PPMS (García et al. 2015). The unfavorable profile together with the low yields of biomass (0.0258 g L^{-1} h^{-1}) and PHA productivity (0.005 g L^{-1} h^{-1}) deemed NSSC-CR unsuitable for the purposes of this study and it was thus eliminated from future work. On the other hand, PHKK PPMS possessed favorable characteristics of containing high glucose (64.21%) and low ash (6.89%) and lignin (19.28%).

In order to lower the ash content of PHKK PPMS thereby increasing the amenability of PPMS fibers to enzymatic saccharification, a pretreatment process as per the methodology of Wang et al. (2010) was pursued. The pretreatment was successful, albeit at a lab scale. In an effort to retrieve the glucose from the de-ashed PPMS fibers, a response surface methodology (RSM) approach was applied to determine the appropriate conditions for enzymatic saccharification to produce a glucose-rich hydrolyzate. The RSM study proved to be beneficial and aided in avoiding the labour intensive “one factor at a time” method. Using the model conditions, a yield of 75% was obtained and characterization of the hydrolyzate revealed that it contained 48.27% glucose. The application phase of this study involved employing the glucose-rich hydrolyzate in a cyclic-fed batch fermentation (CFBF) strategy to enhance PHA productivity (Ibrahim and Steinbüchel 2010). Using another RSM study, the optimal conditions to produce high cell density biomass (OD_{600} of 2.4175) included: 8.77 g L^{-1} yeast extract; 66.63% hydrolyzate (v/v); a fermentation pH of 7.18; and an incubation time of 27.22 h. The CFBF resulted in an almost 3-fold increase in biomass concentration and 4-fold increase in PHA

concentration, respectively, as compared with batch cultivation but, the yields are lower than previous reports on CFBF using *Azohydromonas australica* (Gahlawat and Srivastava 2018), thermophilic bacterium, *Chelatococcus* sp. MW10 (Ibrahim and Steinbüchel 2010) and *Cupriavidus necator* (Haas et al. 2017).

It was also important to elucidate the compositions and the thermal properties of the synthesized PHAs to determine their potential range of applications. Using FTIR the peaks typically representative of PHAs i.e., the ester, methylene, and terminal hydroxyl groups, were identified in the spectra for the commercial PHB and PHBV and for every synthesized PHA, thereby confirming that the synthesized polymers are truly PHAs. Py-GC/MS aided in determining the monomeric composition of the polymers. In addition to the well-known PHB and PHBV, unusual polymers observed in the present study include the HB-HV-HHx terpolymer as well as a HB-HHx copolymer. These types of polymers are flexible polymers due to their elastomeric nature and are suitable for medical applications (Rai et al. 2011). PHAs with a melting temperature lower than commercial PHB or PHBV but with a maximum degradation temperature higher than commercial PHB and PHBV are desirable. The former implies that the polymer can be processed at a low temperature, making the polymer suitable for soft products such as films with improved ductility and flexibility (Rai et al. 2011) and the latter implies that the PHA displays better thermostability than commercial PHB and PHBV (Bhagowati et al. 2015). Another advantageous and valuable trait is a low crystallinity ($X_c \leq$ 50%) as these polymers are less brittle, thus increasing their range of applications (Chaijamrus and Udpuay 2008). In the present study, PHAs that were observed to exhibit these important characteristics include PHAs synthesized using commercial glucose, sucrose and α-cellulose, PHKK PPMS and PHAs obtained from cyclic events 2-4.

7.2. Recommendations

The most valuable recommendation emanating from this study would be to fully characterize the microbial strain intended to be applied for the purposes of PHA production. It is important to profile the growth conditions; carbon and nitrogen substrates able to be metabolized; enzymes produced by the strain; and the class of *phaC* synthase as it also contributes to substrate specificity and ultimately the monomeric constituents of a PHA. A well established profile will aid in ensuring that fermentations are conducted at conditions optimal for cell growth and function in order for PHA production to occur and high yields to be obtained.

Furthermore, the nature of *B. thuringiensis* and its promising PHA-producing ability gives it the potential to be applied in fermentations using other waste biomass such as agro-waste, hemicellulose-rich biomass, effluents, and activated sludge, to name a few.

In addition, prior knowledge on the optimal growth conditions, substrate specificity, and enzymes produced by *B. thuringiensis* is also useful and must be carefully considered when conceptualizing a fermentative strategy. The PHA-producing ability of microbial strains differs vastly therefore, the exploration and implementation of fermentation methods other than the traditional batch cultivation enable the possibility of producing high cell density biomass together with high PHA productivity.

In the event that lignocellulosic biomass is to be used as feedstock, it is imperative to profile the biomass prior to its use. A highly advantageous profile as observed in the present study is a high glucose and low ash content for PHKK PPMS resulted in it being a better feedstock in comparison with NSSC-CR PPMS. Knowledge of the glucose content of the lignocellulosic biomass is valuable as it allows for determining the exact dose of enzyme required for optimal saccharification. It is important to use the correct enzyme dose to avoid wasting expensive commercial enzymes (overdosing) or obtaining a low glucose yield (under dosing). The presence of ash and lignin in the PPMS inhibit enzyme function and high quantities of these components make potential PPMS feedstock undesirable. It will then be advantageous to pretreat the PPMS in order to lower or remove inhibitory components from the PPMS. This also lowers the risk of enzyme inhibition during saccharification which in turn maximizes the yield of glucose in the hydrolyzate. One must also be mindful of the solvents used and water consumed during the pretreatment process. A process might be suitable at a small lab scale for the purposes of an academic study but may not be a cost-effective process to pursue on a large industrial scale and thus additional or alternate strategies must be sought.

In addition to quantifying the PHAs, it is recommended that the PHAs also be characterized. Besides achieving high yields of PHAs, the PHAs must display unique and attractive thermal and mechanical properties that will make the polymer preferable for industrial application. Basically, there is no use in obtaining high yields of PHB that is unappealing due to its brittle nature and needs to be copolymerized to functionalize the polymer thereby incurring PHA processing costs.

7.3. Future possibilities and way forward

Based on the outcome reported herein, it is evident that the *B. thuringiensis* is a robust strain with added advantage of producing hydrolytic enzymes that enable the degradation of lignocellulosic material. Its added ability to grow and produce PHAs using a variety of substrates and fermentation conditions makes this an attractive bacterium to exploit. It may be worthwhile to genetically engineer *B. thuringiensis* with other classes of *phaC* thereby further expanding the range of substrates the isolate can utilize as feedstock as well as increasing the variety of potential copolymers synthesized. The strain can be manipulated using mutation methods or recombinant DNA technologies to synthesize biopolymers with enhanced and/or desirable properties and subsequently widening the scope of applications of the PHA. The nature and types of PHAs synthesized and characterized during this study exhibit attractive properties. To take it further, studies can involve incorporating additives or plasticizers to the existing PHAs to develop a PHA product with superior thermostability and physicochemical properties. PPMS proved to be a favorable substrate for PHA production in its untreated form and a viable candidate for enzymatic saccharification. It will beneficial to explore the possibility of extracting the lignin and hemicellulose from the PPMS and applying these components as substrates for cell proliferation and PHA production. These approaches will definitely contribute to synthesizing value-added products such as PHAs with improved characteristics whilst simultaneously valorizing lignocellulosic waste.

7.4. References

Aljuraifani AA, Berekaa MM, Ghazwani AA (2018) Perspectives of polyhydroxyalkanoate

(PHAs) biopolymer production using indigenous bacteria: Screening and characterization. J Pure Appl Microbiol 12:1997–2009.

Andrady AL, Neal MA (2009) Applications and societal benefits of plastics. Philos Trans R Soc B Biol Sci 364:1977–1984.

Andreeßen B, Steinbüchel A (2010) Biosynthesis and biodegradation of 3-hydroxypropionate-containing polyesters. Appl Environ Microbiol 76:4919–4925.

Bhagowati P, Pradhan S, Dash HR, Das S (2015) Production, optimization and characterization of polyhydroxybutyrate, a biodegradable plastic by *Bacillus* spp. Biosci Biotechnol Biochem 79:1454–1463.

Chaijamrus S, Udpuay N (2008) Production and characterization of polyhydroxybutyrate from molasses and corn steep liquor produced by *Bacillus megaterium* ATCC 6748. Agric Eng Int CIGR Ejournal 1–12.

Gahlawat G, Srivastava AK (2018) Enhancing the production of polyhydroxyalkanoate biopolymer by *Azohydromonas australica* using a simple empty and fill bioreactor cultivation strategy. Chem Biochem Eng Q 31:479–485.

García YG, Carlos, Contreras JCM, Hernández JA, Dueñas RS (2015) Procurement of fermentable sugars from cardboard waste for the cultivation of yeasts for biotechnological use. Rev Mex Ciencias For 6:88–105.

Govender L (2013) Seasonal variation of microflora and their effects on the quality of wood chips intended for pulping. PhD Dissertation. University of KwaZulu-Natal.

Haas C, El-Najjar T, Virgolini N, Smerilli M, Neureiter M (2017) High cell-density production of poly(3-hydroxybutyrate) in a membrane bioreactor. N Biotechnol 37:117–122.

Ibrahim MHA, Steinbüchel A (2010) High-cell-density cyclic fed-batch fermentation of a poly(3-hydroxybutyrate)-accumulating thermophile, *Chelatococcus* sp. strain MW10. Appl Environ Microbiol 76:7890–7895.

Jiang G, Hill DJ, Kowalczuk M, Johnston B, Adamus G, Irorere V, Radecka I (2016) Carbon sources for polyhydroxyalkanoates and an integrated biorefinery. Int J Mol Sci 17:1–21.

Kang L, Wang W, Lee YY (2010) Bioconversion of kraft paper mill sludges to ethanol by SSF and SSCF bioconversion of kraft paper mill sludges to ethanol by SSF and SSCF. Appl Biochem Biotechnol 161:53–66.

Ko CH, Leu SY, Chang CC, Chang CY, Wang YC, Wang YN (2015) Combining cellulosic ethanol fermentation waste and municipal solid waste-derived fiber with a kraft black liquor-derived binder for recycled paper making. BioResources 10:5744–5757.

Naheed N, Jamil N (2014) Optimization of biodegradable plastic production on sugar cane molasses in *Enterobacter* sp. SEL2. Brazilian J Microbiol 426:417–426.

Nandan R, Al-shannag M, Joshua N, Duncan SM, Lawrence E, Alkasrawi M (2015) Bioconversion of paper mill sludge to bioethanol in the presence of accelerants or hydrogen peroxide pretreatment. Bioresour Technol 192:529–539.

Ochoa De Alda JAG (2008) Feasibility of recycling pulp and paper mill sludge in the paper and board industries. Resour Conserv Recycl 52:965–972.

Phillips RB, Jameel H, Chang HM, Biorefinery K, Mill K (2013) Integration of pulp and paper technology with bioethanol production. Biotechnol Biofuels 6:1-12.

Rai R, Keshavarz T, Roether JA, Boccaccini AR, Roy I (2011) Medium chain length

polyhydroxyalkanoates, promising new biomedical materials for the future. Mater Sci Eng R Reports 72:29–47.

Tan GA, Chen C-L, Ge L, Li L, Wang L, Zhao L, Mo Y, Tan SN, Wang J-Y (2014) Enhanced gas chromatography-mass spectrometry method for bacterial polyhydroxyalkanoates analysis. J Biosci Bioeng 117:379–382.

Valappil SP, Boccaccini AR, Bucke C, Roy I (2007) Polyhydroxyalkanoates in Gram-positive bacteria: Insights from the genera *Bacillus* and *Streptomyces*. Antonie Van Leeuwenhoek 91:1–17.

Valappil SP, Rai R, Bucke C, Roy I (2008) Polyhydroxyalkanoate biosynthesis in *Bacillus cereus* SPV under varied limiting conditions and an insight into the biosynthetic genes involved. J Appl Microbiol 104:1624–1635.

Wang W, Kang L, Lee YY (2010) Production of cellulase from kraft paper mill sludge by *Trichoderma reesei* Rut C-30. Appl Biochem Biotechnol 161:382–394.

Zambare V, Christopher L (2020) Integrated biorefinery approach to utilization of pulp and paper mill sludge for value-added products. J Clean Prod 274:122791.

PUBLISHED MANUSCRIPTS

Singh *et al. Bioresour. Bioprocess.* (2021) 8:11
https://doi.org/10.1186/s40643-021-00361-x

Bioresources and Bioprocessing

RESEARCH Open Access

Optimization of cultivation medium and cyclic fed-batch fermentation strategy for enhanced polyhydroxyalkanoate production by *Bacillus thuringiensis* using a glucose-rich hydrolyzate

Sarisha Singh[1*], Bruce Sithole[2,3], Prabashni Lekha[2], Kugenthiren Permaul[4] and Roshini Govinden[1]

Abstract

The accumulation of petrochemical plastic waste is detrimental to the environment. Polyhydroxyalkanoates (PHAs) are bacterial-derived polymers utilized for the production of bioplastics. PHA-plastics exhibit mechanical and thermal properties similar to conventional plastics. However, high production cost and obtaining high PHA yield and productivity impedes the widespread use of bioplastics. This study demonstrates the concept of cyclic fed-batch fermentation (CFBF) for enhanced PHA productivity by *Bacillus thuringiensis* using a glucose-rich hydrolyzate as the sole carbon source. The statistically optimized fermentation conditions used to obtain high cell density biomass (OD_{600} of 2.4175) were: 8.77 g L^{-1} yeast extract; 66.63% hydrolyzate (v/v); a fermentation pH of 7.18; and an incubation time of 27.22 h. The CFBF comprised three cycles of 29 h, 52 h, and 65 h, respectively. After the third cyclic event, cell biomass of 20.99 g L^{-1}, PHA concentration of 14.28 g L^{-1}, PHA yield of 68.03%, and PHA productivity of 0.219 g L^{-1} h^{-1} was achieved. This cyclic strategy yielded an almost threefold increase in biomass concentration and a fourfold increase in PHA concentration compared with batch fermentation. FTIR spectra of the extracted PHAs display prominent peaks at the wavelengths unique to PHAs. A copolymer was elucidated after the first cyclic event, whereas, after cycles CFBF 2–4, a terpolymer was noted. The PHAs obtained after CFBF cycle 3 have a slightly higher thermal stability compared with commercial PHB. The cyclic events decreased the melting temperature and degree of crystallinity of the PHAs. The approach used in this study demonstrates the possibility of coupling fermentation strategies with hydrolyzate derived from lignocellulosic waste as an alternative feedstock to obtain high cell density biomass and enhanced PHA productivity.

Keywords: Polyhydroxyalkanoate, Glucose-rich hydrolyzate, Response surface methodology, Cyclic fed-batch fermentation, PHA productivity, Pulp and paper mill sludge

Introduction

An estimated 240 million tons of plastics are produced globally every year. Most of these plastic materials are petroleum-based and are resistant to degradation resulting in accumulation and pollution of forestry and marine environments (Gholamveisi et al. 2018). With crude oil reserves dwindling, the dependence on exhaustible fossil fuel resources is unsustainable. This can be mitigated by the exploitation of biopolymers, i.e., natural polymers generated by living organisms, consisting of monomeric units that are covalently bonded to form larger molecules. Examples

*Correspondence: sarish_s@yahoo.com; 207506565@stu.ukzn.ac.za
[1] Discipline of Microbiology, University of KwaZulu-Natal (Westville Campus), Durban, South Africa
Full list of author information is available at the end of the article

APPENDIX

Supplementary material 1 (S1)

S 1.1: Pyrogram displaying the profile of commercial PHB

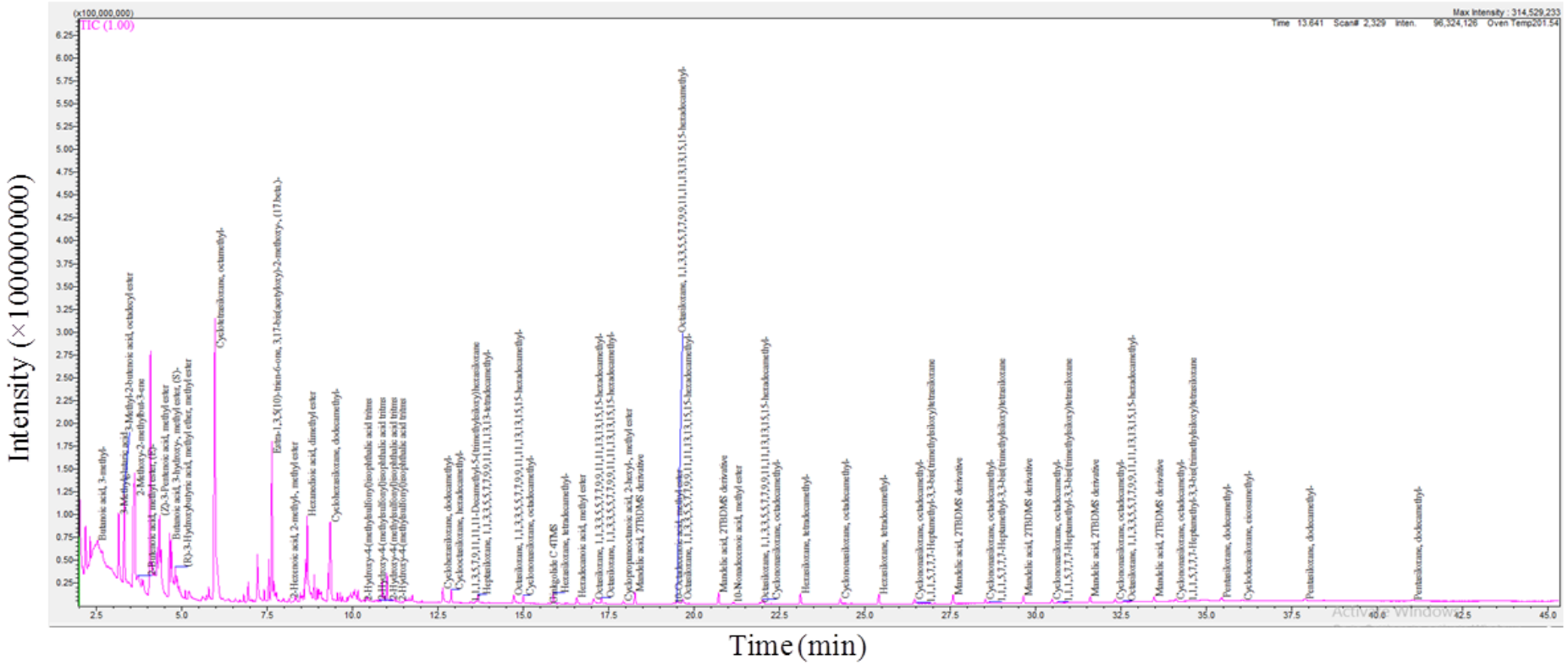

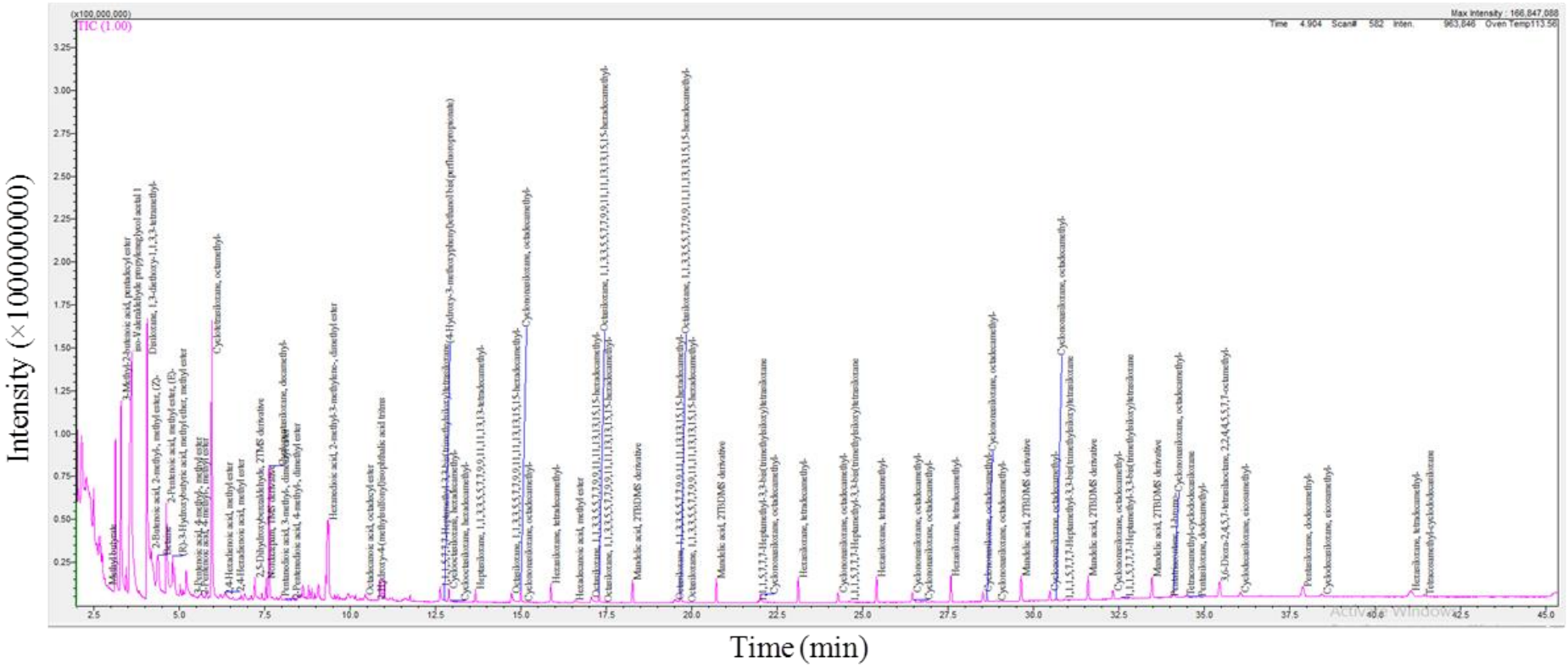

S 1.2: Pyrogram displaying the profile of commercial PHBV

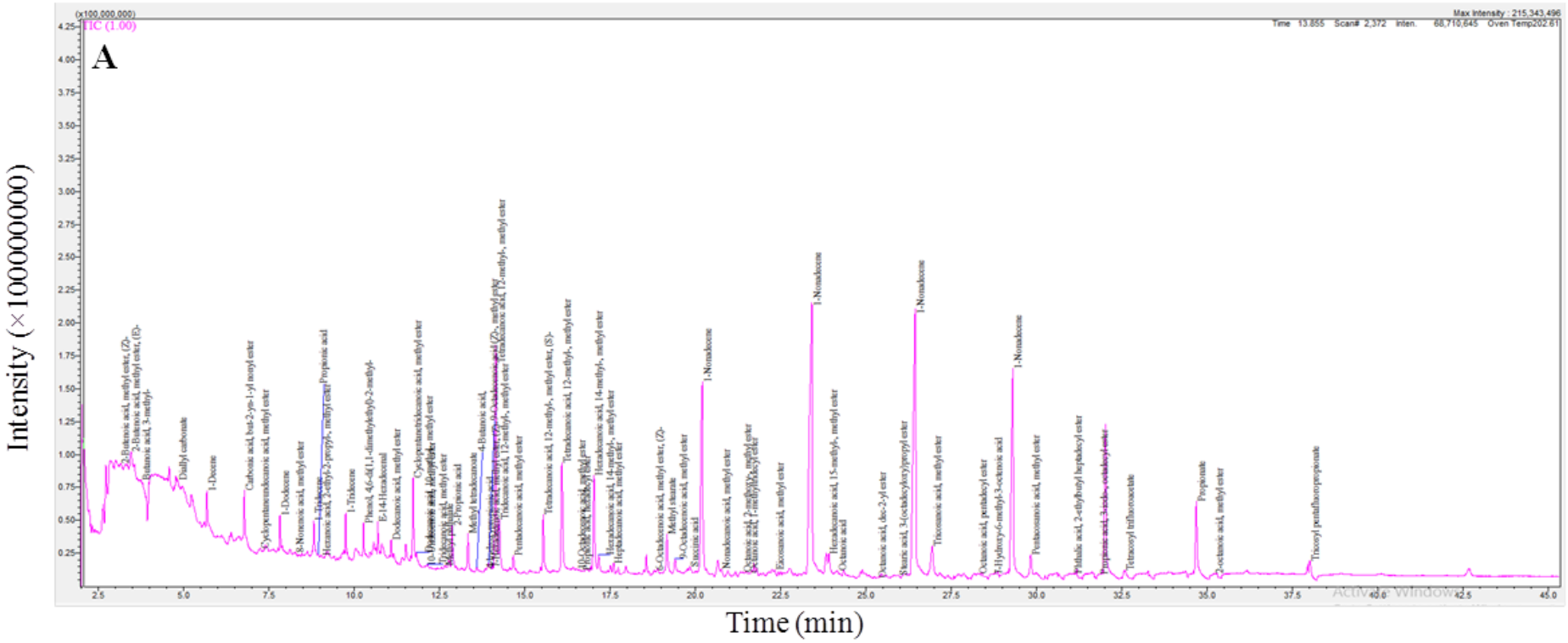
A
TIC (1.00)
Intensity (×100000000)
Time (min)

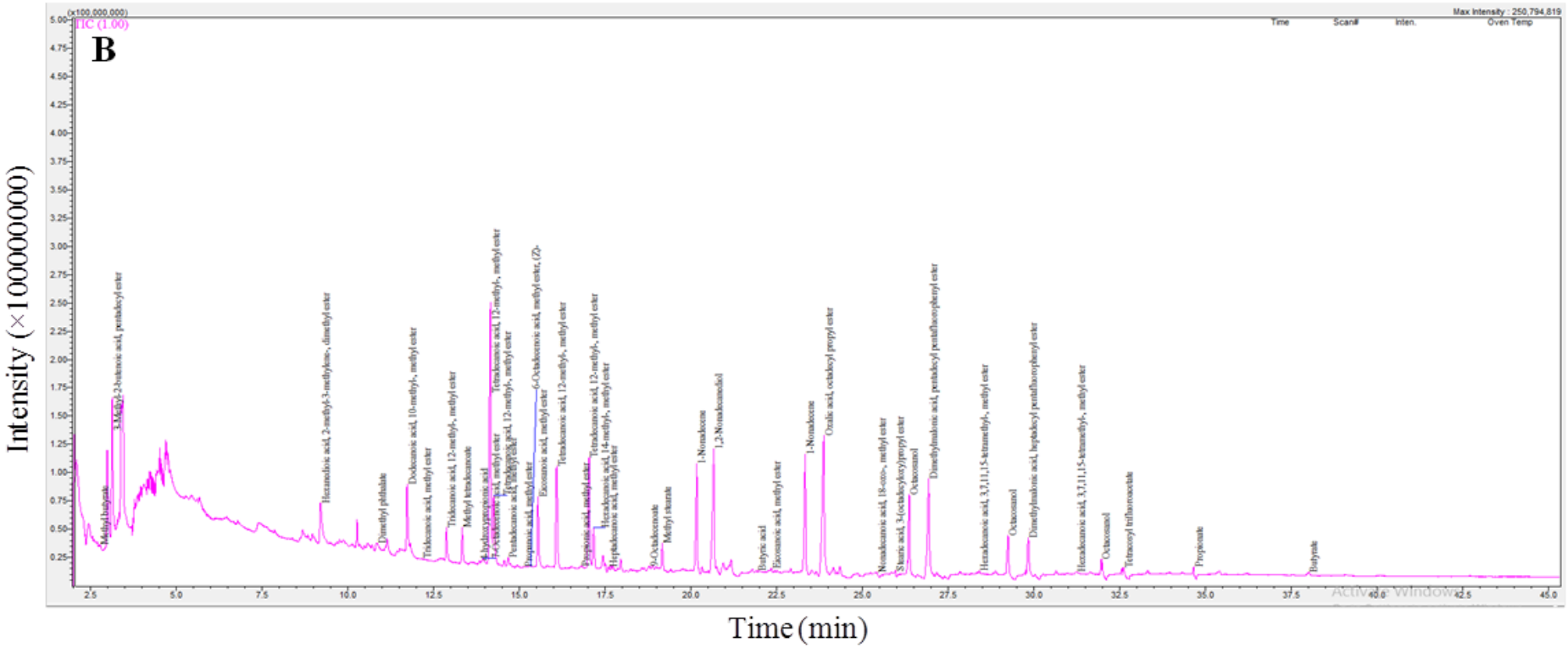
B
Intensity (×100000000)
Time (min)
TIC (1.00)
Max Intensity : 250,794,819
Time
Scan#
Inten.
Oven Temp
Hexanedioic acid, 2-methyl-3-methylene-, dimethyl ester
Dimethyl phthalate
Dodecanoic acid, 10-methyl-, methyl ester
Tridecanoic acid, methyl ester
Tridecanoic acid, 12-methyl-, methyl ester
Methyl tetradecanoate
Tetradecanoic acid, 12-methyl-, methyl ester
Pentadecanoic acid, 12-methyl-, methyl ester
Eicosanoic acid, methyl ester
Tetradecanoic acid, 12-methyl-, methyl ester
Hexadecanoic acid, 14-methyl-, methyl ester
Heptadecanoic acid, methyl ester
9-Octadecenoate
Methyl stearate
1-Nonadecene
1,2-Nonadecanediol
Butyric acid
Eicosanoic acid, methyl ester
1-Nonadecene
Oxalic acid, octadecyl propyl ester
Octacosanol
Dimethylmalonic acid, pentadecyl pentafluorophenyl ester
Octacosanol
Tetracosyl trifluoroacetate
Propionate
Butyrate
Activate Windows

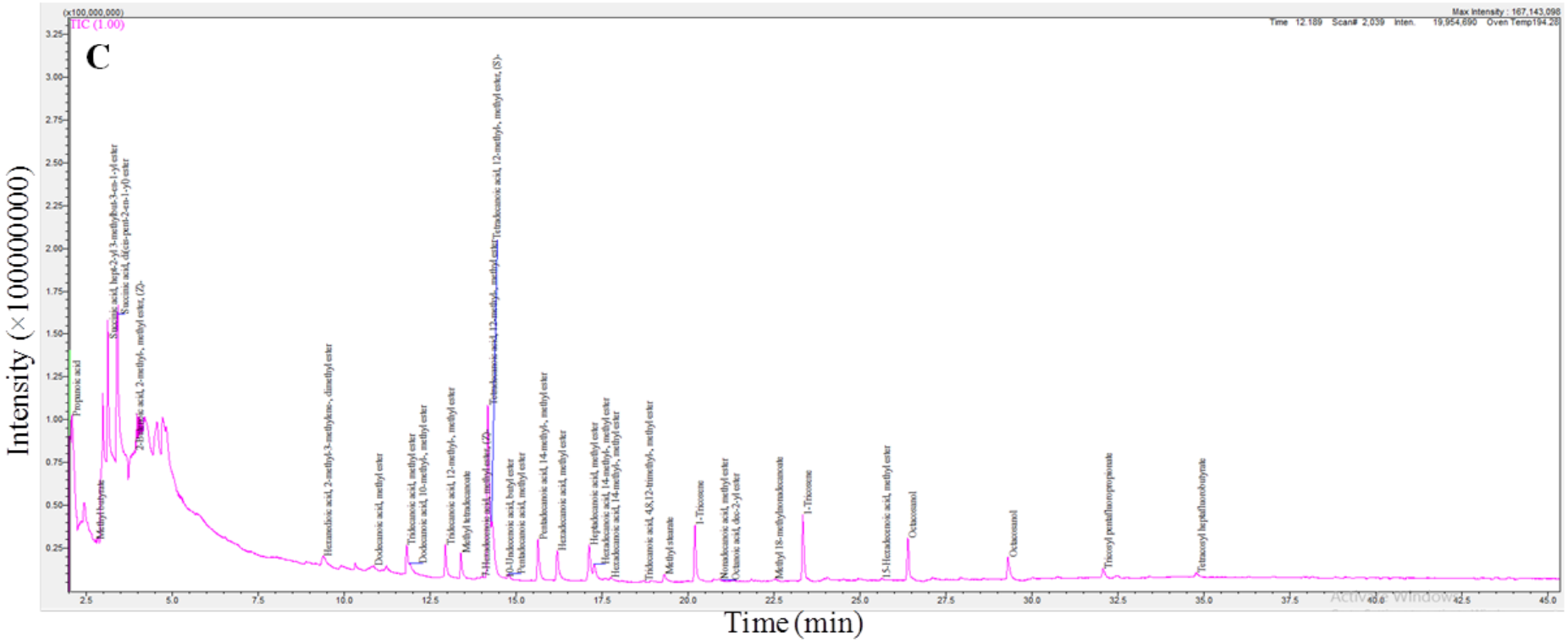
C
TIC (1.00)
Intensity (×100000000)
Time (min)

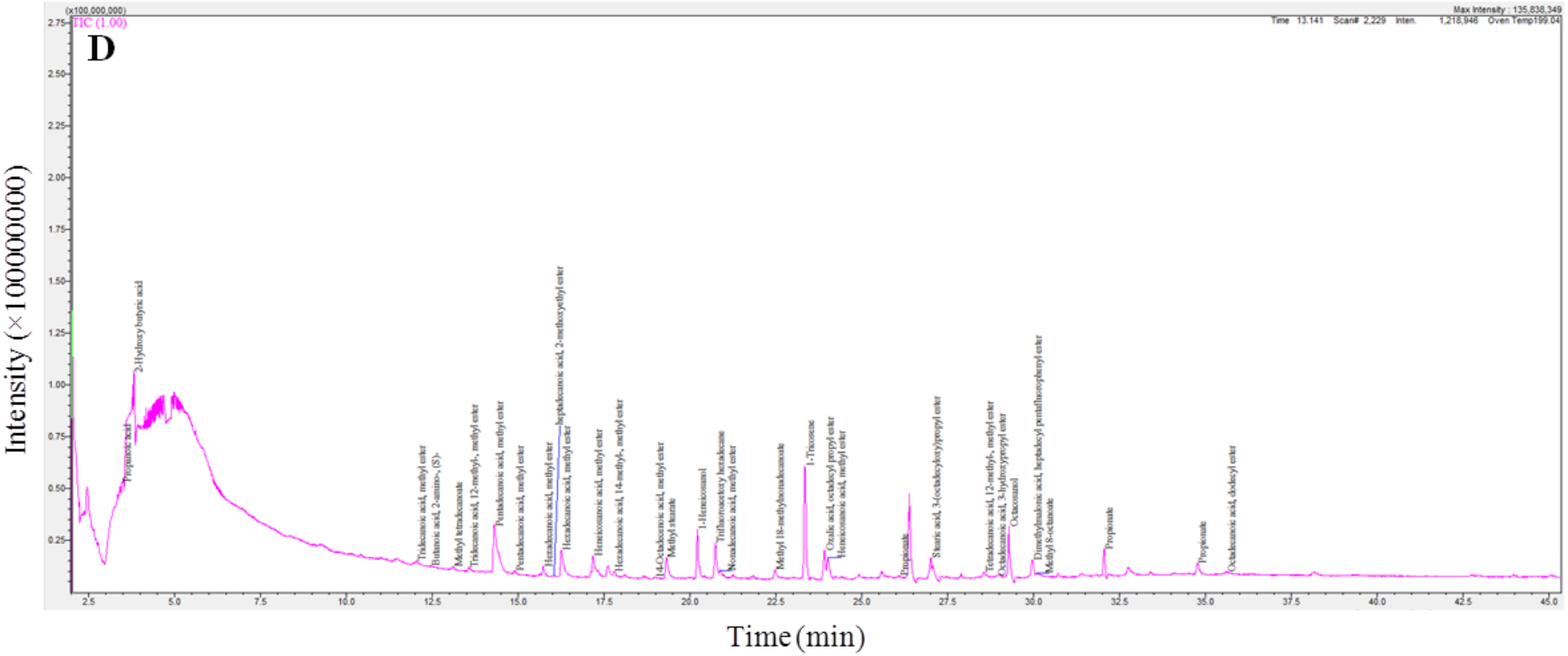
D
TIC (1.00)
Intensity (×100000000)
Time (min)
2-Hydroxy butyric acid
Propanoic acid
Tridecanoic acid, methyl ester
Butanoic acid, 2-amino-, (S)-
Methyl tetradecanoate
Tridecanoic acid, 12-methyl-, methyl ester
Pentadecanoic acid, methyl ester
Pentadecanoic acid, methyl ester
Hexadecanoic acid, methyl ester
heptadecanoic acid, 2-methoxyethyl ester
Hexadecanoic acid, methyl ester
Heneicosanoic acid, methyl ester
Hexadecanoic acid, 14-methyl-, methyl ester
14-Octadecenoic acid, methyl ester
Methyl stearate
1-Heneicosanol
Trifluoroacetoxy hexadecane
Nonadecanoic acid, methyl ester
Methyl 18-methylnonadecanoate
1-Triconene
Oxalic acid, octadecyl propyl ester
Heneicosanoic acid, methyl ester
Dotriacontane
Stearic acid, 3-(octadecyloxy)propyl ester
Tetradecanoic acid, 12-methyl-, methyl ester
Octadecanoic acid, 3-hydroxypropyl ester
Octacosanol
Dimethylmalonic acid, heptadecyl pentafluorophenyl ester
Methyl 8-octynoate
Propionate
Propionate
Octadecanoic acid, dodecyl ester

S 1.3: Pyrograms displaying the profile of the PHAs extracted from *B. thuringiensis* using α-cellulose (A), glucose (B), glycerol (C), starch (D), and sucrose (E) as the sole carbon sources

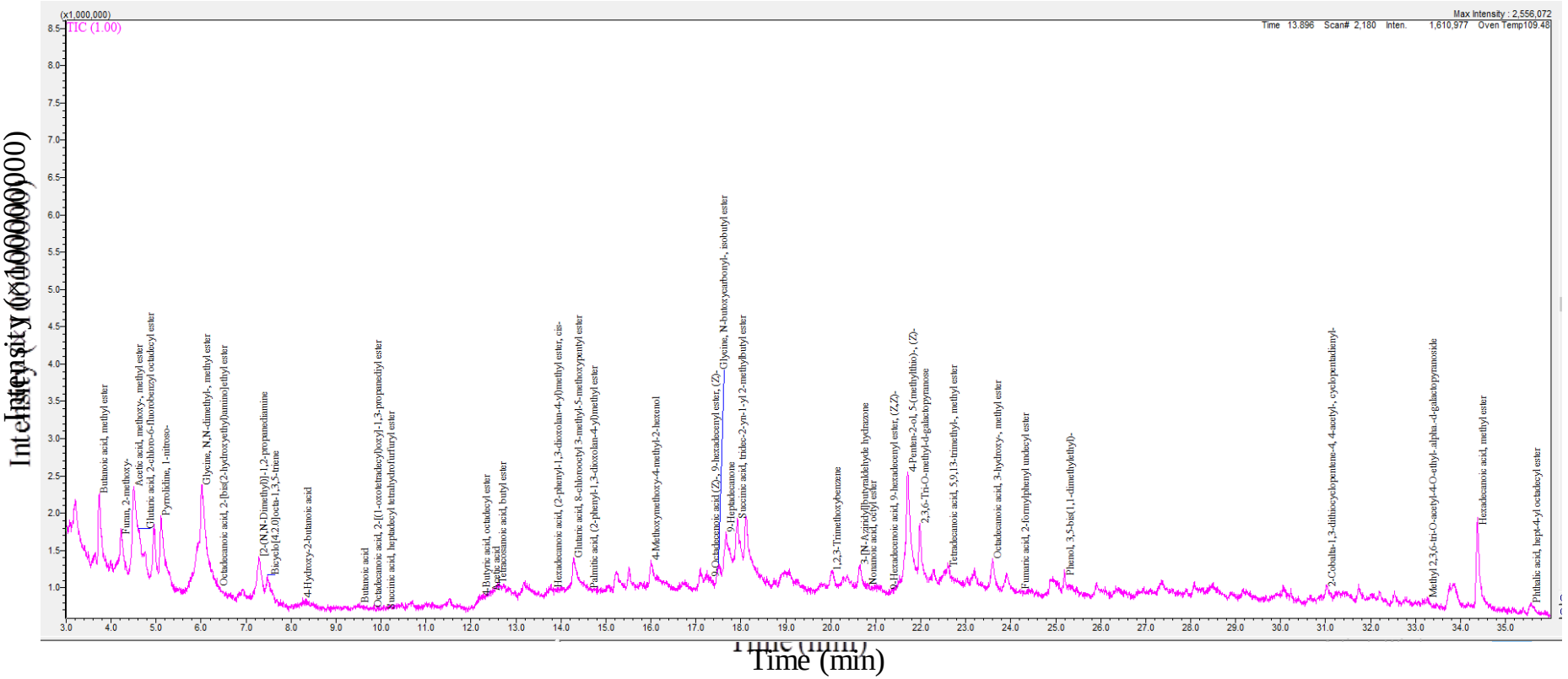

Supplementary material 2 (S2)

S 2.1: Pyrogram displaying the profile NSSC-CR PPMS

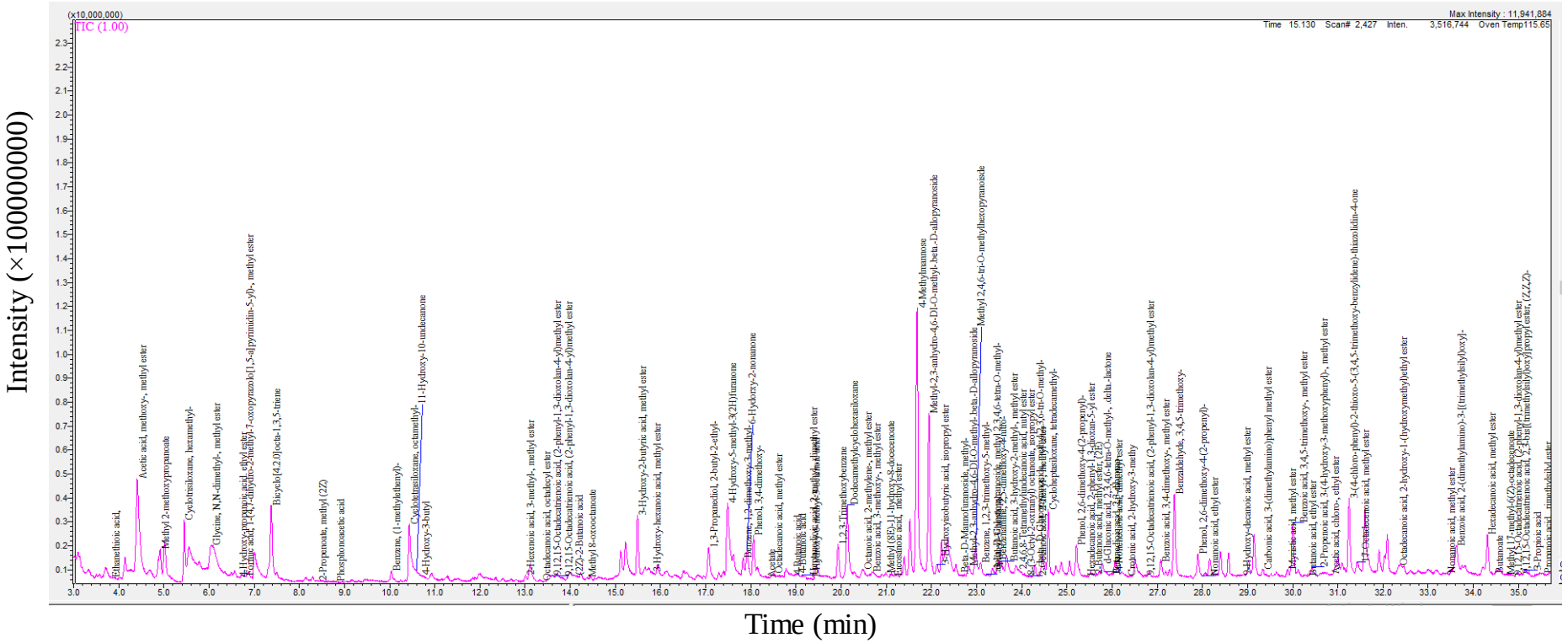

S 2.2: Pyrogram displaying the profile of PHKK PPMS

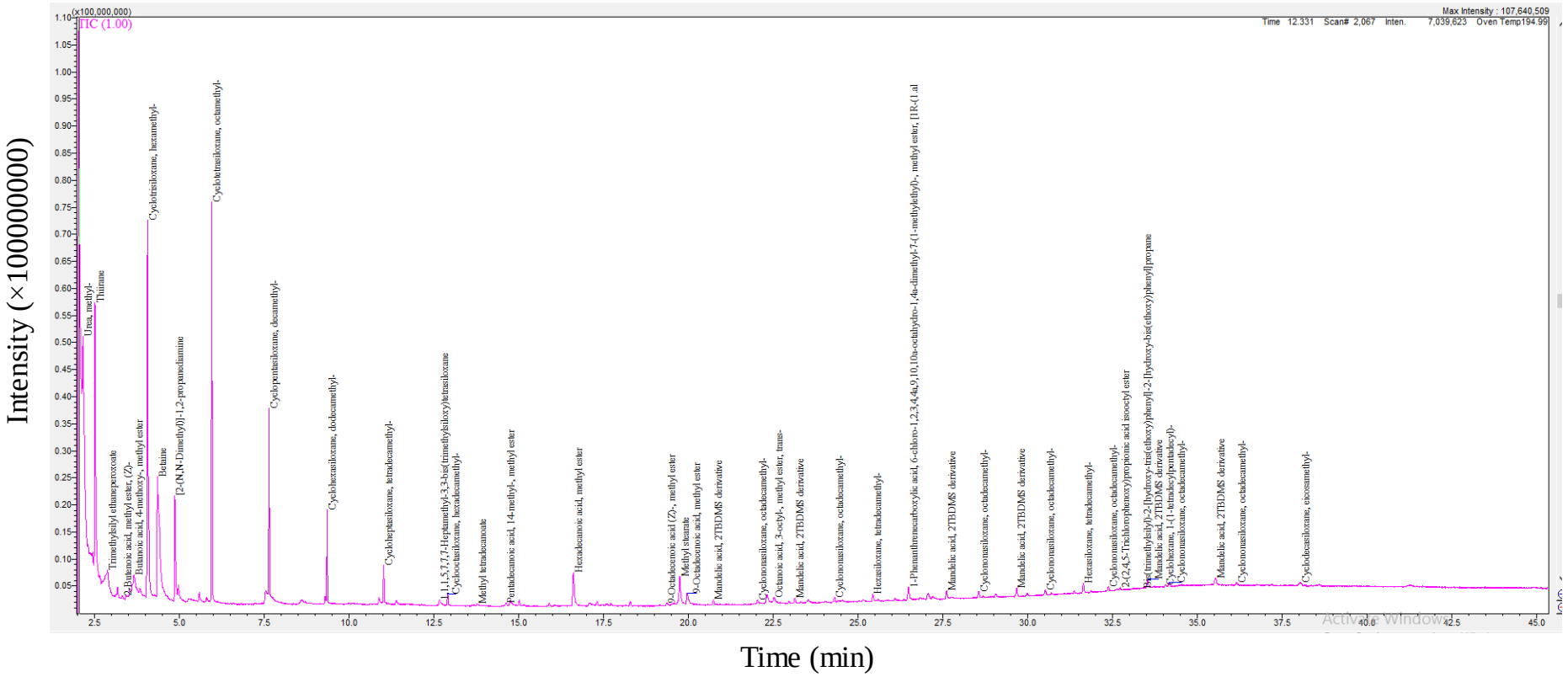

S 2.3: Pyrogram displaying the profile of PHA synthesized using NSSC-CR PPMS as feedstock

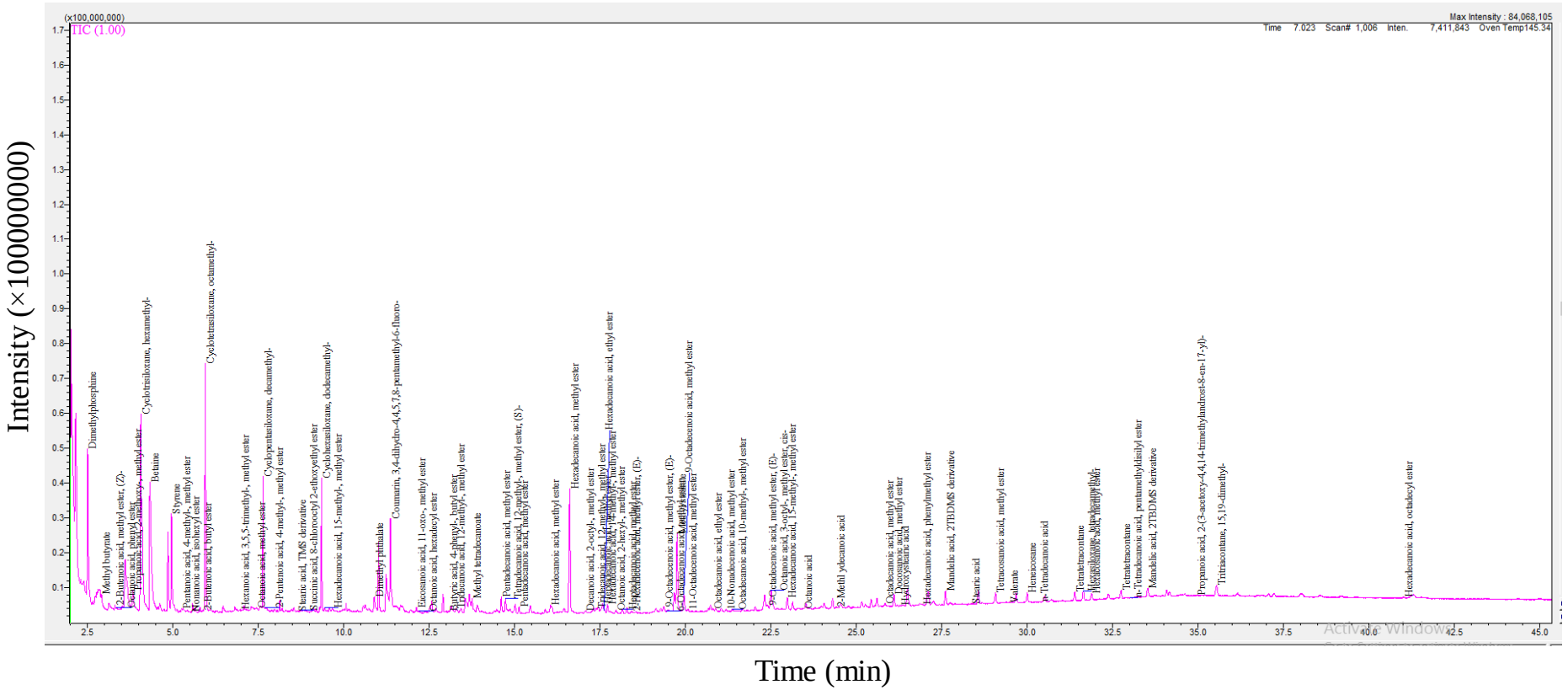

S 2.4: Pyrogram displaying the profile of PHA synthesized using PHKK PPMS as feedstock

Supplementary material 3 (S3)

S 3.1: Pyrogram of PHA extracted after batch fermentation

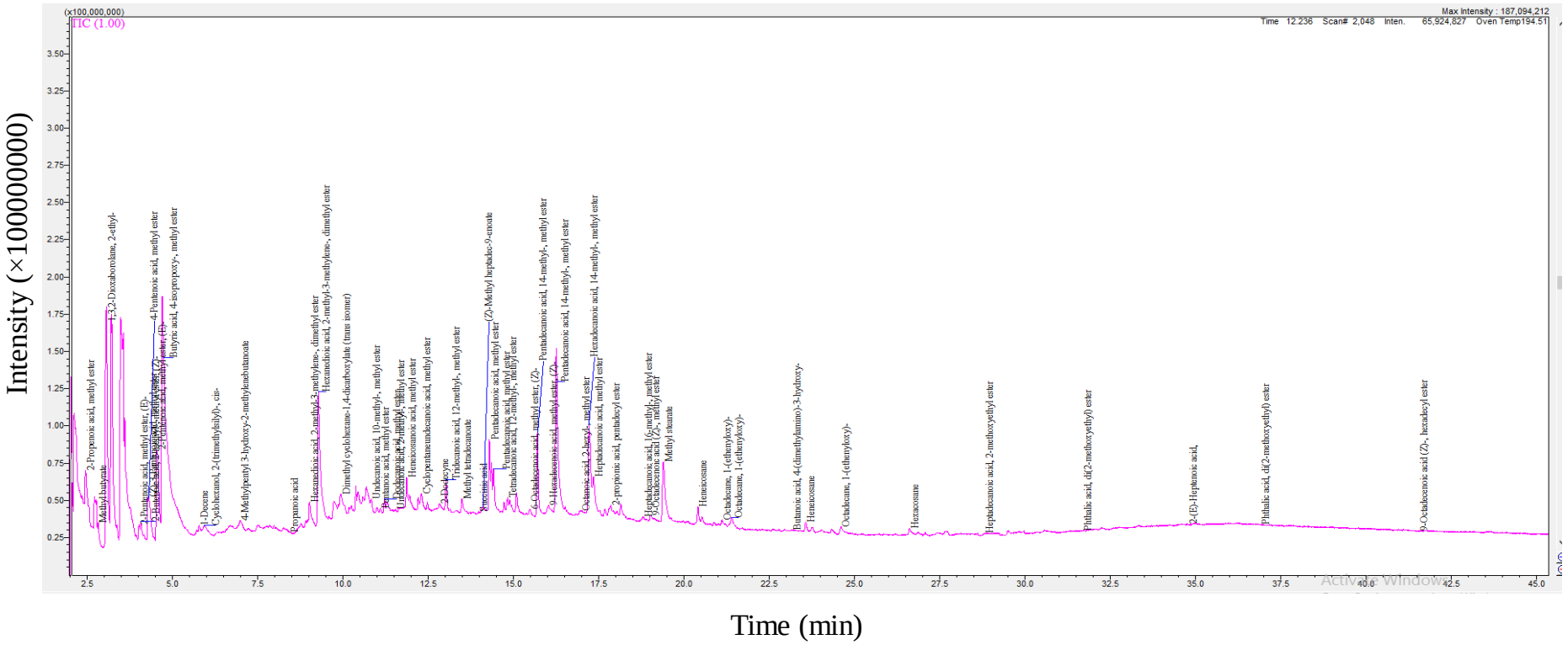

S 3.2: Pyrogram of PHA extracted after CFBF 1

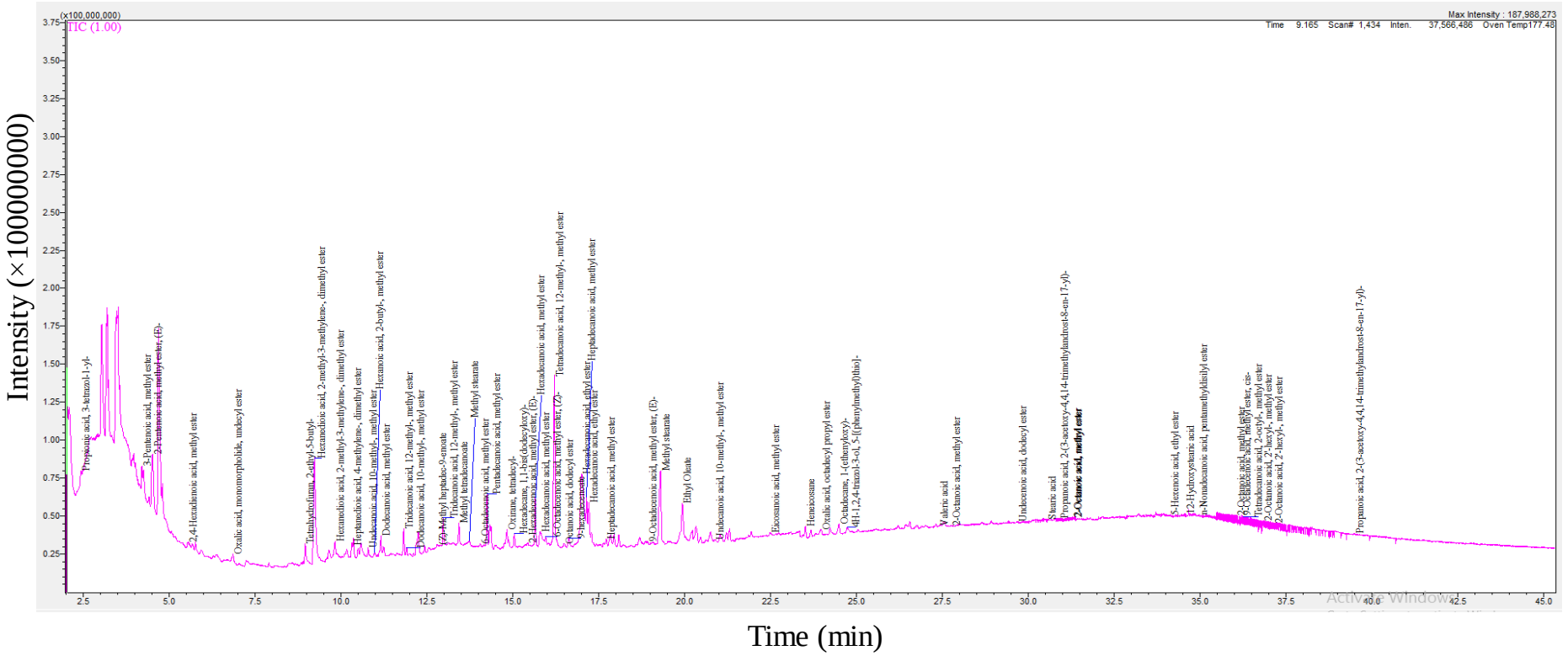

S 3.3: Pyrogram of PHA extracted after CFBF 2

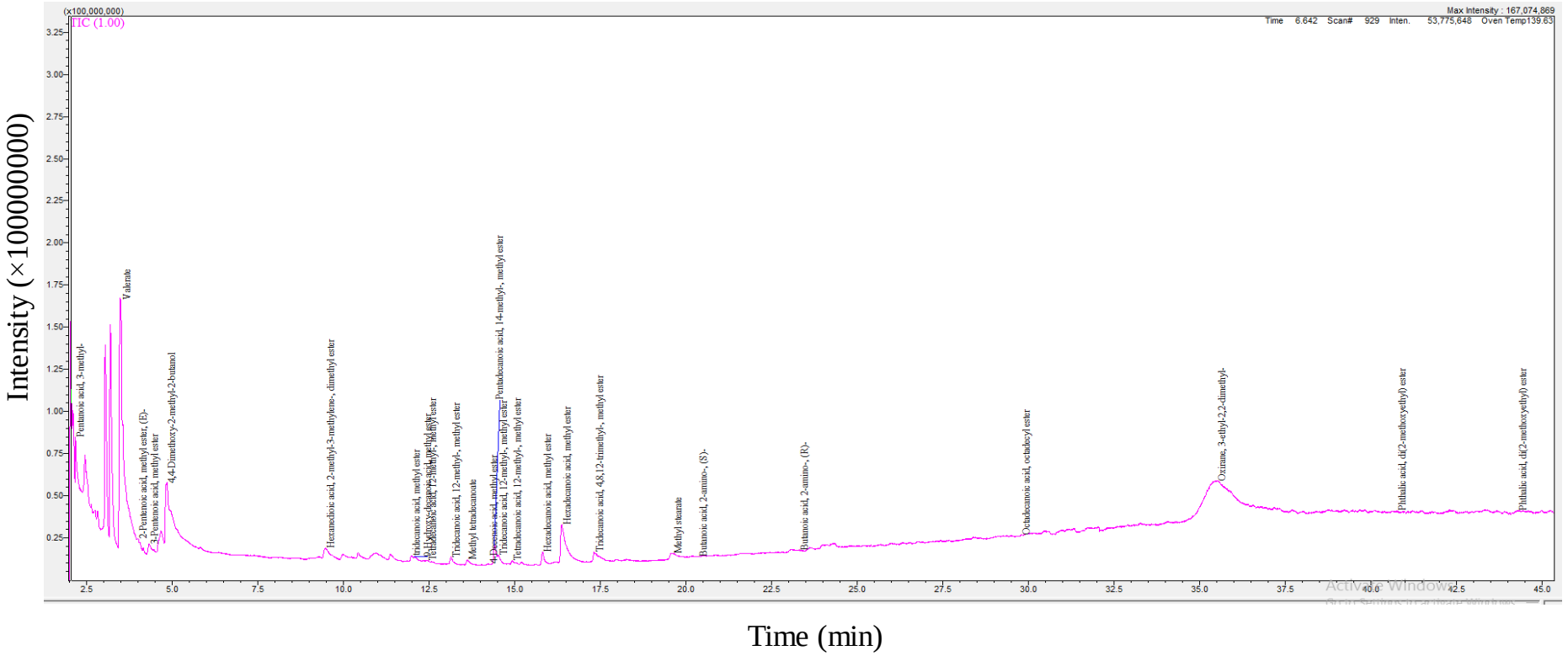

S 3.4: Pyrogram of PHA extracted after CFBF 3

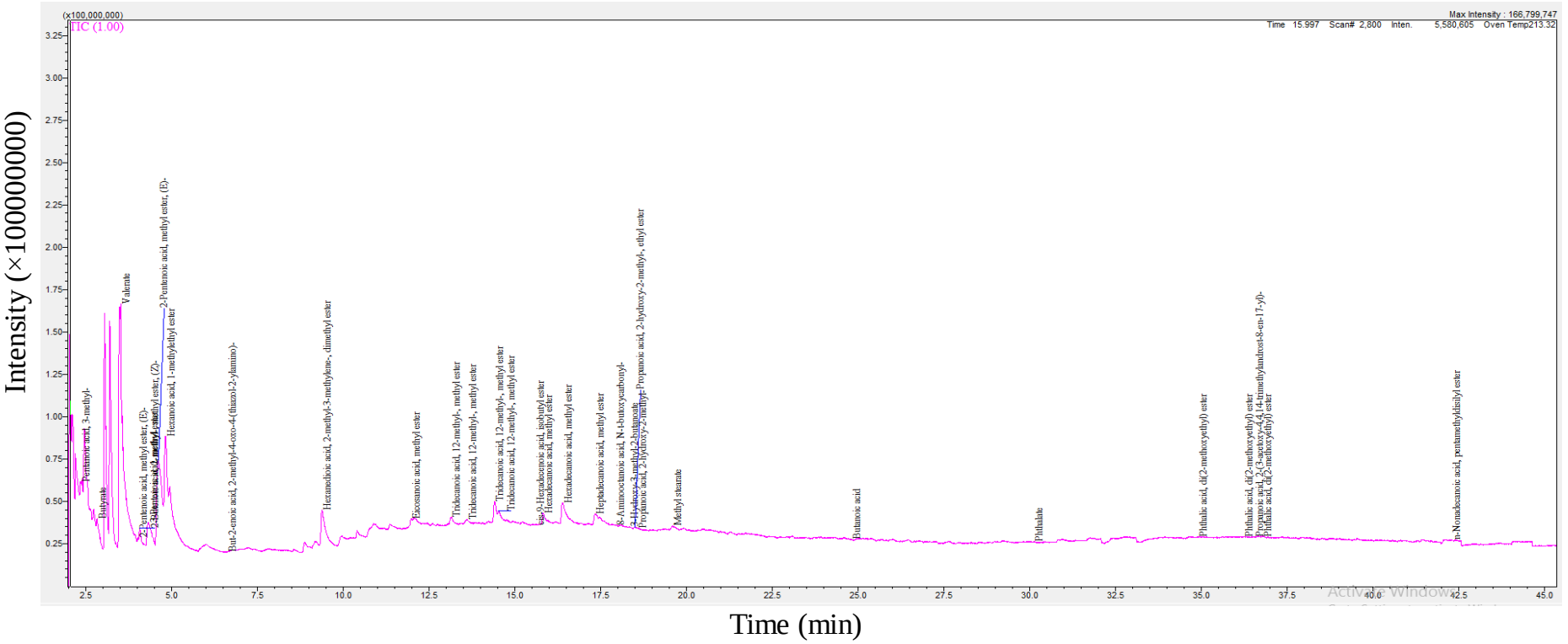

S 3.5: Pyrogram of PHA extracted after CFBF 4